

Final Report

Auger Lifeboat 6 Incident

Shell Oil Company
Houston, Texas, USA

Report No.: O-AP-FINV / BPADG (10165575)
July 9, 2020



Project Name: Auger Lifeboat 6 Incident
Customer: Shell Oil Company
Contact Person: [REDACTED]
Date of Issue: July 7, 2020
Project No.: 10165575
Organization Unit: Incident Investigation
Report No.: O-AP-FINV / BPADG

DNV GL USA, Inc. (Oil and Gas)
Pipeline Services Department
Incident Investigation
5777 Frantz Road
Dublin, OH 43017-1886
United States
Tel: (614) 761-1214
Fax: (614) 761-1633
www.dnvgl.com

Task and Objective:

Please see Executive Summary.

Prepared by

[REDACTED]
[REDACTED], Ph.D.
Principal Engineer

Verified by

[REDACTED]
[REDACTED], Ph.D., FNACE
Senior Principal Engineer

Approved by

[REDACTED]
[REDACTED], P.E.
Head of Department – Pipeline Services

[REDACTED]
[REDACTED], Ph.D., P.E.
Head of Section – Incident Investigation

- ☐ OPEN. Unrestricted Distribution (internal and external)
☐ INTERNAL use only. Internal DNV GL document.
☒ CONFIDENTIAL. Distribution within DNV GL according to applicable contract.*
☐ SECRET. Authorized access only.

* Specify distribution:

Keywords

Copyright © DNV GL 2020 All rights reserved. Reference to part of this publication which may lead to misinterpretation is prohibited. DNV GL and the Horizon Graphic are trademarks of DNV GL AS.

| Rev. No. | Date | Reason for Issue: | Prepared by: | Verified by: | Approved by: |
|----------|------------|-------------------|--------------|--------------|--------------|
| 0 | 2020-03-27 | First Issue | | | |
| 1 | 2020-05-22 | Second Issue | | | |
| | 2020-07-09 | Final | | | |



Executive Summary

Shell Oil Company (SOC) contracted DNV GL USA, Inc. (DNV GL) to assist with a causal investigation of an incident that involved an unintended release of a lifeboat, specifically Lifeboat 6, from the Shell Offshore Inc. (SOI) Auger Tension Leg Platform (TLP). The incident occurred on June 30, 2019 at Auger, located 130 miles off the coast of Louisiana in the Gulf of Mexico (GoM). DNV GL performed inspections of the components associated with the incident as well as testing and analyses of select components.


Lifeboat 6 was manufactured by Watercraft America, Inc., is approximately 24 feet in length, has a full-load capacity of 13,306 lbs, and is approved for 32 persons. Release hooks on the forward and aft of the lifeboat attach to rings suspended from twin fall cables that raise and lower the boat, to and from a davit on the Auger platform.

On June 30, 2019, the Auger lifeboat crew was performing the quarterly launch of Lifeboat 6. As part of the launch, the lifeboat was lowered from the Auger platform using a winch and the rings were released for lifeboat maneuvers in the GoM. The rings reportedly released without issue. While performing maneuvers, the forward and aft hooks were reportedly reset to the closed position. After the maneuvers, Lifeboat 6 returned to the Auger Platform, the rings were re-hooked, and Lifeboat 6 was lifted into the davit using the winch. The aft end of Lifeboat 6 came into contact with the aft bumpers of the davit first, based on measurements performed on the fall cables after the incident.

Personnel onboard started exiting Lifeboat 6 through the man-door located on the starboard side of the vessel. With two personnel still on board, the Aft Hook released the Aft ring and the aft of Lifeboat 6 swung outward away from the Auger Platform, facilitating a sequence of events that resulted in Lifeboat 6 inverted in the water.

The investigation of the unintended Aft Hook release was divided into three main phases: (1) the field investigation, (2) reconstruction and function testing, and (3) examination of key components. The objectives of the investigation were to document the artifacts, determine the immediate cause of the aft hook release, and identify any contributing factors. The investigation by DNV GL is supplemental to a causal analysis being performed by SOI to determine the root cause(s) of the incident.

The results of the investigation indicate that the unintended release of the Subject Aft Hook of Lifeboat 6 was a result of a degraded and compromised aft control cable. The control cable exhibited significant corrosion, full penetration around the circumference, of the structural wire layer allowing for externally applied loads to rotate the locking shaft of the Subject Aft Hook to an open position.



Failure of the Subject Aft Cable is suspected of progressing in the following manner: (1) mechanical damage to the cover due to contact between the control cable and the helmsman's console, (2) water ingress leading to significant corrosion of the wire layer, (3) voluminous corrosion product resulting in fatigue of the cover layer and the cover opening further, and (4) buckling and elongation of the liner layer as a repetitive action associated with the functioning of the control cable. Due to the damage to the Subject Aft Cable, the locking shaft of the Subject Aft Hook was not fully closed (i.e. in a slightly more open position) requiring less rotation to release the hook. The compromised cover and wire layer would have allowed for external loads applied to the control cable to translate onto the inner member of the control cable that is directly linked to the locking shaft, thereby rotating the locking shaft to an open position.

Table of Contents

| | | |
|---------|--|----|
| 1.0 | BACKGROUND | 1 |
| 1.1 | Lifeboat 6 | 1 |
| 1.2 | Summary of the Incident and Recovery Effort..... | 2 |
| 1.3 | Objective of the Investigation | 3 |
| 2.0 | TECHNICAL APPROACH AND ADDITIONAL BACKGROUND | 3 |
| 2.1 | Field Investigation..... | 4 |
| 2.2 | Reconstruction and Function Testing | 4 |
| 2.3 | Examination of Key Components | 4 |
| 2.3.1 | Release Unit – Background Information and Examination | 5 |
| 2.3.2 | Hooks –Background Information and Examination..... | 6 |
| 2.3.3 | Fall Cables and Rings – Background Information and Examination..... | 6 |
| 2.3.4 | Control Cables – Background Information and Examination | 7 |
| 2.3.5 | Fiberglass Hull and Support Structure – Background Information and Examination | 8 |
| 3.0 | RESULTS..... | 9 |
| 3.1 | Field Investigation | 9 |
| 3.1.1 | Inspection at Harvey Terminal – July 29 through August 2, 2019 | 9 |
| 3.1.1.1 | Laser Scanning | 12 |
| 3.1.2 | Inspection at Harvey Terminal – October 3, 2019 | 12 |
| 3.1.3 | Inspection at Harvey Terminal – PSN Visits | 14 |
| 3.1.4 | Auger Lifeboat 6 Davit | 14 |
| 3.2 | Reconstruction..... | 14 |
| 3.2.1 | Description of Reconstruction Process | 15 |
| 3.2.2 | Function Testing | 15 |
| 3.2.2.1 | Subject Hook, Subject Cable, and Subject Release Unit | 15 |
| 3.2.2.2 | Subject Hook, Exemplar Cable, and Subject Release Unit..... | 16 |
| 3.2.2.3 | Exemplar Hook, Exemplar Aft Cable, and Subject Release Unit..... | 17 |
| 3.3 | Examination of Key Components | 17 |
| 3.3.1 | Subject Release Unit..... | 17 |
| 3.3.1.1 | Visual Inspection..... | 17 |
| 3.3.2 | Hooks..... | 17 |

| | | |
|---------|---|----|
| 3.3.2.1 | Subject Hooks | 18 |
| 3.3.2.2 | Exemplar Hook | 24 |
| 3.3.3 | Fall Cables and Rings | 24 |
| 3.3.3.1 | Visual Examination | 24 |
| 3.3.3.2 | Laser Scanning | 26 |
| 3.3.4 | Cables | 26 |
| 3.3.4.1 | Subject Aft Cable | 26 |
| 3.3.4.2 | Lifeboat 7 & 8 Cables | 36 |
| 3.3.4.3 | Mechanical Testing of Exemplar Cable and Subject Aft Cable | 40 |
| 3.3.4.4 | Load Testing with Exemplar Cable, Exemplar Hook, Exemplar Ring, and Subject Release Unit | 40 |
| 3.3.5 | Fiberglass Hull and Support Structure | 42 |
| 3.3.5.1 | Scanning Electron Microscopy | 42 |
| 3.3.5.2 | Mechanical Testing | 43 |
| 3.3.5.3 | Modeling | 44 |
| 4.0 | FAILURE SCENARIOS | 50 |
| 4.1 | Approach | 50 |
| 4.2 | Failure of Non-Hook System Components | 51 |
| 4.3 | Hook Point Load | 51 |
| 4.4 | Locking Shaft of the Subject Aft Hook Rotated Unintentionally | 51 |
| 4.4.1 | Hook System Components Compromised | 52 |
| 4.4.2 | Control Cable Compromised | 52 |
| 4.4.2.1 | Single Overload Event | 52 |
| 4.4.2.2 | Damage Accumulation | 52 |
| 5.0 | CONCLUSIONS | 53 |

List of Figures

| | | |
|------------|--|----|
| Figure 1. | Photograph of Lifeboat 6 in the davit on the Auger Platform prior to the incident. Photograph provided by SOI. | 54 |
| Figure 2. | Laser scan of the davit used with Lifeboat 6 on the Auger Platform. Laser scan data provided by SOI. | 55 |
| Figure 3. | Photographs of the (a) aft and (b) forward ends of Lifeboat 6 in the davit on the Auger Platform before the replacement of the winch, fall cables, and rings (photograph from original equipment manufacturer [OEM] service report FS6540, approximately June 2014). Photographs provided by SOI. | 56 |
| Figure 4. | Photograph of the placard from Lifeboat 6 taken after the incident. | 57 |
| Figure 5. | Drawing Number 7.3 EL-215-Rev A showing the dimensions and the components of an EL Survival Craft. The components used in DNV GL's reconstruction have been highlighted with yellow. Drawing provided by Palfinger to SOI. | 58 |
| Figure 6. | Drawing Number US10088, Sheet 1 of 2 showing the retrofit installation for the LHR3.5M2 hooks in an EL-24 Lifeboat. Drawing provided by Palfinger to SOI. | 59 |
| Figure 7. | Drawing showing the contact between Lifeboat 6 and the bumpers based on the measurements of the twin fall cables that were performed after the incident. The aft is in contact with the bumpers; however, the forward is not in contact. Drawing designed by SOI. | 60 |
| Figure 8. | Photograph showing the condition of Lifeboat 6 in Harvey Terminal after the incident, as viewed from the forward, port side. | 61 |
| Figure 9. | Photograph showing the condition of the Lifeboat 6 in Harvey Terminal after the incident, as viewed from the aft, starboard side. | 62 |
| Figure 10. | Photographs showing the condition of the davit and port bumpers after the incident. Photograph provided by SOI. | 63 |
| Figure 11. | Drawings of the Subject Release Unit showing the different components of the release unit. The drawing on the left is from Drawing Number US10088-Rev B, Sheet 1 of 2 (front) and the drawing on the right is from Palfinger Document F10927. Drawing provided by Palfinger to SOI. Note that the drawing shown is for a hook of similar design and not the as-installed hooks. | 64 |

List of Figures (continued)

- Figure 13. Drawing from Palfinger Document F10927 showing the details of components for the LHR3.5M2 hook with the cover for the locking shaft and control cable removed (Note: drawing modified to remove tab on the clevis so that it is more representative of the clevis from the subject component). Drawing provided by Palfinger to SOI. Note that the drawing shown is for a hook of similar design and not the as-installed hooks.66
- Figure 14. Drawings from Palfinger Document F10927 showing a cross-sectional view of the LHR3.5M2 hook when in the (a) closed position and (b) open position. The location of the clevis, bulkhead nuts, control cable, hook roller, locking shaft, keeper, and locking pawl of the hook are shown. Drawings provided by Palfinger to SOI. Note that the drawings shown is for a hook of similar design and not the as-installed hooks.67
- Figure 15. Drawing from Palfinger Document F10927 combined with an image titled “General-structure-of-push-pull-cable” showing the detail of components for the control cables. Drawing provided by Palfinger to SOI.68
- Figure 16. Schematics of a FEA model showing the nominal wall thicknesses of the fiberglass components of Lifeboat 6 as viewed from (a) the interior and (b) the exterior. The FEA model was produced by Plastic Services Network (PSN) using physical measurements of extracted panels and details from original manufacturer drawings. The colors indicate the following: green is 0.250-inch, pink is 0.375-inch, purple is 0.186-inch, and brown is 0.750-inch wall thickness.69
- Figure 17. Photographs showing Lifeboat 6 and the erected support structure to facilitate inspection of the associated components, as viewed from the (a) forward and (b) aft of Lifeboat 6 at Harvey Terminal after recovery.70
- Figure 18. Photographs showing the aft of Lifeboat 6 and the as-found condition of the Subject Aft Hook as viewed from (a) the starboard side, (b) the stern, and (c) the port side.71
- Figure 19. Photograph of the Subject Aft Cable showing a failure of the outer layers exposing the inner member. The direction of the Subject Aft Hook is noted with the blue arrow. Ruler is in mm.72
- Figure 20. Photograph of the Subject Aft Hook showing the as-found condition of the threaded connections (a) at the clevis and (b) at the bulkhead nuts; the locations of the clevis and bulkhead nuts are shown in embedded schematic. Ruler in top image is in inches.73

List of Figures (continued)

| | | |
|------------|--|----|
| Figure 21. | Photographs showing (a) the bow of Lifeboat 6 and (b) the as-received condition of the Subject Forward Hook at Harvey Terminal. Photograph in (b) provided by USCG. | 74 |
| Figure 22. | Photograph showing a separation of the outer layers from the conduit cap at the bulkhead nuts of the Subject Forward Cable; location shown in the embedded schematic. The direction of the Subject Forward Hook is noted with the blue arrow. | 75 |
| Figure 23. | Photograph showing the as-found condition of the threaded connections of the Subject Forward Hook (a) at the clevis and (b) at the bulkhead nuts; the location of the clevis and bulkhead nuts are shown in the embedded schematic. The direction of the Subject Forward Hook is noted with the blue arrow. | 76 |
| Figure 24. | Photograph showing the as-found condition of the internal subject components of Lifeboat 6. | 77 |
| Figure 25. | Photograph showing the as-found condition of the hydrostatic and safety locks on the Subject Release Unit of Lifeboat 6. | 77 |
| Figure 26. | Photograph showing the as-found condition of the Subject Aft Cable and Subject Forward Cable clevises at the Subject Release Unit of Lifeboat 6. | 78 |
| Figure 27. | Photograph showing the as-found condition of the Subject Aft Cable and Subject Forward Subject at the bulkhead nuts of the Release Unit of Lifeboat 6. | 78 |
| Figure 28. | Photograph of the Subject Release Unit showing the as-found condition of the bulkhead nuts attaching the Subject Hydrostatic Cable to the Subject Release Unit. | 79 |
| Figure 29. | Photograph showing the as-found condition of the hydrostatic actuator of Lifeboat 6. | 79 |
| Figure 30. | Photographs of the key components of Lifeboat 6 after removal and preparing for transit to DNV GL. | 80 |
| Figure 31. | Photographs of the key components of Lifeboat 6 delivered to DNV GL's warehouse on August 6, 2019. | 81 |
| Figure 32. | Photographs showing a failure in an Exemplar Cable when the wire layer and liner were severed at the approximate location of failure as on the Subject Aft Cable. Handle for the Exemplar Release Unit was in the closed position. Ruler is in mm. | 82 |

List of Figures (continued)

| | | |
|------------|--|----|
| Figure 33. | Photographs showing a failure in an Exemplar Cable when the wire layer and liner were severed at the approximate location of failure as on the Subject Aft Cable. Handle for the Exemplar Release Unit was in the open position. Ruler is in mm. | 83 |
| Figure 34. | Photograph showing the orientations of the locking shaft indicator on the Exemplar Hook when the release handle for the Exemplar Release Unit was actuated into the open and close positions before and after the wire layer and liner of the Exemplar Cable were severed. The table summarizes the conditions of each step, with the columns detailing the position of the release handle of the Exemplar Release Unit, the action taken in the step, the measurement of the separation in the Exemplar Cable, and whether the locking shaft prevented the hook from rotating. | 84 |
| Figure 35. | Laser scan of the Lifeboat 6, performed at Harvey Terminal after recovery. | 85 |
| Figure 36. | Photographs showing (a) the starboard of Lifeboat 6 and (b) the reference location for measurements. Tape measure is in feet. | 86 |
| Figure 37. | Photographs showing locations of cracks of interest at (a) the aft shoe plate and (b) 11.4 feet from reference location; locations shown in Figure 36. Tape measure is in feet. | 87 |
| Figure 38. | Photographs showing (a) the reference location for measurements on the interior of the hull and (b) the corresponding location on the engine and engine cradle. Tape measure is in feet. | 88 |
| Figure 39. | Photographs showing (a) indentations / contact damage at the hull interior 2.25 feet from the reference location and (b) the corresponding location on the engine and engine cradle. Tape measure is in feet. | 89 |
| Figure 40. | Photographs showing (a) a missing section of the hull interior 5.8 feet to 6.4 feet from the reference location and (b) the corresponding location on the engine and engine cradle. Tape measure is in feet. | 90 |
| Figure 41. | Photograph showing hole impressions left from the bolt studs used to attach support structure for the engine. Directionality of the damage can be seen adjacent to each hole. Ruler is in inches. | 91 |
| Figure 42. | Photographs showing a transverse crack in the keel of the hull interior located 7.6 feet from the reference location. Tape measure is in feet. | 92 |

List of Figures (continued)

| | | |
|------------|---|-----|
| Figure 43. | Schematic showing the approximate locations of each 24-inch by 24-inch panel extracted from the outer and inner hull of Lifeboat 6. Samples BSO-1, ASO-1, BPO-1, and APO-1 were extracted from the outer hull. Samples AP-2, BP-1, and BS-1 were extracted from the interior seating area. | 93 |
| Figure 44. | 3D representation of the approximate location of Sample C-1. The crack observed was located at the interior of boat at the fiberglass-engine mount interface. | 94 |
| Figure 45. | 3D representation of the approximate location of Sample C-2. The crack observed was located at the exterior of the hull on the keel of the boat. The crack propagated through the thickness of the keel. | 94 |
| Figure 46. | 3D representation of the approximate location of Sample C-3. The crack observed was located at the exterior of the hull on the starboard side. The crack ran from the hull-canopy interface towards the keel. | 95 |
| Figure 47. | Photograph of the reconstruction of the relevant components from Lifeboat 6 located at DNV GL's warehouse. | 96 |
| Figure 48. | Laser scan showing the reconstruction of the relevant components from Lifeboat 6 at DNV GL's warehouse. | 97 |
| Figure 49. | Screenshot of compiled digital recordings from a function test performed using the Subject Aft Hook, the Subject Aft Cable, and the Subject Release Unit. Four views are shown: (a) the port side of the Subject Aft Hook, (b) the break in the Subject Aft Cable located near the Subject Release Unit, (c) the starboard side of the Subject Aft Hook, and (d) the forward side of the Subject Release Unit (note this view is rotated 90° clockwise from its normal orientation). | 98 |
| Figure 50. | Screenshot of compiled digital recordings from a function test performed using the Subject Aft Hook, the Exemplar Cable, and the Subject Release Unit before moving the release handle of the Subject Release Unit. Three views are shown: (a) starboard side of the Subject Aft Hook, (b) the port side of the Subject Aft Hook, and (c) the forward side of the Subject Release Unit. | 99 |
| Figure 51. | Screenshot of compiled digital recordings from a function test performed using the Subject Aft Hook, Exemplar Cable, and Subject Release Unit after moving the release handle of the Subject Release Unit. Three views are shown: (a) starboard side of the Subject Aft Hook, (b) the port side of the Subject Aft Hook, and (c) the forward side of the Subject Release Unit. | 100 |

List of Figures (continued)

| | | |
|------------|--|-----|
| Figure 53. | Screenshot of compiled digital recordings of a function test performed using the Exemplar Hook, Exemplar Cable, and Subject Release Unit after moving the release handle of the Subject Release Unit. Three views are shown: (a) starboard side of the Exemplar Hook, (b) the port side of the Exemplar Hook, and (c) the forward side of the Subject Release Unit. | 102 |
| Figure 54. | Photographs of the Subject Release Unit at DNV GL showing the as-found condition of the clevises and bulkhead nuts, after removing the protective coverings. | 103 |
| Figure 55. | Photographs of the Subject Release Unit at DNV GL showing the as-found condition of the hydrostat cable and end rod jam nuts, after removing the protective coverings. | 104 |
| Figure 56. | Photographs of the Subject Aft Hook with the locking shaft cover removed, viewed from (a) the starboard side and (b) the port side. Ruler is in inches. | 105 |
| Figure 57. | Photographs showing the as-found condition of the threaded connections of the Subject Aft Hook (a) at the clevis and (b) at the bulkhead nuts; the locations of the clevis and bulkhead nuts are shown in Figure 14. Ruler in left image is in inches. | 106 |
| Figure 58. | Photographs of the hook from the Subject Aft Hook assembly showing the (a) starboard side and (b) port side, after disassembly. Ruler is in inches. | 107 |
| Figure 59. | Photographs showing the details of witness marks identified on the hook from the Subject Aft Hook assembly at (a) the inside bend of the hook, (b) the edge of the bend as viewed from the port side, and (c) the point of the hook; locations and viewing directions shown in Figure 58 (a) and (b). Rulers are in inches. | 108 |
| Figure 60. | Photographs showing the hook from the Subject Aft Hook assembly (a) after removing the set screw, pin, and roller, as well as (b) the details of the witness marks present on the contact surface of the roller. Ruler is in inches. | 109 |
| Figure 61. | Photographs of the locking shaft from the Subject Aft Hook showing the (a) round side and (b) the flat, after disassembly. Rulers are in inches. | 110 |
| Figure 62. | Photograph of the locking shaft from the Subject Aft Hook showing the mechanical damage on the edge between the round and the flat of the locking shaft. Ruler is in inches. | 110 |

List of Figures (continued)

| | | |
|------------|---|-----|
| Figure 63. | Photograph of the locking shaft from the Subject Aft Hook showing an area with corrosion attack on the round of the locking shaft. Ruler is in inches. | 110 |
| Figure 64. | Photograph of the locking shaft from the Subject Forward and Aft Hooks comparing the areas of corrosion attack on the round of the locking shaft and comparing the overall geometry. Ruler is in inches. | 111 |
| Figure 65. | Photographs of the keeper from the Subject Aft Hook showing the (a) forward side and (b) aft side, after disassembly. Forward and aft refer to the orientation of the keeper relative to the lifeboat. Ruler is in inches. | 112 |
| Figure 66. | Photographs of the keeper from the Subject Aft Hook showing (a) a possible witness mark and (b) red paint; locations shown in Figure 65. Rulers are in inches. | 112 |
| Figure 67. | Photographs of the locking shaft from the Subject Aft Hook installed (a) in the Subject Aft Hook and (b) in the Exemplar Hook with the clevises and bulkhead nuts set to the as-found condition of the subject components. In both cases, the Subject Release Unit was in the closed position and the Exemplar Cable was used. The blue markings were produced by placing articulating paper between the hook roller and locking shaft contact location. The green line indicates the contact location between the hook roller and locking shaft when the locking shaft arm is fully closed. The red line is consistent with an area of corrosion and wear. The yellow line indicates the contact location between the hook roller and locking shaft when the release unit is closed, but the locking shaft arm is rotated as far as possible towards the open orientation. The red line is consistent with an area of corrosion and wear. | 113 |
| Figure 68. | SEM images showing the detail for a suspected area of contact between the roller of the hook and locking shaft from the Subject Aft Hook. | 114 |
| Figure 69. | SEM images showing mechanical damage near the transition to the flat of the locking shaft from the Subject Aft Hook. | 115 |
| Figure 70. | Photographs of the Subject Forward Hook with the locking shaft cover removed, viewed from (a) the starboard side and (b) the port side. Rulers are in inches. | 116 |
| Figure 71. | Photographs of the hook from the Subject Forward Hook showing the (a) starboard side and (b) port side, after disassembly. Ruler is in inches. | 117 |

List of Figures (continued)

| | | |
|------------|---|-----|
| Figure 72. | Photographs showing the details of witness marks identified on the Subject Forward Hook at (a) the inside bend of the hook, (b) the edge of the bend as viewed from the port side, and (c) the point of the hook; locations and viewing directions shown in Figure 58 (a) and (b). Rulers are in inches. | 118 |
| Figure 73. | Photographs of the locking shaft from the Subject Forward Hook showing the (a) round side and (b) the flat, after disassembly. Rulers are in inches. | 119 |
| Figure 74. | Photograph of the locking shaft from the Subject Forward Hook showing the edge between the round and flat of the locking shaft; area shown in Figure 73. Ruler is in inches. | 119 |
| Figure 75. | Photograph of the locking shaft from the Subject Forward Hook showing an area with corrosion attack on the round of the locking shaft; area shown in Figure 73. Ruler is in inches. | 120 |
| Figure 76. | Photographs of the keeper from the Subject Forward Hook showing the (a) forward side and (b) aft side, after disassembly. Forward and aft refer to the orientation of the keeper relative to the lifeboat. Rulers are in inches. | 120 |
| Figure 77. | Laser scans of Subject Aft Hook components displayed individually. From left to right: the locking shaft (gold), the keeper (yellow), the hook (orange), and the housing (purple). The Locations A, B, and C correlate to the centerlines of the components and their respective positions in the housing. | 121 |
| Figure 78. | Laser scans of Subject Aft Hook components aligned to working positions. | 121 |
| Figure 79. | Laser scans of Subject Aft Hook components aligned to working positions with the locking shaft rotated into contact with the post of the hook body. An outline of the components shows the interacting locations of the hook and locking shaft. | 122 |
| Figure 80. | Laser scans of Subject Aft Hook showing the 3D assembly aligned assuming elongation of the liner equivalent to 2.58 inches. An outline of the components shows the interacting locations of the hook and locking shaft. | 122 |
| Figure 81. | Laser scans of Subject Forward Hook components. From left to right: the locking shaft (teal), the hook (red), and the keeper (light purple). | 122 |

List of Figures (continued)

| | | |
|------------|---|-----|
| Figure 82. | Two right circular cylinders held in contact by forces F uniformly distributed along length l (Left). Elliptical contact stress distribution across contact area $2b$ (Right). Table of variables used in associated calculations (Bottom)..... | 123 |
| Figure 83. | Locking shaft major diameter, locking shaft edge diameter and hook roller diameter illustrated by fitting nominal cylinders to the Subject Aft Locking Shaft (green) and Subject Aft Hook (Orange)..... | 123 |
| Figure 84. | Local Compressive Stress vs. Depth into Material from Contact Surface..... | 124 |
| Figure 85. | Laser scans of Exemplar Hook with a close-up image of the hook tip. | 124 |
| Figure 86. | Photograph of the Subject Aft Ring and a section of the Subject Aft Fall Cable as received at DNV GL. Ruler is in inches..... | 125 |
| Figure 87. | Photographs of (a) the Subject Aft Ring and (b) the section of the Subject Aft Fall Cable after removal from shipping container. Rulers are in inches..... | 125 |
| Figure 88. | Photographs of composite block after removal from the section of the Subject Aft Fall Cable. The direction toward the Subject Aft Ring is shown. Rulers are in inches. | 126 |
| Figure 89. | Photograph showing the cross-section of the Subject Aft Fall Cable. Ruler is in inches..... | 126 |
| Figure 90. | Photographs showing the Subject Aft Ring and locations where witness marks were identified. Ruler in top image is in inches and the ruler in the bottom image is in mm. | 127 |
| Figure 91. | Photographs showing additional witness marks on the Subject Aft Ring; the location of witness mark "B" is shown in Figure 90. Ruler is in mm. | 128 |
| Figure 92. | Photograph of the Subject Forward Ring and a section of the Subject Forward Fall Cable as received at DNV GL. Ruler is in inches..... | 129 |
| Figure 93. | Photograph of the Subject Forward Ring and the section of the Subject Forward Fall Cable after removal from shipping container. Ruler is in inches..... | 129 |
| Figure 94. | Photographs of composite block after removal from the section of the Subject Forward Fall Cable. The direction toward the Subject Forward Ring is shown. Ruler is in inches..... | 130 |

List of Figures (continued)

| | |
|---|-----|
| Figure 95. Photograph showing the cross-section of the Subject Forward Fall Cable. Ruler is in inches. | 130 |
| Figure 96. Photographs showing the Subject Forward Ring and locations where witness marks were identified. Rulers are in inches. | 131 |
| Figure 97. Laser scans of Subject Aft Ring. | 132 |
| Figure 98. Laser scans of Subject Aft Ring with the section of the Subject Aft Fall Cable. | 132 |
| Figure 99. Laser scans of Subject Forward Ring. | 133 |
| Figure 100. Laser scans of Subject Forward Ring with the section of the Subject Forward Fall Cable. | 133 |
| Figure 101. Photograph showing Subject Aft Cable, Subject Forward Cable, and Subject Hydrostat Cable at the Release Unit after reconstruction at DNV GL's facility. | 134 |
| Figure 102. Photographs showing (a) Subject Aft Cable and (b) Subject Forward Cable at the Subject Aft and Subject Forward Hooks, respectively. | 135 |
| Figure 103. Photographs showing mechanical damage to the cover of the Subject Aft Cable (a) 3.70 feet to 4.10 feet, (b) 4.70 feet to 5.70 feet, and (c) 8.10 feet to 8.60 feet from the conduit cap at the Subject Release Unit. These photographs were taken by DNV GL during a site visit to Harvey Terminal on July 31, 2019. Tape measures are in feet. | 136 |
| Figure 104. Photographs showing mechanical damage to the cover layer of the Subject Aft Cable 20.63 feet from the conduit cap at the Subject Release Unit. The top photograph was taken by DNV GL during a site visit to Harvey Terminal on July 31, 2019 and the lower photograph was taken at DNV GL's laboratory in Dublin, Ohio. The direction of the Subject Aft Hook is noted with the blue arrow. Tape measure is in feet and ruler is in inches. | 137 |
| Figure 105. Photographs of the Subject Aft Cable after removing a section with the failure in the outer layers. The direction of the Subject Aft Hook is noted with the blue arrow. Rulers are in inches. | 138 |
| Figure 106. Photographs of the Subject Aft Cable showing the detail of the failure. The direction of the Subject Aft Hook is noted with the blue arrow. Rulers are in inches. | 139 |

List of Figures (continued)

| | |
|---|-----|
| Figure 107. Photograph and montage of photographs of the Subject Aft Cable (a) taken in the field on June 6, 2019 by Palfinger and (b) taken in the laboratory by DNV GL, respectively. For the montage, the fracture surfaces of the cover were matched to generate an image similar to the photograph shown in Figure 107 (a). The numbers in Figure 107 (a) and (b) are corresponding locations along the length the control cable. The direction of the Subject Aft Hook is noted with the blue arrow. Ruler is in inches. | 140 |
| Figure 108. Photograph of the Subject Aft Cable showing the layers of the control cable after dissection near the location of failure. The direction of the Subject Aft Hook is noted with the blue arrow. Ruler is in inches. | 141 |
| Figure 109. Photographs of the cover from the Subject Release Unit side of the failure in the Subject Aft Cable after dissection showing the (a) external surface and (b) internal surface; samples shown in Figure 108. Forward and aft refer to the orientation of the cover relative to the lifeboat. The direction of the Subject Aft Hook is noted with the blue arrow. Results of hardness measurements shown in table. Ruler is in inches. | 142 |
| Figure 110. Photographs of the cover from the Subject Aft Hook side of the failure in the Subject Aft Cable after dissection showing the (a) external surface and (b) internal surface; samples shown in Figure 108. Forward and aft refer to the orientation of the cover relative to the lifeboat. The direction of the Subject Aft Hook is noted with the blue arrow. Ruler is in inches. | 143 |
| Figure 111. Light photomicrographs of the cover from the Subject Aft Cable after matching the fractures surfaces at the failure. The numbers "1" and "2" are reference locations. Forward and aft refer to the orientation of the cover relative to the lifeboat. The direction of the Subject Aft Hook is noted with the blue arrow..... | 144 |
| Figure 112. Montages of SEM images taken of the fracture surfaces from the cover of the Subject Aft Cable showing crack arrest marks and initiation sites; locations for (a) and (b) are shown in Figure 110. The red arrow indicated the direction of fatigue propagation..... | 145 |
| Figure 113. Fourier-transform Infrared Spectroscopy spectrum of the FTIR sample removed from the cover of the Subject Aft Cable; sample location shown in Figure 109..... | 146 |

List of Figures (continued)

| | |
|---|-----|
| Figure 114. Photographs of the wire layer from the Subject Release Unit side of the failure in the Subject Aft Cable after dissection showing the (a) aft side and (b) forward side; samples shown in Figure 108. Forward and aft refer to the orientation of the keeper relative to the lifeboat. The direction of the Subject Aft Hook is noted with the blue arrow. Rulers are in inches. | 147 |
| Figure 115. Photographs of the wire layer from the Subject Aft Hook side of the failure in the Subject Aft Cable after dissection showing the (a) aft side and (b) forward side; samples shown in Figure 108. The direction of the Subject Aft Hook is noted with the blue arrow. Forward and aft refer to the orientation of the keeper relative to the lifeboat. Rulers are in inches. | 148 |
| Figure 116. Light photomicrographs of the wire layer from the Subject Aft Cable showing the corrosion damage at the failure. The direction of the Subject Aft Hook is noted with the blue arrow. | 149 |
| Figure 117. SEM images taken of the strand wires from the wire layer of the Subject Aft Cable showing corrosion damage; viewing direction is shown in Figure 116. | 150 |
| Figure 118. SEM image, EDS spectra, and table of results for white deposits removed from the external surface of the wire layer of the Subject Aft Cable; location shown in Figure 114. | 151 |
| Figure 119. Spectrum and table summarizing the results of an XRD analysis performed on reddish-brown deposits that were removed from the wire layer of Subject Aft Cable near the failure; location shown in Figure 115. | 152 |
| Figure 120. Photograph and photomicrographs of a longitudinal metallographic mount, Mount M1, showing the corrosion attack of the strand wires from the wire layer of the Subject Aft Cable; mount removed from location shown in Figure 114. The direction of the Subject Aft Hook is noted with the blue arrow. The ruler in the upper right photograph is in inches. | 153 |
| Figure 121. Photomicrographs of Mount M1 showing (a) the detail of the corrosion attack and (b) the microstructure of the strand wires from the wire layer of the Subject Aft Cable; locations shown in Figure 120. | 154 |

List of Figures (continued)

| | |
|---|-----|
| Figure 122. Photograph and photomicrographs of a transverse metallographic mount, Mount M2, showing the corrosion attack of the binder and strand wires from the wire layer of the Subject Aft Cable; mount removed from location shown in Figure 114. The blue circle indicates that the direction toward the Subject Aft Hook is out of the paper. The ruler in the upper left photograph is in inches..... | 155 |
| Figure 123. Photomicrographs of Mount M2 showing the microstructure of the (a) binder wire and (b) strand wires from the wire layer of the Subject Aft Cable in the transverse orientation; locations shown in Figure 122. | 156 |
| Figure 124. SEM images, SEM-EDS elemental maps, and EDS results of deposits present on the binder wire from the Subject Aft Cable showing the distribution of iron (Fe), zinc (Zn), chlorine (Cl), and calcium (Ca); area of Mount M1 shown in Figure 120 (rotated 90°)..... | 157 |
| Figure 125. SEM images, SEM-EDS elemental maps, and EDS results of deposits present on the strand wire from the Subject Aft Cable showing the distribution of iron (Fe), chlorine (Cl), and calcium (Ca); area of Mount M1 shown in Figure 120 (rotated 90°). | 158 |
| Figure 126. SEM images and SEM-EDS elemental maps of deposits present on the binder wire from the Subject Aft Cable showing the distribution of iron (Fe), zinc (Zn), and chlorine (Cl); area of Mount M2 shown in Figure 122 (rotated 90° counter clockwise)..... | 159 |
| Figure 127. EDS Spectra, SEM image, and EDS results for wire and binder wire from the Subject Aft Cable; area shown in Figure 122 (rotated 90°). | 160 |
| Figure 128. Photographs of the one failed liner from the Subject Release Unit side after dissection showing the (a) aft side and (b) forward side; samples shown in Figure 108. The mating half of the failed liner is shown in Figure 129. Forward and aft refer to the orientation of the keeper relative to the lifeboat. The direction of the Subject Aft Hook is noted with the blue arrow. Rulers are in inches. | 161 |
| Figure 129. Photographs of the failed liner from the Subject Aft Hook side after dissection showing the (a) aft side and (b) forward side; samples shown in Figure 108. The mating half of the failed liner is shown in Figure 128. Forward and aft refer to the orientation of the keeper relative to the lifeboat. The direction of the Subject Aft Hook is noted with the blue arrow. Rulers are in inches. | 162 |

List of Figures (continued)

| | |
|--|-----|
| Figure 130. Photograph showing the liner from the Subject Release Unit side after removing the wire layer; sample shown in Figure 108. The direction of the Subject Aft Hook is noted with the blue arrow. The results of the hardness testing of the white liner layer are shown in the table. | 163 |
| Figure 131. Light photomicrographs of the liner from the Subject Aft Cable showing the failure. The direction of the Subject Aft Hook is noted with the blue arrow. | 164 |
| Figure 132. SEM images of the liner from the Subject Aft Hook side of the Subject Aft Cable showing the fracture surface; sample location is shown in Figure 131. | 165 |
| Figure 133. SEM images of the liner from the Subject Aft Hook side of the Subject Aft Cable showing the external surface; sample location is shown in Figure 131. | 166 |
| Figure 134. SEM image and EDS Results of the embedded particle in the external surface of the liner of the Subject Aft Cable; location is shown in Figure 131. | 167 |
| Figure 135. Fourier-transform Infrared Spectroscopy spectrum of a sample removed from the liner of the Subject Aft Cable; sample location shown in Figure 114. The wire layer was removed to gain access to the liner layer underneath. | 168 |
| Figure 136. Results of Differential Scanning Calorimetry (DSC) analysis for Oxidative Induction Time (OIT). Samples from liners of Lifeboat 6 (LB6), Lifeboat 7 (LB7), and Lifeboat 8 (LB8) were removed from the aft control cables and tested. | 169 |
| Figure 137. Results of Differential Scanning Calorimetry (DSC) analysis for Glass Transition Temperature (T _g). Samples from liners of Lifeboat 6 (LB6), Lifeboat 7 (LB7), and Lifeboat 8 (LB8) were removed from the aft control cables and tested. | 169 |
| Figure 138. Schematic showing the results of the Thermogravimetric Analysis (TGA). Samples from the liners of Lifeboat 6 (LB6), Lifeboat 7 (LB7), and Lifeboat 8 (LB8) were removed from the aft control cables and tested. | 170 |
| Figure 139. Photograph showing the geometry of tensile specimens extracted from the liners of the aft control cables from of Lifeboat 6 (LB6), Lifeboat 7 (LB7), and Lifeboat 8 (LB8) and a summary table of results of testing. The tests were performed at strain rates of 0.2 in/min, 2 in/min, and 20 in/min. | 171 |

List of Figures (continued)

| | |
|--|-----|
| Figure 140. Photograph of the inner member from the Subject Aft Cable after dissection showing the aft side; samples shown in Figure 108. Aft refers to the orientation of the keeper relative to the lifeboat. The direction of the Subject Aft Hook is noted with the blue arrow. Ruler is in inches. | 172 |
| Figure 141. Light micrographs of the inner member of the Subject Aft Cable showing the detail of the minor corrosion attack to the binder wire and damage to the sheath layer of the inner member. The direction of the Subject Aft Hook is noted with the blue arrow. | 173 |
| Figure 142. Photographs of the (a) hydrostat cable from Lifeboat 7 and (b) the forward control cable from Lifeboat 8 showing evidence of degradation. Photographs were provided by SOI. | 174 |
| Figure 143. Photograph of the hydrostat cable from Lifeboat 7 and the forward control cable from Lifeboat 8, at DNV GL, after partially removing the wrappings from shipment. Ruler is in inches. | 175 |
| Figure 144. Photograph of the hydrostat cable from Lifeboat 7 after removing the wrappings. Ruler is in inches. | 176 |
| Figure 145. Photographs of the hydrostat cable from Lifeboat 7 showing damage at (a) the assumed top orientation and (b) the assumed bottom orientation. Measuring tape is in feet. | 177 |
| Figure 146. Photograph of the forward control cable from Lifeboat 8 after removing the wrappings. Measuring tape is in feet. | 178 |
| Figure 147. Photograph of the forward control cable from Lifeboat 8 showing damage at the assumed top orientation. Measuring tape is in feet. | 179 |
| Figure 148. Photograph of the Lifeboat 7 hydrostat cable after dissection near the damaged location. Ruler is in inches. | 180 |
| Figure 149. Photograph of the Lifeboat 8 forward control cable after dissection near the damaged location. Rulers are in inches. | 181 |
| Figure 150. Photographs of the half the cover from the Lifeboat 7 hydrostat cable after dissection showing the internal surface near the damaged location; samples shown in Figure 148. The reference direction is noted with the blue arrow. Rulers are in inches. | 182 |
| Figure 151. Photographs of the cover from the Lifeboat 7 hydrostat cable after dissection showing the internal surface near the damaged location; samples shown in Figure 148. The reference direction is noted with the blue arrow. Rulers are in inches. | 182 |

List of Figures (continued)

| | |
|--|-----|
| Figure 152. Photographs of the cover from the Lifeboat 8 forward control cable after dissection showing the (a) external surface and (b) internal surface near the damaged location; samples shown in Figure 149 (top). The reference direction is noted with the blue arrow. Rulers are in inches..... | 183 |
| Figure 153. Photographs of the cover from the Lifeboat 8 forward control cable after dissection showing the (a) external surface and (b) internal surface near the damaged location; samples shown in Figure 149 (top). The reference direction is noted with the blue arrow. Rulers are in inches..... | 184 |
| Figure 154. Light photomicrographs of the cover from the Lifeboat 7 hydrostat cable after matching the fractures surfaces. The reference direction is noted with the blue arrow. | 185 |
| Figure 155. Light photomicrographs of the cover from the Lifeboat 8 forward control cable after matching the fractures surfaces. The reference direction is noted with the blue arrow..... | 186 |
| Figure 156. Photographs of the wire layer from the Lifeboat 7 hydrostat cable at the damaged location showing the (a) side exposing the liner and (b) the side with some wires intact; sample location shown in Figure 148 (top). The reference direction is noted with the blue arrow. Rulers are in inches. | 187 |
| Figure 157. Photograph of the wire layer from the Lifeboat 8 forward control cable at the damaged location showing the corrosion attack to the wire layer; sample location shown in Figure 149. The reference direction is noted with the blue arrow. Ruler is in inches. | 188 |
| Figure 158. Light photomicrographs showing the (a) top and (b) bottom of the wire layer from the Lifeboat 7 hydrostat cable showing the corrosion damage; location shown in Figure 156. The reference direction is noted with the blue arrow..... | 189 |
| Figure 159. Light photomicrographs showing the (a) top and (b) bottom of the wire layer from the Lifeboat 8 forward control cable showing the corrosion damage; location shown in Figure 157. The reference direction is noted with the blue arrow..... | 190 |
| Figure 160. Photograph showing the 12-inch lengths of Subject Aft Cable and Exemplar Cable used for mechanical testing. The cover and binder wire were removed from the locations shown. Ruler is in inches..... | 191 |

List of Figures (continued)

| | |
|---|-----|
| Figure 161. Photographs showing the Subject Aft Cable in the hydraulic clamps (a) before and (b) after mechanical testing as well as a table summarizing the results of the mechanical testing of the Subject Aft Cable and Exemplar Cable. | 192 |
| Figure 162. Photographs showing the test rig for the load testing with the Exemplar Cable, Exemplar Hook, Exemplar Ring, and Subject Release Unit. | 193 |
| Figure 163. Photographs showing (a) Scenario 1, (b) Scenario 2, and (c) Scenario 3 of the ring resting on the point of the Exemplar Hook and a table summarizing the results of the load testing. In Scenario 1 and 2, the ring did not move, but in Scenario 3 the ring slipped off the hook point. | 194 |
| Figure 164. Photographs showing (a) the point of the Exemplar Hook compared to the Subject Aft Hook and (b) the mechanical damage to the ring after testing Scenario 1. Rulers are in inches. | 195 |
| Figure 165. Photographs showing (a) the point of the Exemplar Hook compared to the Subject Aft Hook and (b) the mechanical damage to the ring after testing Scenario 2. Rulers are in inches. | 196 |
| Figure 166. Photographs showing (a) the point of the Exemplar Hook compared to the Subject Aft Hook and (b) the mechanical damage to the ring after testing Scenario 3. Rulers are in inches. | 197 |
| Figure 167. Schematic showing the three failure modes, interlaminar, intralaminar, and translaminar for fiberglass materials. | 198 |
| Figure 168. Photograph of Sample C-1 and schematic showing the location where the sample was removed from the inner hull. Sample C-1 was located near the engine mount. The location of the sample examined in the SEM, Sample C-1-A, is shown. Ruler is in inches. | 198 |
| Figure 169. SEM images of Sample C-1-A and schematic showing the fracture surface at a low magnification. Fiber pull-out from the resin matrix is visible near the internal surface. Sample location is shown in Figure 168. | 199 |
| Figure 170. SEM images of Sample C-1-A showing notable fractures of glass fibers. Location of upper left image shown in Figure 169 (right). | 200 |
| Figure 171. Photographs of Sample C-2 and schematic showing the location where the sample was removed from the inner hull. Sample C-2 was located near a crack in the keel. The location of the sample examined in the SEM, Sample C-2-3, is shown. | 201 |

List of Figures (continued)

| | |
|--|-----|
| Figure 172. SEM images of Sample C-2-3 showing notable fractures of glass fibers. | 202 |
| Figure 173. Photograph of Sample C-3 and schematic showing the location where the sample was removed from the outer hull. Sample C-3 was located 11.4 feet from the aft of Lifeboat 6. The location of the sample examined in the SEM, Sample C-3-B, is shown. Ruler are in inches. | 203 |
| Figure 174. SEM images of Sample C-3-B showing notable fractures of glass fibers. | 204 |
| Figure 175. Photograph of an extracted panel (APO-1, location shown in Figure 43) showing the locations where testing coupons were removed using waterjet cutting. Ruler is in inches..... | 205 |
| Figure 176. Photograph of the flexural testing setup on universal testing machine and tables of results for flexural testing of panels extracted from the locations shown in Figure 43. | 206 |
| Figure 177. Photograph showing the sample locations and a table summarizing the results of glass fiber content analysis via ash testing..... | 207 |
| Figure 178. Schematic showing the stress-strain curves generated through compression testing foam from the Lifeboat. Samples with "S" refer to starboard and were removed from under location BS-1 and the samples with "P" refer to port and were removed from under location BP-1; locations of BS-1 and BP-1 are shown in Figure 43. | 208 |
| Figure 179. Schematic showing the material sections assigned to surface regions of the Lifeboat 6 model as viewed from the interior. | 208 |
| Figure 180. Schematic showing the material sections assigned to surface regions of the Lifeboat 6 model as viewed from the exterior. | 209 |
| Figure 181. Schematic showing boundary conditions applied in model: XY symmetry, gravity, engine weight, and vertical displacements. | 209 |
| Figure 182. Von Mises Stress Contour of lifeboat in Step 1 with gravity and engine weight only applied to the lifeboat. | 210 |
| Figure 183. Von Mises Stress Contour of lifeboat in Step 2 with gravity and engine weight and raised ~3.1 inches into the aft davit bumper..... | 210 |
| Figure 184. Von Mises Stress Contour of lifeboat in Step 2 with gravity and engine weight and raised ~3.1 inches into the aft davit bumper..... | 211 |



List of Figures (continued)

| | |
|--|-----|
| Figure 185. Strain Contours of aft bumper with lifeboat raised ~3.1 inches into the aft davit bumper..... | 211 |
| Figure 186. Lateral deflection (port/starboard) of lifeboat raised ~3.1 inches into the aft davit bumper..... | 212 |
| Figure 187. Reaction forces at forward and aft lifting shoes throughout the assessment as a function of vertical displacement considering a bumper..... | 212 |
| Figure 188. Reaction forces at forward and aft lifting shoes throughout the assessment as a function of vertical displacement considering a rigid bumper..... | 213 |
| Figure 189. Schematic showing the fault tree used to identify contributing factors to the unintentional release of the Subject Aft Hook. Green: Evidence from site, laboratory testing, and / or document review support that the fault tree event is a contributing factor. Red: Evidence from site, laboratory testing, and / or document review support that the fault tree event is likely not a contributing factor. | 214 |

1.0 BACKGROUND


Shell Oil Company (SOC) contracted DNV GL USA, Inc. (DNV GL) to assist with a causal investigation of an incident that involved an unintended release of a lifeboat, specifically Lifeboat 6, from the Shell Offshore Inc. (SOI) Auger Tension Leg Platform (TLP). The incident occurred on June 30, 2019 at Auger, located 130 miles off the coast of Louisiana in the Gulf of Mexico (GoM). DNV GL performed site visits to inspect the components associated with the incident as well as testing and analyses of select components to determine the immediate cause of failure in support of the causal investigation led by SOI.

1.1 Lifeboat 6

Figure 1 is a photograph of Lifeboat 6 in the davit on the Auger Platform. The davit has a winch where two cable falls with rings attach to the forward and aft hooks (not visible in photograph). The winch pulls the falls so that the lifeboat rests in the davit against bumpers located at the forward and aft of the lifeboat (not visible in photograph). The bumpers (not visible in photograph) are rubber and attached to A-frames of the davit. Figure 2 is an image of the laser scan data of the Auger Platform with a close-up view of the davit where Lifeboat 6 was located. The locations where the forward and aft of Lifeboat 6 would be located when stored in the davit are noted.

Figure 3 contains photographs of the (a) aft and (b) forward of Lifeboat 6 in the davit on the Auger Platform before replacement of the winch, fall cables, and rings (photograph from June 2014). The falls with rings attached to the forward and aft hooks are visible in these photographs. The contact locations for the aft and forward bumpers of the davit are shown in the photographs (Note: the starboard bumper contact location for the aft is not visible in the photograph). The bumpers primarily contact the fender guards, though some contact with the fiberglass of the canopy appears to occur. The fender guards are comprised of rubber and traces the outer edge of the canopy of the lifeboat.

Figure 4 is a photograph of the placard from Lifeboat 6 taken after the incident. The placard indicates that Lifeboat 6 was manufactured by Watercraft America, Inc. (*Watercraft America*). The approval number and serial number for the lifeboat are 160.035/487/0 and EL24 874/3/84, respectively. The distance between the most forward and most aft element of the boat, permanent fender guards excluded, measured parallel to the design waterline (L) is 23.87 feet. The maximum molded breadth of the hull, without permanent fender guard (B) is 8.75 feet. The vertical distance, at the middle of the length L, from the base line to the top edge of the hull (D) is 3.25 feet. The cubic capacity and the buoyancy capacity are 420.3 ft³ and 123 ft³, respectively. Condition A is 7,212 lbs and refers to the "light load," which is the weight of the complete lifeboat empty and does not include fuel, required equipment, or the equivalent weight of persons. Condition B is 13,306 lbs and



refers to “full load,” which is the weight of the complete lifeboat including all required equipment, provisions, fuel, and the number of persons for which it is approved. The lifeboat is approved for 33 persons. The Officer in Charge, Marine Inspection (OCMI) was denoted as OCMI-JAC. The date of inspection was March 19, 1984.

The original equipment manufacturer (OEM) drawing is shown in Figure 5. Items significant to the work performed by DNV GL are highlighted and include: the forward and aft hooks (Items 8), the forward and aft control cables (not shown in drawing), helmsman’s console (Item 11), release unit (Item 7), hydrostatic actuator (Item 23), and fuel tank complete with air bottle brackets (Item 31).


Palfinger Marine (Palfinger) acquired the EL24-874 lifeboat and retrofitted the vessel with a LHR3.5M2 hook release system in 2011. Figure 6 is Drawing Number US10088, Sheet 1 of 2 showing the retrofit installation for the LHR3.5M2 hooks in an EL-24 Lifeboat. Items significant to the work performed by DNV GL include: the forward and aft hooks (Items 1 and 2), the forward and aft control cables (Items 12 and 13), helmsman’s console (not numbered in drawing), release unit (Item 11), hydrostatic actuator (Item 15), and fuel tank complete with air bottle brackets (not numbered in drawing).

The winch, fall cables, and rings for Lifeboat 6 were replaced in May 2019, approximately one month prior to the incident. After installation, the Lifeboat 6 was completely winched into the davit for storage (i.e. the forward and aft bumpers of the davit were in contact with Lifeboat 6). After the incident, the twin fall cables lengths were measured, and it was determined that the aft of Lifeboat 6 likely contacted the davit dumpers first. Figure 7 is a drawing showing the contact between Lifeboat 6 and the bumpers based on the measurements of the twin fall cables that were performed after the incident.

1.2 Summary of the Incident and Recovery Effort

On June 30, 2019, the Auger lifeboat crew was performing the quarterly launch of Lifeboat 6. As part of the launch, the lifeboat was lowered from the Auger platform using the winch and the rings were released for maneuvers in the GoM. The rings released without issue. While performing maneuvers, the forward and aft hooks were reportedly reset to the closed position and then released to the open position. After the maneuvers, the Lifeboat 6 returned to the Auger Platform, the fall cables were re-hooked, and Lifeboat 6 was lifted into the davit using a winch. Based on measurements of the twin fall cables that were performed after the incident, the aft end of Lifeboat 6 came into contact with the bumpers for the davit first.

Personnel onboard started exiting Lifeboat 6 through the man-door located on the starboard side of the vessel. With two personnel still on board, the Aft Hook released the Aft Ring and



the aft of Lifeboat 6 swung outward away from the Auger Platform, facilitating a sequence of events that resulted in Lifeboat 6 inverted in the water. Loud cracking sounds were noted by witnesses and then a loud bang. The aft of Lifeboat 6 swung outward away from the Auger Platform, putting the entirety of the load of the lifeboat and occupants on the forward hook. A rectangular section of the hull where the forward shoe attached to the forward hook broke away and the lifeboat fell towards the ocean. The forward control cable was stretched, the outer layers of the forward control cable separated from the conduit cap, and the locking shaft of the forward hook rotated to the open position releasing the lifeboat, and Lifeboat 6 fell into the GoM. The recovery effort of the subject components from Lifeboat 6 from the GoM took approximately five (5) days to complete by SOI. Once retrieved, the subject components were sent to Harvey Terminal in New Orleans, Louisiana for the causal investigation.

Figure 8 and Figure 9 are photographs showing the condition of Lifeboat 6 in Harvey Terminal after the incident, as viewed from the forward, port side and the aft, starboard side, respectively. As shown in the figures, Lifeboat 6 is raised from the shipping container to gain safe access to components. A majority of the canopy from the lifeboat was not recovered; however, a majority of the hull and the internal components of the lifeboat were recovered. Significant mechanical damage was sustained to the hull of the lifeboat. Figure 10 contains photographs showing the condition of the davit and port bumpers after the incident. The bumpers exhibit an area of contact, i.e. a witness mark, likely from Lifeboat 6. Similar witness marks were noted on the starboard bumpers in the davit. There was no reported mechanical deformation to the A-frames of the Lifeboat 6 davit. Also, SOI reported that the rings, the falls, and the winch did not exhibit significant evidence of yielding or failure.

1.3 Objective of the Investigation

The objectives of the investigation were to document the artifacts, determine the immediate cause of the aft release, and identify any contributing factors. The investigation by DNV GL is supplemental to a causal analysis being performed by SOI to determine the root cause(s) of the incident.

2.0 TECHNICAL APPROACH AND ADDITIONAL BACKGROUND

The investigation was divided into three main phases: (1) the field investigation, (2) reconstruction and function testing, and (3) examination of key components. The technical approaches are discussed below, and the results are provided in Section 3.0.



2.1 Field Investigation

DNV GL personnel performed two site visits at Harvey Terminal located in New Orleans, Louisiana to inspect and document the as-found condition of Lifeboat 6 and to assist with evidence preservation. The dates of the inspections were July 29 to August 2, 2019 for the first inspection and October 3, 2019 for the second inspection. In addition to these visits, Plastic Services Network (PSN) also performed two site visits to Harvey Terminal on October 14 and 15, 2019 and November 6, 2019. The purpose of PSN's visits were to examine the fiberglass components of Lifeboat 6 and to assist with extraction of fiberglass samples from areas of interest for further testing.


2.2 Reconstruction and Function Testing

Several subject components, discuss below, were delivered to DNV GL Laboratory in Dublin, Ohio for additional testing. A mockup of the Subject Hook Release assembly was constructed, to the extent possible, for the purposes of documenting the relative positions of the subject components and function testing the subject components. The function testing was performed using (1) all subject components from Lifeboat 6, (2) the Subject Components with an Exemplar Cable, and (3) the Subject Release Unit with an Exemplar Hook and Exemplar Cable. It should be noted that for Conditions (2) and (3), the Exemplar Cable was installed on the Subject Aft Hook and that no cable was installed on the Subject Forward Hook. In all function tests, the components were set to the as-found condition of Lifeboat 6. The results were digitally recorded and then examined.

2.3 Examination of Key Components

The following is a list of the components that were provided to DNV GL for testing and analyses:

- Hook System and associated artifacts from Lifeboat 6
 - ◆ Forward and aft hooks
 - ◆ Hydrostatic actuator
 - ◆ Forward and aft control cable
 - ◆ Hydrostatic cable
 - ◆ Release unit
- Helmsman's console from Lifeboat 6

- 
- Bottle brackets and fuel tank assembly, including attached decking, etc. from Lifeboat 6
 - Exemplar artifacts
 - ♦ A hook of the similar design, but a later revision/type approval
 - ♦ A full-length Exemplar Cable of the same design, but a later revision/type approval. The length of the Exemplar Cable was consistent with the length of the Subject Aft Cable removed from service.
 - ♦ A 12-inch length of Exemplar Cable of the same design, but a later revision/type approval
 - Lengths of wire ropes from the falls and attached lifting rings from Lifeboat 6
 - Hydrostatic and aft control cables from on Lifeboat 7 and the forward and aft control cables from Lifeboat 8¹


In the sections that follow, additional background information on the components is provided as well as the technical approach for testing and analyses of the components.

2.3.1 Release Unit – Background Information and Examination

Figure 11 contains drawings of the release unit showing the different components of the system. The hydrostat lock and safety lock are in the closed position in the drawings. To open (release) the hook, the handle of the hydrostat lock, visible from the exterior of the release unit, must move upward while the engaging portion of the hydrostatic lock, not visible from the exterior of the release unit, moves downward out of the way of the safety lock. Then, the handle of the safety lock, visible from the exterior of the release unit, must move upward to allow rotation of the handle on the release unit.

When the lifeboat is waterborne, the inner member of the control cable connected to the hydrostatic lock and the hydrostatic actuator moves upward, moving the engaging end of the hydrostat lock downward and out of the closed position. Access to the hydrostat lock is not possible without removing the protective covers located in the front or back of the release unit. Therefore, when the hooks are set, the release handle is in the closed position, and the protective covers are in place, the hooks should not release when the boat is not waterborne, the release and hydrostatic actuator are properly functioning, and the control cables for the aft and forward hooks are not compromised.

¹ Lifeboat 7 and Lifeboat 8 were in-service on the Auger Platform.



DNV GL visually examined the Subject Release Unit to document the as-received condition and for evidence of mechanical damage.

2.3.2 Hooks –Background Information and Examination

Figure 12 is a portion of Drawing Number US10088-Rev B, Sheet 2 of 2 showing the detail of the installation of the aft and forward LHR3.5M2 hooks using LHR shoes. The LHR shoes are connected to the hull and the hooks are connected to the LHR shoes with a lifting pin. The hooks pass through the canopy above the LHR shoe and are visible from the exterior of the lifeboat.


Figure 13 is a drawing from Palfinger Document F10927 showing the details of components of the LHR3.5M2 hook with the cover for the locking shaft and control cable removed. The LHR3.5M2 hook is comprised of a housing with a hook, keeper, locking pawl (not shown), and locking shaft. A clevis threads to the end rod of the control cable and then connects to the locking shaft using a pin that is held in place with a cotter pin (not shown). The orientation of the locking shaft in the drawing is consistent with a closed position.

Figure 14 contains drawings from Palfinger Document F10927 showing a cross-sectional view of the LHR3.5M2 hook when in the (a) closed position and (b) open position. The roller of the hook rests in contact with the locking shaft when in the closed position. For the hook to open, the locking shaft should rotate counterclockwise, as viewed from the locking arm side of the locking shaft, around axis "A." For this to occur, the inner member of the control cable is pulled downward, pulling the clevis down and rotating the locking shaft into the open position. Note that the external layers of the control cable are held in place with bulkhead nuts that fix the control cable to a horizontal plate on the hook. Only the inner member of the control cable is attached to the clevis and translates; the outer layers of the control cable do not move. The multiple layers of the cable are discussed in more detail in Section 2.3.4. The flat of the locking shaft then rotates into a position allowing the roller of the hook to pass through. Under load, the hook rotates around axis "B," which is the main shaft. The locking pawl rotates into position around axis "C," preventing the locking shaft from rotating clockwise, back into the closed position if the hook is not in the rest position.

DNV GL visually inspected and laser scanned the Subject Aft Hook to document the condition of the aforementioned components. An Exemplar Hook was also laser scanned for comparison to the Subject Aft Hook.

2.3.3 Fall Cables and Rings – Background Information and Examination

As shown in Figure 10, the Subject Aft and Forward Fall Cables were located in the davit and attached to the winch. The Subject Aft and Forward Fall Cables were cut in the field



using a cold cutting technique, packaged and shipped to DNV GL for visual examination and laser scanning.

2.3.4 Control Cables – Background Information and Examination


Figure 15 is a drawing from Palfinger Document F10927 combined with an image titled “General-structure-of-push-pull-cable” showing the detail of components for the control cables. The end of the control cable is comprised of the end rod that travels inside of a support tube. An end rod jam nut is threaded onto the end rod. The annular space of the end rod and support tube junction is sealed with a wiper seal to prevent moisture from entering. The end rod has one end that is threaded, and the other end connects to the inner member of the control cable. The threaded portion of the end rod connects to a clevis that is pinned to the actuating portion of a release unit or LHR hook. The support tube is connected to the grooved conduit cap (herein referred to as conduit cap), which has a threaded portion that is used to adjust the position of the control cable using the bulkhead nuts. At the junction of the support tube and the conduit cap, a swivel seal is present, which prevents moisture from entering the connection.

Within the conduit cap, the conduit of the control cable is held in place. The conduit of the control cable is comprised of several layers including (external layer to internal layer): the plastic cover (herein referred to as cover), the strand and binder wire layer (herein referred to as wire layer), the plastic liner (herein referred to as liner), and the inner member. The plastic cover is comprised of low-density polyethylene (LDPE) and surrounds the wire layer to prevent corrosion. The wire layer is comprised of a single layer of carbon steel, strand wires that are held in place with a carbon steel, binder wire. The liner is comprised of high-density polyethylene (HDPE) and within the liner is the inner member. The inner member is comprised of 19 carbon steel, stranded wires and a carbon steel, flat binder wire that is covered with a thin nylon layer.

The inner member translates within the liner when the end rod of the control cable is pushed or pulled by actuating the release unit to the open or closed positions. The translation of the inner member is restricted by the distance the end rod can translate within the support tube. The maximum distance of translation was measured to be 4.16 inches on the Exemplar Cable.²

The Subject Aft Cable was visually examined in the field and in the laboratory to document the as-found condition. The Subject Aft Cable was dissected in the laboratory for detailed examination. Testing of the cover, liner, and inner member of the Subject Aft Cable included

2 The distance was measured using calibrated calipers and the reported value is the distance between the top of the wiper seal to the first thread on the end rod with the end rod fully extended out of the support tube.



some combination of the following: Shore D hardness testing, light microscopy, scanning electron microscopy (SEM), energy dispersive spectroscopy (EDS) in the SEM, Fourier-transform infrared spectroscopy (FTIR), chemical analyses, differential scanning calorimetry (DSC), thermogravimetric analyses (TGA), and / or mechanical testing. Testing of the wire layer included the following: light microscopy, SEM, EDS in the SEM, x-ray diffraction (XRD), metallography, elemental mapping in the SEM, and chemical analyses.

Control cables were removed from Lifeboat 7 and Lifeboat 8 and were provided to DNV GL for visual examination of the as-found condition and dissection of the layers of the control cable. These control cables were provided because the damage to the cables was consistent with the observed damage to the Subject Aft Cable from Lifeboat 6. Note that Lifeboat 7 and Lifeboat 8 were also in-service on Auger. The results were compared with the findings from Lifeboat 6 for commonalities and differences.

An Exemplar Cable, 12-inches in length and a 12-inch length of the Subject Aft Cable were used for mechanical testing. The outer layers of the control cables were pulled to failure and the failure loads and total extension were recorded.


Load testing was performed in a test rig using the Exemplar Cable, the Exemplar D-Ring, the Exemplar Hook, and the Subject Release Unit. Three scenarios were tested to evaluate a tip or point load, whereby the point of the Exemplar Hook was placed on the flat of the Exemplar Ring (rather than properly seated in the intrados of the hook). For each scenario, the clevises and bulkhead nuts were set to the as-found condition of the subject components and a load equivalent to half the weight of Lifeboat 6 at the time of the incident was applied.

In addition to the load testing, the clevises and the bulkhead nuts were adjusted to the most open position for the locking shaft and a load equivalent to one-half the weight³ of Lifeboat 6 at the time of the incident was applied. The pin holding the Exemplar Cable in place at the release unit was removed under load and an upward force was applied to the control cable to estimate the load required to move the locking shaft into the open position under load.

2.3.5 Fiberglass Hull and Support Structure – Background Information and Examination

The hull and recovered fiberglass components from Lifeboat 6 were visually examined in the field to document the as-found condition. Areas of interest were identified by PSN and

3 One-half the weight of the lifeboat was used as testing was performed using only one hook. The weight of the lifeboat would have been split evenly between the forward and aft hooks.



panels were extracted from the interior and exterior of Lifeboat 6. Testing of the fiberglass panels included the following: SEM, mechanical testing, and finite element analysis (FEA). Figure 16 contains schematics of a FEA model showing the nominal wall thicknesses of the fiberglass components of Lifeboat 6 as viewed from (a) the interior and (b) the exterior. The model was produced by PSN using physical measurements of extracted panels and details from original manufacturer drawings. The fiberglass was modeled with plate elements color-coded to indicate the thickness attributed to the element. The colors indicate the following: green is 0.250-inch, pink is 0.375-inch, purple is 0.186-inch, and brown is 0.750-inch wall thickness. This model was used to simulate the loads imparted on Lifeboat 6 when winched into the davit on Auger.

3.0 RESULTS

3.1 Field Investigation


During the July 29 through August 2, 2019 inspection, DNV GL documented the as-found condition of the subject components and witnessed testing performed by SOI on a reconstruction of the hook system of Lifeboat 6 using exemplar components. A key part of that site visit was to document the condition of the subject hook system. During the October 3, 2019 inspection, DNV GL documented the fiberglass components from the hull and interior of Lifeboat 6 in detail.

Personnel from PSN traveled to Harvey Terminal on October 14 and 15, 2019 to be briefed on the incident and to visually inspect Lifeboat 6. PSN returned to Harvey Terminal on November 6, 2019 to provide guidance on sample extraction of fiberglass and foam insulation from Lifeboat 6 for additional testing and analysis.

3.1.1 Inspection at Harvey Terminal – July 29 through August 2, 2019

Figure 17 contains photographs showing the condition of Lifeboat 6 as viewed from the (a) forward and (b) aft at Harvey Terminal following recovery and staging by SOI. The hull of the vessel was inverted and resting on I-beams supported by cribbing. Clamps were placed at the starboard and port side of the hull of Lifeboat 6 and fixed to the I-beams to prevent movement of the hull in those directions. Two gantry cranes were positioned at the starboard and port. Clamps attached to the falls of the crane were fixed to the I-beams to assist with the support of the weight of the hull. The recovered subject components from the interior of the lifeboat were laying in the shipping container in the positions where they landed during the recovery of the boat.

Figure 18 contains photographs showing the aft of Lifeboat 6 and the as-found condition of the Subject Aft Hook as viewed from (a) the starboard side, (b) the stern, and (c) the port




side. The locking shaft of the Subject Aft Hook was in the fully open position as indicated by the position indicator on the port side. Figure 19 is a photograph showing a failure in the outer layers of the Subject Aft Cable. The cover, the wire layer, and the liner had failed. The liner layer appears elongated, exposing the inner member where no significant damage was noted. Figure 20 contains photographs of the Subject Aft Hook showing the as-found condition of the threaded connections (a) at the clevis and (b) at the bulkhead nuts; the locations of the clevis and bulkhead nuts are shown in Figure 14. The number of exposed threads at the clevis were four (4) threads on the top of the nut and six (6) threads on the bottom of the nut. The number of exposed threads at the bulkhead nuts was five (5) threads.

Figure 21 contain photographs showing (a) the bow of Lifeboat 6 and (b) the as-received condition of the Subject Forward Hook at Harvey Terminal. The hook was rotated to the open position; however, the locking shaft was in the closed position because the control cable was unthreaded from the clevis, allowing for the locking shaft to freely rotate independent of cable/clevis position. A rectangular hull piece is missing from the bow of Lifeboat 6. This piece is attached to the shoe of the Subject Forward Hook. A split in the keel is also visible in Figure 21 (a). The split arrests approximately halfway along the length of the boat. As shown in the image, the hook was open and free to rotate.

Figure 22 is a photograph of the Subject Forward Cable showing a failure at the conduit cap. The failure exposed the inner member of the Subject Forward Cable. The conduit appears to have separated and is in relatively good condition at the conduit cap. Significant mechanical damage to the individual layers was not observed. Figure 23 contains photographs of the Subject Forward Hook showing the as-found condition of the threaded connections (a) at the clevis and (b) at the bulkhead nuts; the locations of the clevis and bulkhead nuts are shown in the embedded schematic. The connection at the clevis had fully unthreaded, such that the inner member was no longer connected with the locking shaft. This likely occurred post incident and prior to recovery due to the movement of the components within the GoM. This allowed the locking shaft to rotate into the fully closed position due to the force applied by the torsion spring. The number of exposed threads at the bulkhead nuts was five (5) threads.

Figure 24 is a photograph showing the as-found condition of the internal subject components of Lifeboat 6. The release unit, the fuel tank with air bottle brackets, engine with engine cradle, part of the helmsman's console, and the control cables for the hook system were recovered. Figure 25 is a photograph showing the as-found condition of the safety lock and the hydrostatic lock on the Subject Release Unit of Lifeboat 6. The hydrostatic lock appeared to be in the open position and the safety lock was in the closed position. A fragment of the protective cover of the hydrostat lock was visible. Figure 26




contains a photograph showing the as-found condition of the Subject Aft Cable and Subject Forward Cable clevises at the Subject Release Unit of Lifeboat 6. The protective covering to the Subject Release Unit was intact. From what is visible, the threaded rods for the Subject Aft and Forward Cables were fully threaded into the clevises. The pins for the clevises were intact and the cotter pins were in place. Figure 27 is a photograph showing the as-found condition of the Subject Aft Cable and Subject Forward Cable at the bulkhead nuts of the Release Unit of Lifeboat 6. The bulkhead nuts were threaded so that, for both control cables, seven (7) threads were visible outside the housing of the release unit. Figure 28 is a photograph of the Subject Release Unit showing the as-found condition of the bulkhead nuts attaching the Subject Hydrostatic Cable to the Subject Release Unit; six (6) threads were visible at the bulkhead nuts. No evidence of significant damage to the housing, handle, plate, clevises, pins, bulkhead nuts, or other internal components to the release unit was visible. Figure 29 is a photograph showing the as-found condition of the hydrostatic actuator of Lifeboat 6. The hydrostatic actuator had partially been pulled into Lifeboat 6; however, its external components appeared undamaged.

In preparation for shipment of select components to DNV GL the following was performed. The bolts holding the hydrostatic actuator in place were unthreaded and the hydrostatic actuator was placed on the deck. Cuts were made in the fiberglass hull adjacent to the Subject Aft Hook to remove the hook without unthreading any components. The fuel tank⁴ with air bottle brackets, Subject Release Unit, Subject Helmsman's Console, Subject Hydrostat, Subject Aft Cable, Subject Forward Cable, Subject Aft Hook, and Subject Forward Hook were wrapped in bubble wrap and fixed with packaging tape. A pallet with a cradle was constructed by SOI to house the fuel tank with air bottle brackets. The remaining components were stacked on the cradle in preparation for shipment. The pallet with the evidence was placed into a shipping container, fixed to the sides of the container using ratchet straps and then wrapped in green plastic wrap, as shown in Figure 30. Figure 31 contains photograph of the key components of Lifeboat 6 delivered to DNV GL's warehouse on August 6, 2019. The pallet did not shift in transit and the wrappings were in good condition.

In addition to the visual inspection and evidence preservation performed by DNV GL at Harvey Terminal described above, DNV GL witnessed testing performed by SOI on a mockup of Lifeboat 6 that included Exemplar Cables, Exemplar Hooks, and an Exemplar Release Unit. Reportedly, SOI set the bulkhead nuts and clevises of the components to the as-found condition of the bulkhead nuts and clevises on Lifeboat 6. To replicate the failure identified in the Subject Aft Cable, the cover, the wire layer, and the liner of the Exemplar Cable were

4 The fuel tank was emptied prior to shipment.



cut. It should be noted that, in the as-found condition, the Exemplar Release Unit would not lock in the open position. In the ideal condition, per Palfinger experts that were onsite, the release handle of the Exemplar Release Unit should lock in both the open and closed positions. Initially, the cover and conduit were cut with no discernable change to the control cable or locking shaft; however, when the liner was cut, a separation immediately formed exposing the inner member of the Exemplar Cable, as shown in Figure 32. This separation resulted in the locking shaft rotating to a slightly more open position. When the Exemplar Release Unit was placed into the open position, the outer layers of the Exemplar Cable came back together, eliminating the separation exposing the inner member, as shown in Figure 33. Note that no load was being applied to the Exemplar Hook during these tests. The process of opening and closing of the Exemplar Hook was repeated several times, the results of which are summarized in Figure 34. The separation exposing the inner member ranged from 2.16 inches to 3.35 inches. In all tests when the Exemplar Release Unit was in the closed position, the locking shaft was at a position preventing opening of the hook, despite the additional rotation of the locking shaft from cutting the liner. In all tests when the Exemplar Release Unit was in the open position, the locking shaft was open allowing the hook to release and rotate freely.


3.1.1.1 Laser Scanning

Figure 35 shows the laser scan of Lifeboat 6, performed at Harvey Terminal after recovery. Lifeboat 6 was laser scanned to document the condition of the interior and exterior of the lifeboat prior to any destructive analyses. The laser scanning was completed by using two scanning devices with one device designed for close range detail and the other for long range data capture. The close-range device used was a FARO Edge ScanArm™ (usable range less than three feet between target and scanner), which can be described as a laser line probe (herein referred to as FARO Edge) integrated to the end of the FARO Edge ScanArm™ measurement arm. The long-range device used was a FARO Focus S70™ (herein referred to as FARO Focus), which has a usable range up to 230 ft.

3.1.2 Inspection at Harvey Terminal – October 3, 2019

During the October visit, DNV GL personnel documented the exterior and interior of the hull of Lifeboat 6 with photography prior to removal of panels of fiberglass for destructive analyses at PSN and DNV GL. The panels were selected by non-metallics experts from PSN for extraction.

Figure 36 contains photographs showing (a) the starboard of Lifeboat 6 and (b) the reference location for measurements. The reference location for the exterior was placed at the aft of the vessel. Figure 37 contains photographs showing the locations of cracks of interest at (a) the aft shoe plate and (b) 11.4 feet from the reference location; locations



shown in Figure 36. In Figure 37 (a), a crack emanating from a bolt hole coincides with an area of inward mechanical deformation of the aft shoe plate. The bend in the shoe plate on the exterior of the hull is adjacent to the termination of the lift shoe on the interior of the hull. The deformation at the plate is consistent with a vertical load in the upward direction, such as overload from being pulled into the davit. Shell indicated that the deformation of the plate was present prior to the incident; however, the crack emanating from the bolt hole may have been related to the incident. In Figure 37 (b), a crack in the hull along the entirety of the starboard side is visible. It is approximately 1 foot away from a crack visible in the keel.

Figure 38 contains photographs showing (a) the reference location for measurements on the interior of the hull and (b) the corresponding location on the engine and engine cradle. A fracture in the hull at the location where the propeller shaft penetrated the exterior hull is noted in Figure 38 (a). Also, blue paint from the bottom of the engine appears to have flaked off in Figure 38 (b).

Figure 39 contains photographs showing (a) an indentation at the hull interior 2.25 feet from the reference location and (b) the corresponding location on the engine and engine cradle. The indentation at the interior was likely due to contact with the edge of the engine cradle at the location shown.

Figure 40 contains photographs showing (a) a missing section of the hull interior 5.8 feet to 6.4 feet from the reference location and (b) the corresponding location on the engine and engine cradle. The corresponding positions of the holes in the foam are shown in the photographs. A steel plate embedded in the foam and beneath the fiberglass interior was used to mount the engine cradle. The size and position of the steel plate are such that the plate was supported by the bottom of the hull. Additionally, a blue paint chip is visible on what would be the bottom of the lifeboat, 5.45 feet from the reference location. The blue paint chip was not well adhered to the surface. Additional blue paint chips were identified in the keel of the lifeboat near the aft end (i.e. reference end). These likely originated from the bottom of the engine block where blue paint was flaked off. Corrosion of the engine block resulted in the blue paint peeling and the water typically present in the keel distributed the blue paint chips at various areas within the bottom of the lifeboat.

Figure 41 is a photograph showing the detail of the holes in the foam and damage / scoring marks adjacent to each of the holes. All damage is in the same direction, toward the canopy. This indicates that the engine cradle moved towards the canopy of Lifeboat 6.




Figure 42 contains photographs showing a transverse crack in the keel of the hull interior located 7.6 feet from the reference location. The fracture in the keel is visible in Figure 37 (b), indicating that it is completely through wall.

3.1.3 Inspection at Harvey Terminal – PSN Visits

Figure 43 is a schematic showing the approximate locations of each 24-inch by 24-inch panel extracted from the outer and inner hull of Lifeboat 6. Samples BSO-1, ASO-1, BPO-1, and APO-1 were extracted from the outer hull. Samples AP-2, BP-1, and BS-1 were extracted from the interior seating area. In addition to these samples, foam samples were removed from the interior of Lifeboat 6. The foam and fiberglass samples were used for mechanical and analytical testing, and chemical analyses.

Figure 44 through Figure 46 are three dimensional representations of the approximate locations of Samples C-1, C-2, and C-3. Sample C-1 contained a crack located at the interior of the boat at the interface of the starboard side and fiberglass-engine mount. Sample C-2 contained a crack located at the exterior of the hull on the keel of the boat. The crack propagated through the thickness of the keel. Sample C-3 contained a crack located at the exterior of the hull on the starboard side. The crack ran from the hull-canopy interface towards the keel. These samples were selected for additional analyses to determine if they were primary to the incident (i.e. occurred prior to impact with the water).


The foam and fiberglass samples were removed using a reciprocating saw. The foam samples were approximately 18 inches by 18 inches in size and the fiberglass samples were approximately 24 inches by 24 inches in size.

3.1.4 Auger Lifeboat 6 Davit

SOI inspected the davit of Lifeboat 6 and recorded the lengths of the fall cables. The replacement of the winch, fall cables, and the Rings had occurred approximately one month prior to the incident. After measurements were performed by SOI, it was determined that a gap of approximately 12.5 inches was present between the forward bumpers and Lifeboat 6 when the aft bumpers came in contact with Lifeboat 6. During the time between the replacements and the incident, it was reported that the forward and the aft of Lifeboat 6 were in contact with the bumpers of the davit.

3.2 Reconstruction

The objective of reconstruction was to reassemble the subject components, to the extent possible, to positions within the lifeboat prior to the incident. The reconstruction was performed at DNV GL and documented with photography and laser scanning for comparison



to a similar lifeboat of the same make and model located in Lafayette, Louisiana and / or 3D models, if available.

3.2.1 Description of Reconstruction Process

The relative distances and the heights of the components used in the reconstruction were set using Drawing Number 7.3 EL-215-Rev A, shown in Figure 5. The components used in the reconstruction are highlighted with yellow in the figure. The reconstruction is comprised of the hooks that were removed from the forward and aft of Lifeboat 6 (Items 8), as well as the corresponding control cables (not shown in the drawing), helmsman's console (Item 11), Subject Release Unit (Item 7), hydrostatic actuator (Item 23), and fuel tank complete with air bottle brackets (Item 31).

Figure 47 is a photograph of the completed reconstruction of the relevant components from Lifeboat 6. The fuel tank complete with air bottle brackets, helmsman's console, and release unit were supported using a pallet and lumber. Wooden stands were built for the forward and aft hooks. These stands were adjusted to the appropriate heights using bottle jacks and then secured in place using short lengths of lumber. The stands holding the components were then adjusted to the appropriate distances from one another and white paint was used to mark their locations on the floor.


Figure 48 is a laser scan showing the completed reconstruction of the relevant components from Lifeboat 6. The laser scan was compared to the positions of the components from a laser scan of a lifeboat of similar vintage and construction located in Lafayette, Louisiana. The differences between the scans were minimal. Reportedly, the Subject Aft Cable was routed down the starboard side of the cableway in the bottle rack and wire guide. The Subject Aft Cable then crossed to the port side of the bilge at the front of the engine, not the starboard side as shown in the laser scan. The Subject Aft Cable crossed back to the starboard side of the bilge area behind the reduction gear and ran to the hook along the starboard side of the propeller tunnel.

3.2.2 Function Testing

The objective of the functional testing was to determine if the subject components performed as-intended when tested in the as-found conditions. Testing was also conducted using an Exemplar Cable.

3.2.2.1 Subject Hook, Subject Cable, and Subject Release Unit

Figure 49 is a screenshot of compiled digital recordings from a function test performed using the Subject Aft Hook, the Subject Aft Cable, and the Subject Release Unit. Four views are shown: (a) the port side of the Subject Aft Hook, (b) the break in the Subject Aft Cable located near the Subject Release Unit, (c) the starboard side of the Subject Aft Hook, and



(d) the forward side of the Subject Release Unit (note this view is rotated 90° clockwise from its normal orientation).

It is worth noting that the function test using subject components resulted in a unique condition. As shown, the Subject Release Unit is in the closed position; however, the locking shaft of the Subject Aft Hook is in the fully open position. To operate as designed, when the Subject Release Unit is in the closed position, the locking shaft of the Subject Aft Hook should be in the closed position as well. The orientation of the locking shaft was noted on the starboard side of the locking shaft “as received at DNV GL.”

To perform the function testing of the subject components, the releases of the hydrostatic and safety locks were placed in the open position and the release handle of the release unit was pulled towards the open position. For the condition described, the release handle for the release unit would not move, likely due to the bent and deformed subject control cables near the conduit caps at the release unit (see Figure 27). No changes to the position of the components were noted.

3.2.2.2 Subject Hook, Exemplar Cable, and Subject Release Unit

Figure 50 and Figure 51 are screenshots of compiled digital recordings from a function test performed using the Subject Aft Hook, the Exemplar Cable, and the Subject Release Unit before and after, respectively, moving the release handle of the Subject Release Unit. Three views are shown: (a) starboard side of the Subject Aft Hook, (b) the port side of the Subject Aft Hook, and (c) the forward side of the Subject Release Unit. The Exemplar Cable was installed using the same positioning / nut spacing as the Subject Aft Cable.

To perform the function testing of the Subject Aft Hook, the Exemplar Cable, and the Subject Release Unit, the hydrostatic and safety locks were placed in the open position and the release handle of the Subject Release Unit was pulled towards the open position. For the condition described, the release handle for the Subject Release Unit moved freely. The inner member of the Exemplar Cable moved upward at the Subject Release Unit and downward at the Subject Aft Hook. The locking shaft of the Exemplar Hook rotated 94.4°, when viewing from the starboard side. The rotation of the locking shaft in this manner moved the flat of the locking shaft into a position that allowed the hook to open. The orientation of the indicator on the port side of the locking shaft after the function testing was consistent with the orientation of the indicator on the port side of the locking shaft as received at DNV GL. It should be noted that the release handle of the Subject Release Unit did not lock in the open position. Though atypical, the release handle not locking into the open position did not prevent the hooks from being reset and locked in the closed position.

3.2.2.3 Exemplar Hook, Exemplar Aft Cable, and Subject Release Unit

Figure 52 and Figure 53 are screenshots of compiled digital recordings from a function test performed using the Exemplar Hook, the Exemplar Cable, and the Subject Release Unit before and after, respectively, moving the release handle of the Subject Release Unit. Three views are shown: (a) starboard side of the Subject Aft Hook, (b) the port side of the Subject Aft Hook, and (c) the forward side of the Subject Release Unit.

The function testing was performed in the same manner as described in Section 3.2.2.2 and the results were comparable. The locking shaft of the Exemplar Hook rotated 89.3°, slightly less than the previous setup. Again, it was noted that the release handle of the Subject Release Unit did not lock in the open position, which is atypical.

3.3 Examination of Key Components

3.3.1 Subject Release Unit

3.3.1.1 Visual Inspection

Figure 54 contains photographs of the Subject Release Unit at DNV GL showing the as-found condition of the clevises and bulkhead nuts, after removing the protective coverings from the Subject Release Unit. The Subject Release Unit was in the closed position. No end rod jam nuts were present. The clevises for the forward and aft control cables were nearly fully threaded onto the end rod of the control cable with seven (7) threads exposed on each. The bulkhead nuts were threaded so that one (1) thread was visible within the housing of the Subject Release Unit (not visible in photographs) and seven (7) threads were visible outside the housing of the Subject Release Unit. This positioned the height of the control cable at its lowest possible position within the housing. Figure 55 contains photographs of the Subject Release Unit at DNV GL showing the as-found condition of the hydrostat cable and end rod jam nuts, after removing the protective coverings. The end rod jam nuts attaching the end rod to the hydrostat cable are partially threaded with five (5) threads exposed on the top side and six (6) threads exposed on the bottom side. No evidence of significant damage to the housing, handle, plate, clevises, pins, bulkhead nuts, end rod jam nuts, or other internal components to the Subject Release Unit was visible. The hydrostatic and safety locks operated freely.

3.3.2 Hooks

The investigation includes detailed examination of the Subject Aft Hook and the Exemplar Hook. Where appropriate, examination of the Subject Forward Hook was also performed for comparison.

3.3.2.1 Subject Hooks


3.3.2.1.1 Visual Inspection – Subject Aft Hook

Figure 56 contains photographs of the Subject Aft Hook with the locking shaft cover removed, viewed from (a) the starboard side and (b) the port side. The locking shaft of the Subject Aft Hook was in the fully open position, as-found, as indicated by the position of the locking shaft arm visible on the starboard view and the position indicator on the port side. The keeper and hook rotated freely. The locking shaft could not be moved due to damage associated with the Subject Aft Cable. Figure 57 contains photographs showing the as-found condition of the threaded connections of the Subject Aft Hook (a) at the clevis and (b) at the bulkhead nuts; the location of the clevis and bulkhead nuts are shown in Figure 14. The number of exposed threads at the clevis were four (4) threads on top of the end rod jam nut and six (6) threads on bottom of the end rod jam nut. Five (5) threads were exposed at the bulkhead nuts. The Subject Aft hook was disassembled so that the hook, keeper, and locking shaft could be individually examined and documented.

Figure 58 contains photographs of the hook from the Subject Aft Hook assembly showing the (a) starboard side and (b) port side, after disassembly. The location of the roller for the hook is partially visible in the photographs. A set screw holds the pin of the roller in place. The roller for the Subject Aft Hook did rotate, but with some effort.

Figure 59 contains photographs showing witness marks identified on the hook from the Subject Aft Hook at (a) the inside bend of the hook, (b) the edge of the bend as viewed from the port side, and (c) the point of the hook; image locations and viewing directions shown in Figure 58 (a) and (b). Witness marks are visible at the inside bend of the hook and the starboard side of the hook point, as shown in Figure 59 (a). Some scratch-like witness marks are also visible near the hook point. Red paint is also visible at the inside of the hook, likely from transfer of paint from the rings. Discoloration is visible on the inside bend of the hook, which is likely from superficial corrosion attack. Witness marks on the edge of port side of the hook are visible in Figure 59 (b). Orange paint is also visible on the port side of the hook from the Subject Aft Hook. The Orange paint is like from the coating of the lifeboat. A witness mark is visible on the port side of the hook point in Figure 59 (c). Scratch-like witness marks are visible on the port side of the hook point.

Figure 60 contains photographs showing the Subject Aft Hook after removing the set screw, pin, and roller, as well as the witness marks present on the contact surface of the roller. The roller contained a white, plastic bushing. The pin is solid and showed no evidence of plastic deformation. The white plastic bushing has some wear, which may account for the difficulty in rotating the roller when assembled. On the roller, linear witness marks that are oriented left to right in the photograph are visible near the 90° and 270° orientations. Witness marks



are also visible at the 180° orientation and appear to be more indentation-like in appearance. The width of the roller is 0.579 inches (average of four measurements taken at 0°, 90°, 180°, and 270° orientations).

Figure 61 contains photographs of the locking shaft from the Subject Aft Hook showing the (a) round side and (b) the flat, after disassembly. There is no evidence of plastic deformation at the arm of the locking shaft. Figure 62 is a photograph of the locking shaft from the Subject Aft Hook showing the mechanical damage on the edge of the round and the flat of the locking shaft. The mechanical damage and witness mark are 0.571 inches and 0.550 inches in width, respectively. These values are consistent with the width of the roller from the Subject Aft Hook.

Figure 63 is a photograph of the locking shaft from the Subject Aft Hook showing an area with corrosion attack on the round of the locking shaft. The width of the area of corrosion attack is 0.618 inches, which is consistent with the width of the roller from the hook. The presence of corrosion at this location (in comparison to other locations on the locking shaft), suggests that the roller was in contact at this location for extended periods of time, such as storage in the davit.

Figure 64 is a photograph of the locking shaft from the Subject Forward and Aft Hooks comparing the areas of corrosion attack on the round of the locking shaft and comparing the overall geometry. As shown, the areas of corrosion for the locking shafts from the Subject Aft Hook and Subject Forward Hook are 36° and 39°, respectively, from the flat of the locking shaft. With respect to the geometry, a slight variation in the orientation of the flats of the locking shafts is visible. This may be due to the manufacturing. The arm and the body of the locking shaft are keyed. The arm of the locking shaft is placed into the body of the locking shaft and welded. There is likely variability in the orientations in the flat as a result of this manufacturing process.

Figure 65 contains photographs of the keeper from the Subject Aft Hook showing the (a) forward side and (b) aft side, after disassembly. Red paint is visible on the forward side of the keeper, likely from transfer of red paint from the ring. There is no evidence of witness marks in the vicinity of the red paint. Figure 66 contains photographs of the keeper from the Subject Aft Hook showing (a) a possible witness mark and (b) red paint; locations shown in Figure 65. The possible witness mark appears to be in an area where some additional material is present. Red paint is visible on the aft side of the keeper, likely from transfer of the red paint from the ring.

3.3.2.1.1.1 CONTACT WITH THE HOOK ROLLER AND LOCKING SHAFT

Figure 67 contains photographs of the locking shaft from the Subject Aft Hook installed (a) in the Subject Aft Hook and (b) installed on the Exemplar Hook with the clevises and bulkhead nuts set to the as-found condition of the subject components. In both cases, the Subject Release Unit was in the closed position and the Exemplar Cable was used. No load was applied.

The blue markings were produced by placing articulating paper between the hook roller and locking shaft contact location. The green line is the contact location between the hook roller and the locking shaft when the arm of the locking shaft is placed in the fully closed position (i.e. the arm of the locking shaft is in contact with the standoff for the locking shaft cover, see Figure 52 (a)). The degrees of rotation from the green line to the flat of the locking shaft are 60°. A yellow line is located between the green and red lines. The yellow line indicates the contact location between the hook roller and locking shaft when the release unit is closed, but the locking shaft arm is rotated as far as possible towards the open orientation. This was of interest as it was noted that this situation occurred when the Subject Aft Hook was released to the open position and then reset (i.e. there is some travel in the control cable possible that is due to the design of the release handle for the release unit even though the Subject Release Unit is in the locked position). The degrees of rotation from the yellow line to the flat of the locking shaft are 42°. The red line is consistent with the area of significant corrosion and wear, which suggests that, for a portion of the service history, the hook roller and locking shaft were in contact at this location. The degrees of rotation from the red line to the flat of the locking shaft are 36°.

The position of the red line relative to the green and yellow line may have been created in two possible ways: (1) under load, the location of contact between the hook roller and the locking shaft rotates to a more open position or (2) the separation in the conduit of the Subject Aft Cable.

3.3.2.1.2 Scanning Electron Microscopy – Subject Aft Hook

Figure 68 contains SEM images showing details for the area of corrosion denoting the contact location between the roller of the hook and locking shaft from the Subject Aft Hook. The area exhibits evidence of two different morphologies; smearing / abrasive wear morphology and a flattened / contact morphology. Some corrosion attack can also be seen in the figure. Figure 69 contains SEM images showing mechanical damage near the transition to the flat of the locking shaft from the Subject Aft Hook. The area of damage is about 20 mils in width and associated with either mechanical damage or wear.

3.3.2.1.3 Visual Inspection – Subject Forward Hook




Figure 70 contains photographs of the Subject Forward Hook with the locking shaft cover removed, viewed from (a) the starboard side and (b) the port side. As received at DNV GL, the locking shaft of the Subject Forward Hook was in the fully open position as indicated by the position of the locking shaft arm visible on the starboard view and the position indicator on the starboard side. Note that this differs from the as-found condition at recovery and Harvey Terminal, where the locking shaft was in the fully closed position. The keeper and hook rotated freely. The locking shaft could be moved freely since the clevis was unthreaded from the Subject Forward Cable. The Subject Forward Hook was disassembled so that the hook, keeper, and locking shaft could be individually examined and documented.

Figure 71 contains photographs of the hook from the Subject Forward Hook showing the (a) starboard side and (b) port side, after disassembly. The location of the roller for the hook is partially visible in the photographs. As with the Subject Aft Hook, a set screw holds the pin of the roller in place.

Figure 72 contains photographs showing the details of witness marks identified on the hook from the Subject Forward Hook at (a) the inside bend of the hook, (b) the edge of the bend as viewed from the port side, and (c) the point of the hook; image locations and viewing directions shown in Figure 71 (a) and (b). Witness marks are visible at the inside bend of the hook, as shown in Figure 72 (a). Red paint is also visible at the inside of the hook, likely from transfer of paint from the rings. Discoloration is visible on the inside bend of the hook, which is likely from superficial corrosion attack. No witness marks are visible on the edge of the port side of the hook, but some discoloration from superficial corrosion attack is visible (see Figure 72 (b)). A scratch-like witness mark is visible on the starboard side of the hook point in Figure 72 (c).

Figure 73 contains photographs of the locking shaft from the Subject Forward Hook showing the (a) round side and (b) the flat, after disassembly. There is no evidence of plastic deformation at the arm of the locking shaft. Figure 74 is a photograph of the locking shaft from the Subject Forward Hook showing a witness mark, 0.567 inches in width, on the flat of the locking shaft. This value is consistent with the width of the roller from the hook. Compared to the Subject Aft Hook, the mechanical damage at the round is absent on the locking shaft from the Subject Forward Hook.

Figure 75 is a photograph of the locking shaft from the Subject Forward Hook showing an area with corrosion attack on the round of the locking shaft. The width of the area of corrosion attack is 0.604 inches, which is consistent with the width of the roller from the hook. Similar to the Subject Aft Hook, this area of corrosion suggests that the roller was in contact at this location for extended periods of time, such as storage in the davit.




Figure 76 contains photographs of the keeper from the Subject Forward Hook showing the (a) forward side and (b) aft side, after disassembly. Red paint is visible on the forward and aft sides of the keeper, likely from transfer of the red paint from the ring. There is no evidence of witness marks in the vicinity of the red paint. There is also some discoloration on the forward side of the keeper, likely from superficial corrosion.

The primary difference between the Subject Aft Hook and the Subject Forward Hook was the mechanical damage to the round of the locking shaft from the Subject Aft Hook (see Figure 62). Small differences in the manner of construction were also noted (see Figure 64). Otherwise, comparable damage from service was identified on the other components.

3.3.2.1.4 Laser Scanning

The hook, keeper, locking shaft and housing of the Subject Aft Hook were scanned using the FARO Edge after disassembly, as shown in Figure 77. The components were aligned in 3D space by using geometrical characteristics of the components. Centerline axes were fit to the centerlines of the hole in the hook (Location A in Figure 77), bolt hole of the keeper (Location B in Figure 77), and the locking shaft (Location C in Figure 77). Those centerlines were aligned to the centerlines of the respective holes in the hook housing. The result is the assembly shown in Figure 78, which can be manipulated to investigate relationships between component contact areas and component positions.

The 3D assembly shown in Figure 78 was utilized to investigate the relationship between the contact area of the locking shaft and hook for various locking shaft orientations. Figure 79 shows the assembly positioned to create contact between the arm of the locking shaft and standoff for the locking shaft cover (see Figure 52 (a)), which is the fully closed position . Both starboard and port views of the assembly as well as a wire outline cross-section extracted from the centerline of the hook are shown.

Figure 80 shows laser scans of Subject Aft Hook showing the 3D assembly aligned assuming elongation of the liner equivalent to 2.58 inches.⁵ Both starboard and port views of the assembly as well as a wire outline cross-section extracted from the centerline of the hook are shown. Figure 79 and Figure 80 highlight the effect of the rotation of the locking shaft on the contact location between the hook and locking shaft.

Figure 81 shows the 3D scans of the Subject Forward Hook, locking shaft, keeper, and hook. These items were documented using laser scanning for comparison to the Subject Aft Hook components. No significant differences were noted.

5 The origin of the value 2.58 inches is discussed in detail in Section 3.3.4.1.1.

3.3.2.1.5 Calculations for Interaction Force of Hook Roller and Locking Shaft

Analysis was done to estimate the stresses at the contact area between the locking shaft and hook due to loading from the weight of the lifeboat when the locking shaft is in the closed position and at a nearly open position (i.e. the roller of the hook is in contact with the edge radius of the locking shaft). The approach taken focused on estimating the dimensions of the contact area and maximum pressure created by the contact between the cylindrical surfaces of the locking shaft and hook roller. Contact stress between two bodies exhibiting curved surfaces can be classified as Hertzian stresses. The half-width b of the contact area between two cylindrical bodies is described by the equation below.

$$b = \sqrt{\pi l \frac{2F \left(\frac{1 - \nu_1^2}{E_1} + \frac{1 - \nu_2^2}{E_2} \right)}{1/d_1 + 1/d_2}}$$

The diameters of the cylinders d_1 and d_2 are pressed together with a force F across a length l . The elastic modulus and Poisson's ratio of the component materials are represented by E_1 , E_2 , and ν_1 and ν_2 , respectively. The Hertzian equations calculate compressive stresses. The maximum pressure (p_{max}), as defined by the equation below, occurs at the center of the contact area defined by $2b$ and l .


$$p_{max} = \frac{2F}{\pi b l}$$

Stresses due to contact of cylindrical components can have large magnitudes and are compressive in nature. The stress fields in the material tend to be very shallow leading to surface damage. Figure 82 illustrates the interaction of the components and the elliptical stress distribution with width $2b^6$ as well as lists the quantities used in this analysis. Figure 83 illustrates the major diameter of the locking shaft, edge diameter of the locking shaft⁷, and diameter of the hook roller using the laser scan data of the Subject Aft Hook components. The analysis was performed assuming the locking shaft was in contact with the major diameter of the hook roller and again assuming the locking shaft was in contact with the edge diameter of the locking shaft near the transition to the flat portion of the locking shaft.

When the major diameter of the locking shaft is in contact with the hook roller, the half-width of the contact area is 0.0143 inches with a maximum pressure of 331 ksi. Conversely, when the edge diameter of the locking shaft is in contact with the hook roller the half-width of the contact area is 0.0067 inches with a maximum pressure of 708 ksi. The contact area

6 Budynas, R., Nisbett, K. (2008). Shigley's Mechanical Engineering Design. 8th edition. McGraw-Hill.

7 The edge diameter of the locking shaft is the radius transition from the major diameter into the flat of the locking shaft.



between the hook roller and locking shaft is 2.14 times larger when contacting the major diameter versus the edge diameter. The larger contact area created between the hook roller and major diameter of the locking shaft corresponds to a lower maximum pressure (stress) since the loading remains constant for both cases. Figure 84 illustrates the local compressive stress in the locking shaft and hook roller material with depth into the material. The largest stress manifests on the surface of the components and decreases below an assumed yield strength of 80.0 ksi at an approximate depth of 0.06 inches. The magnitude of the stress is likely an overestimation as the equation relies on only the elastic modulus and does not include plastic characteristics of the materials. It does however serve as a way to compare the stresses and contact areas that would result due to the different positions of the locking shaft.

3.3.2.2 Exemplar Hook

An Exemplar Hook was provided for mechanical testing and scenario development. DNV GL laser scanned the condition of the Exemplar Hook prior to the mechanical testing.

3.3.2.2.1 Laser Scanning


Figure 85 contains laser scans of the Exemplar Hook with a close-up image of the hook tip. The laser scanning was performed to document the as-received condition of the Exemplar Hook. Load testing using the Exemplar Hook was performed to understand the damage accumulation at the hook point when the ring and the hook point were in contact (i.e. improper installation of the ring into the hook). The load testing is discussed in Section 3.3.4.4. The laser scan data of the Exemplar Hook and Subject Hook were compared to ensure the Exemplar Hook was suitable for testing. The dimensions between the two hooks are similar with some subtle differences at the hook point. This is likely because the point is reportedly hand-ground as a final manufacturing step, per Palfinger, thus differences would be anticipated at this location.

3.3.3 Fall Cables and Rings

3.3.3.1 Visual Examination

Figure 86 is a photograph of the Subject Aft Ring and a section of the Subject Aft Fall Cable as received at DNV GL. The ring was wrapped in white cloth covered with orange bubble wrap and fixed in place with black electrical tape. The ferrule of the eye splice was also covered in white cloth held in place with black electrical tape. The entirety of the assembly was placed in a case for transport.

Figure 87 contains photographs of (a) the Subject Aft Ring and (b) the section of the Subject Aft Fall Cable after removing the protective wrappings. The fall cable had an eye at the end into which the ring was set. A thimble was located at the intrados of the eye. A



ferrule covered the ends of the splice that created the eye. The fall cable had two composite blocks (labelled A and B in the photograph) located 5.5 inches from upper end of the ferrule. The composite blocks were 2.0 inches in thickness and held in place with two sets of bolts and nuts. The wire rope was consistent with right hand, regular lay.

Figure 88 contains photographs of the composite blocks after removal from the section of the Subject Aft Fall Cable. The direction toward the Subject Aft Ring is shown. The contact surfaces of the composite blocks with the fall cable has indentations. The indentations clearly show the lay of the fall cable and beyond the indentation markings, there is no evidence of mechanical damage to the other surfaces of the composite blocks. This suggests little to no movement of the composite blocks position along the fall cable (i.e. no slippage). There is also no evidence of transfer of material from slippage of the composite blocks on the fall cable.

Figure 89 is a photograph of the cross-section of the Subject Aft Fall Cable. The wire rope is comprised of six strands of bundled metallic wires and a center core of nylon. There is no evidence of significant necking or failed wires along the length inspected.

Figure 90 and Figure 91 contains photographs showing the Subject Aft Ring and locations where witness marks were identified. The coating for the ring is a red paint. The witness marks labeled "A" and "D" are round and appear to be superficial corrosion in an area of coating damage. The witness marks labeled "B" and "E" are more linear and located on the outer or inner flat of the ring, respectively. The witness mark labelled "C" is also an area of coating damage and superficial corrosion, but to a lesser extent than the other locations.

Figure 92 is a photograph of the Subject Forward Ring and a section of the Subject Forward Fall Cable as received at DNV GL. The ring was wrapped in white cloth covered with orange bubble wrap fixed in place with black electrical tape. The ferrule of the eye splice was also covered in white cloth held in place with black electrical tape. The entirety of the assembly was placed in a case for transport.

Figure 93 contains a photograph of the Subject Forward Ring and the section of the Subject Forward Fall Cable after removing the protective wrappings. The construction of the fall cable was similar to the Subject Aft Ring and Fall Cables, with the exception that the composite blocks for the limit switch were in contact with the ferrule.

Figure 94 contains photographs of composite blocks after removal from the section of the Subject Forward Fall Cable. The direction toward the Subject Forward Ring is shown. As with the composite blocks removed from the aft, there was also no evidence of transfer of material from slippage of the composite blocks on the fall cable. The primary difference was that some degradation to the composite blocks was visible.




Figure 95 is a photograph the cross-section of the Subject Forward Fall Cable. The wire rope is comprised of six strands of bundled metallic wires and a center core of nylon. The nylon core for the fall cable appears more yellowed than the core from the Subject Aft Fall Cable. There was no evidence of significant necking or failed wires along the length inspected.

Figure 96 contains photographs showing the Subject Forward Ring and locations where witness marks were identified. The coating for the ring is a red paint. The witness marks labeled "A," "D," and "E" are linear and located on the inner flat of the ring. The witness marks labelled "B" and "C" are rounder and similarly sized. The witness marks are coincident with an area of coating damage and superficial corrosion. The markings were similar to mechanical damage identified on the aft components.

3.3.3.2 Laser Scanning

The Subject Aft Ring, the section of the Subject Aft Fall cable, the Subject Forward Ring, and the section of the Subject Forward Fall cable were scanned using the FARO Edge. Figure 97 shows the laser scans of both sides of the Subject Aft Ring illustrating the manufacturing markings and witness marks. Figure 98 shows the laser scans of the Subject Aft Ring and the section of the Subject Aft Fall cable. Figure 99 shows the laser scans of both sides of the Subject Forward Ring illustrating the manufacturing markings and witness marks. Figure 100 shows the laser scans of the Subject Forward Ring and the section of Subject Forward Fall cable.

3.3.4 Cables

3.3.4.1 Subject Aft Cable

3.3.4.1.1 Visual Inspection

Figure 101 contains photographs showing the Subject Aft Cable, Subject Forward Cable, and Subject Hydrostat Cable at the Release Unit after reconstruction at DNV GL's facility. Damage is evident in the cover, wire layer, and liner layers of the Subject Aft Cable, which exposes the inner member. The Subject Forward Cable is damaged at the cover layer, but the inner layers are intact. The cover layer of the Subject Hydrostat Cable is stripped off and some mechanical damage to the wire layer is visible.

Figure 102 contains photographs showing (a) the Subject Aft Cable and (b) the Subject Forward Cable at the Subject Aft and Subject Forward Hooks, respectively. The Subject Aft Cable does not show any damage at the connection points to the Subject Aft Hook. The Subject Forward Cable does show damage at the conduit cap, exposing the inner member. The cover, wire layer, and liner were not mechanically damaged significantly, suggesting that failure at this location was due to the failure at the connection of the conduit cap to the outer layers.





Figure 103 contains photographs showing mechanical damage to the cover of the Subject Aft Cable (a) 3.70 feet to 4.10 feet, (b) 4.70 feet to 5.70 feet, and (c) 8.10 feet to 8.60 feet from the conduit cap at the Subject Release Unit. These photographs were taken by DNV GL during the site visit to Harvey Terminal on July 31, 2019. In service, the Subject Aft Cable was reportedly outed down the starboard side of the cableway in the bottle rack and wire guide. The Subject Aft Cable then crossed to the port side of the bilge at the front of the engine, not the starboard side as shown in the laser scan. The Subject Aft Cable crossed back to the starboard side of the bilge area behind the reduction gear and ran to the hook along the starboard side of the propeller tunnel. Significant corrosion damage to the wire layer was not observed at the breaks in the cover layer. The superficial corrosion damage suggests that the breaks in the cover layer likely formed during or post incident as a result of the Subject Aft Cable making contact with the equipment through which it was routed. Similar mechanical damage to the cover layer and superficial corrosion to the wire layer were noted at similar locations along the length of the Subject Aft Cable and are likely due to damage after the incident (i.e. secondary damage).

Figure 104 contains photographs showing mechanical damage to the cover layer of the Subject Aft Cable 20.63 feet from the conduit cap at the Subject Release Unit. At the location where the Subject Aft Cable would make contact with the rudder assembly, there is an indentation in the cover layer of the Subject Aft Cable. The location of the mechanical damage to the cover layer suggests contact between the rudder assembly and the Subject Aft Cable during and / or after the incident. The damage noted is likely secondary damage.

Figure 105 contains photographs of the Subject Aft Cable after removing a section with the failure in the outer layers; cut location shown in Figure 101. The failure was located 0.72 feet to 1.34 feet from the conduit cap at the Subject Release Unit. The inner member would not slide freely likely because the control cable was bent. Figure 106 contains photographs of the Subject Aft Cable showing the detail of the failure. The failure of the liner layer was 1.42 inches and the failure of the cover layer was 4.00 inches at the orientation shown. The cover does not show evidence of elongation; however, elongation is visible in the liner. Therefore, the difference between the separation in the cover and the separation of the liner is approximately the elongation of the liner layer (2.58 inches). Detail photographs of the liner layer show locations of tearing and buckling, and the primary fracture surface. The buckling suggests that the liner layer may have been compressed.

Figure 107 contains a photograph and montage of the Subject Aft Cable (a) taken in the field on June 6, 2019 by Palfinger, 24 days prior to the incident, and (b) taken in the laboratory by DNV GL following the incident, respectively. For the montage, shown in Figure 107 (b), the fracture surfaces of the cover were matched to generate an image similar to the photograph shown in Figure 107 (a). The numbers in Figure 107 (a) and (b)




are corresponding locations along the length the control cable. The field photograph, Figure 107 (a), shows that the cover of the Subject Aft Cable had been compromised. The strand wires were no longer laying parallel, but rather were protruding at various angles. As shown in the image, the Subject Aft and Forward Cables were routed through an opening cut in the helmsman's console. The exposed wire layer was severely corroded, which resulted in bulging at the opening of the cover. The directionality of some of the corroded wires were not along the axis of the control cable but jut out at a variety of angles. This indicates that the Subject Release Unit was cycled prior to the June 6 photograph taken by Palfinger. The montage in Figure 107 (b) shows that a portion of the strand wires as well as a portion of the binder wire had corroded away. This indicates that the load carrying capacities of the Subject Aft Cable in tension and compression were likely diminished. As viewed, the opening in the laboratory images correspond to the side pointing towards the forward of the lifeboat, and the side not shown is the pointing towards the aft of the lifeboat. These references were used to track the orientations of the components for the dissection and testing discussed below.

3.3.4.1.2 Dissection and Testing

A transverse cut was made to the Subject Aft Cable using a hand grinder with a silicon carbide blade at the location shown in Figure 105 to remove the failed portion of the control cable. The section of the Subject Aft Cable was then dissected for detailed analyses of the layers of the control cable. Figure 108 is a photograph of the Subject Aft Cable showing the layers of the control cable after dissection near the location of the failure. The direction of the Subject Aft Hook is noted with the blue arrow. The cover was removed by splitting axially using a razor blade and a Dremel with a silicon carbide blade. The wire and liner layers were left intact. The inner member slid freely from the liner once the transverse cut shown in Figure 105 was made. The layers of the Subject Aft Cable were examined using a combination of visual inspection, light microscopy, SEM, energy dispersive spectroscopy (EDS) in the SEM, x-ray diffraction (XRD), chemical analysis, metallography, and / or mechanical testing. The layers and testing performed on each are discussed individually in Sections 3.3.4.1.2.1 through 3.3.4.1.2.3 below.

3.3.4.1.2.1 Subject Aft Cable – Cover

Figure 109 and Figure 110 contain photographs of the cover as viewed from the Subject Release Unit and Subject Aft Hook sides, respectively. The (a) external surfaces and (b) internal surfaces of the cover are shown; samples shown in Figure 108. The external surfaces have minor mechanical damage at the high spots in the cover. These high spots correlate to the binder wire from the wire layer. The internal surfaces have white and reddish-brown deposits. The white deposits are likely zinc oxides, which suggests that the



wire layer was galvanized. The reddish-brown deposits are consistent with an iron oxide and are due to the corrosion of the wire layer. The white deposits are more evident on the Subject Release Unit side of the failure, while the reddish-brown deposits are primarily on the Subject Aft Hook side of the failure. This is likely a result of the in-service orientation of the Subject Aft Cable, such that water ingress would drain down towards the Subject Aft Hook. The fracture surfaces of the cover are noted in the figures and are discussed in more detail below.

3.3.4.1.2.1.1 Shore D Hardness


Figure 109 contains photographs showing the cover from the Subject Release Unit side after dissection; sample shown in Figure 108. The direction of the Subject Aft Hook is noted with the blue arrow. The results of the hardness testing of the cover was 51.0 Shore D hardness.

3.3.4.1.2.1.2 Light Microscopy

Figure 111 contains light photomicrographs of the Subject Aft Cable after matching the fractures surfaces at the failure. The fractures surface paths are both axial and circumferential in nature. Abrasive wear, i.e. chafing, of the external surface is visible in the left most image. This damage corresponds to the location of contact with the opening cut in the helmsman's console and the Subject Aft Cable (see Figure 107). Some mechanical damage and a gouge are visible on the external surface in the region of the opening in the cover. Mechanical damage in the form of impact, gouging, and / or rubbing was likely the primary cause(s) of failure of the cover layer. With the cover layer compromised, water could ingress leading to the corrosion of the wire layer. However, the mechanical damage alone does not account for the cracking observed, which is examined in more detail in the SEM work provided below.

3.3.4.1.2.1.3 Scanning Electron Microscopy

Figure 112 contains montages of SEM images taken of the fracture surfaces from the cover of the Subject Aft Cable showing crack arrest marks and initiation sites; locations for Figure 112 (a) and (b) are shown in Figure 110. The red arrow indicated the directions of fatigue propagation. The initiation sites are located on the external surface or mid-wall of the cover where there is a change in plane (i.e. the crack is no longer axial in direction and becomes more circumferential). The initiation sites on the external surface are coincidence with the thinnest parts of the cover, which coincide with the binder wire of the wire layer. The initiation sites on the external surface suggest that a force was exerted circumferentially at the internal surface. It is suspected that this force was associated with an increase in volume that results when steel corrodes. This voluminous corrosion product



exerts a force on the cover from the inside. Hence, the fatigue is a consequence of mechanical damage to the cover, water ingress, and corrosion of the wire layer.

3.3.4.1.2.1.4 Fourier-transform Infrared Spectroscopy

Figure 113 contains an FTIR spectrum of a sample removed from the cover of the Subject Aft Cable; sample location shown in Figure 109. The spectrum shows absorbance bands at 2915 cm^{-1} , 2848 cm^{-1} , 1469 cm^{-1} , and 718 cm^{-1} . These absorbance bands are consistent with the characteristic absorbance bands for polyethylene (PE) materials, which are located at 2914 cm^{-1} , 2847 cm^{-1} , 1470 cm^{-1} , and 718 cm^{-1} . The FTIR results and the hardness results shown in Section 3.3.4.1.2.1.1 indicate that the cover was likely comprised of a LDPE, which is consistent with the manufacturer specifications.

3.3.4.1.2.2 Subject Aft Cable - Wire Layer

Figure 114 and Figure 115 contain photographs of the wire layer as viewed from the Subject Release Unit and Subject Aft Hook sides, respectively. The (a) aft side and (b) forward side of the wire layer are shown; samples shown in Figure 107. The Subject Release unit side has severe corrosion and reddish-brown deposits near the failure and white deposits away from the failure. The Subject Aft Hook side has severe corrosion near the failure and primarily reddish-brown deposits with some white deposits along its length. The strand wires at the failure have a reduced cross-sectional area, either from corrosion or necking. The binder wire has been corroded away at the failure. The reddish-brown deposits are consistent with an iron oxide and are due to the corrosion of the wire layer. Spot testing of the deposits using 2N HCl at the location shown in Figure 115 showed negative results for carbonates and sulfides. The white deposits are likely zinc oxides, which suggests that the wire layer was galvanized. The white deposits are more evident on the Subject Release Unit side of the failure, while the reddish-brown deposits are primarily on the Subject Aft Hook side of the failure. This is likely a result of the in-service orientation of the Subject Aft Cable, such that water ingress drained down towards the Subject Aft Hook.

3.3.4.1.2.2.1 Light Microscopy

Figure 116 contains light photomicrographs of the wire layer from the Subject Aft Cable showing the corrosion damage at the failure. Some mechanical damage is evident in the areas where there is a reduced cross-section area for the strand wires. Penetrations (i.e. holes) to the liner and the transfer of corrosion product to the external surface of the liner are visible and investigated further in Section 3.3.4.1.2.4.

3.3.4.1.2.2.2 Scanning Electron Microscopy

Figure 117 contains SEM images taken of the strand wires from the wire layer of the Subject Aft Cable showing corrosion damage; location is shown in Figure 116. The wires are covered in corrosion product and thinned. The ends of the wires are between 40 mils to 85 mils in spacing. There is no evidence of mechanical overload to the wires, such as ductile or brittle fracture. All wires appear to be compromised as a result of through-thickness corrosion.

3.3.4.1.2.2.3 Energy Dispersive Spectroscopy

Energy dispersive spectroscopy was performed on white deposits removed from the external surface of the wire layer of the Subject Aft Cable using carbon tape; results shown in Figure 118 and sample location shown in Figure 114. The results indicate that the white deposit consisted primarily of zinc (Zn) and oxygen (O). Moderate amounts of sodium (Na), magnesium (Mg), iron (Fe), nickel (Ni), and copper (Cu) were detected. Low amounts of silicon (Si), phosphorous (P), sulfur (S), chlorine (Cl), potassium (K), chromium (Cr), and manganese (Mn) were also detected. The high concentrations of Zn and O indicate that the deposits are primarily comprised of zinc oxide, indicating that the wires were galvanized.


3.3.4.1.2.2.4 X-Ray Diffraction

Figure 119 contains spectra and a table summarizing the results of an x-ray diffraction (XRD) analysis performed on reddish-brown deposits that were removed from the wire layer of the Subject Aft Cable near the failure; location shown in Figure 114. The chemical composition of the deposit consists of magnetite (Fe_3O_4), goethite ($\alpha\text{-FeO(OH)}$), and lepidocrocite ($\gamma\text{-FeO(OH)}$).

Magnetite is a metastable iron oxide phase formed under low oxygen conditions. Goethite and lepidocrocite are thermodynamically stable, hydrated, iron oxides that form in association with aqueous corrosion under aerobic (high oxygen) conditions. Under aerated aqueous conditions, it is not uncommon to find magnetite at the metal surface and the higher oxidation state oxides located on top of the magnetite.

3.3.4.1.2.2.5 Metallography

Figure 120 contains a photograph and photomicrographs of a longitudinal metallographic mount, Mount M1, showing the corrosion attack of the strand wires from the wire layer of the Subject Aft Cable; mount removed from location shown in Figure 114. The corrosion attack appears to be preferentially oriented along the longitudinal direction (i.e. in the drawing direction of the wires). Figure 121 contains photomicrographs of Mount M1 showing (a) the details of the corrosion attack and (b) the microstructure of the strand wires from the wire layer of the Subject Aft Cable; locations shown in Figure 120. The microstructure of



the strand wire consists of ferrite and pearlite with inclusions (dark gray, elongated particles). The corrosion is preferentially located along axial stringers in the steel.


Figure 122 contains a photograph and photomicrographs of a transverse metallographic mount, Mount M2, showing the corrosion attack of the binder and strand wires from the wire layer of the Subject Aft Cable; mount removed from location shown in Figure 114. Corrosion attack in the form of pitting appears to have initiated at the crevice between the strand wires and binder wire. Figure 123 contains photomicrographs of Mount M2 showing the microstructure of (a) the binder wire and (b) the strand wire from the wire layer of the Subject Aft Cable; locations shown in Figure 122. The microstructure of the binder wire is comprised of ferrite (white areas) and spheroidized pearlite (black areas), while the strand wire microstructure is comprised of pearlite (dark gray areas) with cold worked ferrite (white areas).

3.3.4.1.2.2.6 Elemental Mapping and Energy Dispersive Spectroscopy in the Scanning Electron Microscope

More detailed SEM and SEM-EDS mapping analyses were performed on the mounted and polished cross-sections Mount M1 (the longitudinal cross-section) and Mount M2 (the transverse cross-section). Figure 120 and Figure 122 include photographs of the mounted and polished cross-sections, Mount M1 and Mount M2.

Figure 124 and Figure 125 contain SEM images, SEM-EDS elemental maps, and EDS results of the deposits found within Mount M1 (binder wire); see Figure 120 for locations. The SEM-EDS elemental map in Figure 124 shows that there is a relatively uniform distribution of Cl through the thickness of the deposit and that the Zn is present as layers through the deposit. Some Ca is present near the metal -deposit interface. The deposits of the binder wire have high amounts of Fe and O at the metal interface (Location A), which are likely present in the form of an iron oxide. There are higher concentrations of Zn at Locations B, C, and D that are remnants from the galvanized layer. Relatively low to trace concentrations of Na, magnesium (Mg), aluminum (Al), Si, S, Cl, Ca, Cr, manganese (Mn), and copper (Cu) were also detected. The Cl is likely present in the form of chlorides and the remaining elements were likely from the environment and / or impurities from the galvanizing process.

The SEM-EDS elemental map in Figure 125 (strand wire) shows that there are high concentrations of Cl at pits near the metal and deposit interface. Some Ca is also detected within a deposit layer and on the outer edge of the deposits. The deposits of the wire have high amounts of Fe and O at the metal interface (Locations B and C), which are likely present in the form of an iron oxide. Calcium and oxygen are present in high amounts at Location A, which is typically consistent with carbonates; however, none were detected during spot testing. As such, it is most likely these elements are from the environment.



There is no evidence of Zn at any of the locations, indicating the galvanized layer had fully corroded away. Relatively low to trace concentrations of Na, Mg, Al, Si, S, Cl, potassium (K), Ca, Cr, Mn, and strontium (Sr) were also detected at some locations. The Cl is likely present in the form of chlorides and the remaining elements were likely from the environment and / or impurities from the galvanizing process.

The SEM-EDS elemental map in Figure 126 (binder wire) shows that there are high concentrations of Zn and Cl in the galvanized layer. The galvanized layer of the wire has high amounts of Zn, Fe, and O at the metal interface (Locations A and B), which are likely present in the form of a zinc oxide and / or an iron oxide. There is also a high concentration of Na in the galvanized layer. The Fe concentration is slightly higher at the metal / galvanized layer interface. Relatively low to trace concentrations of Si, S, and Cl were also detected at both locations. The Cl is likely present in the form of chlorides and the remaining elements were likely from the environment and / or impurities from the galvanizing process.


The presence of a galvanized layer was confirmed. Near the failure location of the Subject Aft Cable, the galvanized layer of the wires layer was fully or partly corroded away. The presence of Cl indicates that chlorides are likely present, which are known to accelerate corrosion of carbon steels.

3.3.4.1.2.2.7 Chemical Analyses

Semi-quantitative, EDS analyses were performed on the strand wire and binder wire to determine the approximate compositions of the strand wire and binder wire. Figure 127 contains an EDS Spectra, SEM image, and EDS Results for strand wire and binder wire from the Subject Aft Cable; area shown in Figure 122 (rotated 90°). The wires are primarily comprised of Fe with low amounts of Si, Cr, Mn, and Cu present. The main difference between the strand wire and binder wire is that the strand wire appears to contain more chromium than the binder wire. Please note that carbon was not included in the spectra as the mount used for testing was carbon coated. Based on the chemistry and metallography, the strand wire and binder wire are carbon steel alloys.

3.3.4.1.2.3 Subject Aft Cable – Liner

Figure 128 and Figure 129 contain photographs of the liner from the Subject Release Unit and Subject Aft Hook sides, respectively. The photographs show of the failure in the Subject Aft Cable after dissection on the (a) aft side and (b) forward side; samples shown in Figure 108. The photographs of the liner layer show locations of tearing and buckling as well as the location for the fracture surface. The buckling suggests that the liner layer may have



been compressed. The fracture surfaces of the liner are noted in the figures and are discussed in more detail below.

3.3.4.1.2.3.1 Shore D Hardness

Figure 130 contains the results of the hardness testing of the white liner, which had an average hardness of 51.0 Shore D.

3.3.4.1.2.3.2 Light Microscopy


Figure 131 contains light photomicrographs of the liner removed from the Subject Aft Cable at the failure location after matching the fractures surfaces. The fracture paths are primarily circumferential in nature. The previously noted tearing and buckling are visible in the micrographs. The buckling suggests that the liner layer had been compressed; however, the morphology of the fracture surfaces indicate that the tube failed in tension. Additionally, a thinned area on the aft side of the Subject Release Unit side of the failure is visible. A reddish-brown, embedded particle, as well as reddish brown deposits, are visible near the failure on the external surface of the liner. Punctures are visible on the aft side of the Subject Aft Hook side of the failure, and correlate with the size and spacing of the individual wires that make up the wire layer.

3.3.4.1.2.3.3 Scanning Electron Microscopy

Figure 132 contains SEM images taken of the liner from the Subject Aft Hook side of the Subject Aft Cable showing the fracture surface; viewing direction is shown in Figure 131. The fracture exhibits evidence of necking, indicating that the tensile load applied to the liner was not extremely fast. Fast loading conditions of polyethylene result in little to no necking corresponding to a brittle fracture. Some areas of the fracture surface do exhibit minimal necking, which likely correspond to the final areas of overload. The cube-shaped objects shown in the images are likely salt deposits. Figure 133 contains SEM images of the liner from the Subject Aft Hook side of the Subject Aft Cable showing the external surface; sample location is shown in Figure 131. Punctures at a buckle, as well as gouging that is oriented longitudinally on the external surface of the liner, are visible. The punctures are spaced 35 mils to 45 mils from one another, which is similar to the spacing identified between the tips of the corroded strand wires from the wire layer; thus, the punctures and gouging are likely from the strand wires in the wire layer.

3.3.4.1.2.3.4 Energy Dispersive Spectroscopy in the Scanning Electron Microscope

Figure 134 contains an SEM image and EDS results for an embedded particle in the external surface of the liner of the Subject Aft Cable; location is shown in Figure 131. Some gouging



is visible in the external surface of the liner and is oriented in the longitudinal direction (similar to the punctures previously observed). The embedded particle is mainly comprised of Cl, Na, O and Fe, which suggest that an iron oxide and NaCl are present. Low amounts of Mg, Si, S, K, and Ca are also present, which are consistent with the elements detected in the corrosion deposits and galvanized layer of the wire layer from the Subject Aft Cable. These elements are likely from the environment and / or impurities from the galvanizing process.

3.3.4.1.2.3.5 Fourier-Transform Infrared Spectroscopy

Figure 135 contains an FTIR spectrum of a sample removed from the liner of the Subject Aft Cable; sample location shown in Figure 114. The wire layer was removed to gain access to the liner layer underneath. The spectrum shows absorbance bands at 2914 cm^{-1} , 2847 cm^{-1} , 1472 cm^{-1} , and 730 cm^{-1} . These absorbance bands are consistent with the characteristic absorbance bands for PE materials, which are located at 2914 cm^{-1} , 2847 cm^{-1} , 1470 cm^{-1} , and 718 cm^{-1} . Minor peaks are noted at 1368 cm^{-1} , 1260 cm^{-1} , 1100 cm^{-1} , 1019 cm^{-1} , 908 cm^{-1} , 804 cm^{-1} , and 430 cm^{-1} , which are likely related to additives to the PE of the liner. The FTIR results and the hardness results shown in Section 3.3.4.1.2.3.1 indicate that that liner is likely comprised of a LPDE. It should be noted the manufacturer specification of the liner material is HDPE.

3.3.4.1.2.3.6 Differential Scanning Calorimetry – Oxidative Induction Time

Differential Scanning Calorimetry (DSC) was performed to understand the Oxidative Induction Time of the liner material. A shorter time to oxidation would indicate degradation of the liner due to environmental exposure. The test was performed on liners extracted from the Subject Aft Cable of Lifeboat 6, the aft control cable of Lifeboat 7, and aft control cable of Lifeboat 8. Figure 136 displays the results of the analysis. The results indicate no significant difference in Oxidative Induction Time between the samples removed from the liners.

3.3.4.1.2.3.7 Differential Scanning Calorimetry – Glass Transition Temperature

Differential Scanning Calorimetry (DSC) per ASTM D3418 was performed to quantify the Glass Transition Temperature (T_g) of the liner material. Significant differences in the T_g of the liner material would suggest a higher degree of degradation in the cable of one boat as compared to another. The test was performed on liners extracted from the Subject Aft Cable of Lifeboat 6, the aft control cable of Lifeboat 7, and aft control cable of Lifeboat 8. Figure 137 displays the results of the analysis. The results suggest no significant difference in Glass Transition Temperature between the samples removed from the liners.

3.3.4.1.2.3.8 Thermogravimetric Analysis

Thermogravimetric Analysis (TGA) was performed to determine the Glass Transition Temperature (T_g) of the liner material. Significant differences in the T_g of the liner material would suggest a higher degree of degradation in the cable of one boat as compared to another. The test was performed on liners extracted from Lifeboat 6, Lifeboat 7, and Lifeboat 8. Figure 138 displays the results of the analysis. The results suggest no significant difference in Glass Transition Temperature between the samples removed from the liners.

3.3.4.1.2.3.9 Mechanical Testing

Tensile testing via ASTM D638 was performed on the die-cut test coupons extracted from liners of the Subject Aft Cable of Lifeboat 6, the aft control cable of Lifeboat 7, and aft control cable of Lifeboat 8. The testing was performed at varying strain rates (0.2 in/min, 2 in/min, 20 in/min) to investigate the rate dependent mechanical properties of the liner material. The variation in strain rate was used to simulate quasi-static and quasi-dynamic failure scenarios. The testing was also performed to determine the differences in mechanical properties between the liners of each lifeboat. Significant differences in mechanical properties may suggest degradation between samples. The results are shown in Figure 139. The results do not suggest a higher degree of degradation between samples. The results display the rate dependent properties of the liner material, meaning as the strain rate increases there is reduction in ductility.

3.3.4.1.2.4 Subject Aft Cable – Inner Member


Figure 140 contains a photograph of the inner member from the Subject Aft Cable after dissection showing the aft side; sample location shown in Figure 108. The area of the inner member exposed due to the break in the liner is noted. Minor corrosion attack to the binder wire is evident inside and outside of the exposed area. No mechanical deformation was noted in the inner member at the location shown.

3.3.4.1.2.4.1 Light Microscopy

Figure 141 contains light micrographs of the inner member of the Subject Aft Cable showing the detail of the corrosion attack to the binder wire and damage to the sheath layer of the inner member. The minor corrosion attack to the binder wire is below the nylon cover. Scratches along the axis of the inner member are noted on the cover of the inner member.

3.3.4.2 Lifeboat 7 & 8 Cables

Figure 142 contains field photographs of the (a) hydrostat cable from Lifeboat 7 and (b) the forward control cable from Lifeboat 8 showing evidence of degradation. Photographs were provided by SOI. As shown in the images, the hydrostat cable from Lifeboat 7 and the



forward control cable from Lifeboat 8 were routed through openings in / near the helmsman's console. As was identified for the Subject Aft Cable in Lifeboat 6, the cover failed with fracture paths in both the axial and circumferential orientations. Bulging of the cover layer is visible in both cables. The wire layer that is visible is severely corroded, likely causing the opening / bulging of the cover.

The cables were removed from service and prepared for shipment. Figure 143 is a photograph showing the hydrostat cable from Lifeboat 7 and the forward control cable from Lifeboat 8, at DNV GL, after partially removing the wrappings from shipment. The cables had been wrapped in bubble wrap fixed with green painter's tape. The cables were then coiled into a bundle and fixed with green painter's tape. The bundle was received on a wooden pallet, which was wrapped in clear plastic. The shipping materials were intact and in good condition upon arrival to DNV GL.

At DNV GL, the wrappings were removed, and the cables were visually inspected and then dissected. The objectives of the analysis were to compare the degradation of the cables from Lifeboat 7 and Lifeboat 8 with the failure location identified on the Subject Aft Cable from Lifeboat 6.

3.3.4.2.1 Visual Inspection of Lifeboat 7 Hydrostat Cable and Lifeboat 8 Forward Cable

Figure 144 is a photograph of the hydrostat cable from Lifeboat 7 after removing the wrappings. The damage location on the cable is noted in the image. Measurements were performed using the reference end located at the shoulder of the conduit cap, which is noted in the photograph.

Figure 145 contains photographs of the hydrostat cable from Lifeboat 7 showing (a) the assumed top orientation and (b) the assumed bottom orientation. The external surface of the cover exhibits evidence of gouging and scraping associated with the installation and / or removal of the cable through a penetration in plywood. The cracking in the cover is located between 1.30 feet and 1.38 feet from the shoulder of the conduit cap. The cracking is both axially and circumferentially oriented; however, the cracking is not continuous around the circumference of the cable. Severe corrosion attack to the wire layer is visible in Figure 145 (a), exposing the liner between 1.31 inches and 1.35 inches from the shoulder of the conduit cap.

Figure 146 is a photograph of the forward control cable from Lifeboat 8 after removing the wrappings. The damage location of the cable is noted in the image. Measurements were performed using the reference end located at the shoulder of the conduit cap, which is noted in the photograph.




Figure 147 contains a photograph of the forward control cable from Lifeboat 8 showing the assumed top orientation. The external surface of the cover exhibits evidence of gouging and scraping associated with the installation and / or removal of the cable through a penetration in plywood. The cracking in the cover is located between 3.07 feet and 3.21 feet from the shoulder of the conduit cap. The cracking is both axially and circumferentially oriented; however, the cracking is not continuous around the circumference of the cable and only present at the top orientation. Severe corrosion attack to the wire layer is visible in Figure 147; however, the liner is not exposed.

3.3.4.2.2 Dissection and Testing

Transverse cuts were made to the Lifeboat 7 hydrostat cable to remove the portions of the cables containing the damage location. The cuts were made using a hand grinder with silicon carbide blade at the locations shown in Figure 144 and Figure 146. The sections of the cable were then dissected for detailed visual analyses of the layers of the cable. Figure 148 and Figure 149 are photographs of the Lifeboat 7 hydrostat cable and Lifeboat 8 forward control cable showing the layers of the cable after dissection. The cover was removed by splitting axially using a razor and / or a Dremel® tool with a silicon carbide blade. The wire and liner layers were left intact. The inner member was not removed but slid freely within the liner. The layers of the cables were examined using visual inspection and light microscopy. The layers and testing performed on each are discussed individually in Sections 3.3.4.2.2.1 and 3.3.4.2.2.2 below.

3.3.4.2.2.1 Lifeboat 7 Hydrostat Cable and Lifeboat 8 Forward Cable - Cover

Figure 150 and Figure 151 contain photographs of the cover from the Lifeboat 7 hydrostat cable at the damage location after dissection showing the internal surfaces; sample location shown in Figure 144. The internal surfaces have white and reddish-brown deposits. The white deposits are likely zinc oxides, which suggests that the wire layer was galvanized. The reddish-brown deposits are consistent with an iron oxide and are due to the corrosion of the wire layer. The fracture surfaces of the cover are noted in the figures and are discussed in more detail below. The external surfaces have minor mechanical damage at the high spots in the cover (not shown in the images). These high spots correlate to the binder wire from the wire layer.

Figure 152 and Figure 153 contain photographs of the cover from the Lifeboat 8 forward control cable at the damage location after dissection showing the (a) external surfaces and (b) internal surfaces; sample location shown in Figure 149 (top). The appearance of the cover from Lifeboat 8 was similar to the cables from Lifeboat 6 and Lifeboat 7.

3.3.4.2.2.1.1 Light Microscopy


Figure 154 and Figure 155 contain light photomicrographs of the Lifeboat 7 hydrostat cable and Lifeboat 8 forward control cable, respectively, after matching the fractures surfaces. The fracture surface paths are both axial and circumferential in nature. Some mechanical damage and gouging are visible on the external surface where the cable is compromised. This damage corresponds to the location of contact with the plywood where the cables in Lifeboat 7 and Lifeboat 8 (see Figure 142) were routed. Mechanical damage in the form of impact and / or gouging was likely the primary cause(s) of failure of the cover layers of Lifeboat 7 and Lifeboat 8. With the cover layer compromised, water could ingress leading to the corrosion of the wire layer. As with the Subject Aft Cable, the cracking of the cover layer likely propagated by fatigue due to the voluminous corrosion product from the corrosion of the wire layer, which is similar to the appearance of the cover from the Subject Aft Cable of Lifeboat 6.

3.3.4.2.2.2 Lifeboat 7 Hydrostat Cable and Lifeboat 8 Forward Cable - Wire Layer

Figure 156 and Figure 157 contain photographs of the wire layers from the Lifeboat 7 hydrostat cable and Lifeboat 8 forward control cable, respectively, showing the corrosion damage; samples shown in Figure 144 and Figure 146, respectively. The corrosion attack to the Lifeboat 7 hydrostat cable is less severe than the Subject Aft Cable from Lifeboat 6, but more severe than the Lifeboat 8 forward control cable. Both cables show white deposits and reddish-brown deposits near the failure location. The reddish-brown deposits are consistent with an iron oxide and are due to the corrosion of the wire layer. The white deposits are likely zinc oxides, which suggests that the wire layer was galvanized. The strand wires in hydrostat cable of Lifeboat 7 have a reduced cross-sectional area from corrosion attack. The binder wire has been corroded away at both locations.

3.3.4.2.2.2.1 Light Microscopy

Figure 158 and Figure 159 contains light photomicrographs of the wire layer from the Lifeboat 7 hydrostat cable and Lifeboat 8 forward control cable, respectively, showing the detail of the corrosion at the damage location. The reduced cross-section area for the wires from the wire layer of Lifeboat 7 hydrostat cable is more evident. Some transfer of the corrosion product of wire layer to the liner is evident in Figure 158. Pitting in the area of most severe corrosion is evident for the wire layer from the Lifeboat 8 forward control cable. This area is coincident with the area where the spiral cable would have been. It is worth noting that the corrosion damage accumulation on the wire layer from forward control cable of Lifeboat 8 was less severe the wire layer from the hydrostat cable of Lifeboat 7. The bottom side of Lifeboat 8 forward control cable did not show significant corrosion attack.



The corrosion morphology observed on the cables from Lifeboat 7 and 8 is similar to that observed on the aft control cable of Lifeboat 6, with one notable exception. The individual wires pertaining to Lifeboat 7 and 8 are laying at the expected orientation based on the general lay of the wire strands. The individual wires on the aft control cable of Lifeboat 6 are pointing at various angles that are not necessarily in the same direction as the lay of the wire strands, and can be seen in Figure 107 (a). This suggests that the Subject Aft Cable was operated while the wire layer was compromised at some point prior to June 6, 2019, such that the mating wires were pushed into contact with other portions of the control cable, deflecting and bending the wires during operation.


3.3.4.3 Mechanical Testing of Exemplar Cable and Subject Aft Cable

Figure 160 is a photograph showing the Subject Aft Cable and Exemplar Cable used for mechanical testing. The cover and binder wire were removed from the locations shown to improve the grip of the hydraulic clamps with the control cables. The Subject Aft Cable was removed between 9.0 feet and 10.0 feet from the shoulder of the conduit cap. The Exemplar Cable was provided by the United States Coast Guard (USCG); the USCG acquired the cable from an authorized cable assembler. The inner member was left intact for the exemplar test and was removed at the ends of the sample for the subject test to minimize ovalization.

Figure 161 contains photographs showing the Subject Aft Cable in the hydraulic clamps (a) before and (b) after mechanical testing, as well as a table summarizing the results of the mechanical testing of the Subject Aft Cable and Exemplar Cable. The Subject Aft Cable had a maximum load of 2175 lbs with an extension of 1.10 inches. The Exemplar Cable had a maximum load of 6622 lbs with a maximum extension of 2.65 inches. No significant corrosion or pre-existing damage was noted on the Subject Aft Cable that could account for the lower load value. Both tests failed at the hydraulic grips. It is possible that the notches were introduced when gripping the Subject Aft Cable were more severe, resulting in a lower load value. The results may also vary due to the difference in cable manufacture, degradation associated with in the subject cable, and / or the testing approach.

3.3.4.4 Load Testing with Exemplar Cable, Exemplar Hook, Exemplar Ring, and Subject Release Unit

Figure 162 contains photographs showing the test rig for the load testing with the Exemplar Cable, Exemplar Hook, Exemplar Ring, and Subject Release Unit. The Exemplar Hook was fixed to the test frame using threaded rods attached to an eye where the lifting pin had been threaded. A clevis was attached to the ring, and the ring was placed in the fully engaged position of the Exemplar Hook. The ring was free to rotate within the clevis, as it would in the thimble in-service. The clevis was attached to the load cell using a threaded



rod and eye. The lower portion of the Exemplar Hook was prevented from rotating by placing two steel plates on either side of the hook and clamping them in place (represented by the red box in the left photograph in Figure 162). Load was applied to the test setup by adding weights to the back of the test frame. All clevises and bulkhead nuts for the Exemplar Hook, Subject Release Unit, and Exemplar Cable were set to the as-found condition. A load of 4391 lbs, half the estimated weight of Lifeboat 6 at the time of the incident, was applied to the test setup in the fully engaged position to remove any slack in the test frame and setup. This value was selected as it was representative of the weight of Lifeboat 6 with equipment and occupants at the time of the failure.

The test setup was used to understand the damage accumulation at the hook point and the ring when the ring is improperly installed in the Exemplar Hook. Three scenarios were tested. Figure 163 contains photographs showing (a) Scenario 1, (b) Scenario 2, and (c) Scenario 3 of the ring resting on the point of the Exemplar Hook. In Scenario 1 and Scenario 2, the point of the hook was placed on the flat of the ring that was present on the internal surface. The primary difference between the two was the orientation of the ring being rotated towards the starboard (Scenario 1) or towards the port (Scenario 2). For Scenario 3, the point of the hook was placed such that the ring was parallel to the hook point. For Scenario 1 and 2, a load of 4391 lbs was applied, and the load was held by the test setup. The ring of the setup was then struck with a rubber mallet to force rotation of the ring when under load. In Scenario 3, the ring slipped off the hook point after 3400 lbs was applied. Figure 164 through Figure 166 show (a) the point of the Exemplar Hook compared to the Subject Aft Hook and (b) the mechanical damage to the ring after testing Scenario 1, Scenario 2, and Scenario 3, respectively. In all cases, mechanical damage to the point of the Exemplar Hook was severe and there was evidence of red paint transfer. The damages identified did not match the damage noted on the Subject Aft Hook. Similarly, the ring sustained mechanical damage to the flat of the ring where the point of the hook rested in each scenario. However, the damages identified were not similar to the damage identified on the Subject Aft ring.

In addition to the load testing, the clevises and the bulkhead nuts were adjusted to the most open position for the locking shaft and a 4391 lbs load was applied. The load held such that the pin at the clevis attaching the Exemplar Cable to the Subject Release Unit was able to be removed under load. Testing was then performed to determine the load necessary to rotate the locking shaft to an open position. A scale was attached to the clevis where the pin was removed, and an upward load was applied to the control cable. The load was increased until the locking shaft rotated into the open position, which occurred at approximately 65 lbs.

3.3.5 Fiberglass Hull and Support Structure

3.3.5.1 Scanning Electron Microscopy

Fractographic analysis was performed on the composite samples removed from Lifeboat 6. Broadly, failure of composites can be grouped into three specific and unique modes: translaminar, interlaminar and intralaminar. A schematic illustrating the three modes is shown in Figure 167.⁸


Translaminar failure involves fracture of the reinforcing fibers, typically across multiple plies or orientations. When describing fracture surfaces in generic terms, it is important to note that the other methods of failure do not generally involve fiber fracture. Interlaminar failure (delamination) involves fracture between the layers. This is more commonly described as layer failure or delamination. This mode is generally devoid of fiber fracture. Intralaminar fracture involves through-thickness fractures of the matrix between the fibers. This mode is generally devoid of fiber fracture. It is also necessary to acknowledge that when conducting fractography of composite structures, the presence of numerous multiple different modes within a singular failure or even plane of failure is not just possible, but common. The interfaces interact and the degree to which is dependent on factors such as loading conditions, material architecture, chemistry, physical, component geometry, environment of use, and other application specific factors.

Figure 168 is a photograph of Sample C-1 and a schematic showing the location where the sample was removed from the inner hull. Sample C-1 was located near the engine mount. Figure 169 contains low magnification SEM images of Sample C-1-A. Fiber pull-out from the resin matrix is visible near the internal surface.

Figure 170 contains higher magnification SEM images of Sample C-1-A showing notable fracture surfaces of glass fibers. The top images display examples of interlaminar, intralaminar, and translaminar fracture. The bottom images display the brittle fracture morphology of individual glass fibers. The fracture morphologies identified are consistent with a brittle failure mode and indicative of fast fracture from a dynamic event.

Figure 171 contains photographs of Sample C-2 and a schematic showing the location where the sample was removed from the inner hull. Sample C-2 was located near a crack in the keel. The location of the sample examined in the SEM, Sample C-2-3, is shown. The sample was located within the through-wall portion of the crack. Figure 172 contains SEM images of Sample C-2-3 showing notable fracture surfaces of glass fibers. The images display

⁸ For a reference on typical fracture surfaces of fibers, reference M. Elices and J. Llorca, *Fiber Fracture*, First Edition (2002).



examples of interlaminar, intralaminar, and translaminar fracture. Brittle resin fracture and brittle glass fiber fractures are also shown.

Figure 173 contains a photograph of Sample C-3 and schematic showing the location where the sample was removed from the outer hull. Sample C-3 was located 11.4 feet from the aft of Lifeboat 6. The location of the sample examined in the SEM, Sample C-3-B, is shown. The crack was not through wall in this area. Figure 174 contains SEM images of Sample C-3-B showing notable fracture surfaces of glass fibers. The images display examples of mixed mode interlaminar and intralaminar fracture. Brittle fracture of the resin and glass fibers is also shown.

The fracture morphologies for all locations examined (C-1, C-2, and C-3) are consistent with a brittle failure mode and indicative of a single, high load event.

3.3.5.2 Mechanical Testing


Mechanical analysis of the lifeboat's constituent materials was performed to obtain material properties to apply to a computer-simulated Finite Element model.

3.3.5.2.1 Three-Point Bend Flexural Testing

Tensile and flexural test coupons were extracted from each fiberglass panel via waterjet cutting. The dimensions of each tensile coupon were determined through reference ASTM D3039-17 Polymer Matrix Composite Tensile Testing. The dimensions of each flexural coupon were determined through Reference ASTM D790-17 Standard Test Methods for Flexural Properties of Unreinforced and Reinforced Plastics and Electrical Insulating Materials. The thickness of the fiberglass material deviated from the specifications in the testing standard; however, the thickness was not altered, as machining of the panel to meet the standard thickness dimension could introduce micro-cracks or otherwise damage the test specimen. The locations where the waterjet cut specimens were removed from one panel are shown in Figure 175.

Flexural testing was performed on the fiberglass material to obtain flexural modulus, yield stress, yield strain, break stress, and break strain. The flexural response of the material was applied directly to the model to understand the material's behavior under the incident's loading scenario.

Flexural testing was performed on panels from six locations to confirm global uniformity in material properties. The results of this testing are shown in Figure 176. The ultimate stress for the exterior panels ranged between 11.1 ksi and 13.8 ksi, while the ultimate stress for the interior panels ranged from 9.0 ksi and 13.7 ksi. The panels extracted from the interior of the boat (AP-2 and BS-1) exhibited a lower average strength than the exterior panels



(ASO-1, APO-1, BPO-1, BSO-1) so two unique material properties for each location were calculated. The flexural response of the exterior fiberglass was a calculated average of the results for panels ASO-1, APO-1, BPO-1, and BSO-1. The flexural response of the interior fiberglass was a calculated average of the results for panels AP-2 and BS-1.

In addition, flexural testing was carried out on coupons removed from two orientations (0° and 90°) to confirm isotropy. Isotropy signifies that the material properties of the fiberglass are not directionally dependent, and a single material property can be applied. The results of this testing also are shown in Figure 176, and show isotropic properties at the 0° and 90° orientations of the specimens.

3.3.5.2.2 Glass-Fiber Content Analysis

In addition to flexural testing, a glass fiber content analysis was performed at five locations within each panel to determine the average percentage of glass fiber within each panel. As stated previously, the glass fiber within the composite matrix provides the majority of the material's strength. The tests were carried out in accordance with ASTM D5630 – 13 Standard Test Method for Ash Content in Plastics. The results are shown in Figure 177 and indicate that the interior panels (AP-2 and BS-1, i.e. non-structural) have a lower glass-fiber content than the exterior panels (i.e. structural). This correlates with the findings of the flexural testing performed that indicated that the interior panels had lower strength.


3.3.5.2.3 Compression Testing of Foam

Compression testing was performed on the inner foam to obtain material properties to be applied to the Finite Element Model. The foam samples were removed from the interior of the vessel from under the fiberglass panels BP-1 and BS-1, which are shown in Figure 43. The testing was carried out in accordance with ASTM D3574 – 17 Standard Test Methods for Flexible Cellular Materials—Slab, Bonded, and Molded Urethane Foams. The foam samples were extracted from one port location and one starboard location. An average compression modulus was calculated from testing the two locations and the results were applied to the Finite Element model. The resulting Stress-Strain curve is shown in Figure 178. Samples with "S" refer to starboard and were removed from under location BS-1 and the samples with "P" refer to port and were removed from under location BP-1.

3.3.5.3 Modeling

3.3.5.3.1 Background

Loading at the contacts of the aft bumpers with Lifeboat 6 was investigated as a possible contributor to the incident using finite element analysis (FEA) modeling. Fall cable measurements were taken by the SOI team at the davit of Lifeboat 6 after the incident. The difference in length between the forward and aft fall cables was estimated to be 12.5



inches. As a result, there was a 7.556 inch difference⁹ between the aft and forward ends of Lifeboat 6 (i.e. Lifeboat 6 was tilted towards the bow of the lifeboat), as depicted in the schematic in Figure 7. Based on the measurements performed by the SOI team, the aft bumpers would have made contact before the forward bumpers. At the time the Subject Aft Hook released, the estimated vertical displacement after contact of the aft bumpers with Lifeboat 6 was 9.444 inches. Note that this indicates that the forward portion of Lifeboat 6 did not contact the forward bumpers. The estimated gap between the lifeboat and the forward bumpers is 3.073 inches. As a consequence of the 9.444-inch vertical displacement, loading at the bumper contact locations at the aft of the Lifeboat 6 likely occurred. The loading may have also resulted in stresses and deflections that caused damage to Lifeboat 6. For example, the failure at the engine mount region (see Figure 40) or the failure at the keel (see Figure 42) may have resulted from loading at the aft when Lifeboat 6 was being pulled into the davit.

A series of analyses were performed to simulate this loading scenario of Lifeboat 6. The FEA model was used to identify regions of high stress and strain that could have contributed to the unintentional release of the Subject Aft Hook and to evaluate the likelihood of this loading scenario being the causal failure mechanism.

Using laser scanning imagery and design drawings, a representative 3D model of Lifeboat 6 was generated. As discussed in Section 3.3.5.2, samples were removed from various locations on Lifeboat 6 and tested to acquire representative material properties used in the structural analysis of Lifeboat 6. The analysis was performed using ABAQUS (ABAQUS/CAE 2018) FEA software.


3.3.5.3.2 Material Inputs

3.3.5.3.2.1 Fiberglass

The majority of the structure of Lifeboat 6 is fiberglass. Mechanical testing was completed on extracted fiberglass coupons to acquire material properties for the structural analysis work completed during this investigation.

Flexural properties of the fiberglass structure were measured according to ASTM D790-15. Multiple regions were tested with multiple coupons from each region. The varying layout structure and thickness of Lifeboat 6 was taken into account. Mechanical testing of the

⁹ The difference between the height of the lifting point from the keel of the lifeboat at the Forward Hook (87.25 inches) and the height of the lifting point from the keel of the lifeboat at Aft Hook (67.25 inches), as designed, is 20 inches (see Figure 5 for the original design drawing). The as-installed height difference between the forward and aft hooks of Lifeboat 6 is unknown. However, the 20-inch height difference is known to vary from installation to installation.



fiberglass, reported in Section 3.3.5.2, were used as material inputs for the model. The fiberglass structure had an average flexural strength of 12,000 psi.

The stress-strain response of the fiberglass material was modeled as bi-linear and linear elastic properties up until the point of yielding were assumed for the model.

3.3.5.3.2.2 Foam

The mechanical properties of the foam were determined in compression according to ASTM D3574-17. The modulus of the foam is several orders of magnitude lower than that of the fiberglass; therefore, the foam is likely not a significant contributor to overall stiffness and was not utilized in the model.

3.3.5.3.2.3 Steel and Stainless Steel

Steel and stainless-steel components that may have added stiffness to the lifeboat structure were included in the structural model. These components include the lifting shoes where the hooks connect to the lifeboat, the engine mount, the engine cradle, the fuel tank, the propeller shaft, and rudder support structure. Per drawings provided by Palfinger, the steel components of the lifeboat were specified as Grade A-36 carbon steel or Grade 2205 duplex stainless steel. The A-36 carbon steel components (engine mount, engine cradle, fuel tank, propeller shaft, and rudder support structure) have a specified minimum yield strength (SMYS) of 36 ksi and the duplex stainless-steel components (lifting shoes) have a SMYS of 65.0 ksi. These components were modeled considering an elastic-plastic material model with the appropriate yield strengths in the Abaqus model.

3.3.5.3.2.4 Davit Bumper


The bumper material properties were not measured in the laboratory and were approximated using a hyperelastic material model in Abaqus. These hyperelastic material models allow for large deformations and strain response, typical of rubber materials. A representative hyperelastic material model using the Ogden strain energy potential formulation within Abaqus was used for the assessment. The geometry of the bumpers was modeled based on laser scans and photography performed on Auger.

3.3.5.3.3 Structural Model Mesh

The finite element model consists of 48,697 total elements, 22,093 of which are linear quadrilateral elements of Type S4 and 1,654 are linear triangular elements of Type S3.^{10, 11} The remaining elements in the model were used to model the bumpers, consisting of 24,650

¹⁰ S4: 4-node general purpose shell element.

¹¹ S3: 3-node general purpose shell element.



linear hexahedral elements of Type C3D8H and 300 linear wedge elements of Type C3D6H.¹² The model is comprised of 51,969 nodes. The body was meshed continuously using shell elements. The stiffness of these shell elements is determined by the assigned thickness and material properties.

Measurements provided from Lifeboat 6 and examination of the Lifeboat 6 drawings indicate that the thickness of the fiberglass varied throughout the structure. The modeling effort assumed that the thicknesses on the mechanical drawing were representative of Lifeboat 6. These thicknesses were applied to each applicable region of the lifeboat. Diagram illustrating the thicknesses of the various components of Lifeboat 6 are shown in Figure 179 and Figure 180.

3.3.5.3.4 Standard Analysis


The analysis was completed in Abaqus Standard, which is appropriate for static or quasi-static analyses, such as the loading the lifeboat was subjected to in the Davit. The specifics of the model setup, loading, and boundary conditions are described below.

3.3.5.3.4.1 Boundary Conditions and Constraints

The loading and geometry are symmetric about the x-y plane, aligned with the centerline of the lifeboat dividing the starboard and port sides. Half of the Lifeboat 6 structure was modeled, and a symmetry boundary constraint was applied to this boundary, mirroring stresses and deflections across this plane. An overview of the boundary conditions applied to the model is shown in Figure 181.

All nodes on the circumference of each lift shoe bracket were constrained to a node at the center of each mounting pin hole using a kinematic coupling constraint. This allows for a simplified method of modeling the interaction between the lifting shoe and the fall cables without explicitly modeling the contact and interaction between each of the components involved, as these are not the primary interest of this assessment. This constraint was applied to both the forward and aft lift shoe. Beam connectors were used at each of these mounting pin holes to represent the fall cables tethered to the lifting shoe brackets. These were incorporated to allow for the lifeboat to translate in the forward and aft directions, while also being able to apply the vertical boundary condition. A displacement of 9.444 inches was applied in the negative y-direction (upward) to the top of these beam connectors. The forward and aft of the lifeboat were raised into the davit at the same rate. The central nodes of the forward and aft lift shoes were free to translate in the x and z directions and were allowed to rotate about all axes.

¹² C3D8H – 8-node linear brick element with hybrid formulation.



The location, orientation, and geometry of the aft bumper was modeled using the laser scan images of the actual Lifeboat 6 davit on the Auger platform, performed by SOI and provided to DNV GL. Sensitivity studies were performed considering the aft bumper as rigid as well as rubber in order to examine the impact on the conclusions of the assessment.

In the actual construction of the boat, the canopy and the hull are connected using a combination of bolted joints and adhesives. For this analysis, the interface between the hull and the canopy was modeled as a singular body with a thickness of 0.75 inches (the sum of the hull and canopy thicknesses in the overlapping region). This is a reasonable assumption as it does not contribute to the overall structural stiffness of the lifeboat.

Interfaces between steel surfaces and fiberglass surfaces were modeled using the shell composite lay-up method. Composite shell elements containing the appropriate thicknesses and material properties of the metallic and fiberglass layers were assigned to the composite shell at these interfaces. For example, the interface between the engine mount and the fiberglass was modeled as a 2-layer shell composite with steel thickness and material properties assigned to one layer of the composite and fiberglass thickness and material properties assigned to the other layer.

SOI and the USCG determined that the total weight of Lifeboat 6 was approximately 8,781 lbs at the time of the incident. Certain objects and features (e.g. engine, steering module, water pump system, etc.) that contributed to the overall weight of the lifeboat were not modeled in the finite element model to reduce the complexity of the model. The weight of the engine was simulated via a traction load of 250 lbs (500 lbs accounting for symmetry) applied at the center of the engine cradle as shown in Figure 181. The acceleration of gravity was then calculated such that the target weight of 8781 lbs was achieved. This method assumes that the weight of the boat is distributed evenly throughout the model. The total weight of the lifeboat in the Abaqus model was 8,686 lbs when solving for the dead weight of the lifeboat with the applied engine weight.

As the lifeboat is being raised into the davit, the fiberglass canopy contacts the aft bumper. Hard contact was assumed between the aft bumper and the lifeboat using the surface-surface contact formulation in Abaqus.

3.3.5.3.4.2 Load Steps

The simulation was performed in two static steps as follows:

- Step 1 considered only gravity and the engine weight loads on the model, essentially capturing the baseline condition of the boat hanging from a static condition prior to being raised into the davit.


- Step 2 considered the same gravity and engine weight loads while also the introducing the 9.444-inch vertical displacement at the forward and aft lifting shoes. The intent of this step was to capture the contact interaction between the lifeboat and the aft bumper as the lifeboat was raised into the davit.

3.3.5.3.4.3 Results

Convergence difficulties were observed with the finite element model as the lifeboat was forced up into the aft bumper. With all the complexities incorporated into the finite element model, contact was established between the two components but then as the two were forced together, thereby compressing the bumper and the lifeboat, the deformation was such that a converged solution was unachievable beyond a certain vertical displacement with the data that were available. Therefore, the decision was made to perform a sensitivity study whereby the aft bumper would be modeled with a representative rubber material, able to deform extensively, and also as a rigid bumper, allowing for minimal deformation of the bumper.

For the model with the aft bumper modeled as rubber, the lifeboat was lifted into the bumper approximately 3.1 inches before the model was unable to achieve a converged solution. For the model with the rigid bumper, the lifeboat was raised approximately 1.08 inches into the bumper before the break stress of the fiberglass was achieved. If it is assumed that the point at which the bumper model fails to converge is the point at which the rubber material ceases to absorb any additional elasticity (i.e. begins to behave as a rigid bumper). One could then approximate the total travel up into the bumper by summing the maximum vertical displacement between the bumper model and the rigid bumper model. Considering this and the model results, the total vertical displacement into the aft bumper would have been approximately 4.18 inches before the break stress of the fiberglass near the bumper was achieved. Stress contours for the lifeboat with only gravity and engine weight loading applied are shown in Figure 182 while stress contours of the lifeboat raised approximately 3.1 inches into the aft bumper are shown in Figure 183 – Figure 184 for various lifeboat components.

With the lifeboat raised approximately 3.1 inches into the aft bumper, the maximum stress at the aft lift shoe was 869 MPa (126 ksi), which exceeds the SMYS of the aft shoes. Note that no yielding was noted at the aft shoes during visual examination. The extreme deformation and strain contours of the aft bumper are shown in Figure 185. Minimal lateral deflection in the starboard direction was noted in the model in the vicinity of the engine cradle. A contour plot showing the lateral deflection is shown in Figure 186, with negative values indicating a deflection towards the starboard side and positive values indicating



deflection towards the port side of the lifeboat. The maximum deflection near the engine cradle was approximately 0.2 mm in the starboard direction.

Considerable forces were observed at the aft lift shoe as the boat was raised into the aft bumper. These forces were significantly greater in the rigid bumper case than in the bumper case. A plot of the reaction forces at the forward and aft lift shoes as a function of vertical displacement is shown in Figure 187 and Figure 188 considering a rubber and rigid bumper, respectively.

3.3.5.3.4.4 Conclusions

As indicated in Section 3.3.5.3.1, the objective of the FEA modeling was to investigate loading at the contacts of the aft bumpers with Lifeboat 6 as a possible contributor to the incident. At the engine mount region (see Figure 40) or the failure at the keel (see Figure 42), aforementioned areas of interest, significant deflections or stresses were not observed in the model. Additionally, stresses within the hull at the aft bumper contact were insufficient to result in failure of the hull. This is consistent with the observations from the field investigation. As the model had convergence issues, additional work is needed to determine if it is possible for the lifeboat to have been pulled the full 9.444 inches of vertical displacement at the aft and / or if there is another physical element of the lifeboat being pulled into the davit that has not been properly incorporated.

4.0 FAILURE SCENARIOS

4.1 Approach

A fault tree analysis was performed as part of the investigation of the Lifeboat 6 incident. Three fault trees were evaluated using laboratory testing performed at DNVGL, documentation related to the incident, and information provided by SOI. The results of the fault tree analysis are discussed below. Within the fault tree, contributing factors were identified and evaluated for their contribution to the release of the aft hook of Lifeboat 6. The contributing factors (located at the bottom of each branch of the fault tree) are color-coded as green or red. This color coding is representative of the following categories:

1. Green: Evidence from site, laboratory testing, and / or document review support that the fault tree event is a contributing factor.
2. Red: Evidence from site, laboratory testing, and / or document review support that the fault tree event is likely not a contributing factor.

Figure 189 is a schematic showing the fault tree used to identify contributing factors to the release of the Subject Aft Hook.

4.2 Failure of Non-Hook System Components

The possibilities of fiberglass components, fall cables, and / or ring failure(s) were considered as potential contributing factors to the release at the aft hook.

The recovered portions of Lifeboat 6 were inspected at Harvey Terminal. Areas of interest from the fiberglass components were removed from the interior and exterior of Lifeboat 6 for examination in the laboratory. The results of the laboratory examination indicated that the fiberglass components failed due to a single overload event. Finite element analysis of the Lifeboat 6 being pulled into the davit to simulate loading conditions showed that the damage identified at these areas of interest would not have failed at 3.1 inches of vertical displacement. Additional work to the FEA model would be required to determine if the remaining ~6.3 inches of vertical displacement would have resulted in failure at areas of interest or if the areas of interest failed due to the lifeboat striking the water.

Lengths of the fall cables with rings from the aft and forward of Lifeboat 6 were provided to DNV GL for visual inspection and laser scanning. There was no evidence of elongation or broken wires within the fall cables. Similarly, no ovality or elongation of the rings was noted.

Based on the testing performed, it is unlikely that failure(s) of the non-hook system components contributed to the incident.

4.3 Hook Point Load

The possibility of a hook point load due to improper installation of the ring into the aft hook was considered. Load tests, using an Exemplar Cable, Exemplar Hook, Exemplar Ring, and Subject Release Unit, were performed. The results of the load testing indicated that the damage accumulation at the hook point of the Exemplar Hook and the Exemplar ring were not consistent with the damage identified at the point of the Subject Aft Hook.

4.4 Locking Shaft of the Subject Aft Hook Rotated Unintentionally

The possibility of the locking shaft from the Subject Aft Hook rotating unintentionally was considered as a contributing factor to the incident. The term “unintentionally” is being used in this case to describe rotation of the locking shaft without a human purposefully activating the release handle of the Subject Release Unit. For the locking shaft to operate unintentionally, the control cable and / or the Subject Release Unit would have to be compromised.



4.4.1 Hook System Components Compromised

Damage to the locking shaft, the release handle, and / or the clevises and bulkhead nuts was considered as a possible contributing factor. No evidence of a compromised function due to significant mechanical damage was identified on these components. It should be noted that some minor mechanical damage was identified on the edge of the locking shaft from the Subject Aft Hook. The mechanical damage was the same width as the roller for the hook and appeared to be in the direction of the hook moving passed the locking shaft. This may indicate that a sufficiently high load at the Subject Aft Hook caused the roller of the hook to move from the near edge or edge across the flat of the locking shaft.

4.4.2 Control Cable Compromised

Several of the layers comprising the Subject Aft Cable were compromised. Specifically, the outer layer (cover) exhibited mechanical damage and fatigue, the wire layer exhibited significant corrosion damage, and the liner layer exhibited tearing and puncture. Each of the damage mechanisms described above were evaluated and classified as either corresponding to a single overload event or an extended damage accumulation event.

4.4.2.1 Single Overload Event

In this case, a single overload event is defined as a tensile load applied along the axis of the control cable at a sufficiently high stress to fail the outer layers. Laboratory examination of the Subject Aft Cable showed evidence of wear and cracking in the cover, corrosion within the wire layer, and cycling of the liner layer. Though a final overload likely occurred to fail the liner layer, a single overload event was not associated with the failure of the Subject Aft Cable.

4.4.2.2 Damage Accumulation

Damage accumulation to the Subject Aft Cable was evaluated as a contributing factor to the incident. Contributions from the environment and mechanical damage are discussed separately below.

4.4.2.2.1 Environment

Laboratory testing of the cover and liner layers (i.e. plastic components), did not show evidence of degradation associated with chemicals or thermal exposure. However, the wire layer showed evidence of significant corrosion. The corrosion appeared to have occurred at a break within the cover that allowed water ingress. Once the water penetrated the cover layer, corrosion of the carbon steel wire layer initiated. The corrosion at the failure location was more significant than the corrosion at other breaks in the cover. This suggests that the wire layer had corroded prior to the incident and this was corroborated with photographs from an inspection of Lifeboat 6, approximately one month prior to the incident.

4.4.2.2.2 Mechanical Damage

The possibility of cyclic loading to the wire layer was considered. During laboratory testing, no evidence of fatigue was identified at the conduit. However, mechanical damage and cracking to the cover as well as elongation and compression of the liner layer were identified. An area of contact between the cover and the helmsman's station appears to have been the initiation site for mechanical damage. Due to the cover becoming compromised, water ingress occurred resulting in significant corrosion of the wire layer. As the voluminous corrosion continued, cracks within the cover layer developed and propagated, as evidenced by the progressive crack fronts within the cover that opened the cover layer further. Buckling, plastic deformation, and punctures were visible in the liner suggesting that intended functioning of the control cable from the release unit resulted in the damage.

5.0 CONCLUSIONS

The results of the investigation indicate that the unintended release of the Subject Aft Hook of Lifeboat 6 was a result of a degraded and compromised aft control cable. The control cable exhibited significant corrosion, full penetration around the circumference, of the structural wire layer allowing for externally applied loads to rotate the locking shaft of the Subject Aft Hook to an open position.

Failure of the Subject Aft Cable is suspected of progressing in the following manner: (1) mechanical damage to the cover due to contact between the control cable and the helmsman's console, (2) water ingress leading to significant corrosion of the wire layer, (3) voluminous corrosion product resulting in fatigue of the cover layer and the cover opening further, and (4) buckling and elongation of the liner layer as a repetitive action associated with the functioning of the control cable. Due to the damage to the Subject Aft Cable, the locking shaft of the Subject Aft Hook was not fully closed (i.e. in a slightly more open position) requiring less rotation to release the hook. The compromised cover and wire layer would have allowed for external loads applied to the control cable to translate onto the inner member of the control cable that is directly linked to the locking shaft, thereby rotating the locking shaft to an open position.



Figure 1. Photograph of Lifeboat 6 in the davit on the Auger Platform prior to the incident. Photograph provided by SOI.

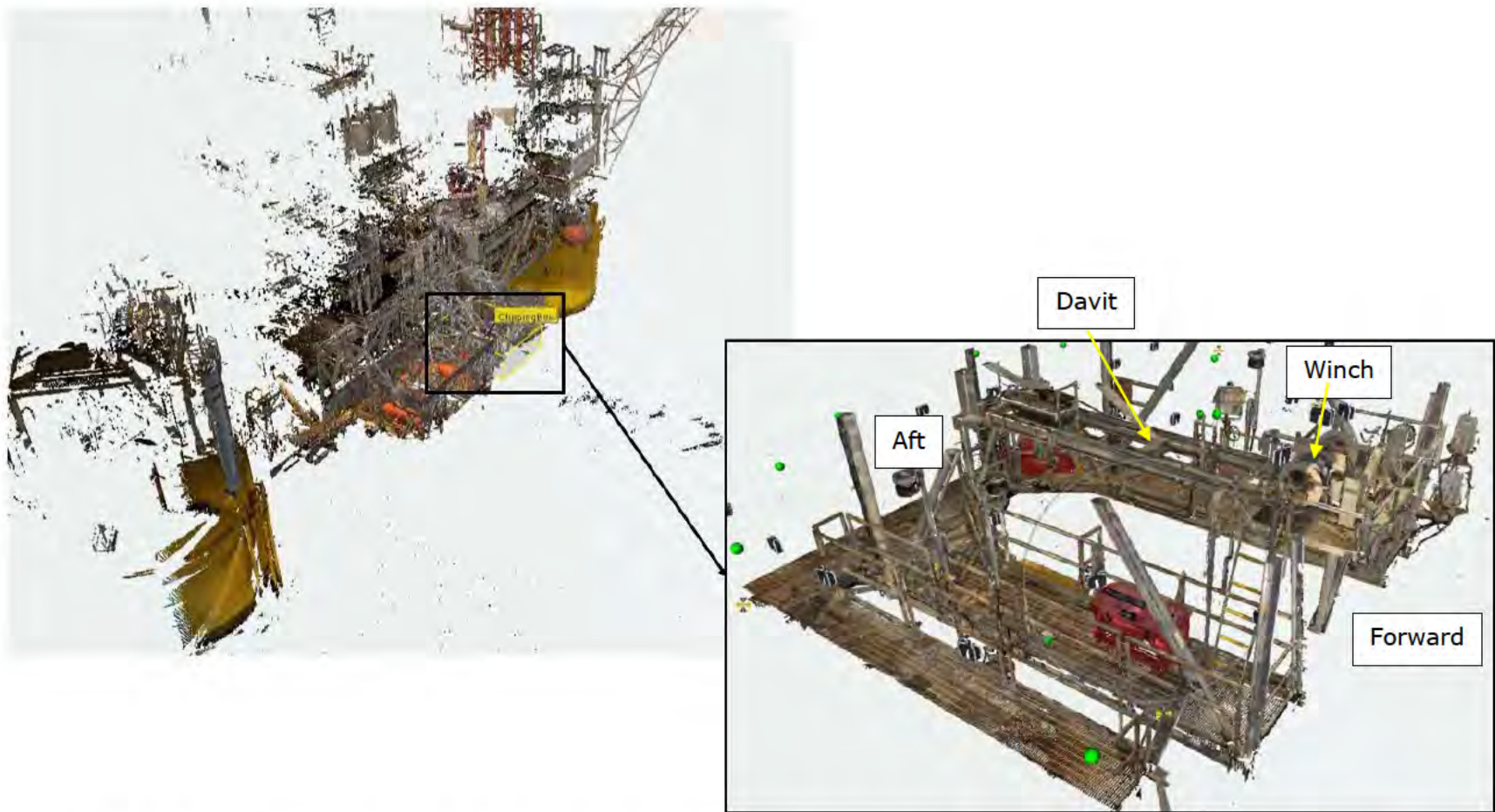


Figure 2. Laser scan of the davit used with Lifeboat 6 on the Auger Platform. Laser scan data provided by SOI.

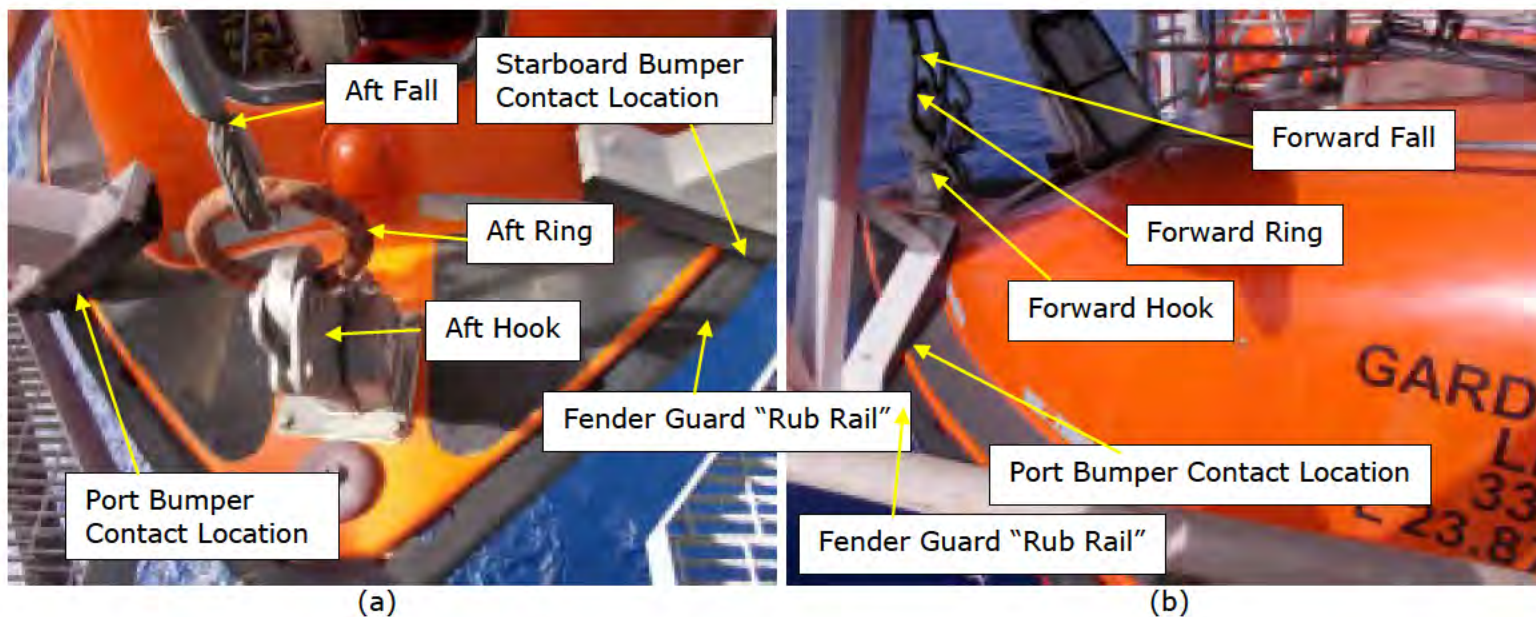


Figure 3. Photographs of the (a) aft and (b) forward ends of Lifeboat 6 in the davit on the Auger Platform before the replacement of the winch, fall cables, and rings (photograph from original equipment manufacturer [OEM] service report FS6540, approximately June 2014). Photographs provided by SOI.



Figure 4. Photograph of the placard from Lifeboat 6 taken after the incident.

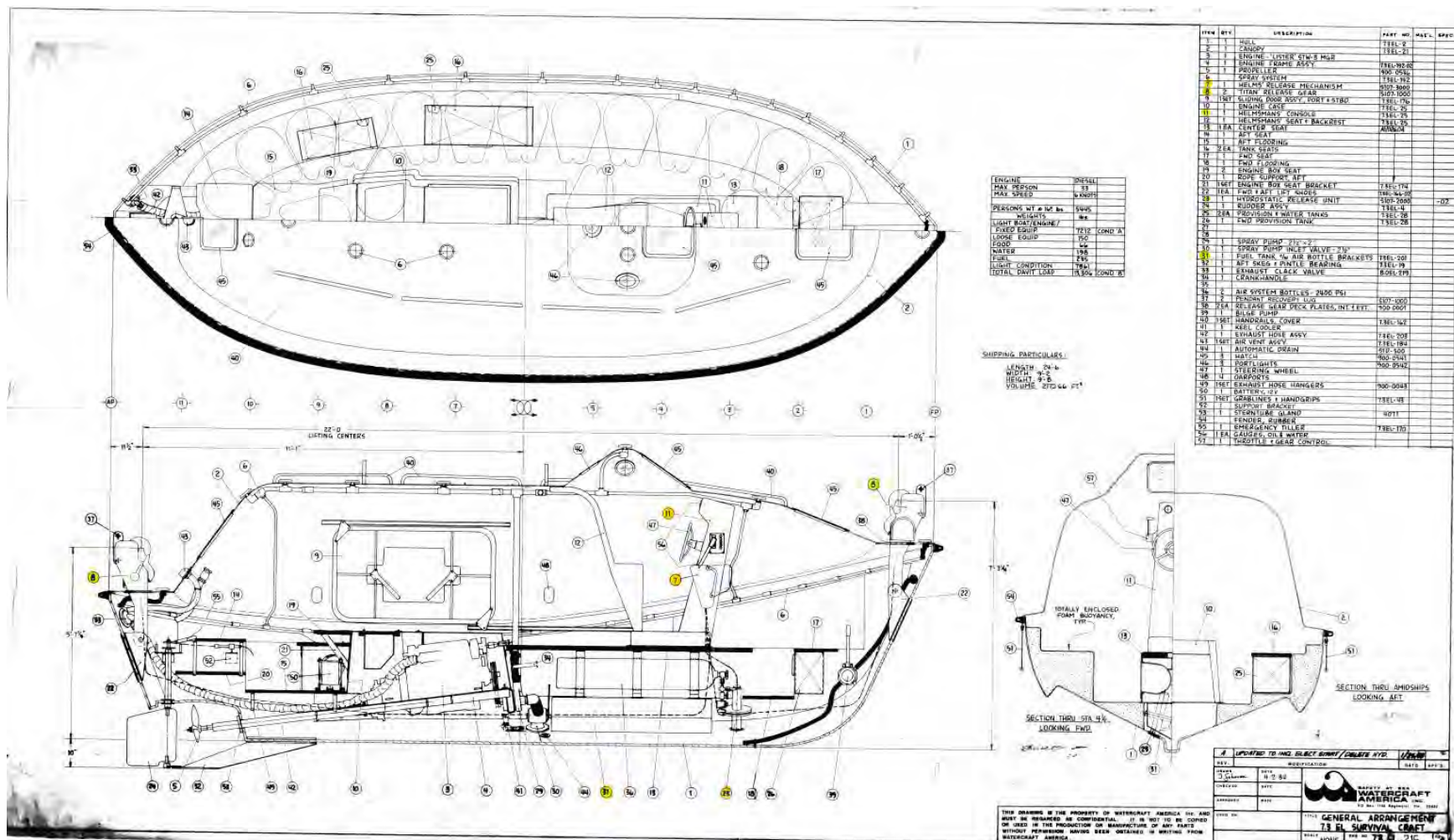


Figure 5. Drawing Number 7.3 EL-215-Rev A showing the dimensions and the components of an EL Survival Craft. The components used in DNV GL's reconstruction have been highlighted with yellow. Drawing provided by Palfinger to SOI.

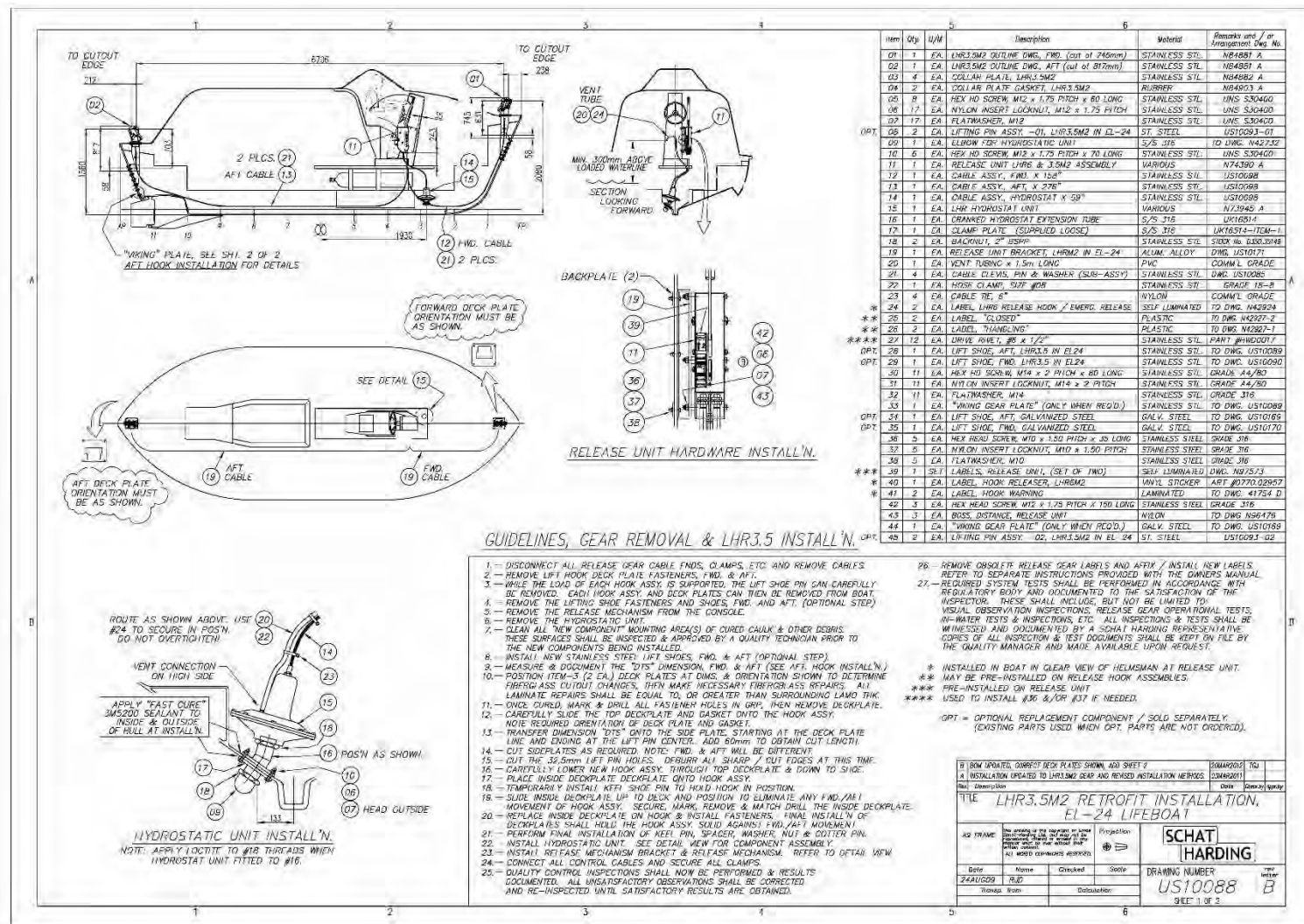


Figure 6. Drawing Number US10088, Sheet 1 of 2 showing the retrofit installation for the LHR3.5M2 hooks in an EL-24 Lifeboat. Drawing provided by Palfinger to SOI.

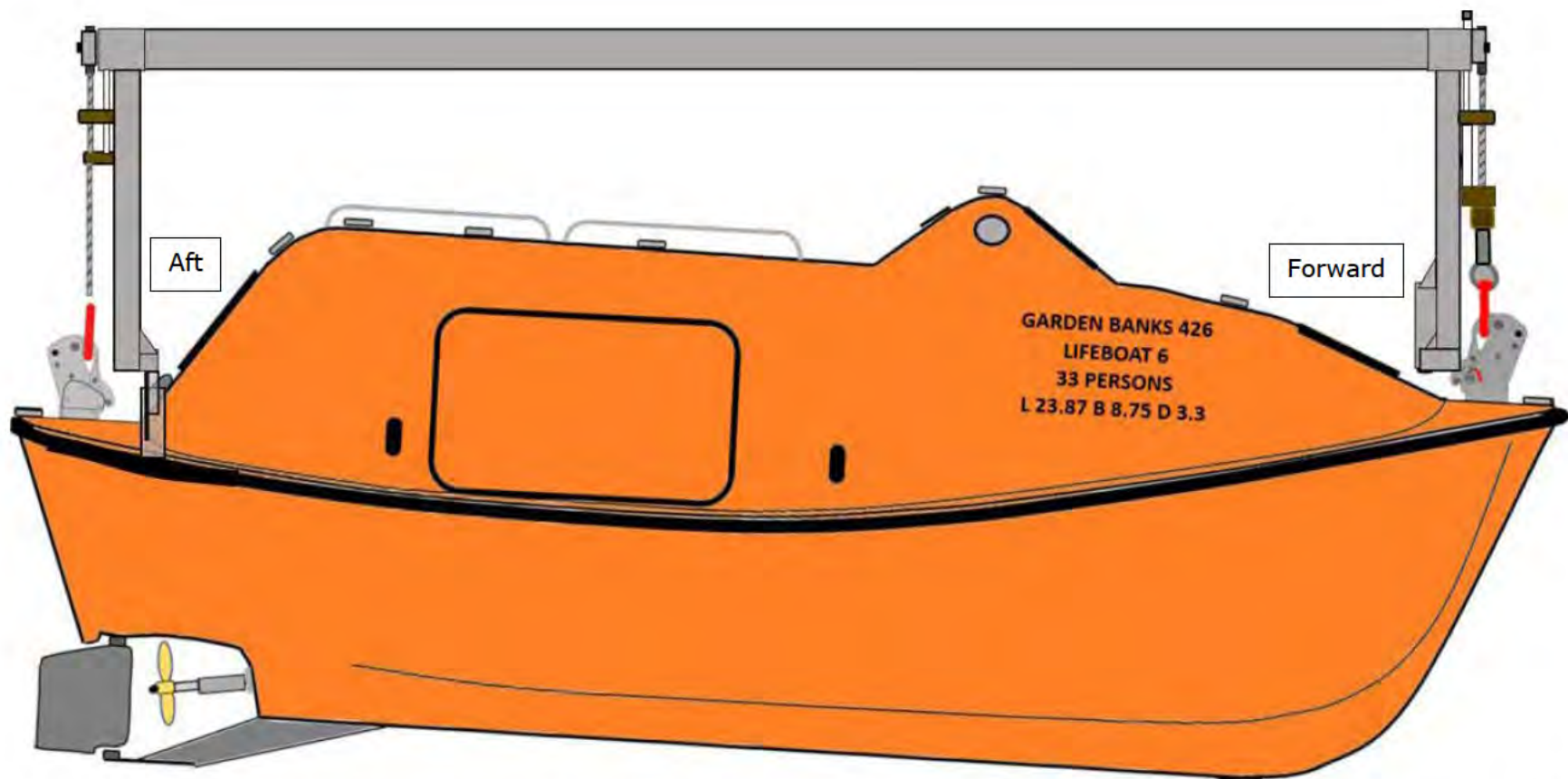


Figure 7. Drawing showing the contact between Lifeboat 6 and the bumpers based on the measurements of the twin fall cables that were performed after the incident. The aft is in contact with the bumpers; however, the forward is not in contact. Drawing designed by SOI.



Figure 8. Photograph showing the condition of Lifeboat 6 in Harvey Terminal after the incident, as viewed from the forward, port side.



Figure 9. Photograph showing the condition of the Lifeboat 6 in Harvey Terminal after the incident, as viewed from the aft, starboard side.

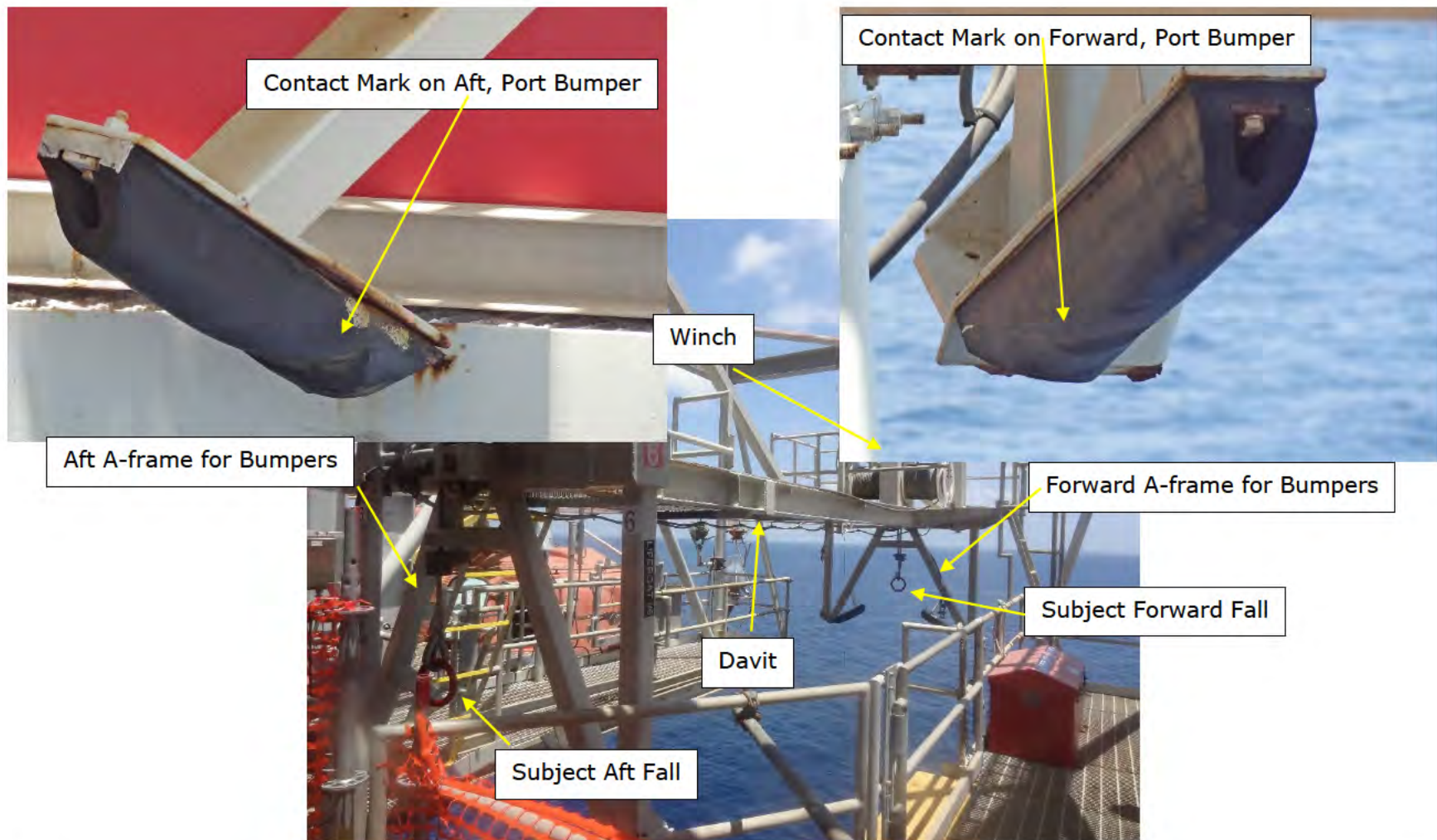


Figure 10. Photographs showing the condition of the davit and port bumpers after the incident. Photograph provided by SOI.

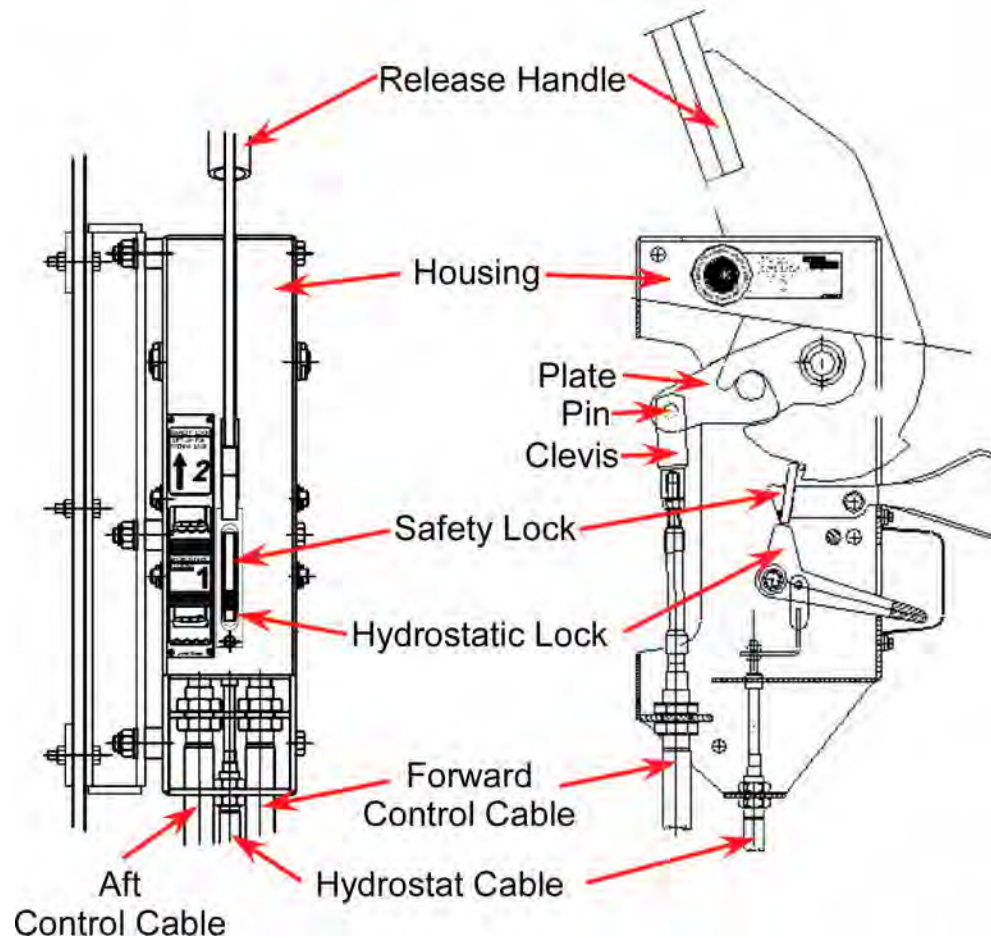


Figure 11. Drawings of the Subject Release Unit showing the different components of the release unit. The drawing on the left is from Drawing Number US10088-Rev B, Sheet 1 of 2 (front) and the drawing on the right is from Palfinger Document F10927. Drawing provided by Palfinger to SOI. Note that the drawing shown is for a hook of similar design and not the as-installed hooks.

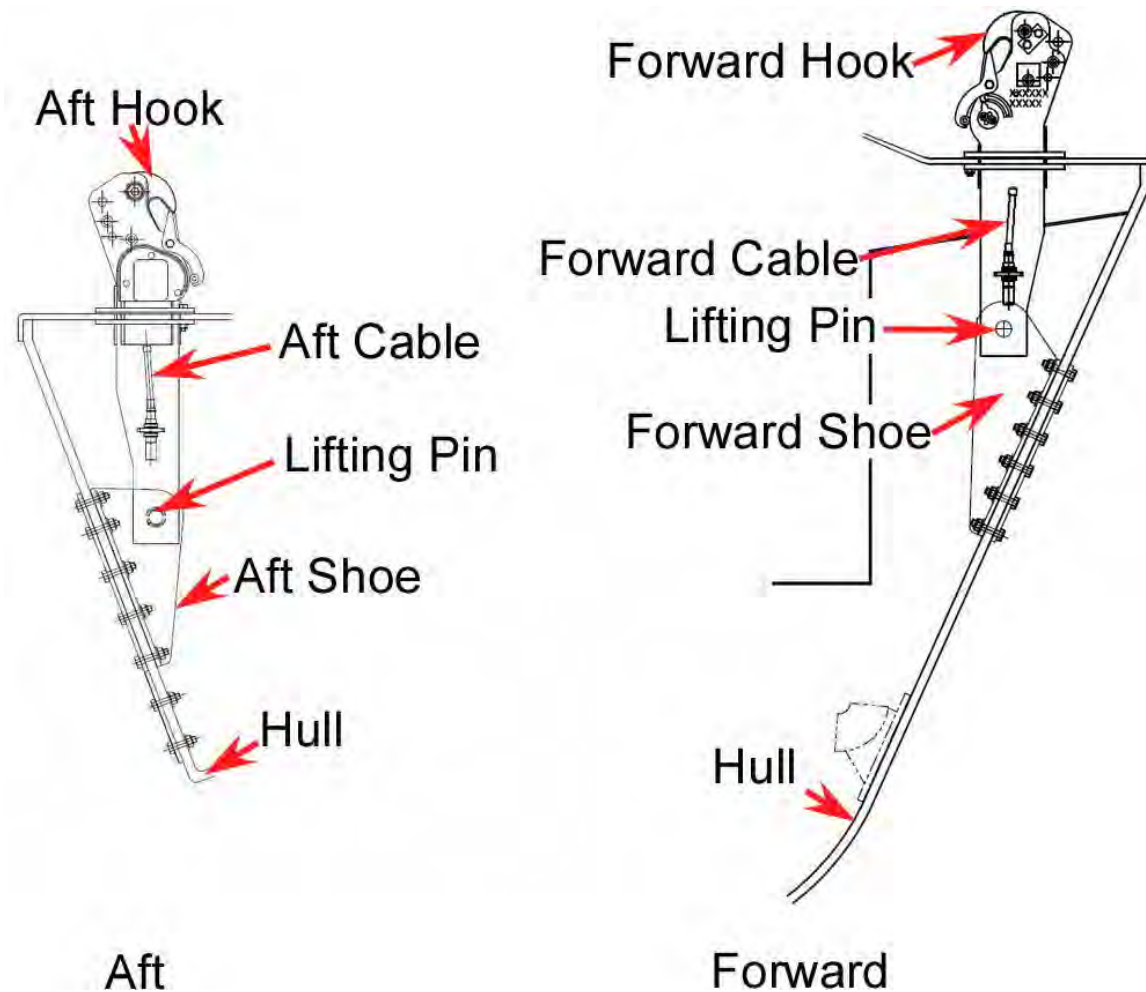


Figure 12. Portion of Drawing Number US10088-Rev B, Sheet 2 of 2 showing the detail of the installation of the aft and forward LHR3.5M2 hooks using LHR shoes. Drawing provided by Palfinger to SOI. Note that the drawing shown is for a hook of similar design and not the as-installed hooks.

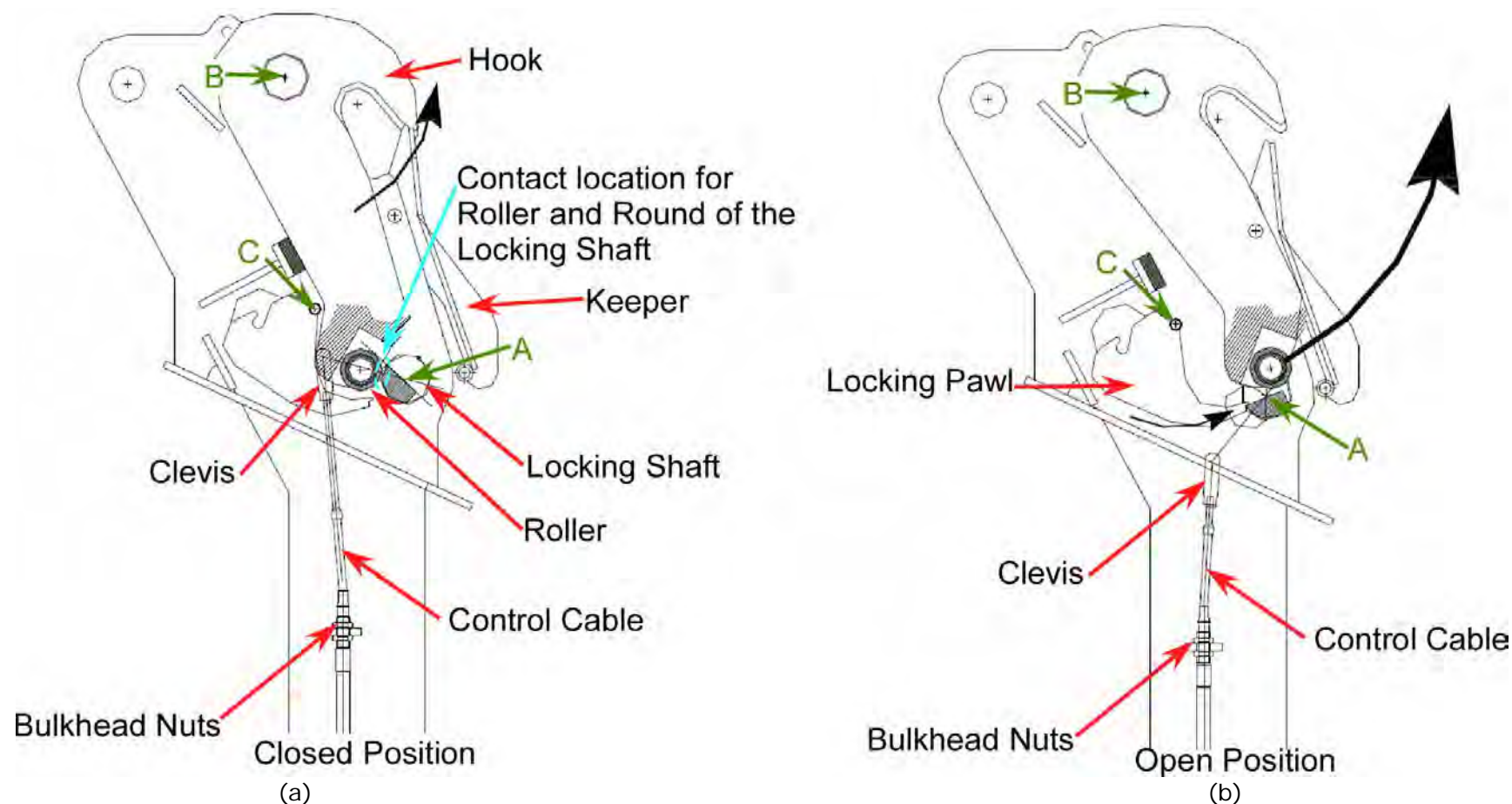


Figure 14. Drawings from Palfinger Document F10927 showing a cross-sectional view of the LHR3.5M2 hook when in the (a) closed position and (b) open position. The location of the clevis, bulkhead nuts, control cable, hook roller, locking shaft, keeper, and locking pawl of the hook are shown. Drawings provided by Palfinger to SOI. Note that the drawings shown is for a hook of similar design and not the as-installed hooks.

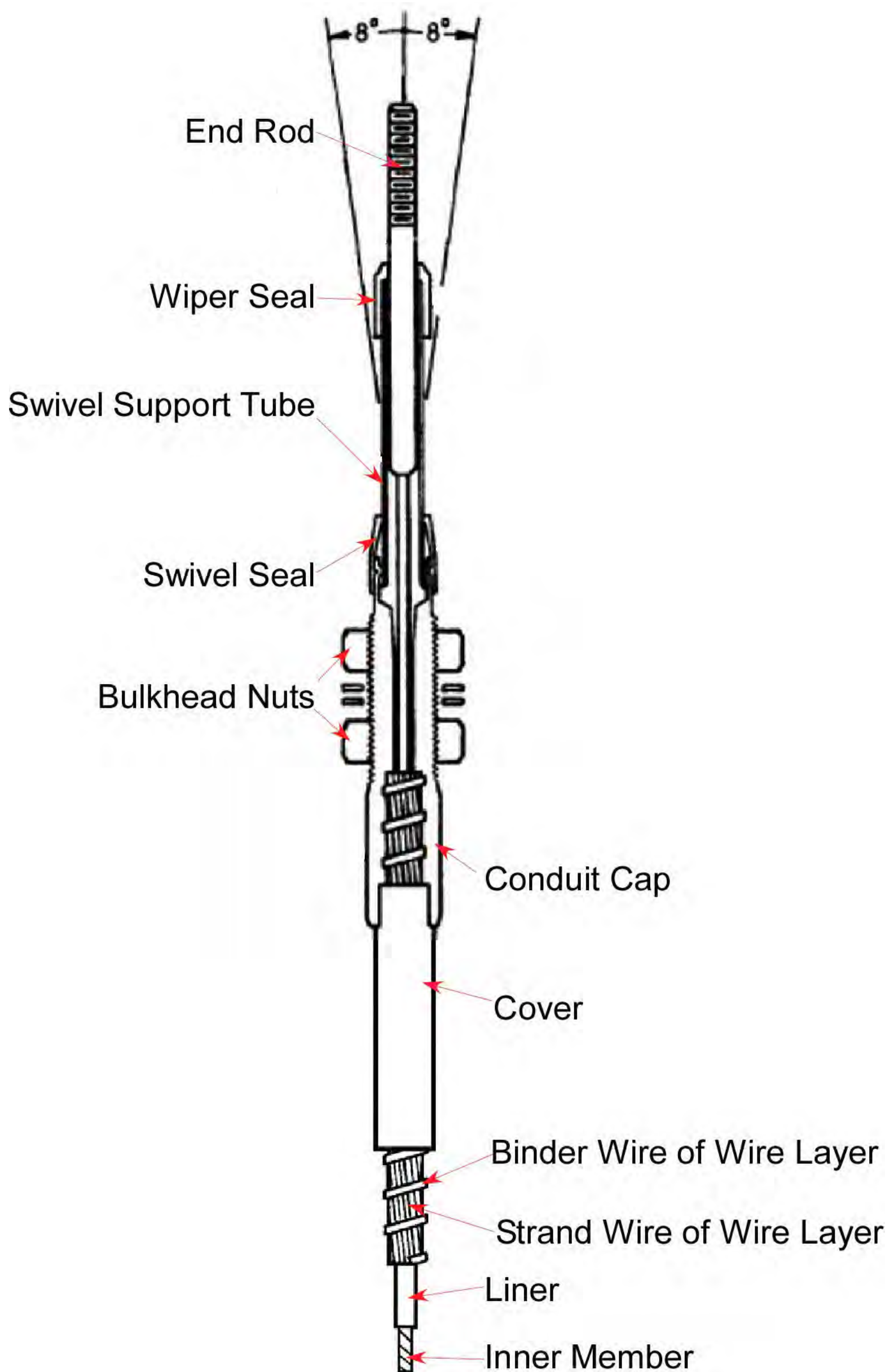
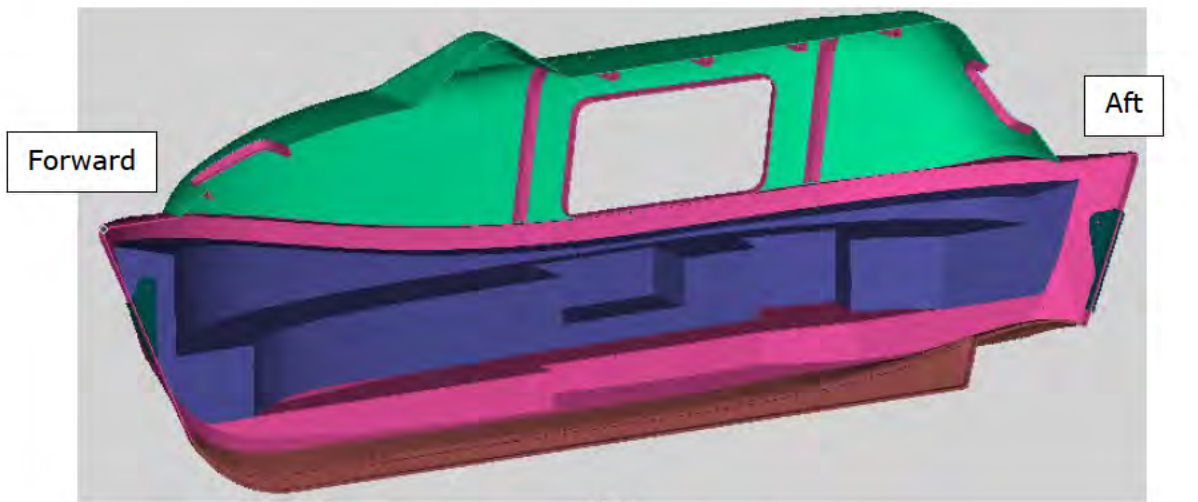
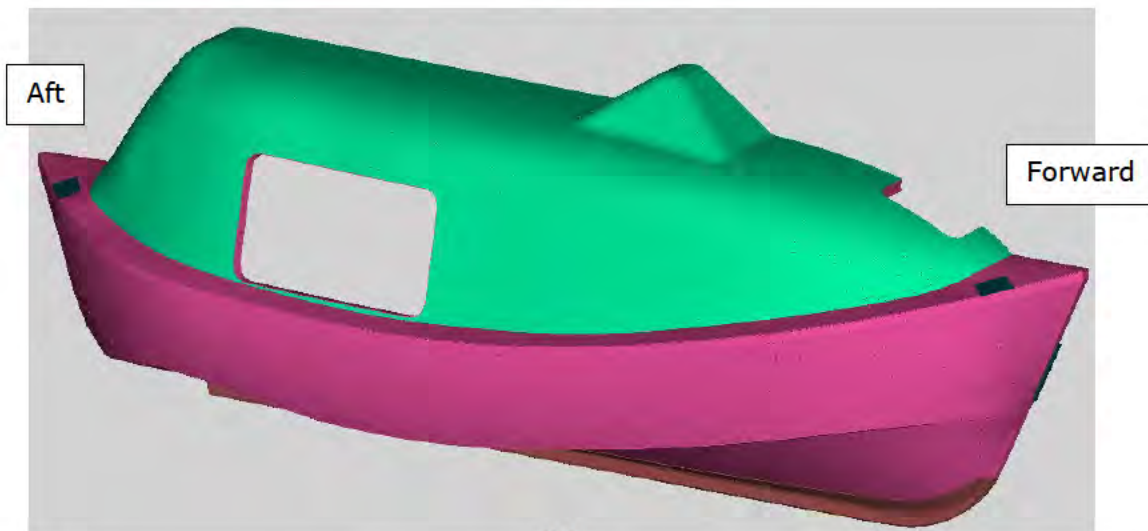


Figure 15. Drawing from Palfinger Document F10927 combined with an image titled “General-structure-of-push-pull-cable” showing the detail of components for the control cables. Drawing provided by Palfinger to SOI.

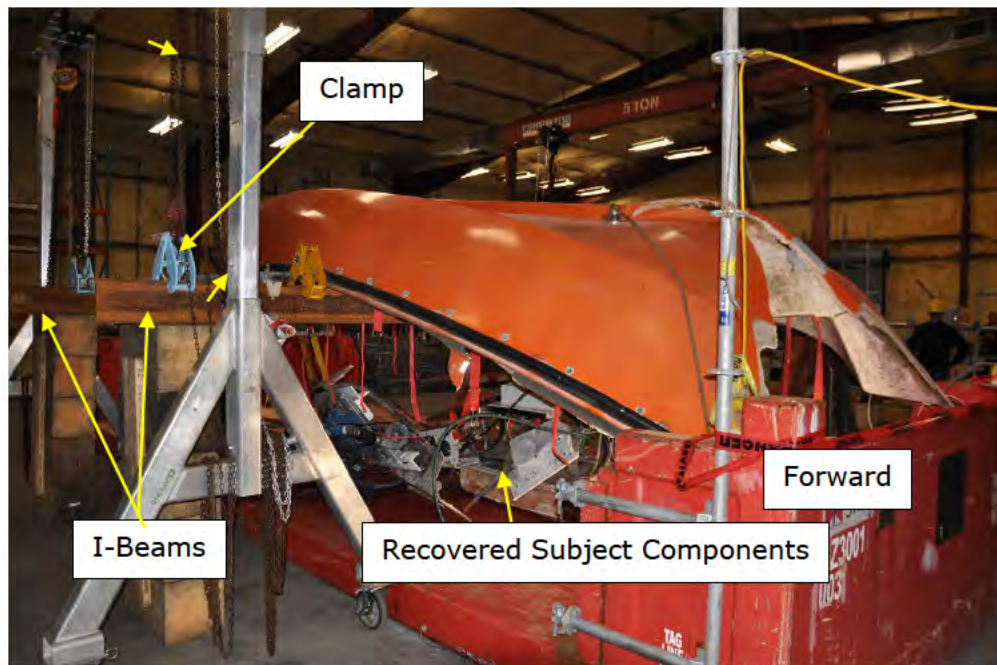


(a)

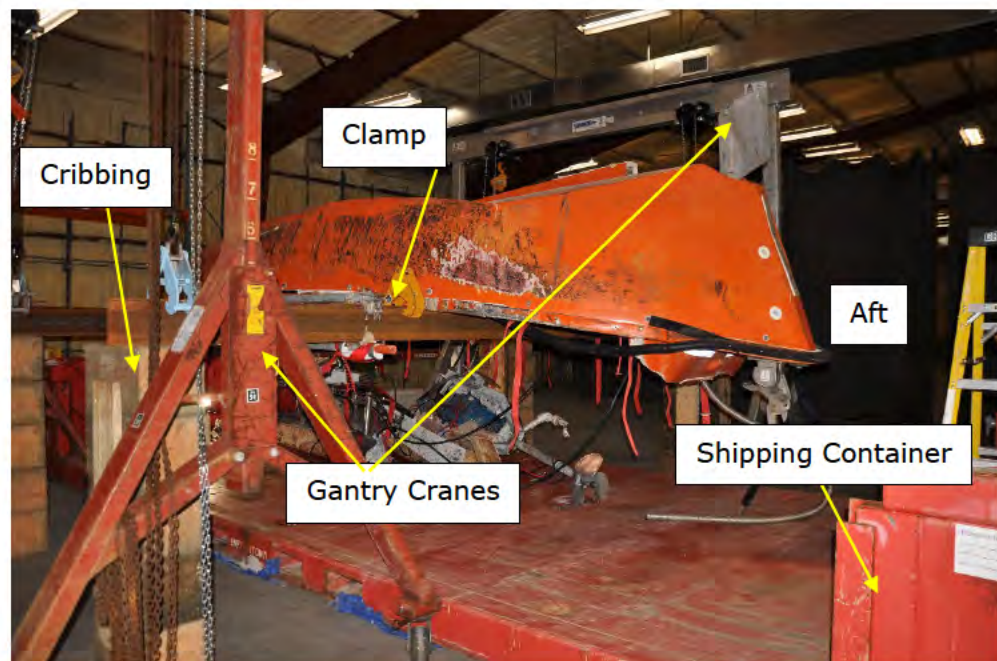


(b)

Figure 16. Schematics of a FEA model showing the nominal wall thicknesses of the fiberglass components of Lifeboat 6 as viewed from (a) the interior and (b) the exterior. The FEA model was produced by Plastic Services Network (PSN) using physical measurements of extracted panels and details from original manufacturer drawings. The colors indicate the following: green is 0.250-inch, pink is 0.375-inch, purple is 0.186-inch, and brown is 0.750-inch wall thickness.



(a)



(b)

Figure 17. Photographs showing Lifeboat 6 and the erected support structure to facilitate inspection of the associated components, as viewed from the (a) forward and (b) aft of Lifeboat 6 at Harvey Terminal after recovery.

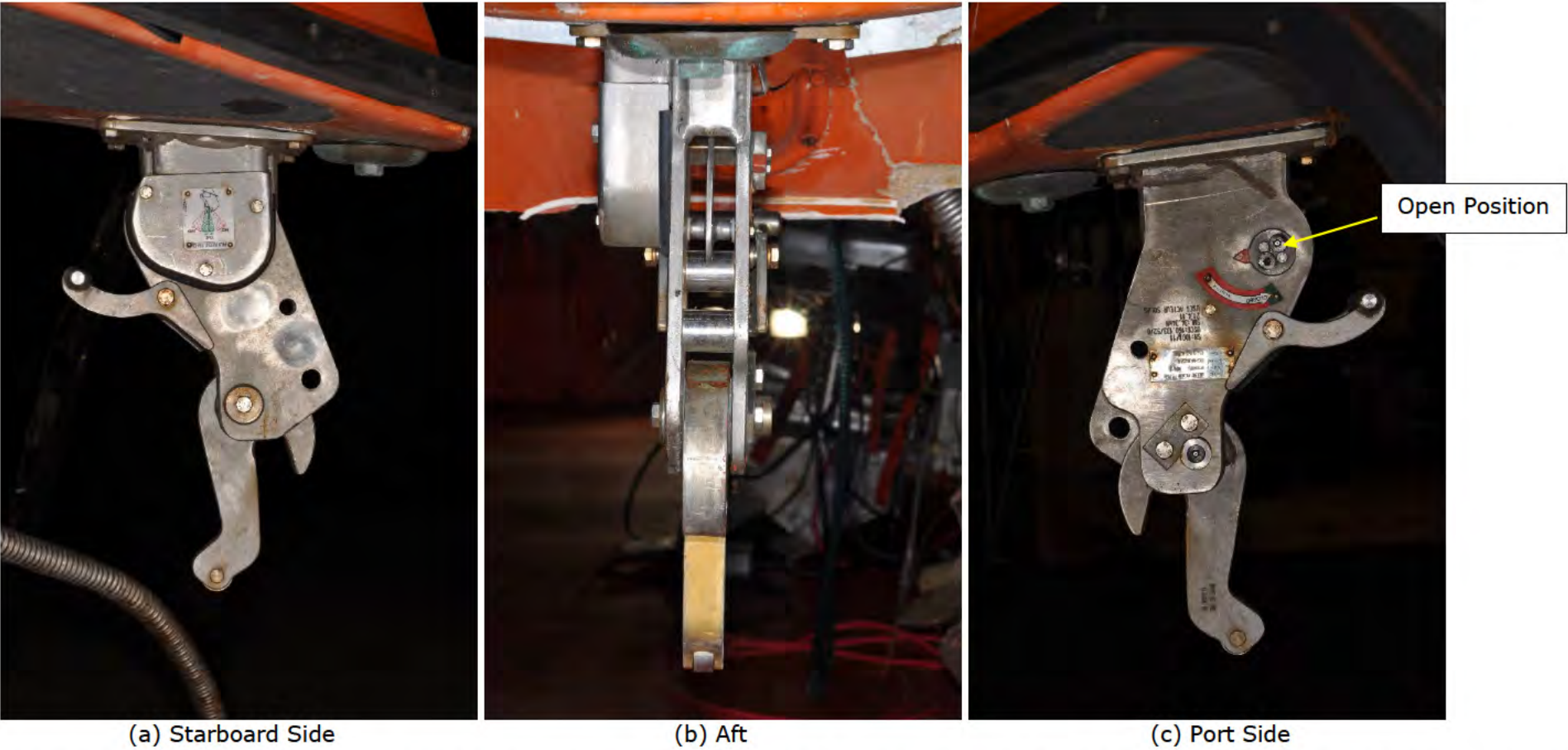
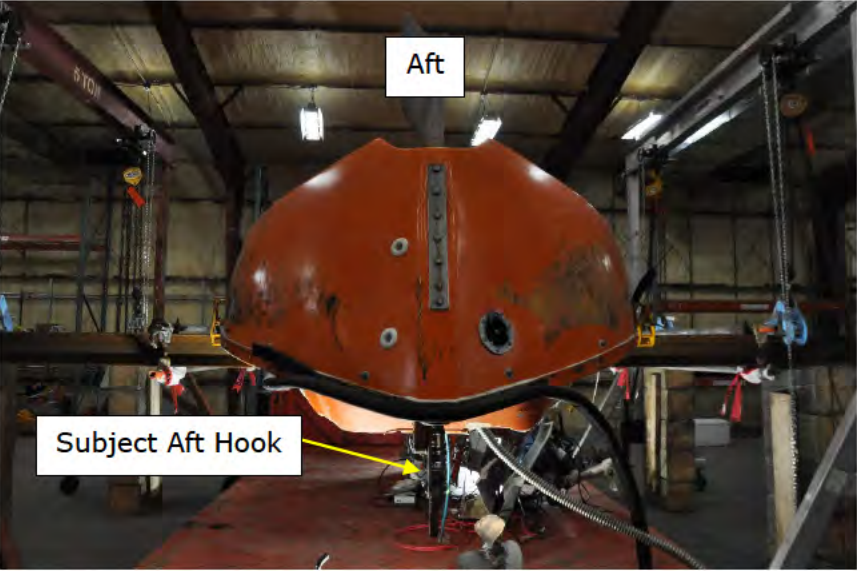
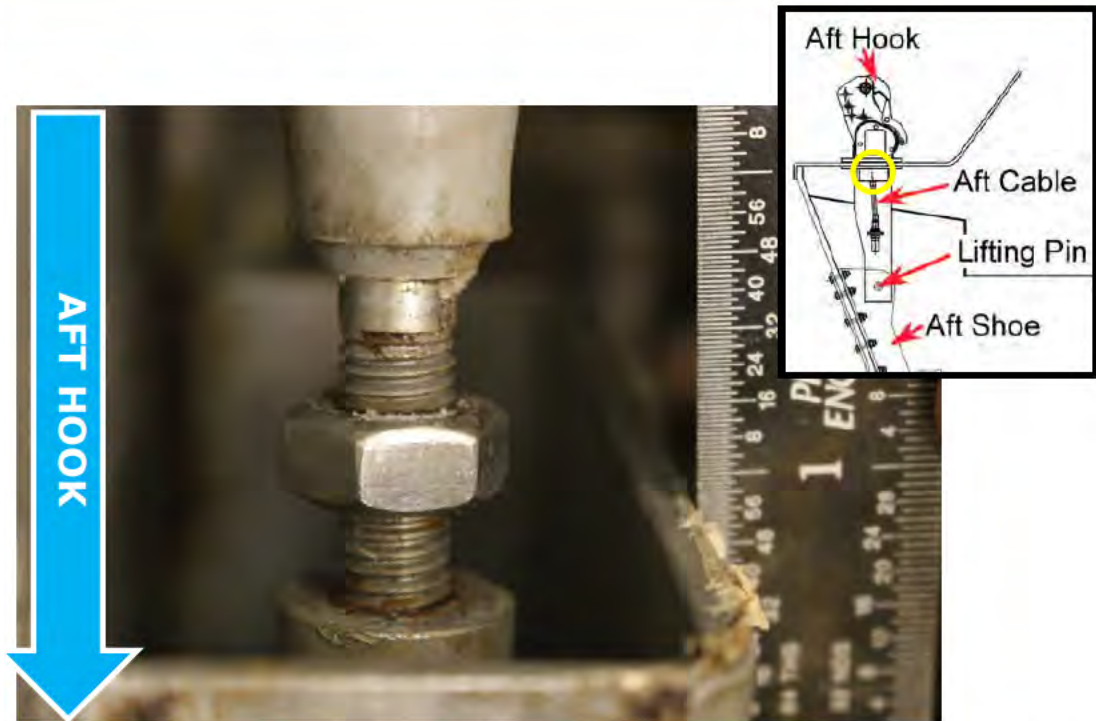


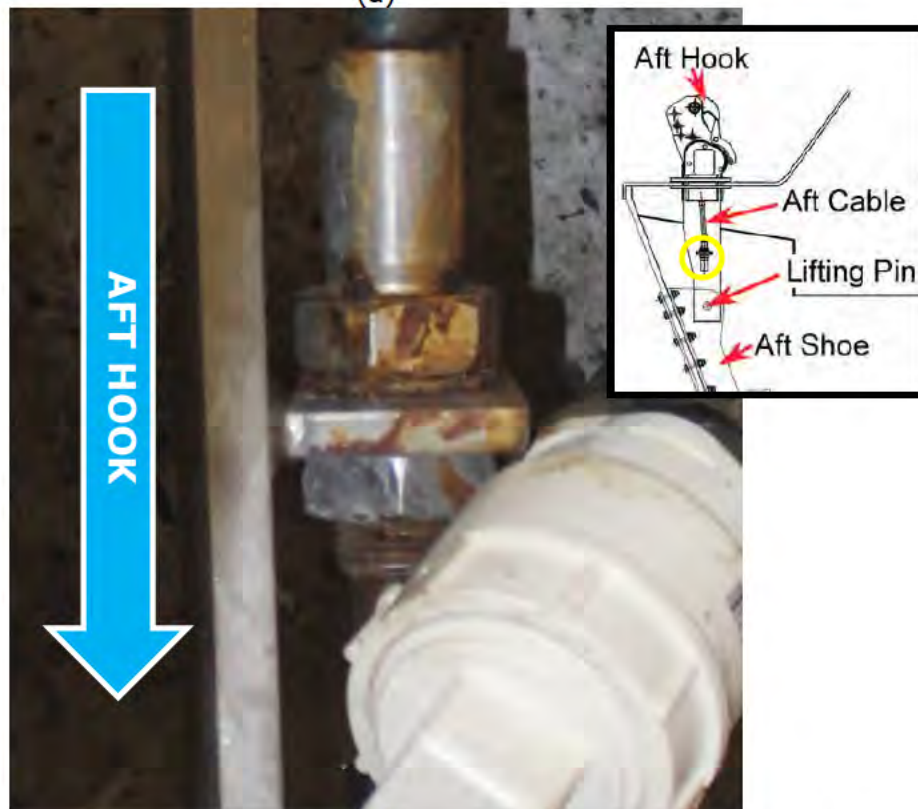
Figure 18. Photographs showing the aft of Lifeboat 6 and the as-found condition of the Subject Aft Hook as viewed from (a) the starboard side, (b) the stern, and (c) the port side.



Figure 19. Photograph of the Subject Aft Cable showing a failure of the outer layers exposing the inner member. The direction of the Subject Aft Hook is noted with the blue arrow. Ruler is in mm.



(a)



(b)

Figure 20. Photograph of the Subject Aft Hook showing the as-found condition of the threaded connections (a) at the clevis and (b) at the bulkhead nuts; the locations of the clevis and bulkhead nuts are shown in embedded schematic. Ruler in top image is in inches.

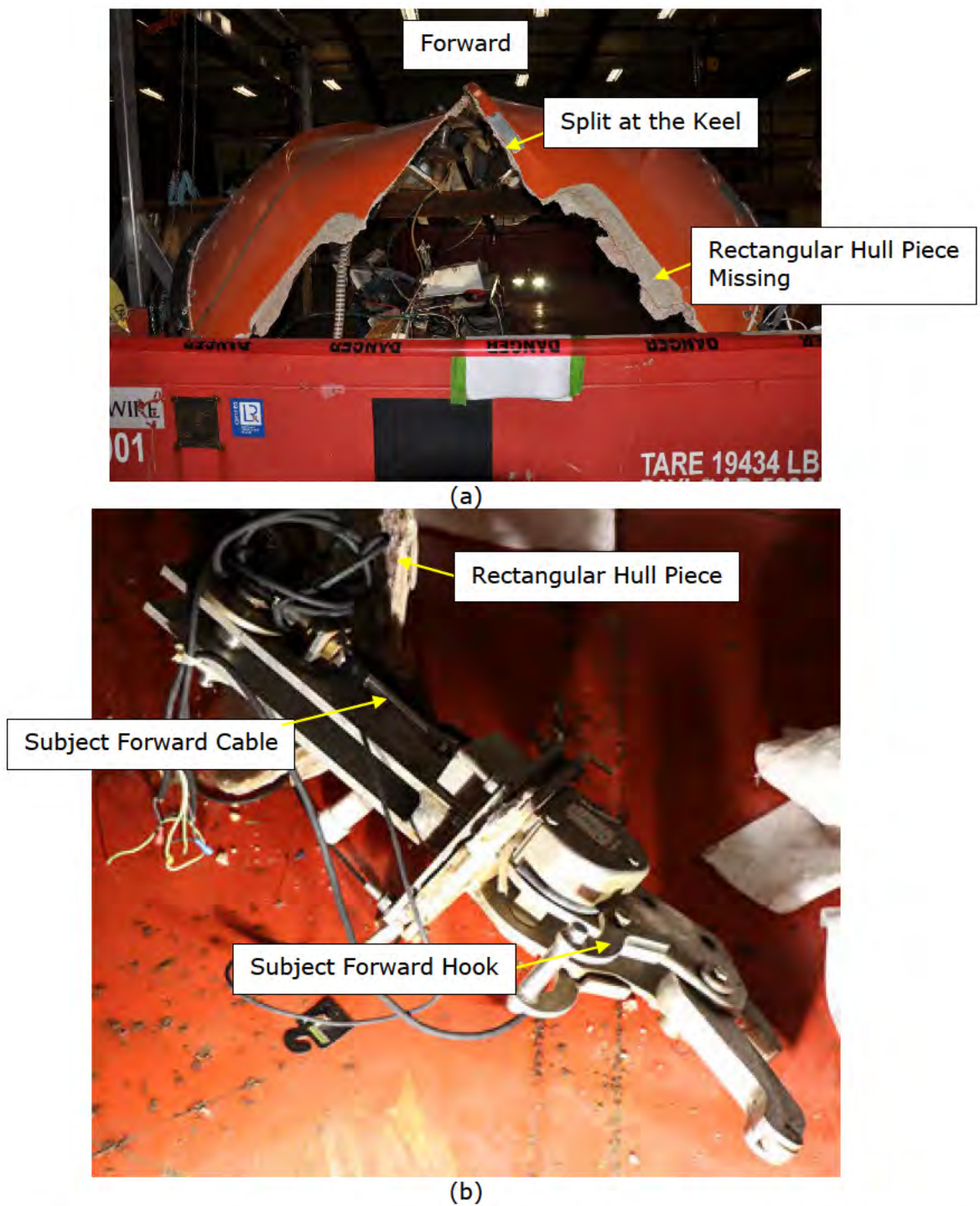


Figure 21. Photographs showing (a) the bow of Lifeboat 6 and (b) the as-received condition of the Subject Forward Hook at Harvey Terminal. Photograph in (b) provided by USCG.

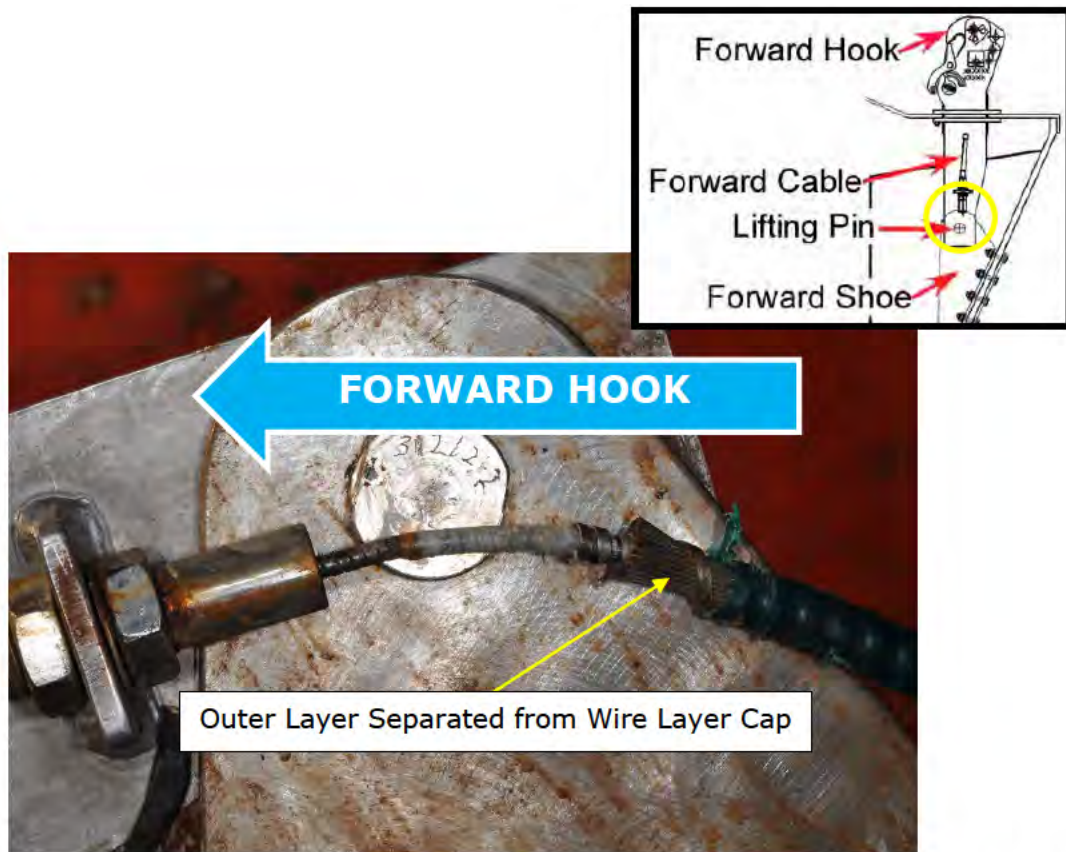
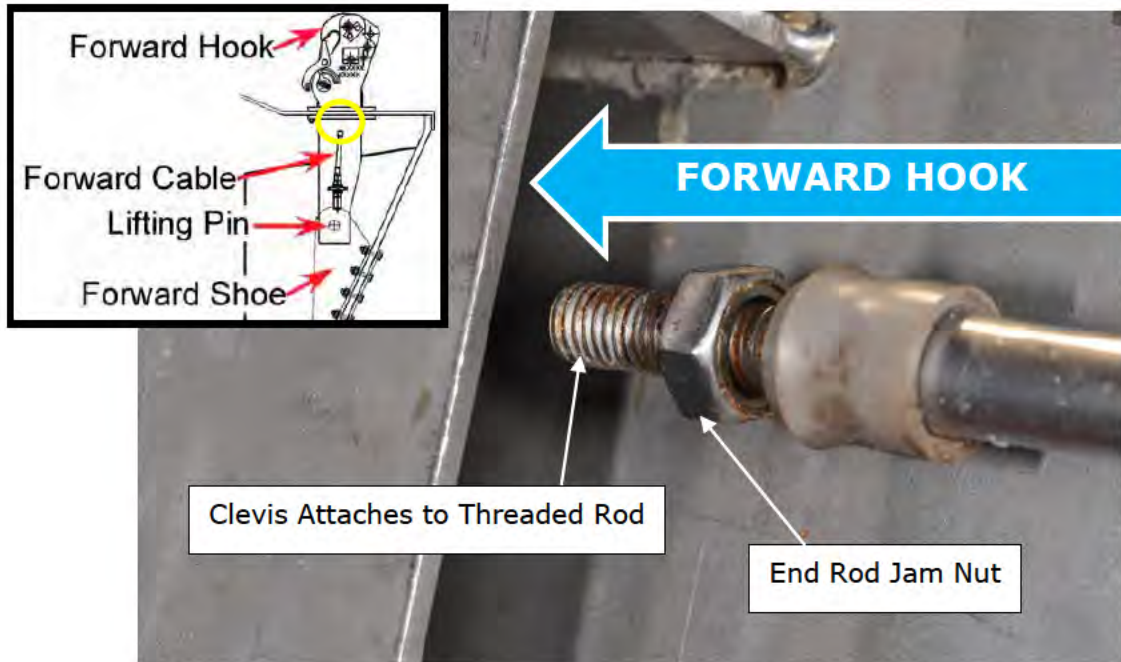
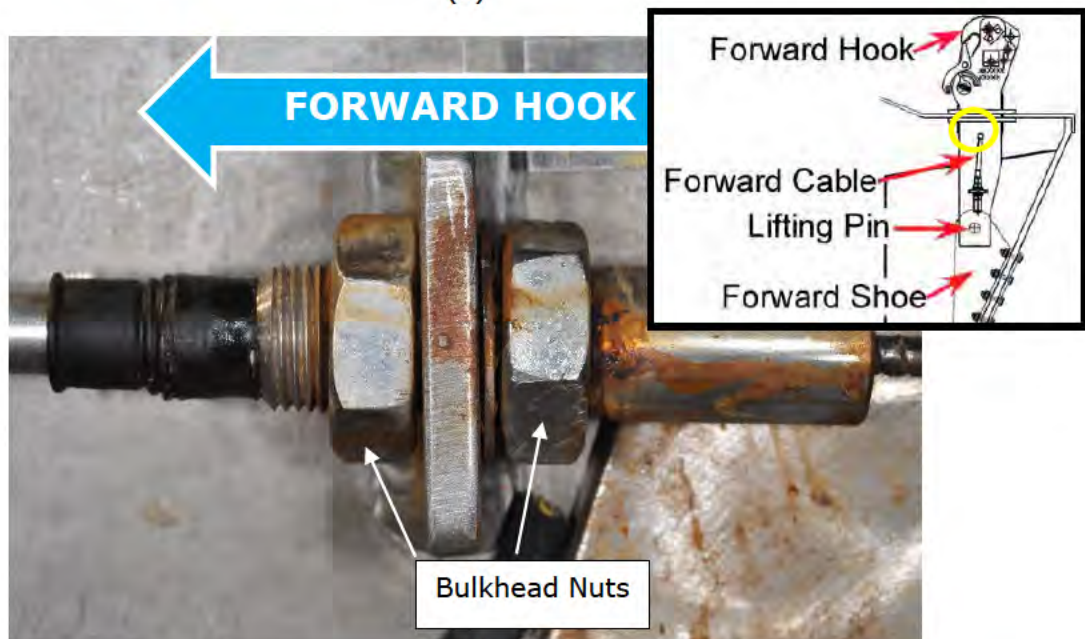


Figure 22. Photograph showing a separation of the outer layers from the conduit cap at the bulkhead nuts of the Subject Forward Cable; location shown in the embedded schematic. The direction of the Subject Forward Hook is noted with the blue arrow.



(a)



(b)

Figure 23. Photograph showing the as-found condition of the threaded connections of the Subject Forward Hook (a) at the clevis and (b) at the bulkhead nuts; the location of the clevis and bulkhead nuts are shown in the embedded schematic. The direction of the Subject Forward Hook is noted with the blue arrow.

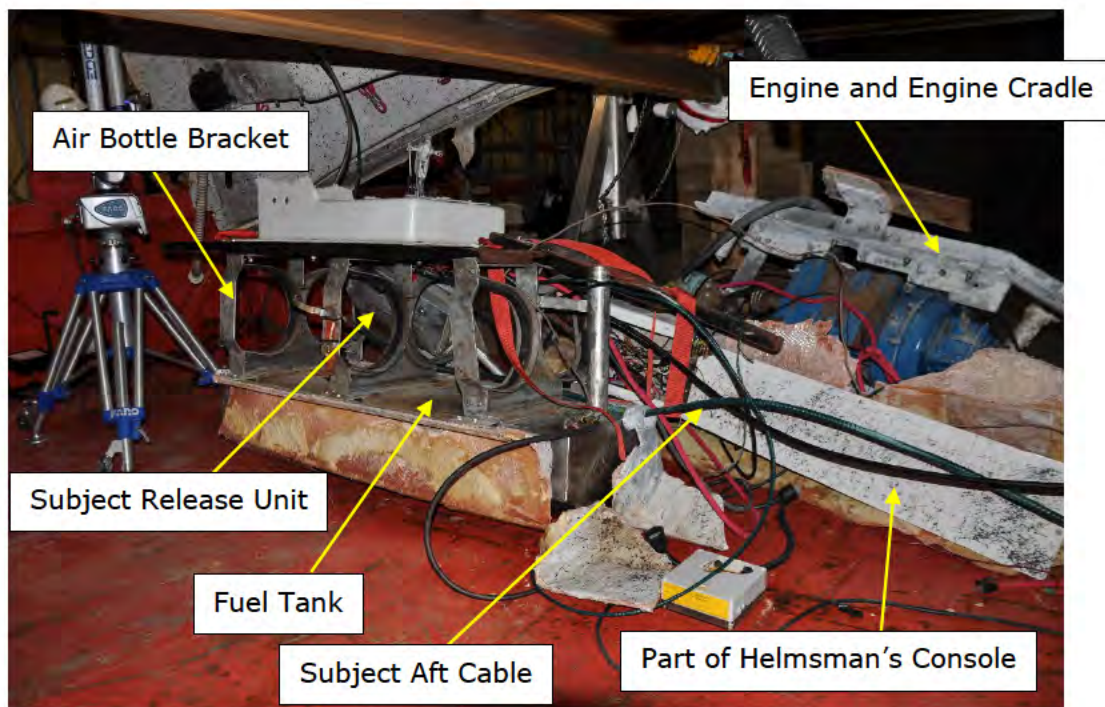


Figure 24. Photograph showing the as-found condition of the internal subject components of Lifeboat 6.

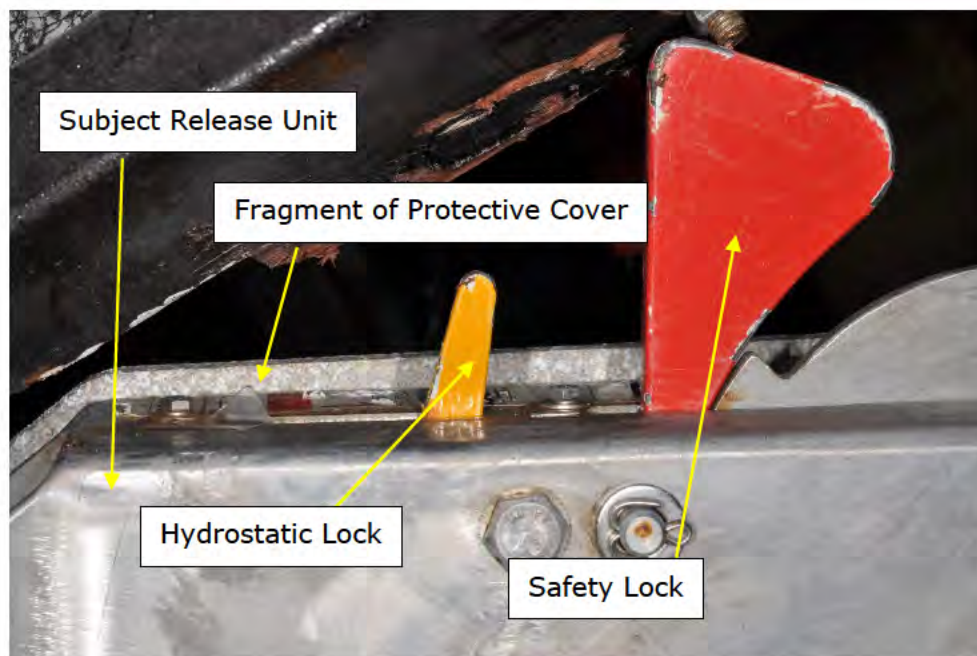


Figure 25. Photograph showing the as-found condition of the hydrostatic and safety locks on the Subject Release Unit of Lifeboat 6.

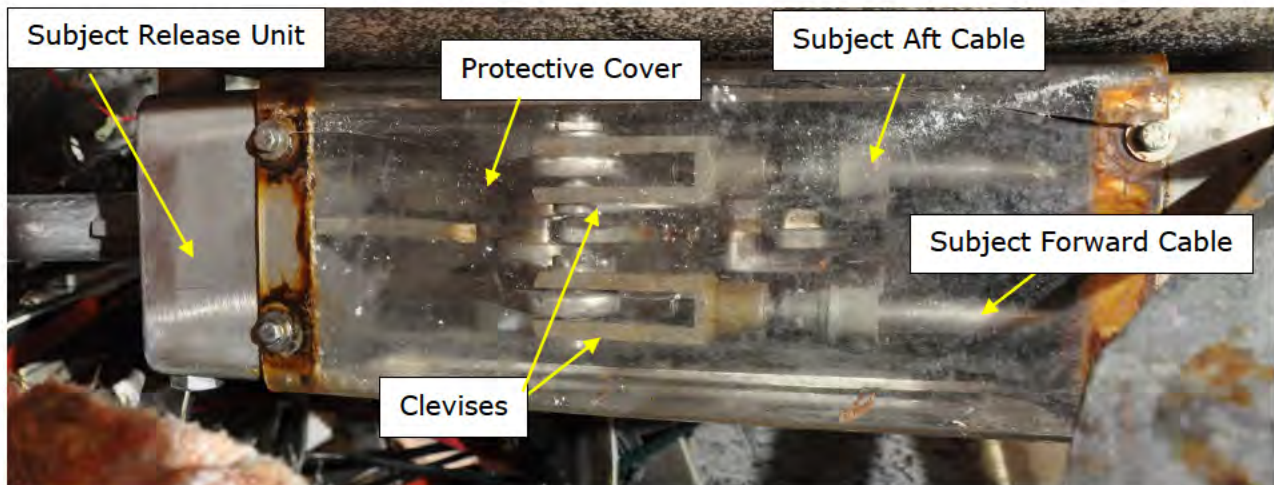


Figure 26. Photograph showing the as-found condition of the Subject Aft Cable and Subject Forward Cable clevises at the Subject Release Unit of Lifeboat 6.

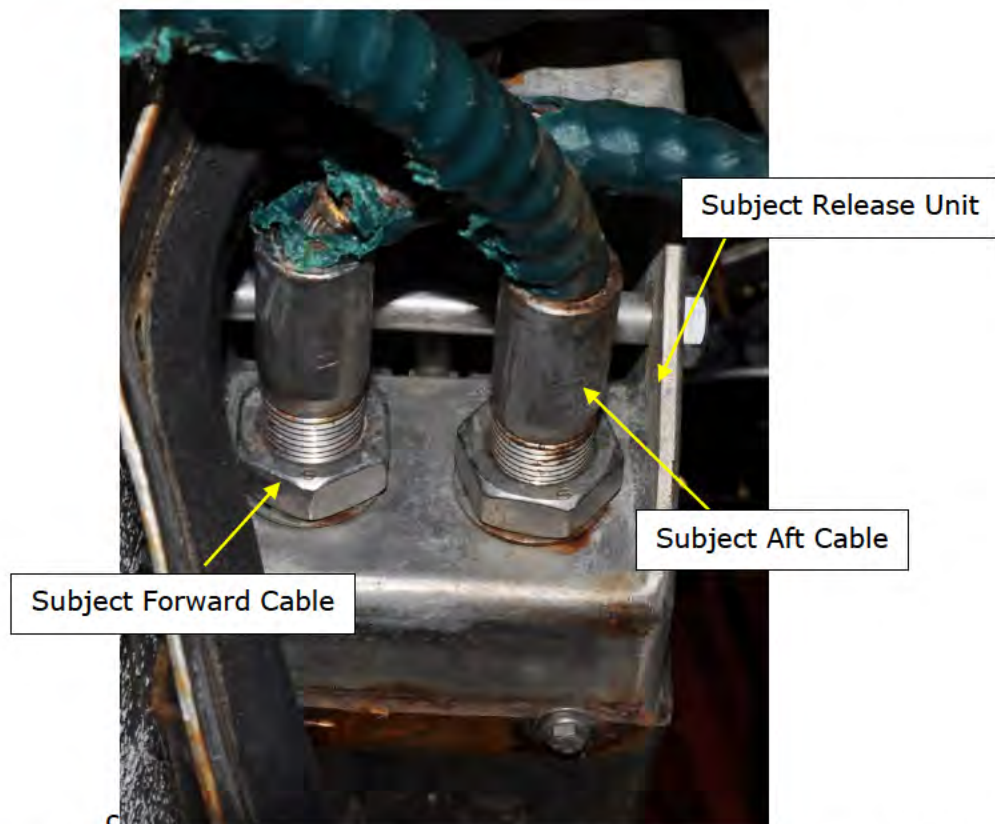


Figure 27. Photograph showing the as-found condition of the Subject Aft Cable and Subject Forward Subject at the bulkhead nuts of the Release Unit of Lifeboat 6.



Figure 28. Photograph of the Subject Release Unit showing the as-found condition of the bulkhead nuts attaching the Subject Hydrostatic Cable to the Subject Release Unit.

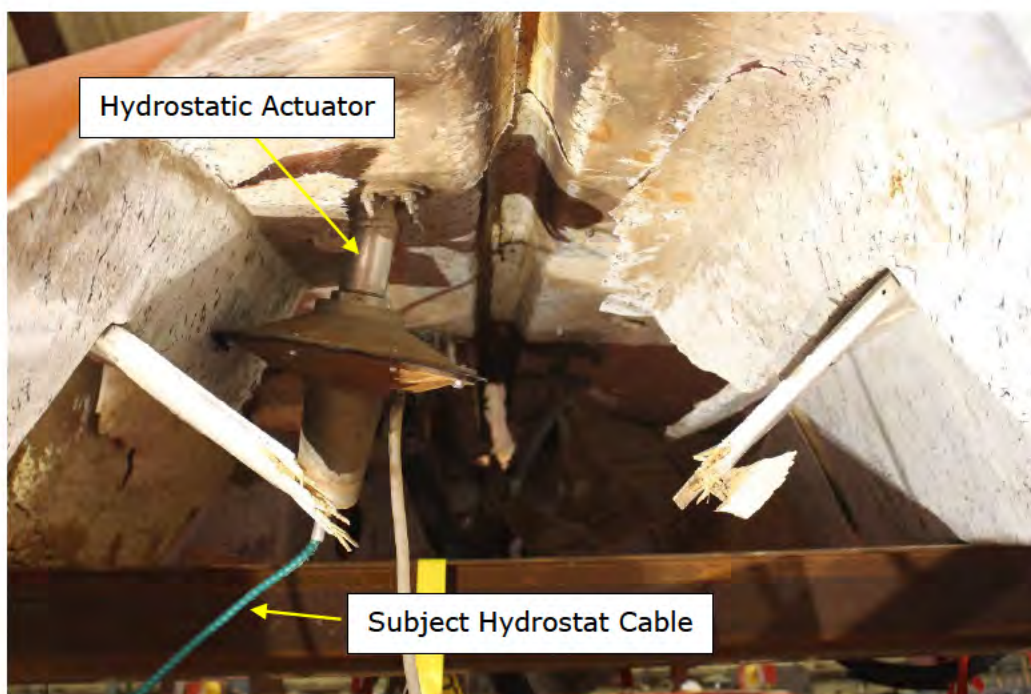


Figure 29. Photograph showing the as-found condition of the hydrostatic actuator of Lifeboat 6.



Figure 30. Photographs of the key components of Lifeboat 6 after removal and preparing for transit to DNV GL.



Figure 31. Photographs of the key components of Lifeboat 6 delivered to DNV GL's warehouse on August 6, 2019.

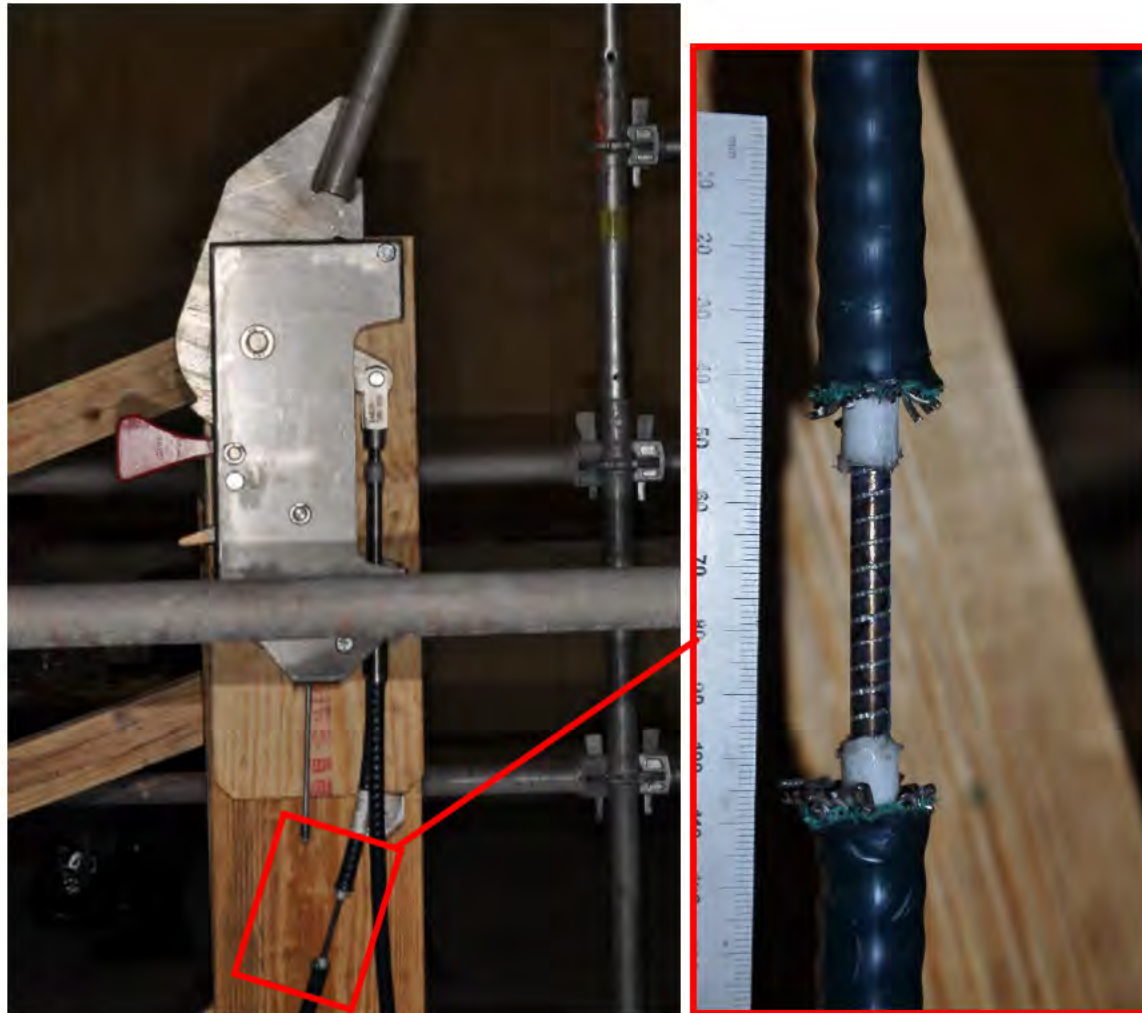


Figure 32. Photographs showing a failure in an Exemplar Cable when the wire layer and liner were severed at the approximate location of failure as on the Subject Aft Cable. Handle for the Exemplar Release Unit was in the closed position. Ruler is in mm.

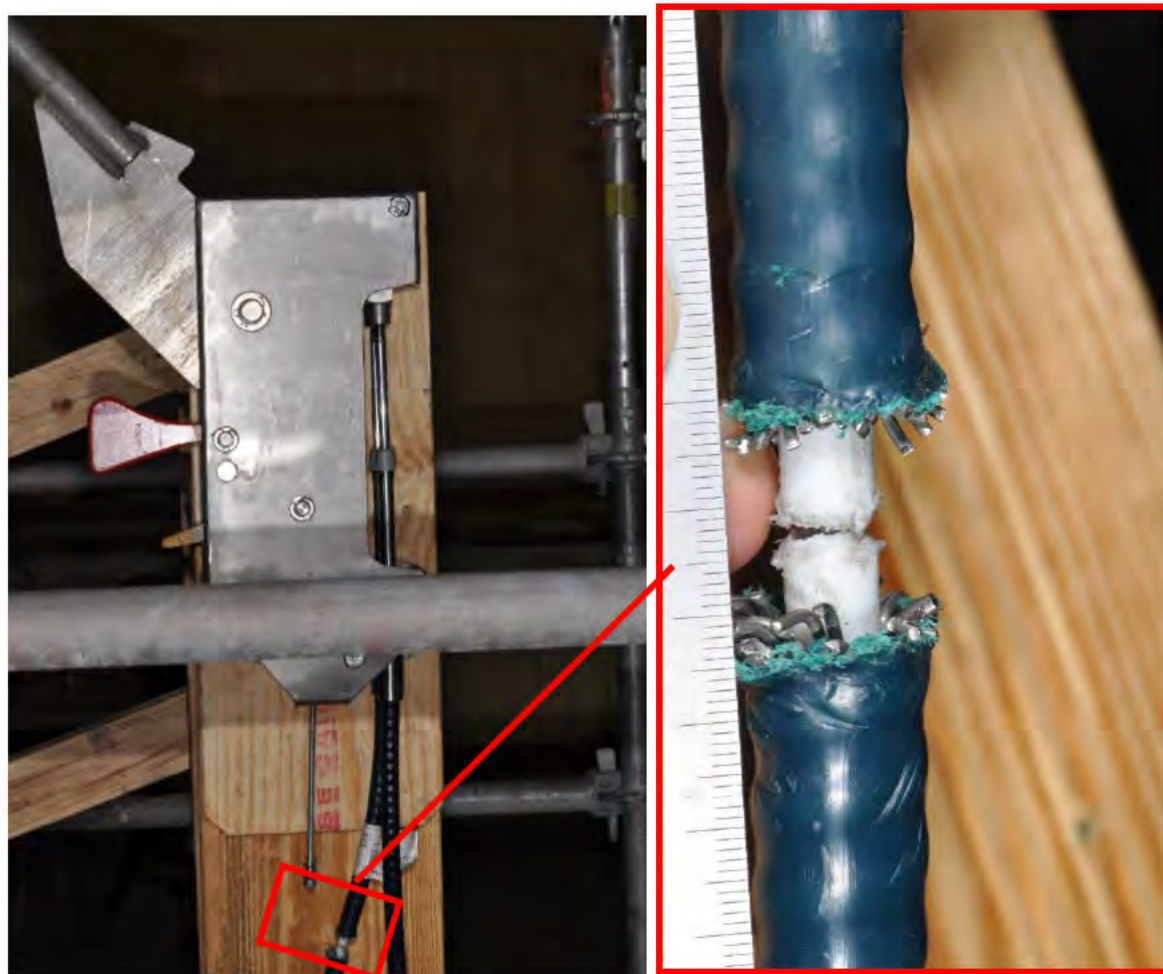
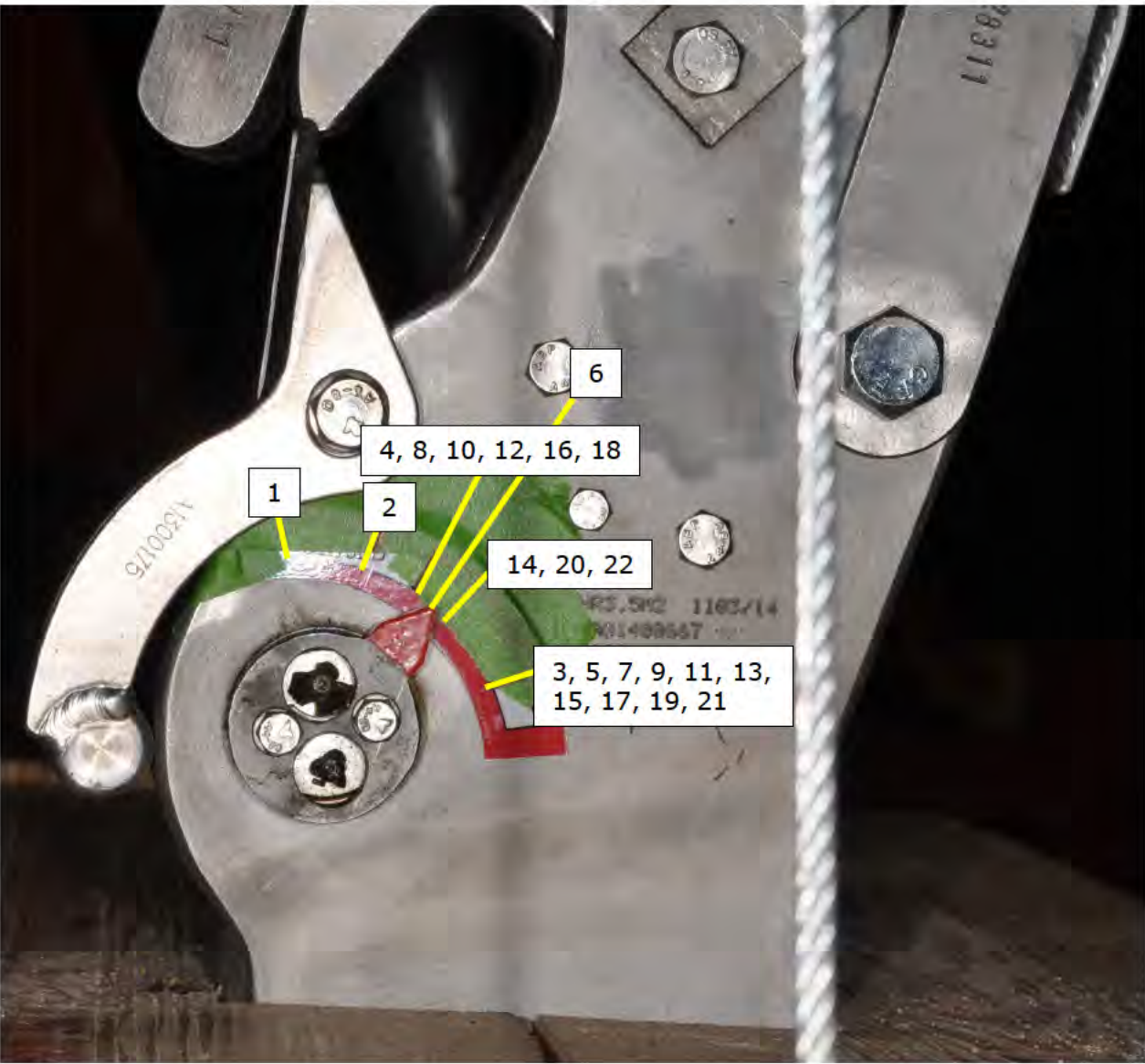


Figure 33. Photographs showing a failure in an Exemplar Cable when the wire layer and liner were severed at the approximate location of failure as on the Subject Aft Cable. Handle for the Exemplar Release Unit was in the open position. Ruler is in mm.



| Step | Position of Exemplar Release Unit | Action | Measurement at Gap (inches) | Estimated Degrees of Rotation to Open Position (Degrees) | Locking Shaft Prevents Hook from Rotating |
|------|-----------------------------------|---|-----------------------------|--|---|
| 1 | Closed | As-setup | – | 88 | Y |
| 2 | Closed | Cut Exemplar Cable Wire Layer and Liner | 2.16 | 60 | Y |
| 3 | Open | Open Exemplar Release Unit | 0.00 | 0 | N |
| 4 | Close | Close Exemplar Release Unit | 2.52 | 43 | Y |
| 5 | Open | Open Exemplar Release Unit | 0.00 | 0 | N |
| 6 | Close | Close Exemplar Release Unit | 2.67 | 33 | Y |
| 7 | Open | Open Exemplar Release Unit | 0.00 | 0 | N |
| 8 | Close | Close Exemplar Release Unit | 2.55 | 43 | Y |
| 9 | Open | Open Exemplar Release Unit | 0.00 | 0 | N |
| 10 | Close | Close Exemplar Release Unit | 2.56 | 43 | Y |
| 11 | Open | Open Exemplar Release Unit | 0.00 | 0 | N |
| 12 | Close | Close Exemplar Release Unit | 2.56 | 43 | Y |
| 13 | Open | Open Exemplar Release Unit | 0.00 | 0 | N |
| 14 | Close | Close Exemplar Release Unit | 3.03 | 28 | Y |
| 15 | Open | Open Exemplar Release Unit | 0.00 | 0 | N |
| 16 | Close | Close Exemplar Release Unit | 2.60 | 43 | Y |
| 17 | Open | Open Exemplar Release Unit | 0.00 | 0 | N |
| 18 | Close | Close Exemplar Release Unit | 2.44 | 43 | Y |
| 19 | Open | Open Exemplar Release Unit | 0.00 | 0 | N |
| 20 | Close | Close Exemplar Release Unit | 2.99 | 28 | Y |
| 21 | Open | Open Exemplar Release Unit | 0.00 | 0 | N |
| 22 | Close | Close Exemplar Release Unit | 3.35 | 28 | Y |

Figure 34. Photograph showing the orientations of the locking shaft indicator on the Exemplar Hook when the release handle for the Exemplar Release Unit was actuated into the open and close positions before and after the wire layer and liner of the Exemplar Cable were severed. The table summarizes the conditions of each step, with the columns detailing the position of the release handle of the Exemplar Release Unit, the action taken in the step, the measurement of the separation in the Exemplar Cable, and whether the locking shaft prevented the hook from rotating.

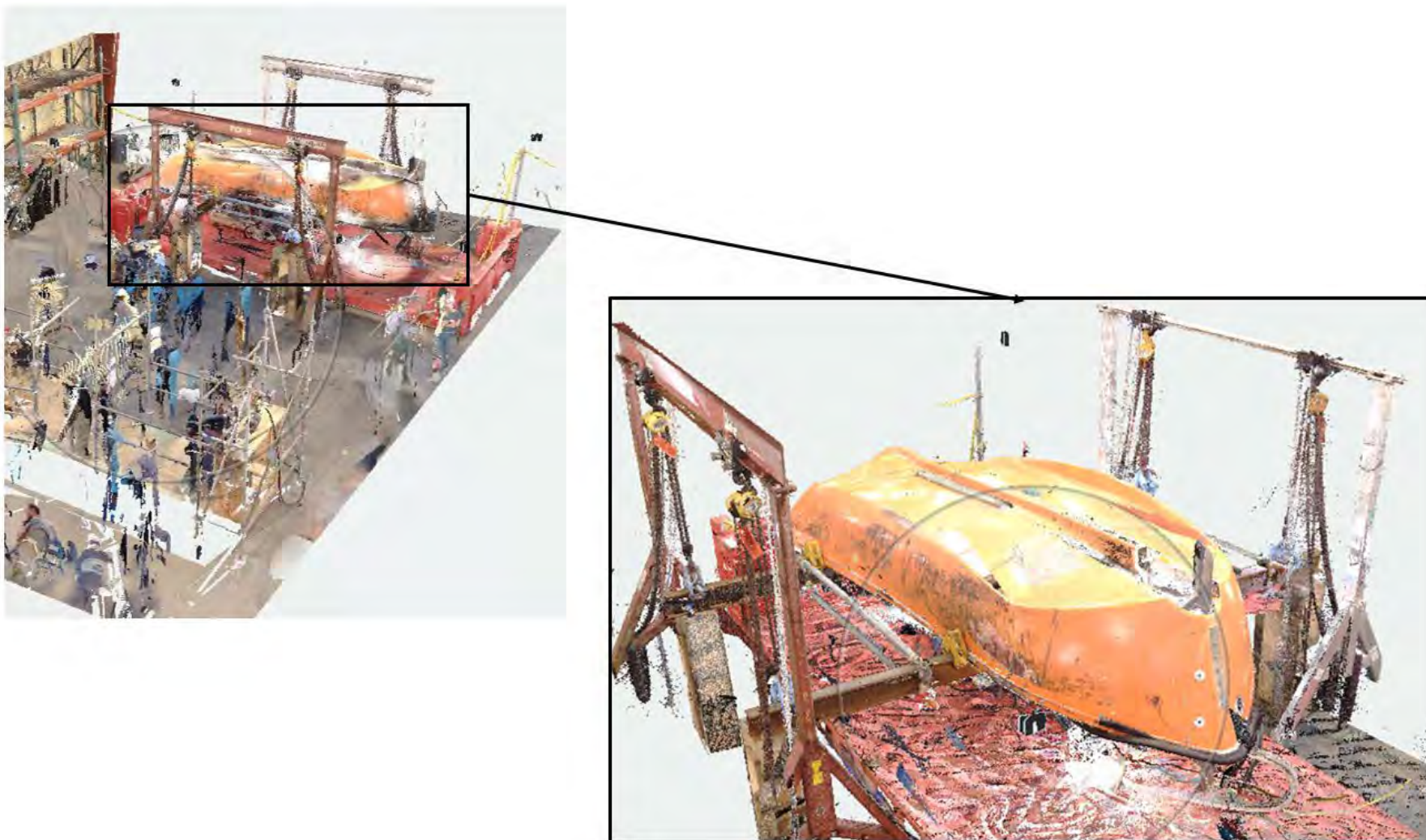


Figure 35. Laser scan of the Lifeboat 6, performed at Harvey Terminal after recovery.

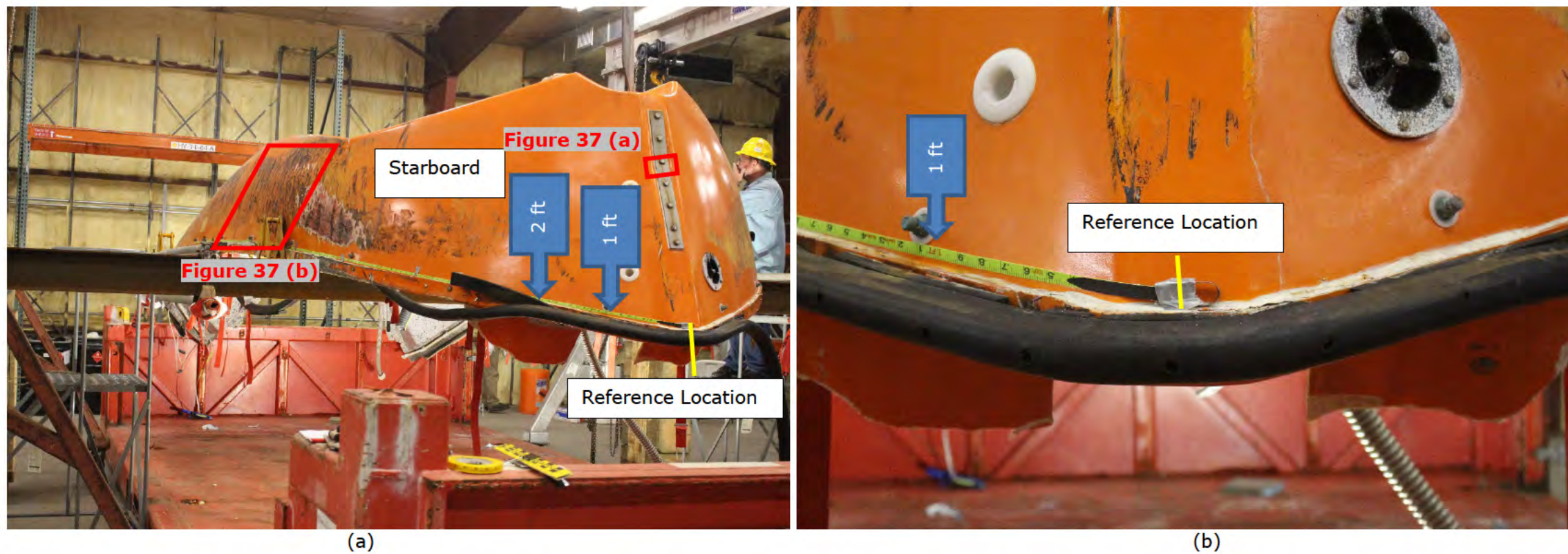


Figure 36. Photographs showing (a) the starboard of Lifeboat 6 and (b) the reference location for measurements. Tape measure is in feet.

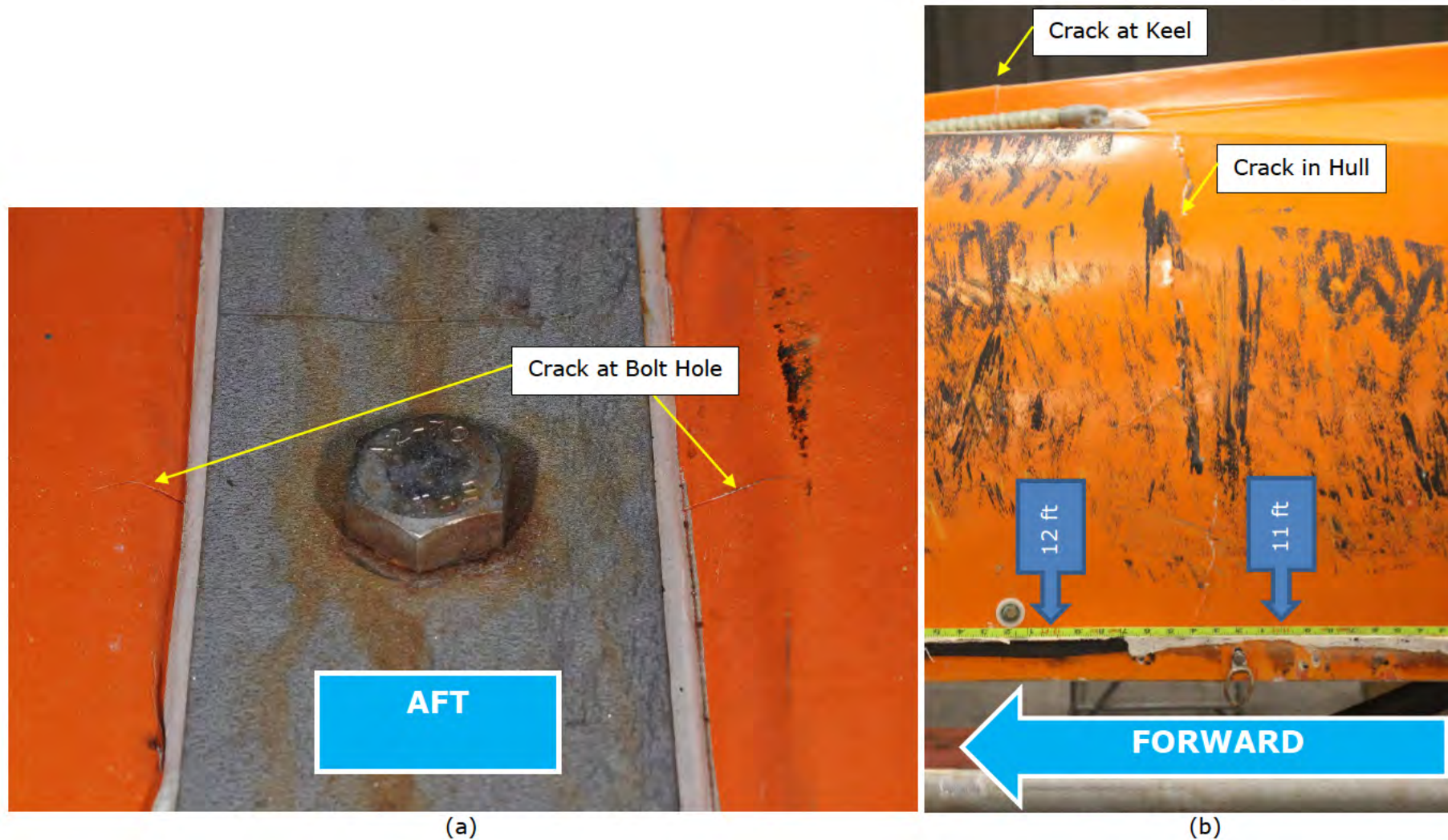


Figure 37. Photographs showing locations of cracks of interest at (a) the aft shoe plate and (b) 11.4 feet from reference location; locations shown in Figure 36. Tape measure is in feet.

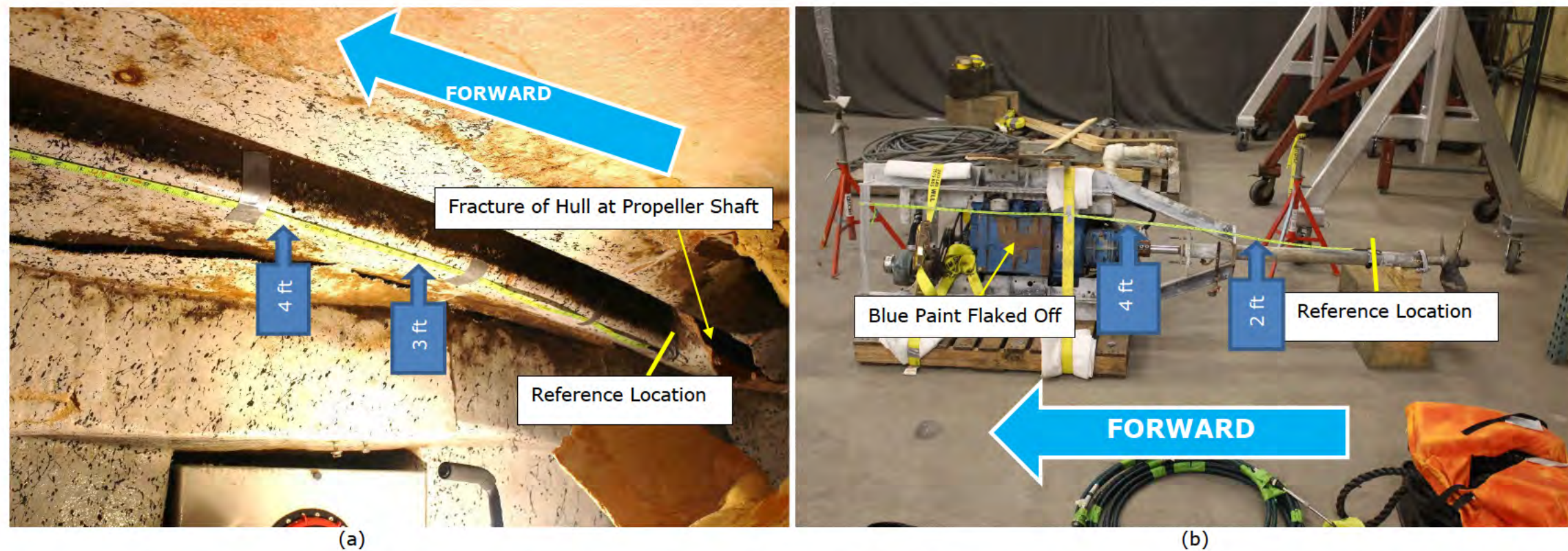


Figure 38. Photographs showing (a) the reference location for measurements on the interior of the hull and (b) the corresponding location on the engine and engine cradle. Tape measure is in feet.

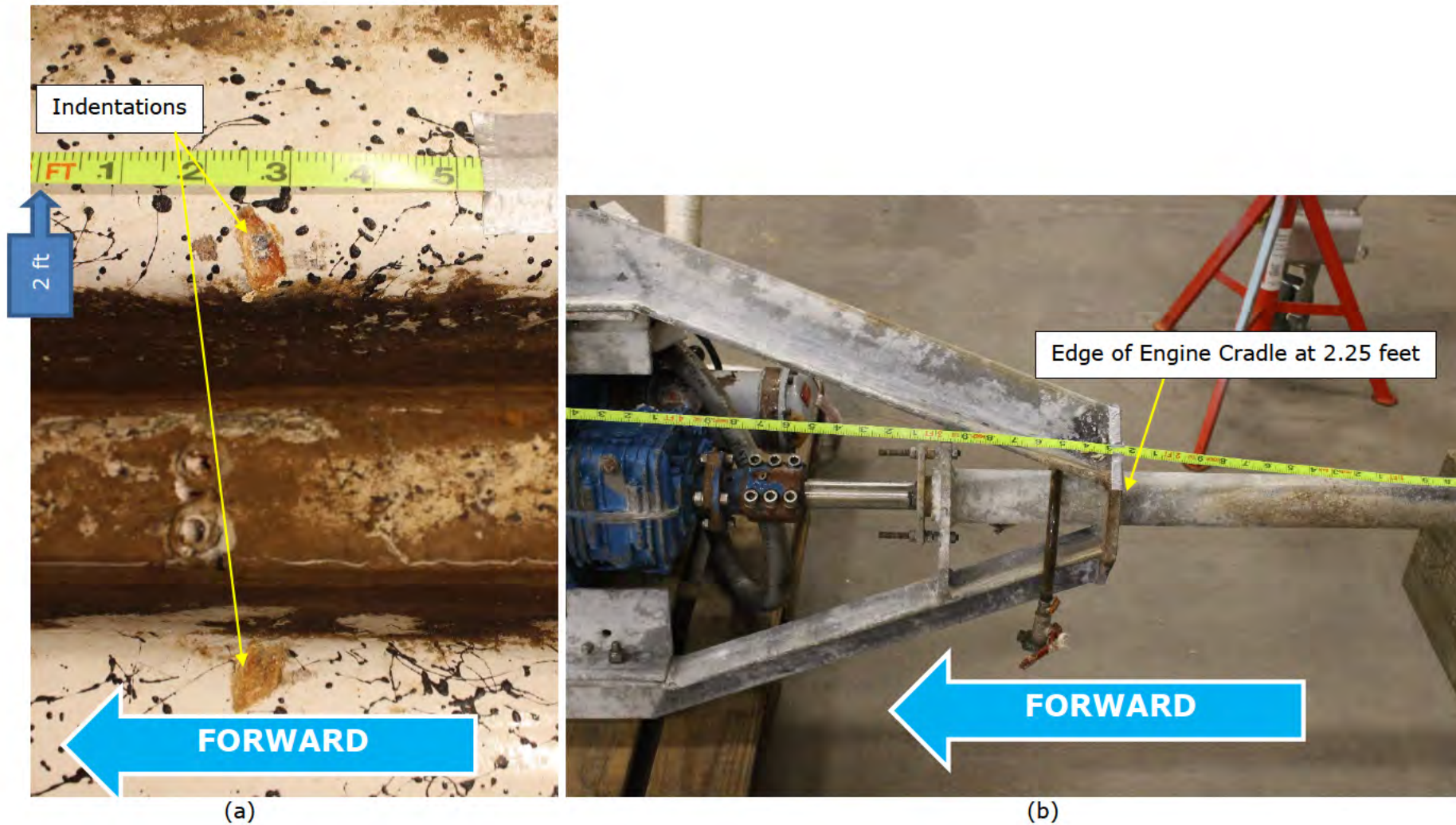


Figure 39. Photographs showing (a) indentations / contact damage at the hull interior 2.25 feet from the reference location and (b) the corresponding location on the engine and engine cradle. Tape measure is in feet.

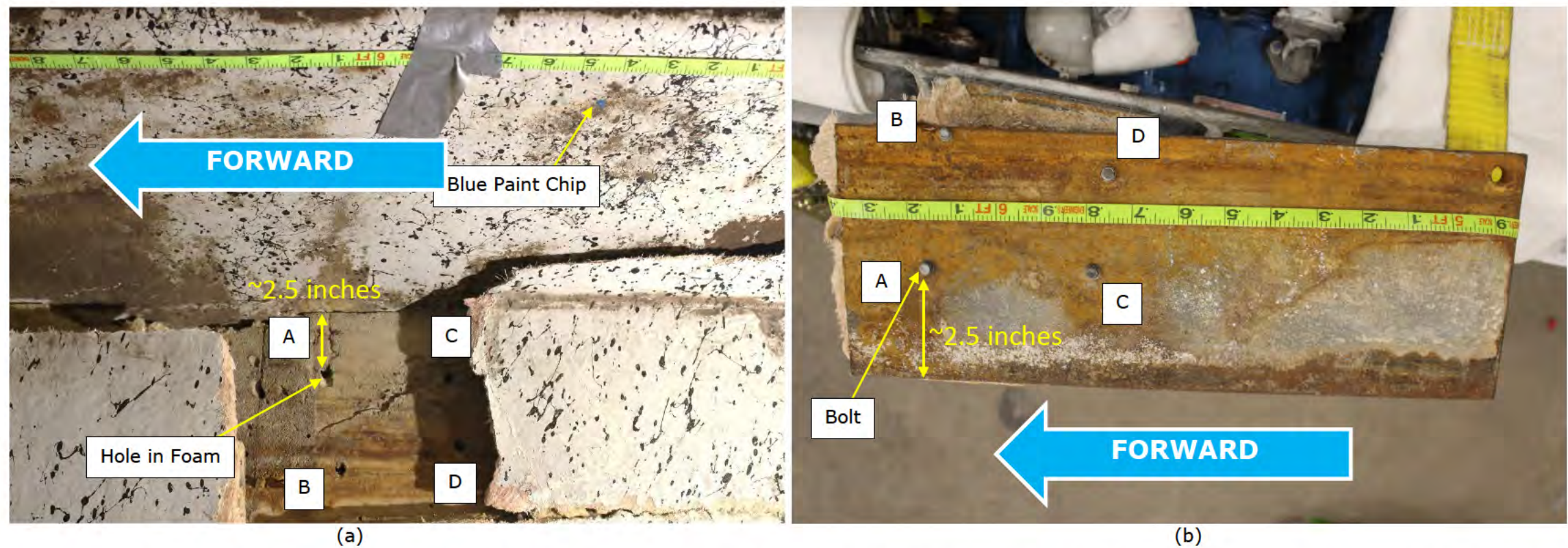


Figure 40. Photographs showing (a) a missing section of the hull interior 5.8 feet to 6.4 feet from the reference location and (b) the corresponding location on the engine and engine cradle. Tape measure is in feet.

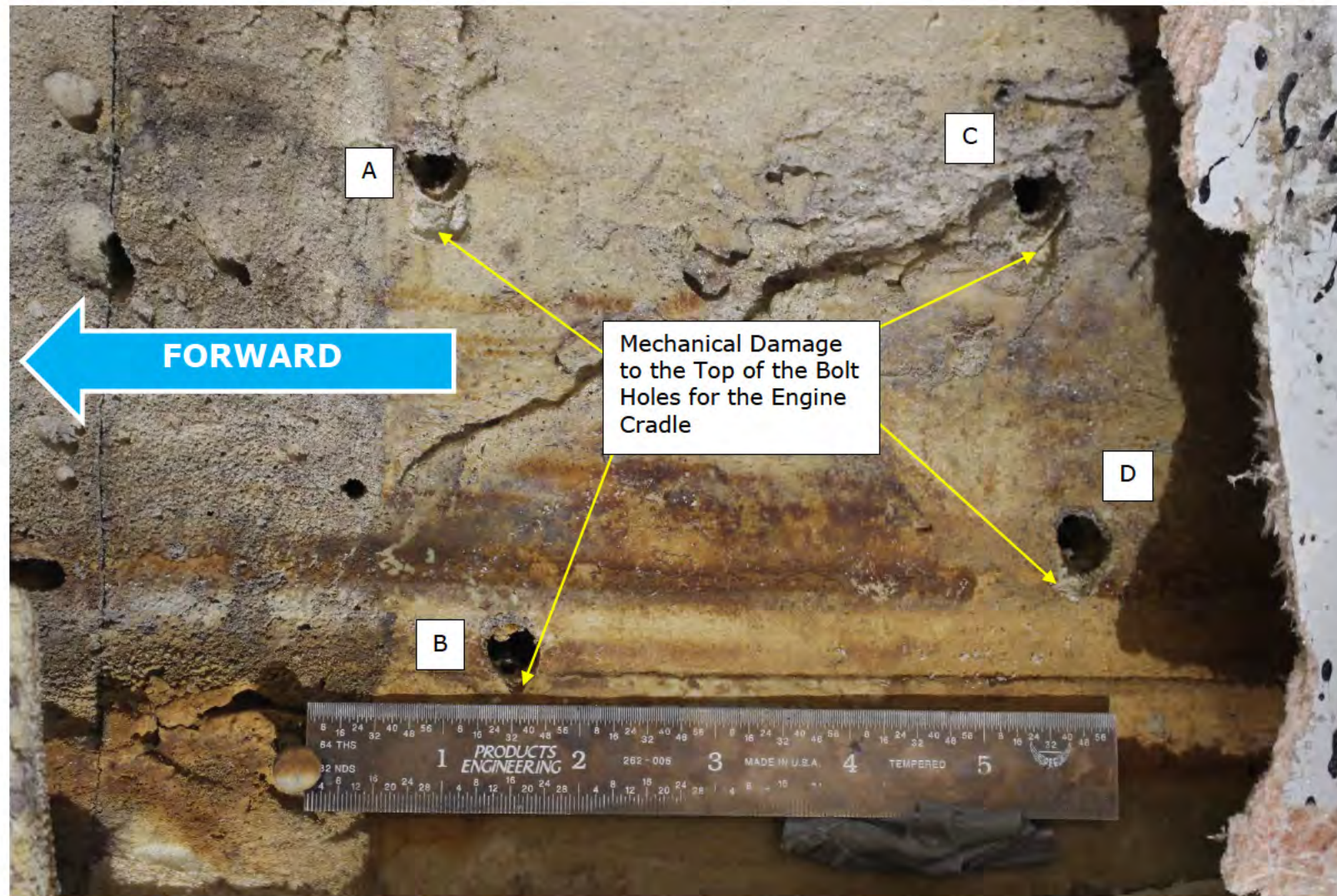


Figure 41. Photograph showing hole impressions left from the bolt studs used to attach support structure for the engine. Directionality of the damage can be seen adjacent to each hole. Ruler is in inches.



Figure 42. Photographs showing a transverse crack in the keel of the hull interior located 7.6 feet from the reference location. Tape measure is in feet.

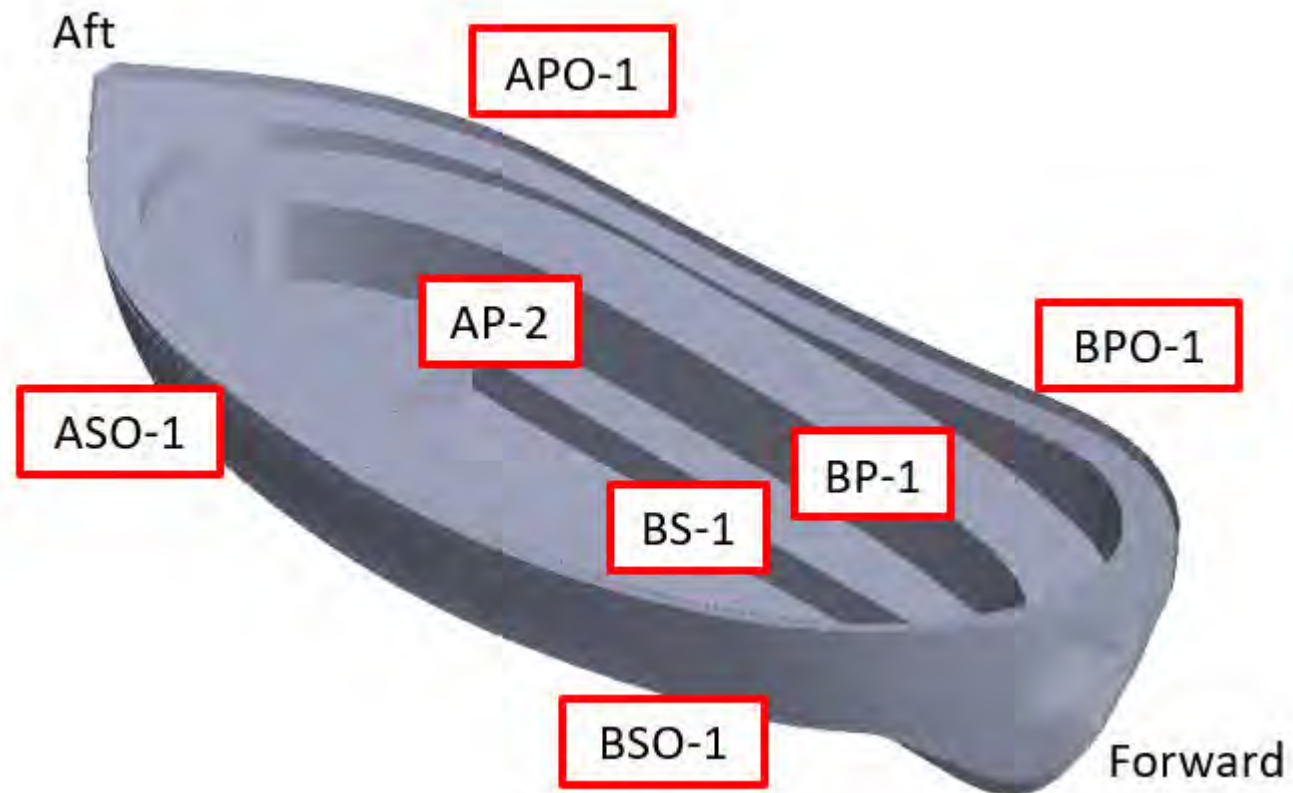


Figure 43. Schematic showing the approximate locations of each 24-inch by 24-inch panel extracted from the outer and inner hull of Lifeboat 6. Samples BSO-1, ASO-1, BPO-1, and APO-1 were extracted from the outer hull. Samples AP-2, BP-1, and BS-1 were extracted from the interior seating area.



Figure 44. 3D representation of the approximate location of Sample C-1. The crack observed was located at the interior of boat at the fiberglass-engine mount interface.



Figure 45. 3D representation of the approximate location of Sample C-2. The crack observed was located at the exterior of the hull on the keel of the boat. The crack propagated through the thickness of the keel.



Figure 46. 3D representation of the approximate location of Sample C-3. The crack observed was located at the exterior of the hull on the starboard side. The crack ran from the hull-canopy interface towards the keel.

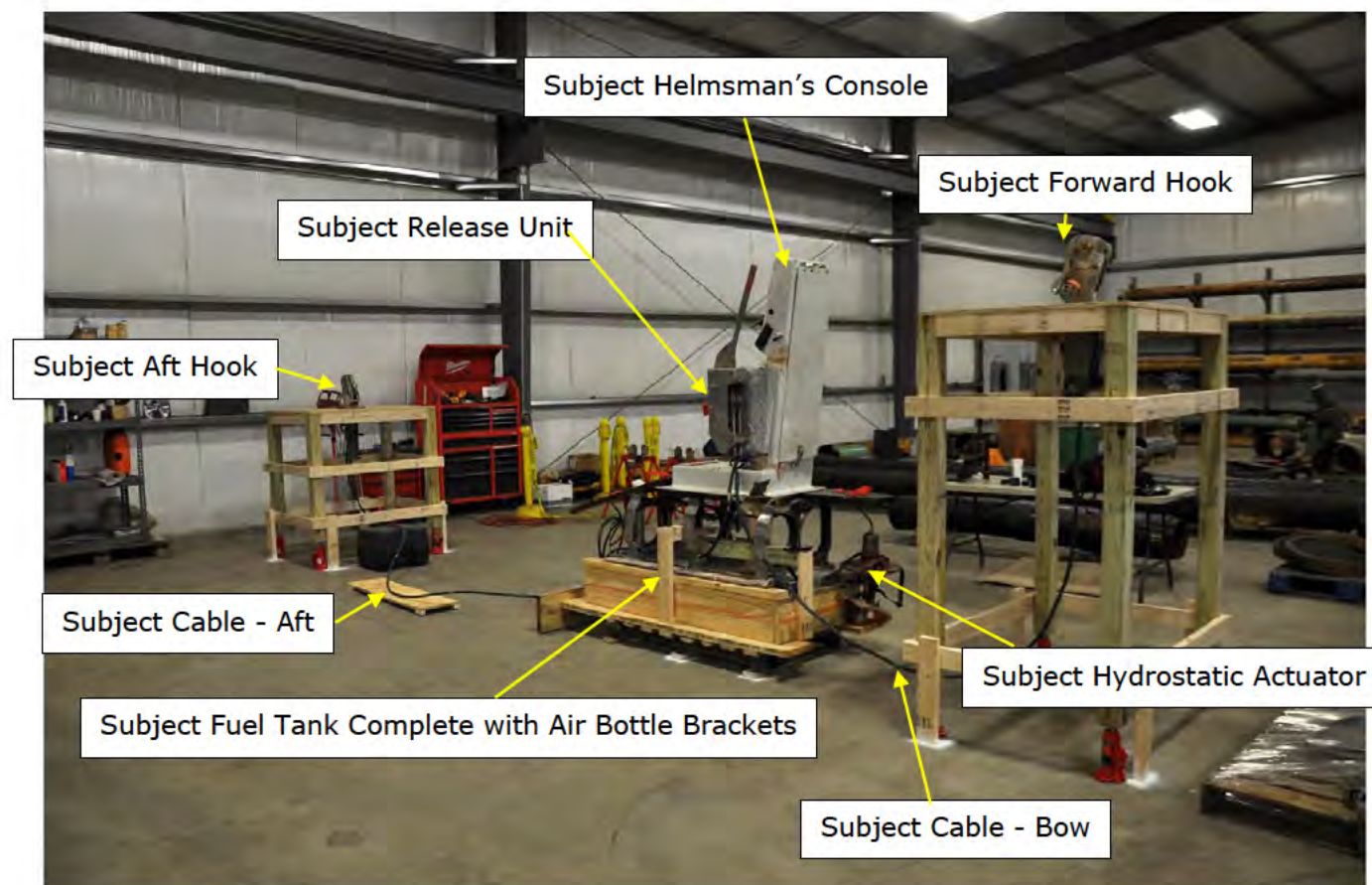


Figure 47. Photograph of the reconstruction of the relevant components from Lifeboat 6 located at DNV GL's warehouse.

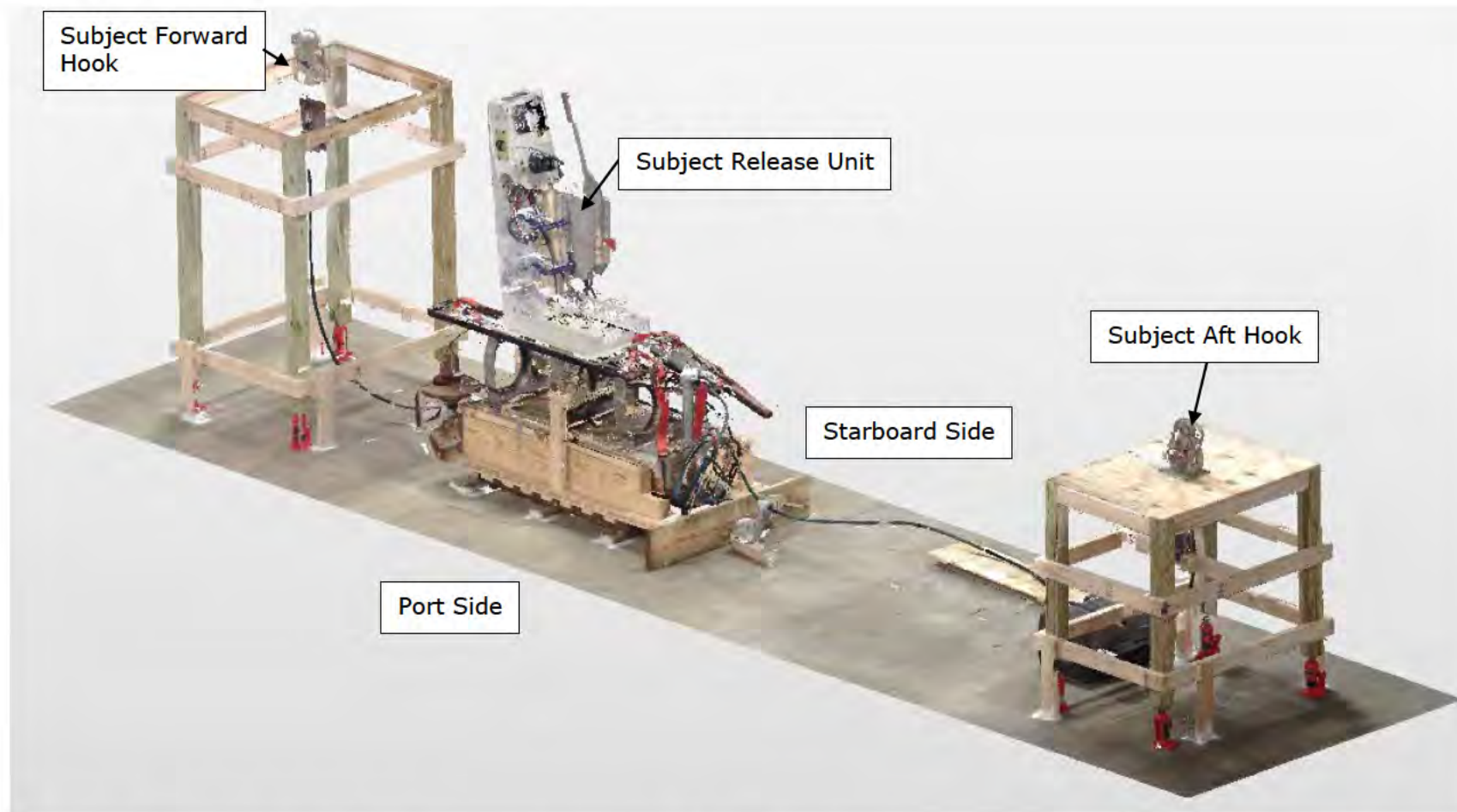


Figure 48. Laser scan showing the reconstruction of the relevant components from Lifeboat 6 at DNV GL's warehouse.

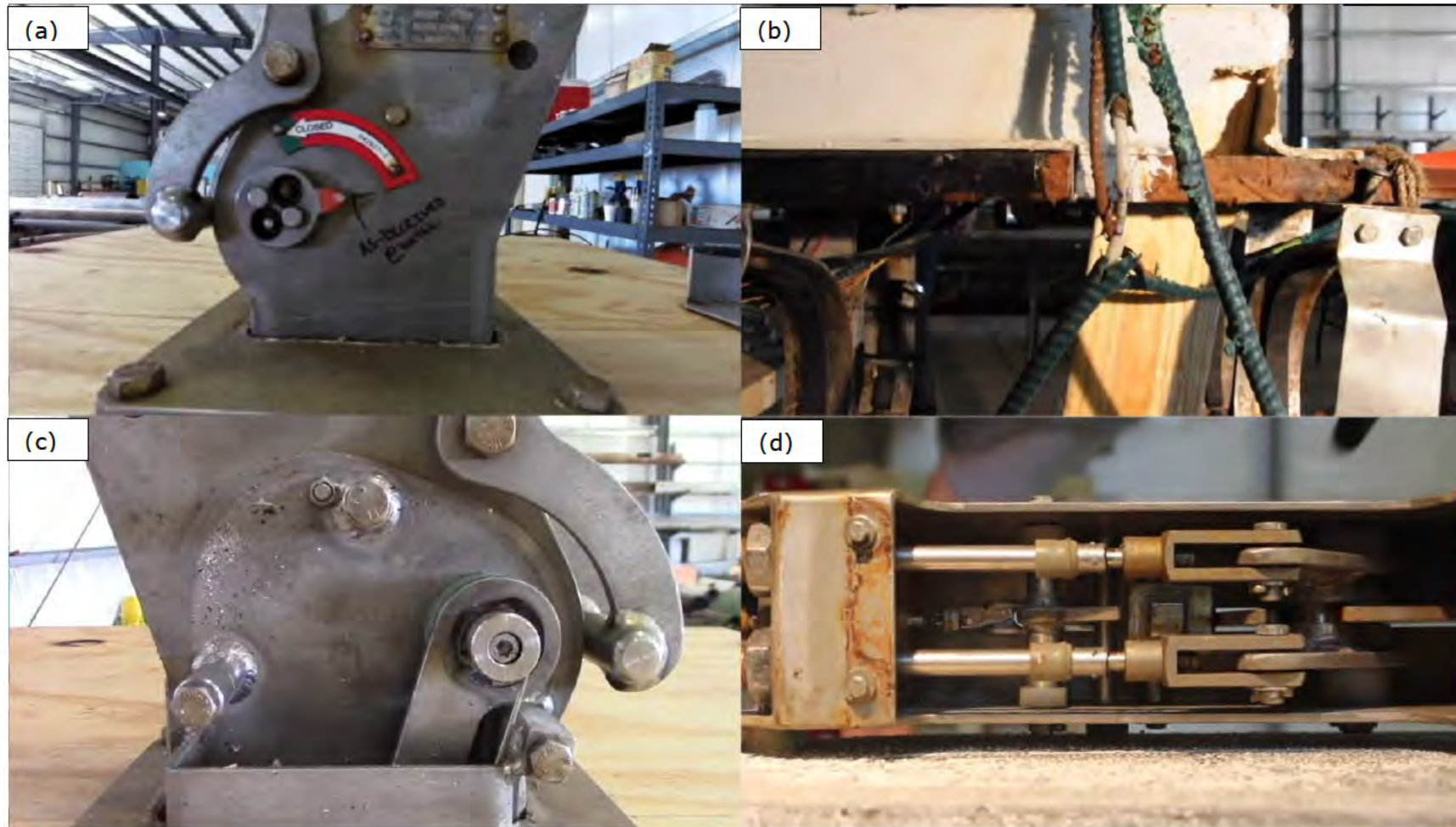


Figure 49. Screenshot of compiled digital recordings from a function test performed using the Subject Aft Hook, the Subject Aft Cable, and the Subject Release Unit. Four views are shown: (a) the port side of the Subject Aft Hook, (b) the break in the Subject Aft Cable located near the Subject Release Unit, (c) the starboard side of the Subject Aft Hook, and (d) the forward side of the Subject Release Unit (note this view is rotated 90° clockwise from its normal orientation).

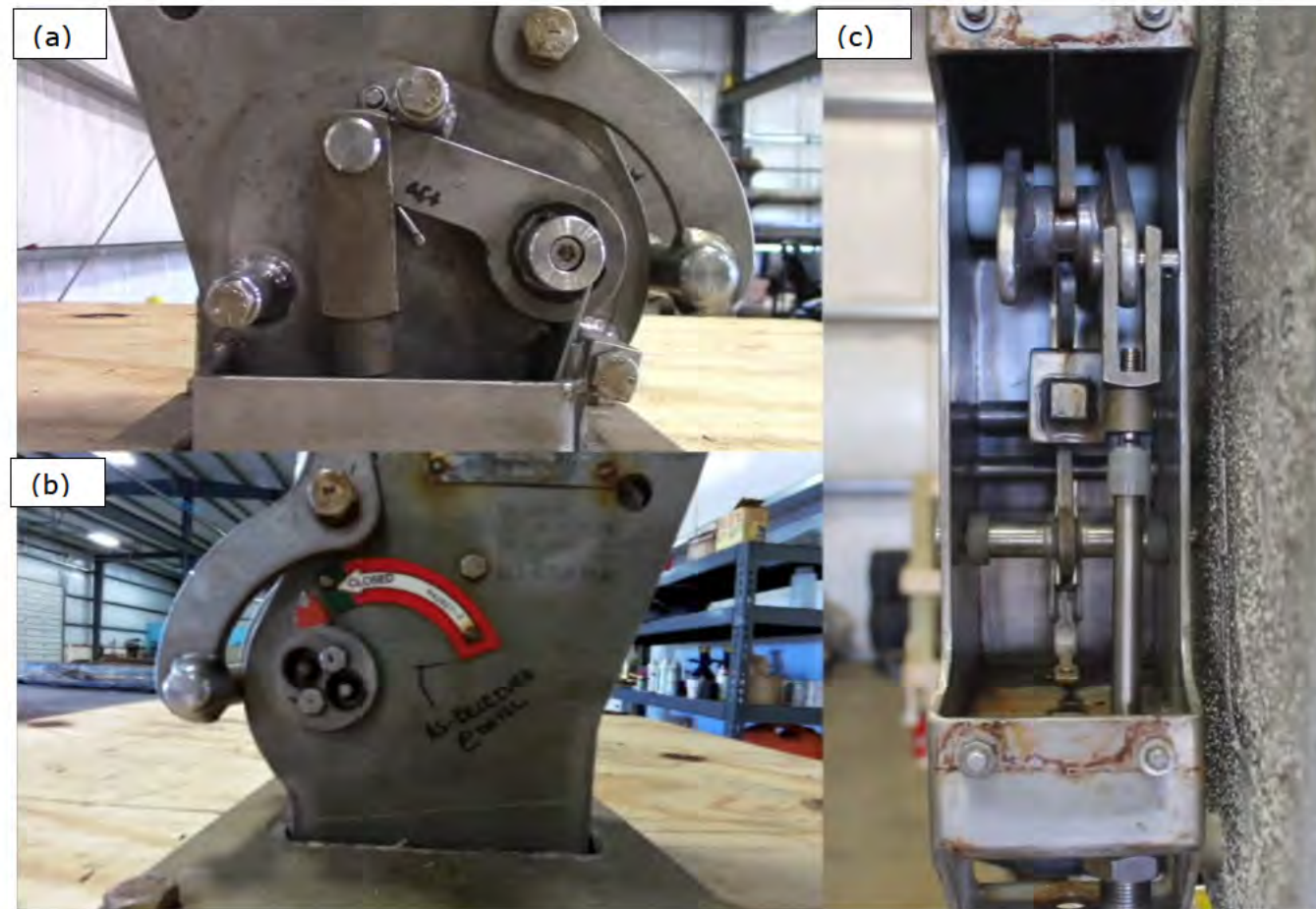


Figure 50. Screenshot of compiled digital recordings from a function test performed using the Subject Aft Hook, the Exemplar Cable, and the Subject Release Unit before moving the release handle of the Subject Release Unit. Three views are shown: (a) starboard side of the Subject Aft Hook, (b) the port side of the Subject Aft Hook, and (c) the forward side of the Subject Release Unit.

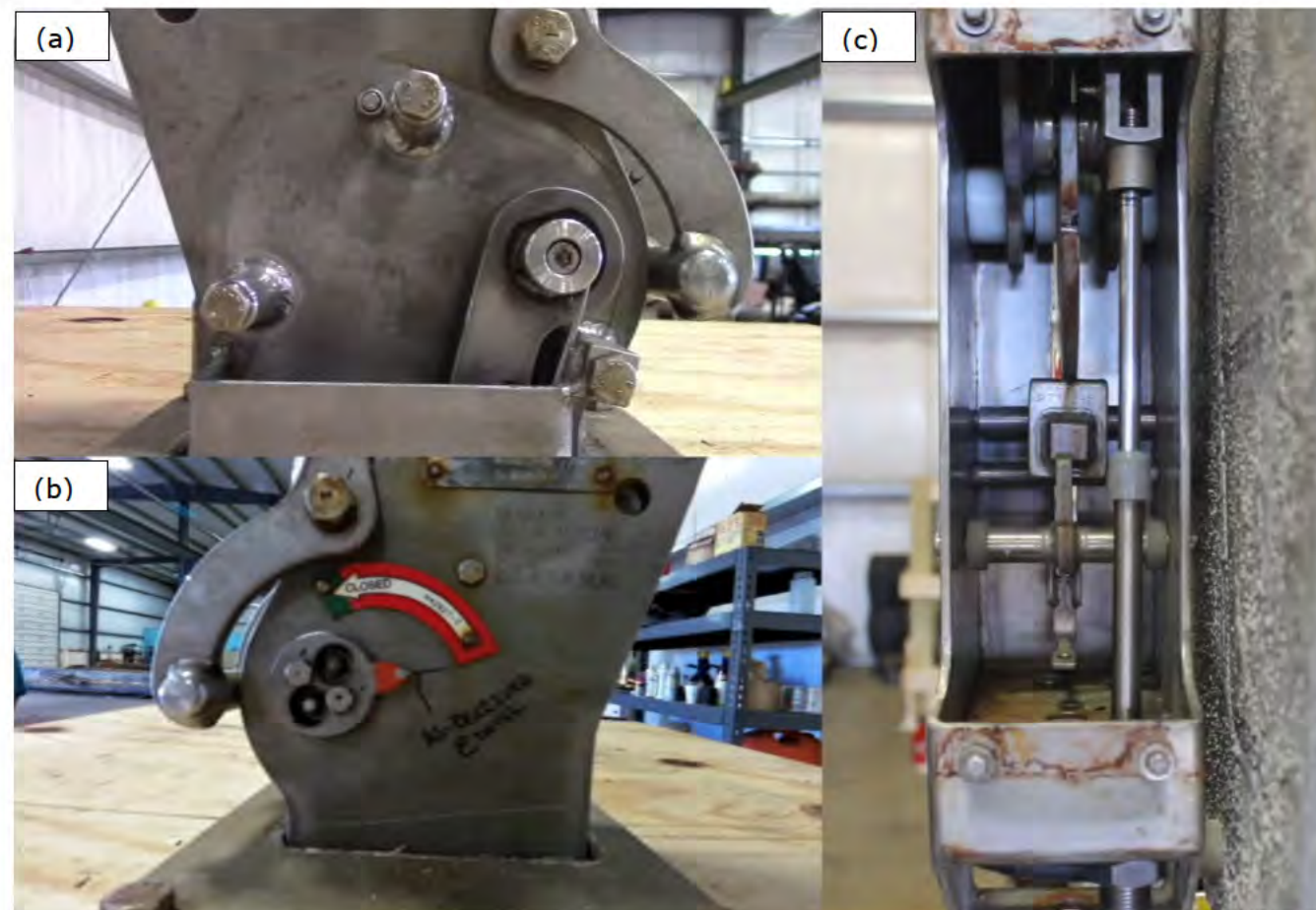


Figure 51. Screenshot of compiled digital recordings from a function test performed using the Subject Aft Hook, Exemplar Cable, and Subject Release Unit after moving the release handle of the Subject Release Unit. Three views are shown: (a) starboard side of the Subject Aft Hook, (b) the port side of the Subject Aft Hook, and (c) the forward side of the Subject Release Unit.

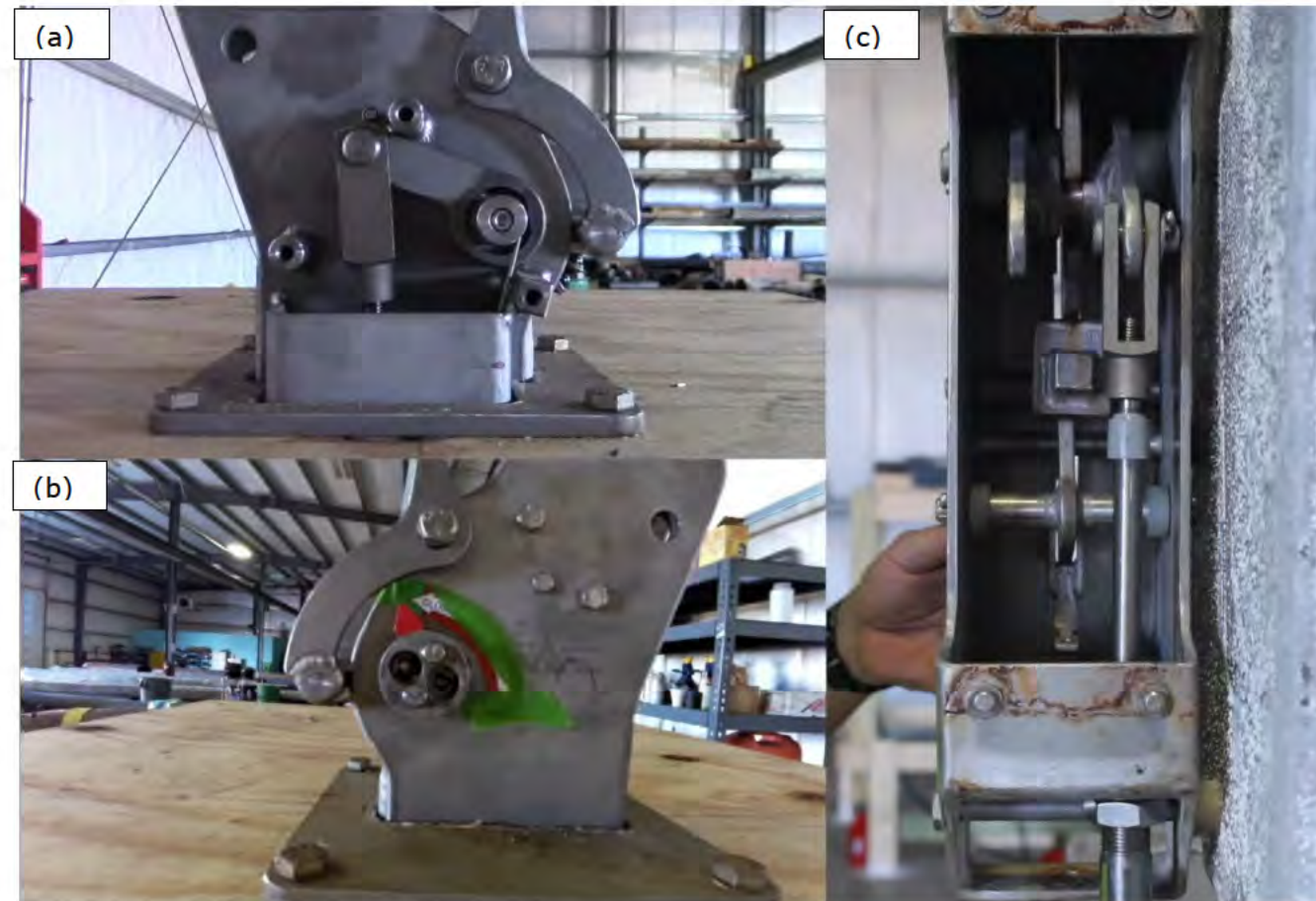


Figure 52. Screenshot of compiled digital recordings of a function test performed using the Exemplar Hook, Exemplar Cable, and Subject Release Unit before moving the release handle of the Subject Release Unit. Three views are shown: (a) starboard side of the Exemplar Hook, (b) the port side of the Exemplar Hook, and (c) the forward side of the Subject Release Unit.

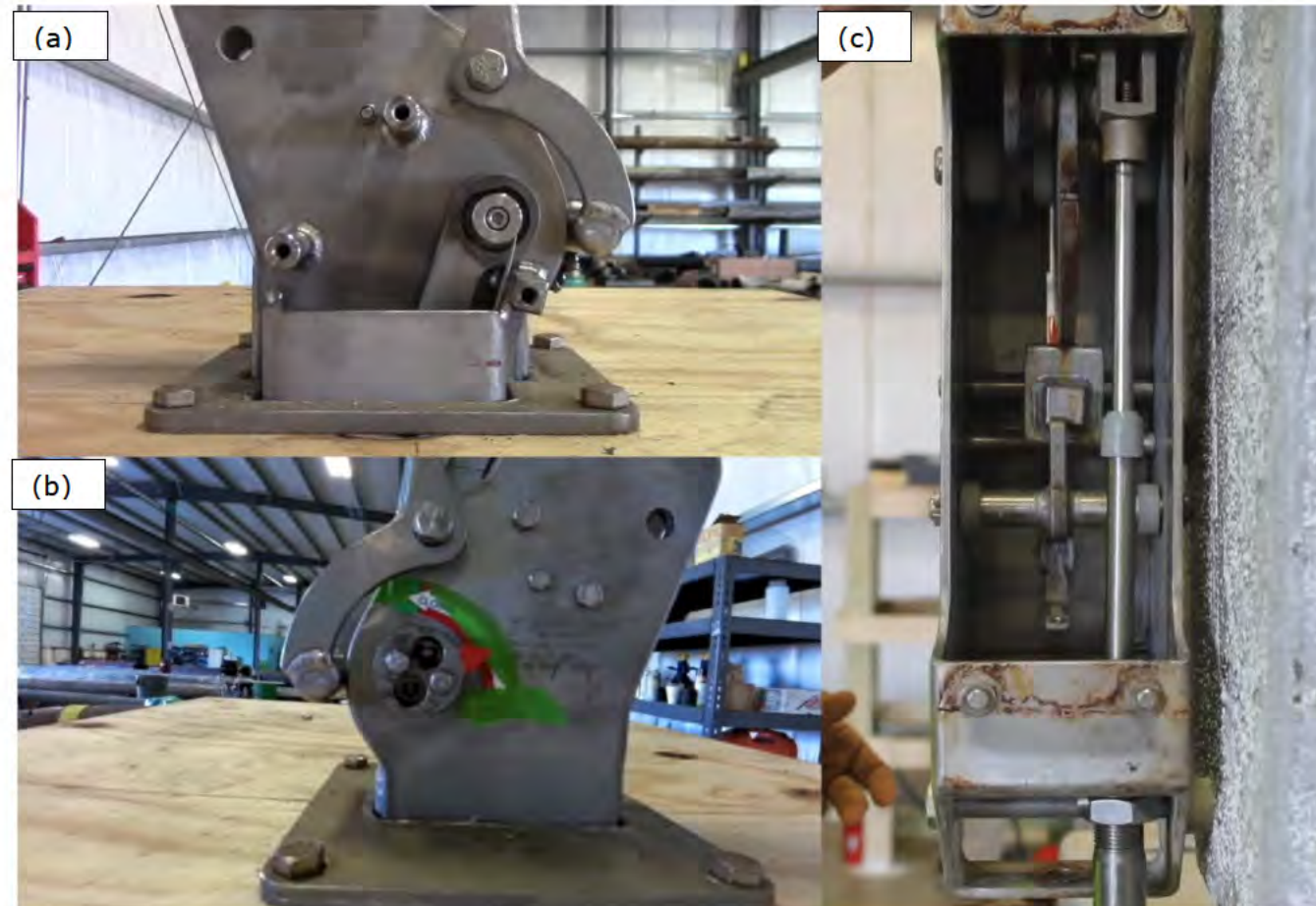


Figure 53. Screenshot of compiled digital recordings of a function test performed using the Exemplar Hook, Exemplar Cable, and Subject Release Unit after moving the release handle of the Subject Release Unit. Three views are shown: (a) starboard side of the Exemplar Hook, (b) the port side of the Exemplar Hook, and (c) the forward side of the Subject Release Unit.

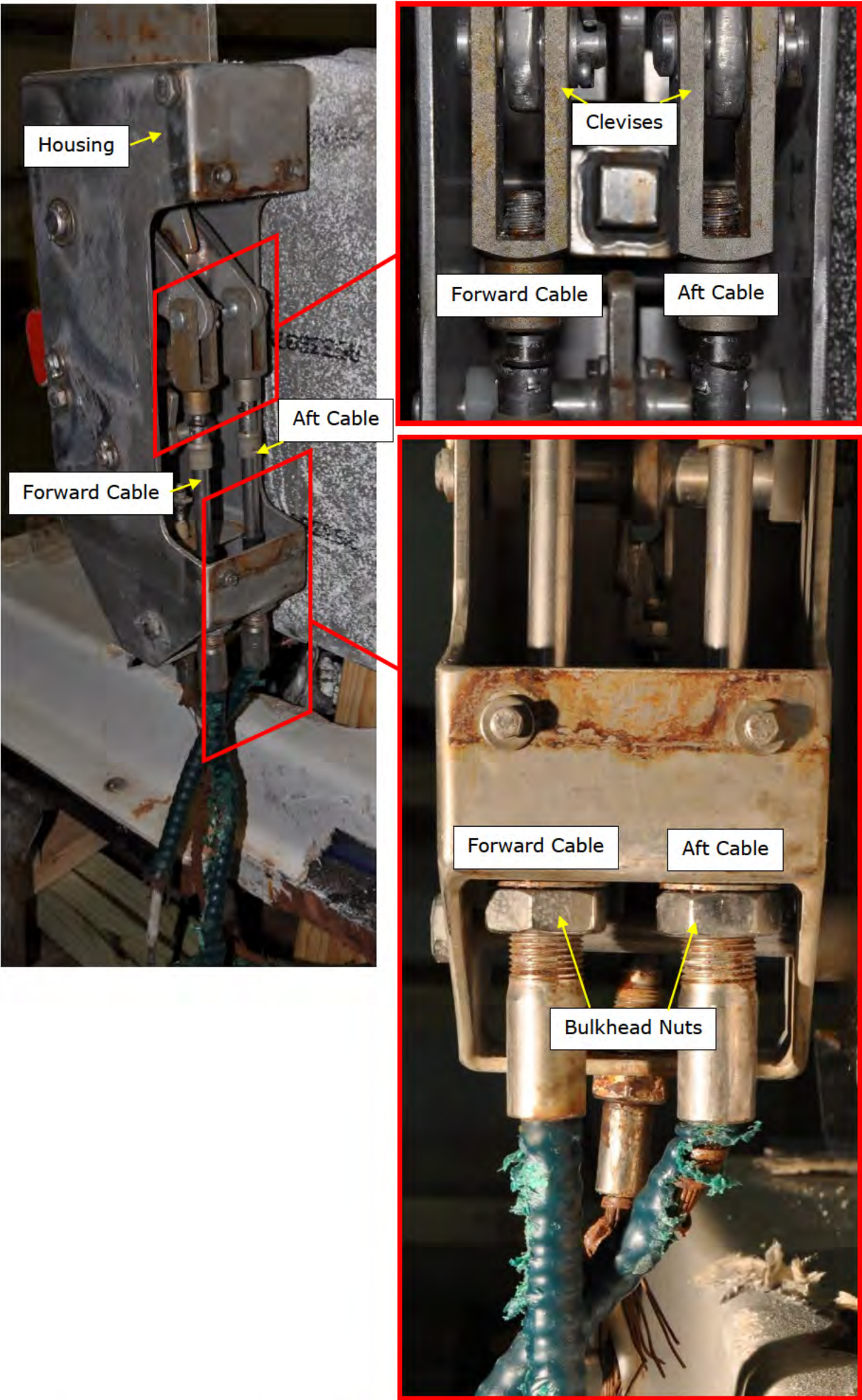


Figure 54. Photographs of the Subject Release Unit at DNV GL showing the as-found condition of the clevises and bulkhead nuts, after removing the protective coverings.

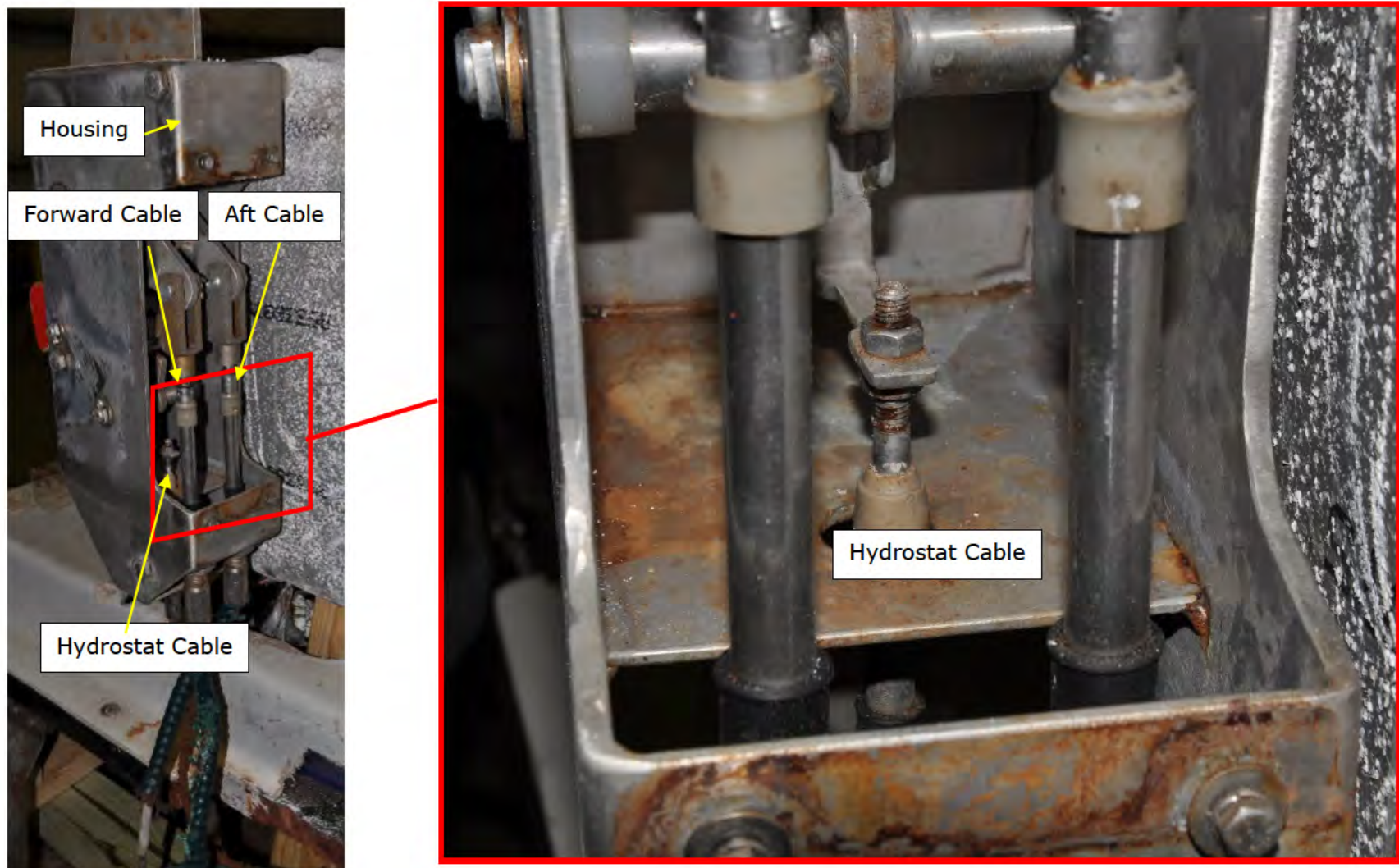


Figure 55. Photographs of the Subject Release Unit at DNV GL showing the as-found condition of the hydrostat cable and end rod jam nuts, after removing the protective coverings.

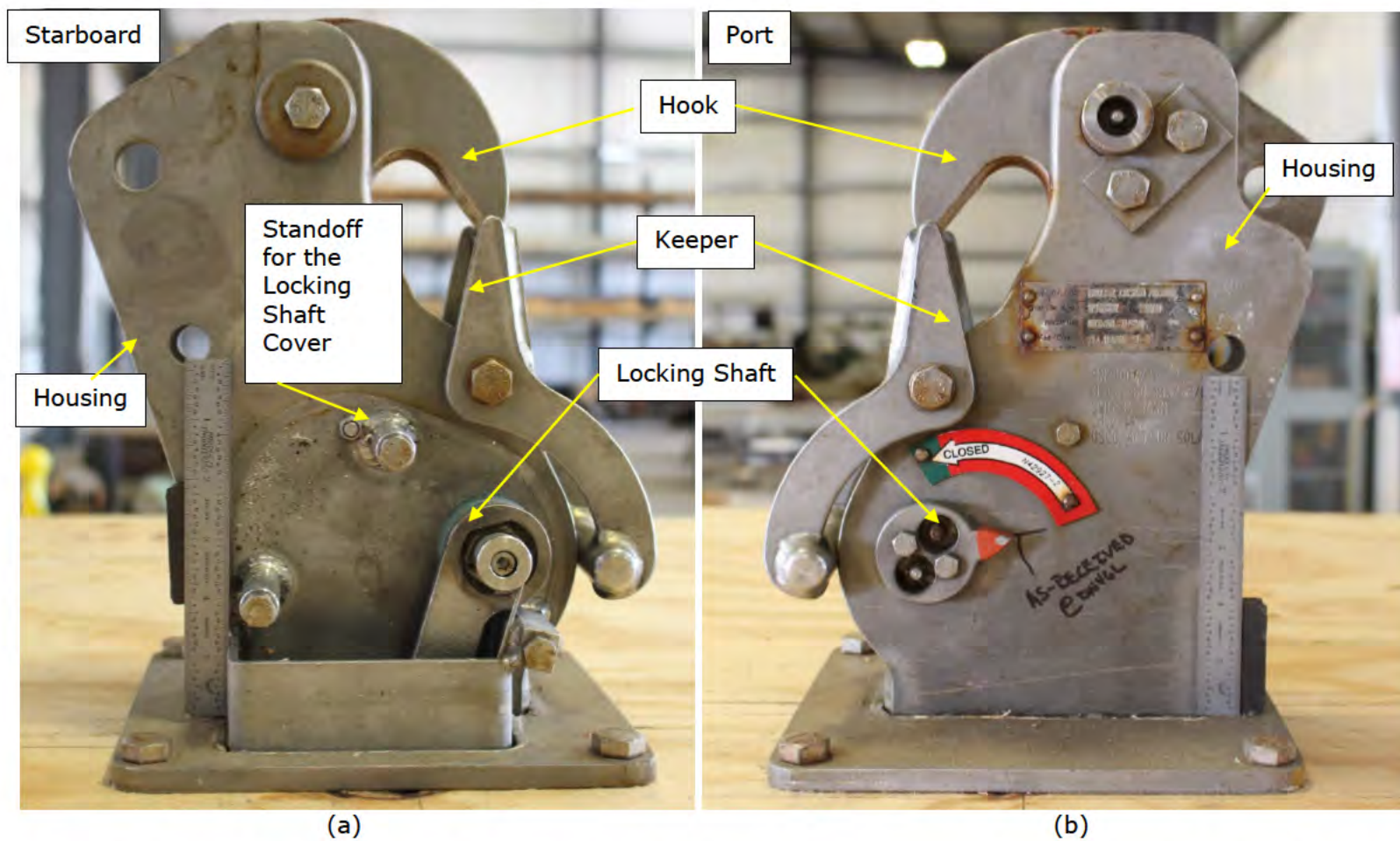
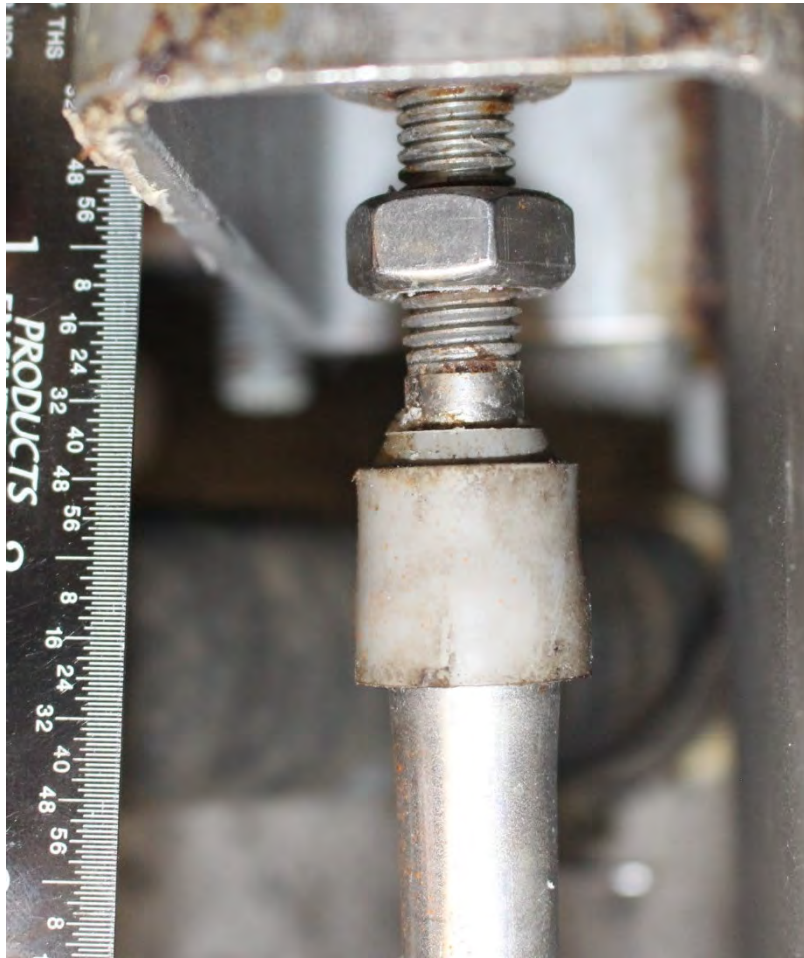


Figure 56. Photographs of the Subject Aft Hook with the locking shaft cover removed, viewed from (a) the starboard side and (b) the port side. Ruler is in inches.

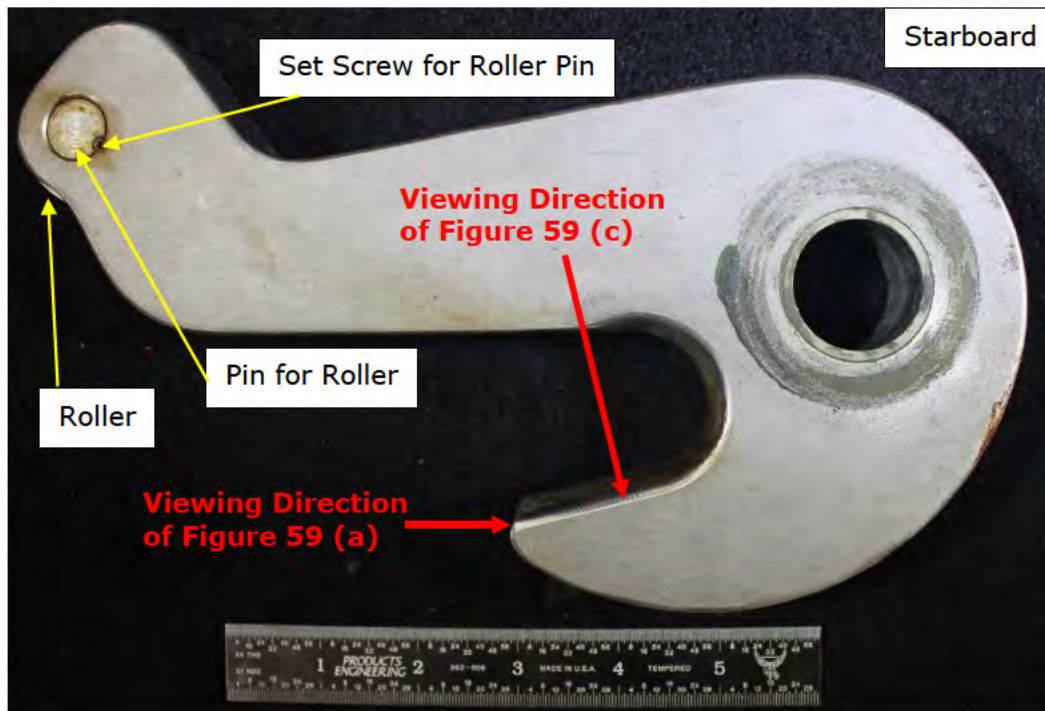


(a)

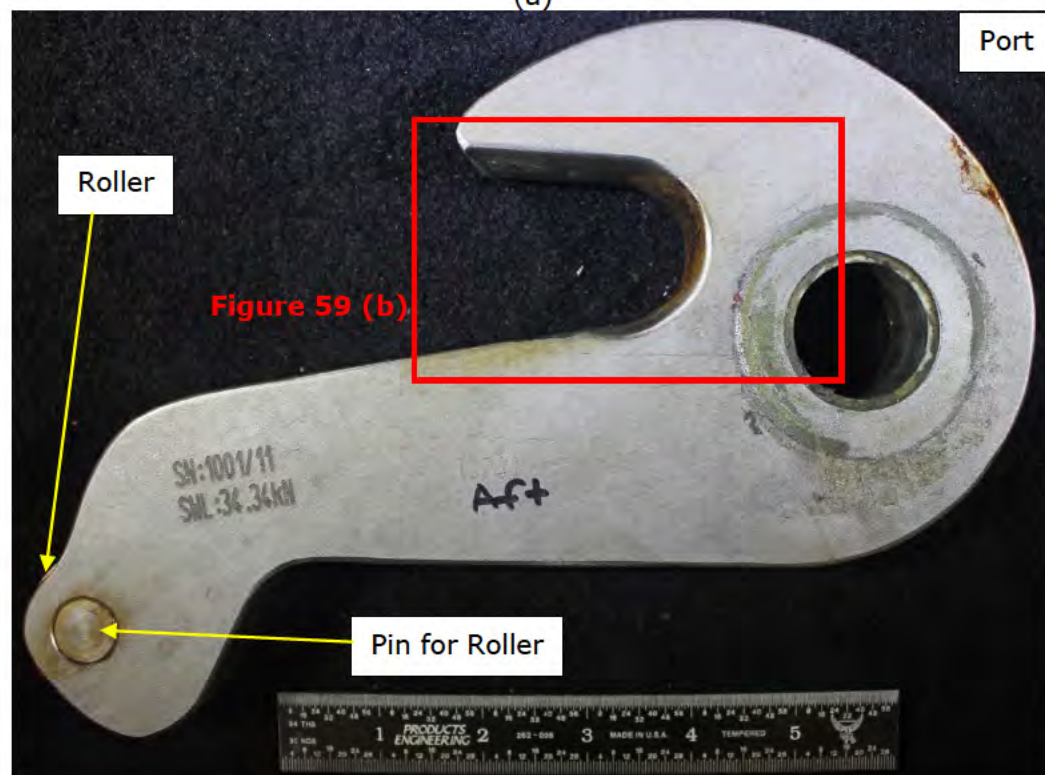


(b)

Figure 57. Photographs showing the as-found condition of the threaded connections of the Subject Aft Hook (a) at the clevis and (b) at the bulkhead nuts; the locations of the clevis and bulkhead nuts are shown in Figure 14. Ruler in left image is in inches.



(a)



(b)

Figure 58. Photographs of the hook from the Subject Aft Hook assembly showing the (a) starboard side and (b) port side, after disassembly. Ruler is in inches.

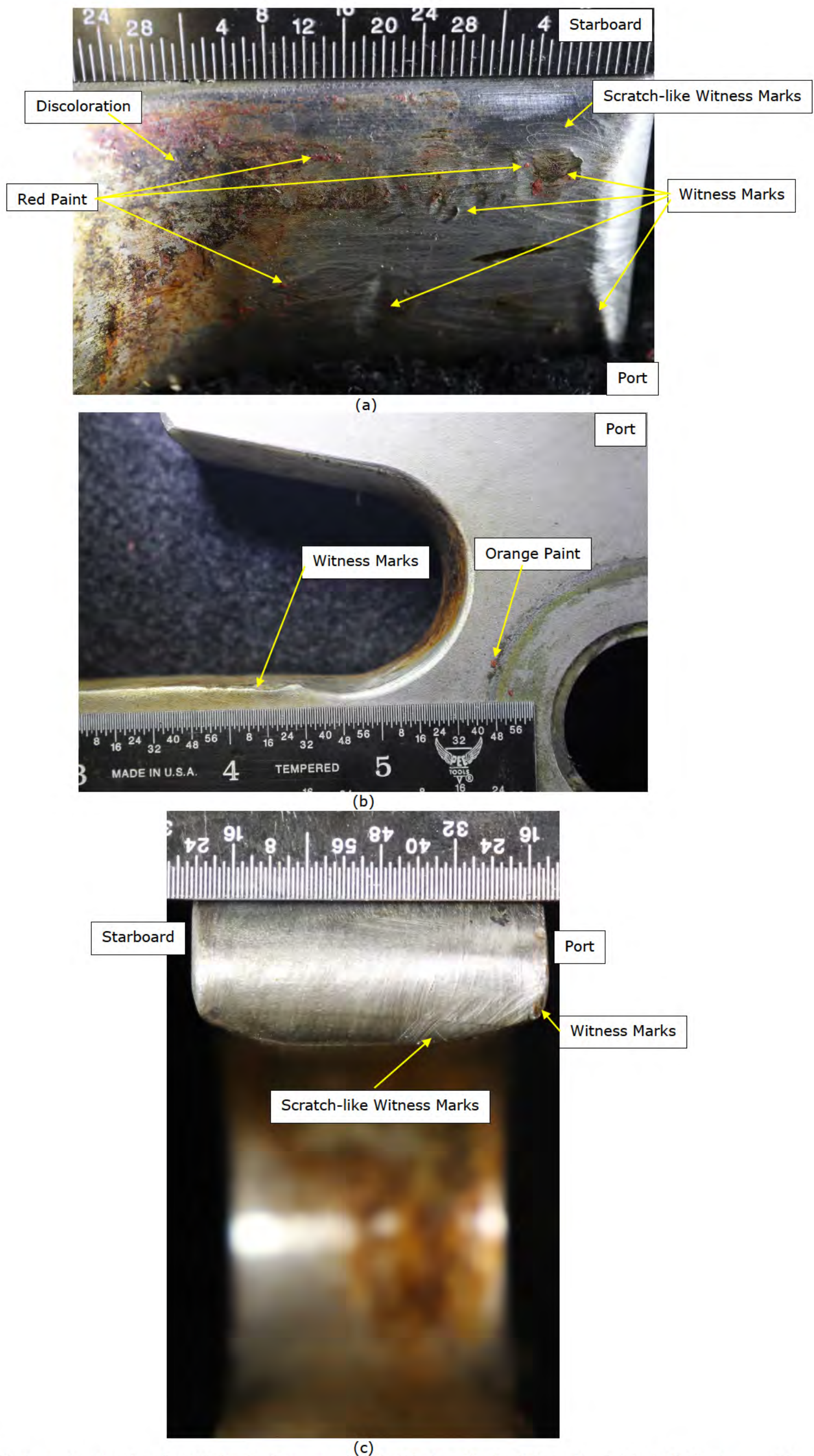
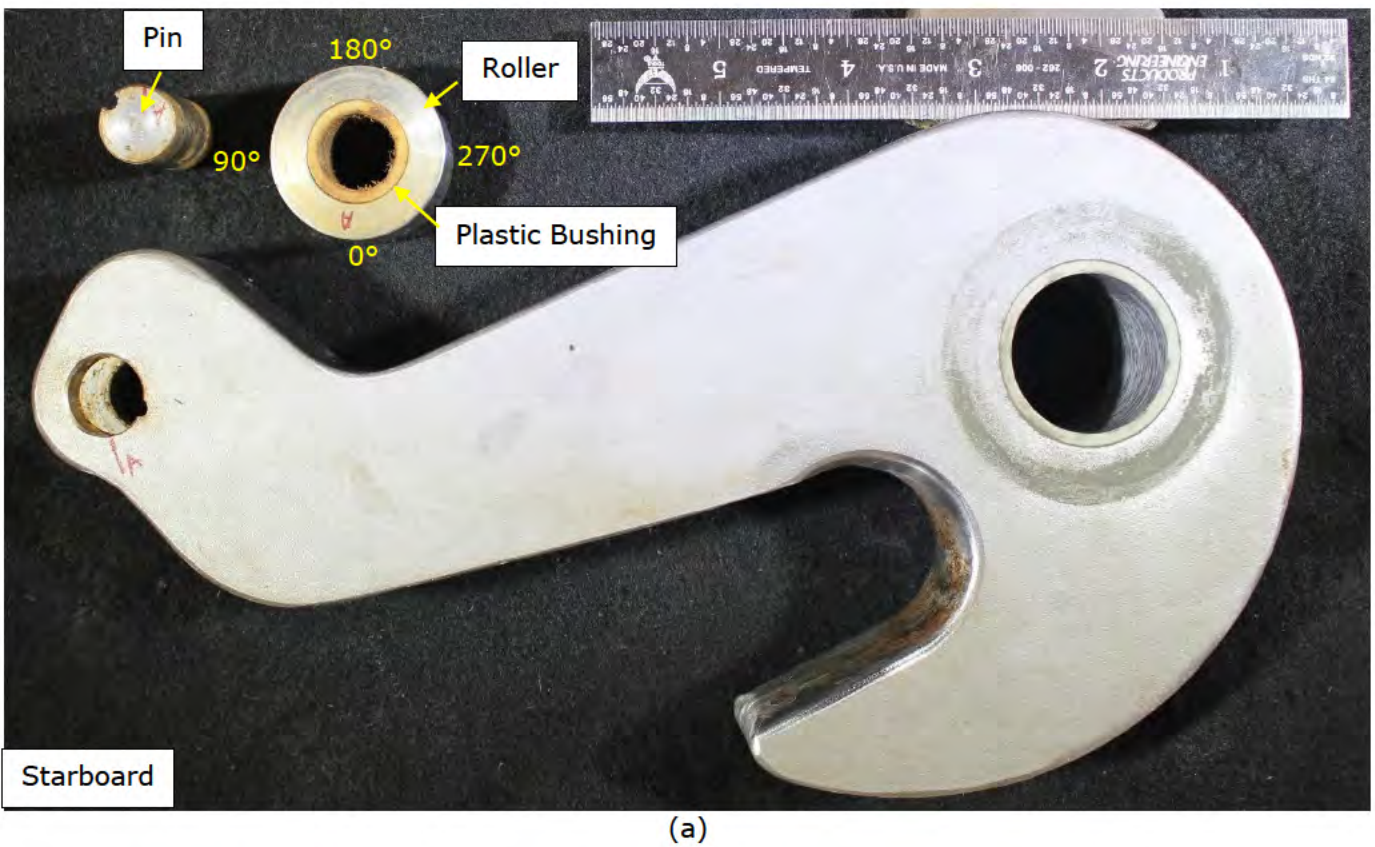
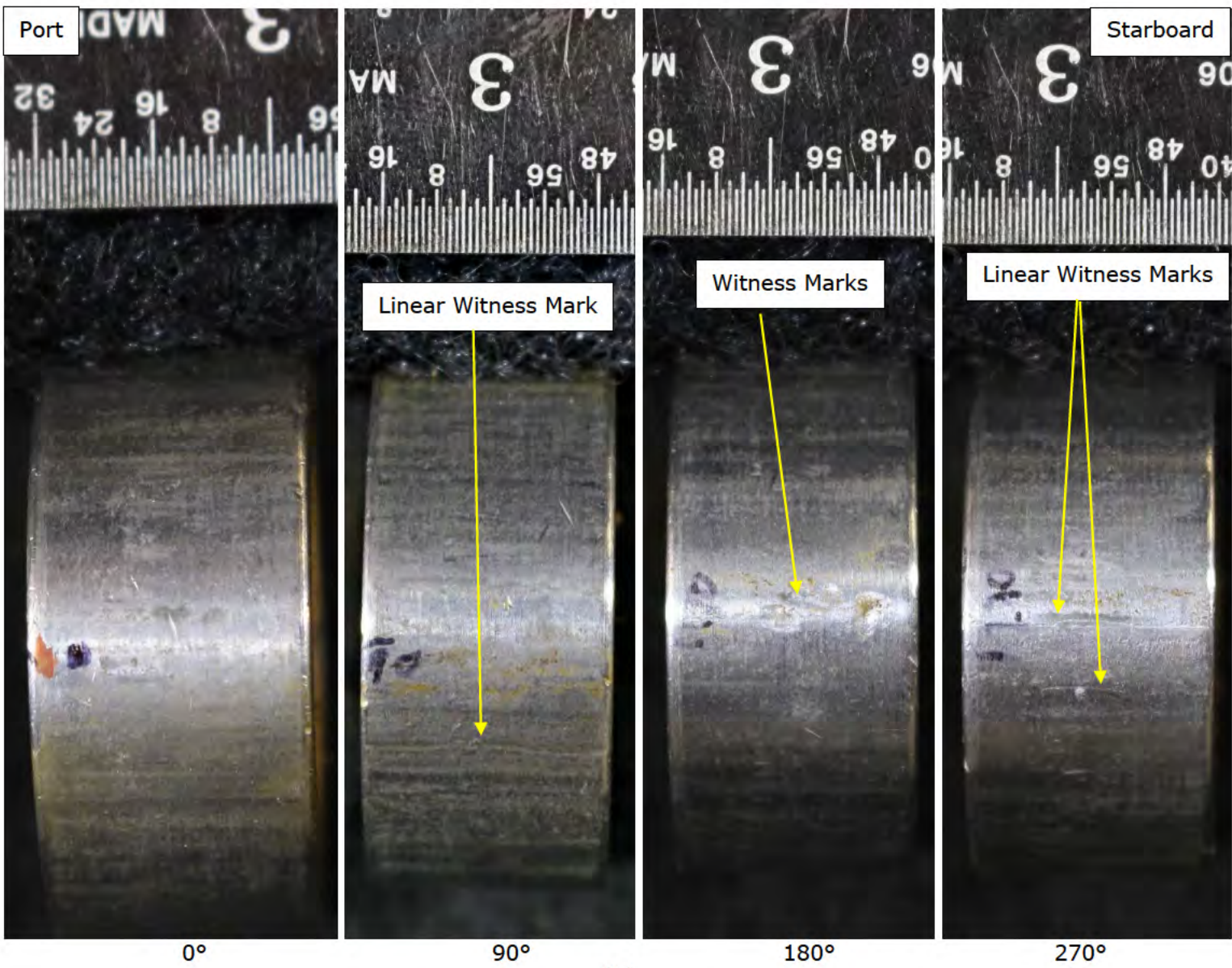


Figure 59. Photographs showing the details of witness marks identified on the hook from the Subject Aft Hook assembly at (a) the inside bend of the hook, (b) the edge of the bend as viewed from the port side, and (c) the point of the hook; locations and viewing directions shown in Figure 58 (a) and (b). Rulers are in inches.



(a)



(b)

Figure 60. Photographs showing the hook from the Subject Aft Hook assembly (a) after removing the set screw, pin, and roller, as well as (b) the details of the witness marks present on the contact surface of the roller. Ruler is in inches.

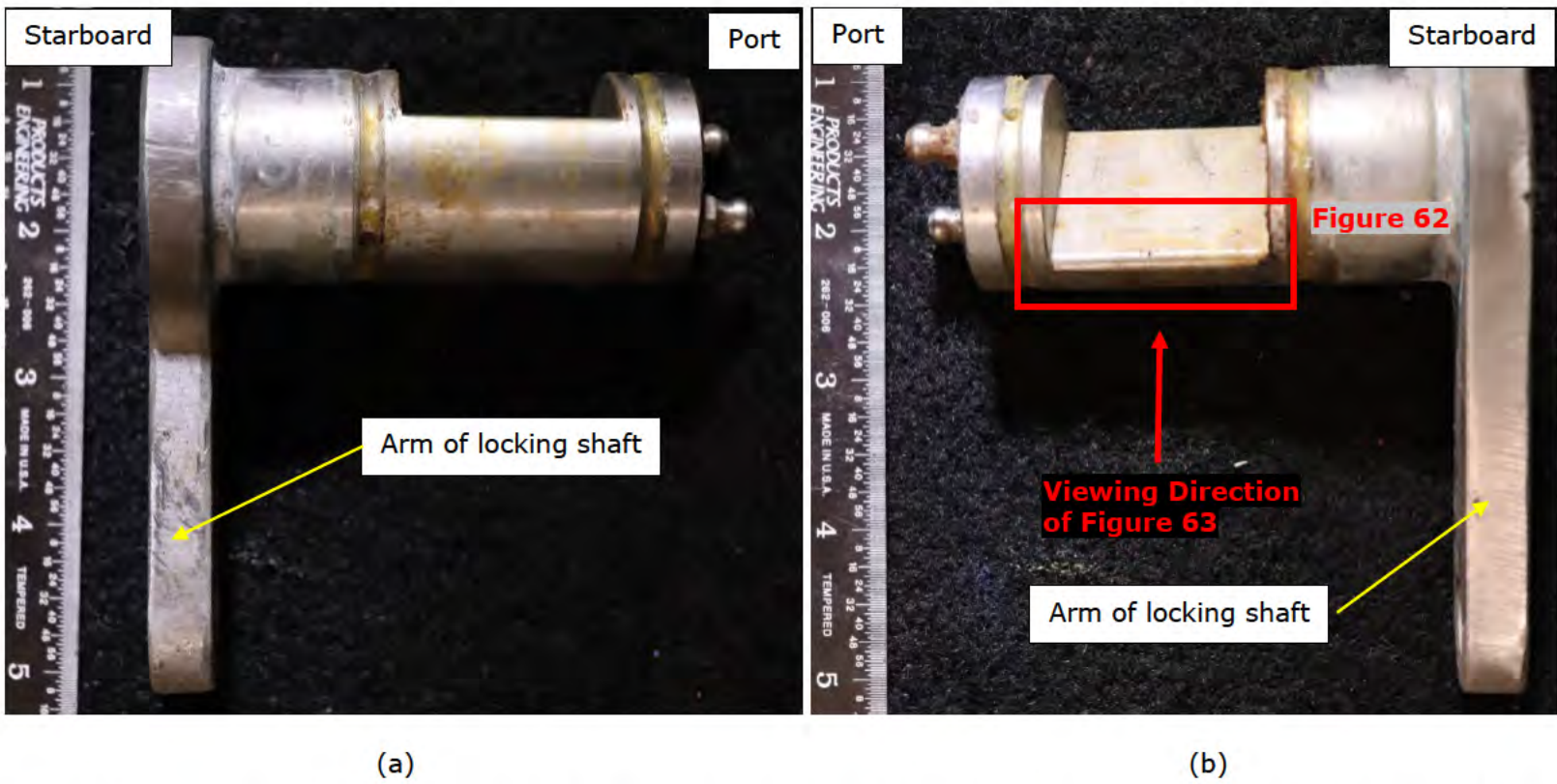


Figure 61. Photographs of the locking shaft from the Subject Aft Hook showing the (a) round side and (b) the flat, after disassembly. Rulers are in inches.

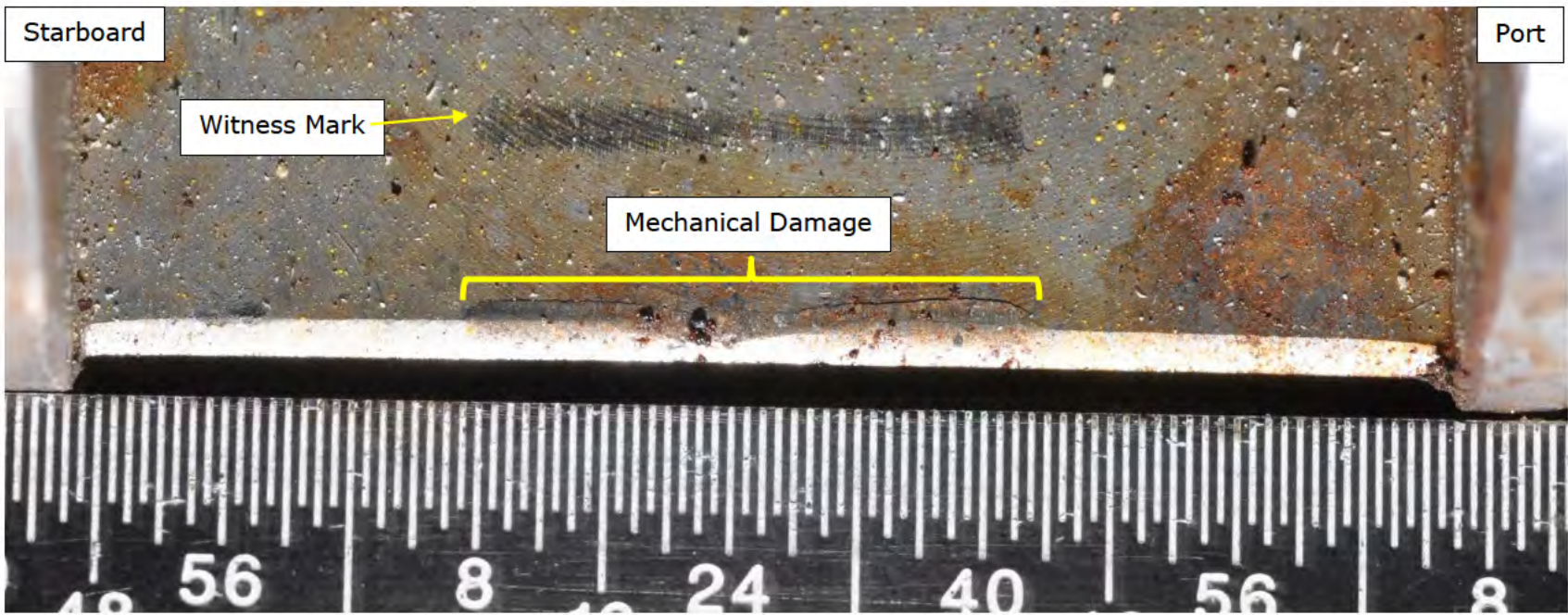


Figure 62. Photograph of the locking shaft from the Subject Aft Hook showing the mechanical damage on the edge between the round and the flat of the locking shaft. Ruler is in inches.



Figure 63. Photograph of the locking shaft from the Subject Aft Hook showing an area with corrosion attack on the round of the locking shaft. Ruler is in inches.

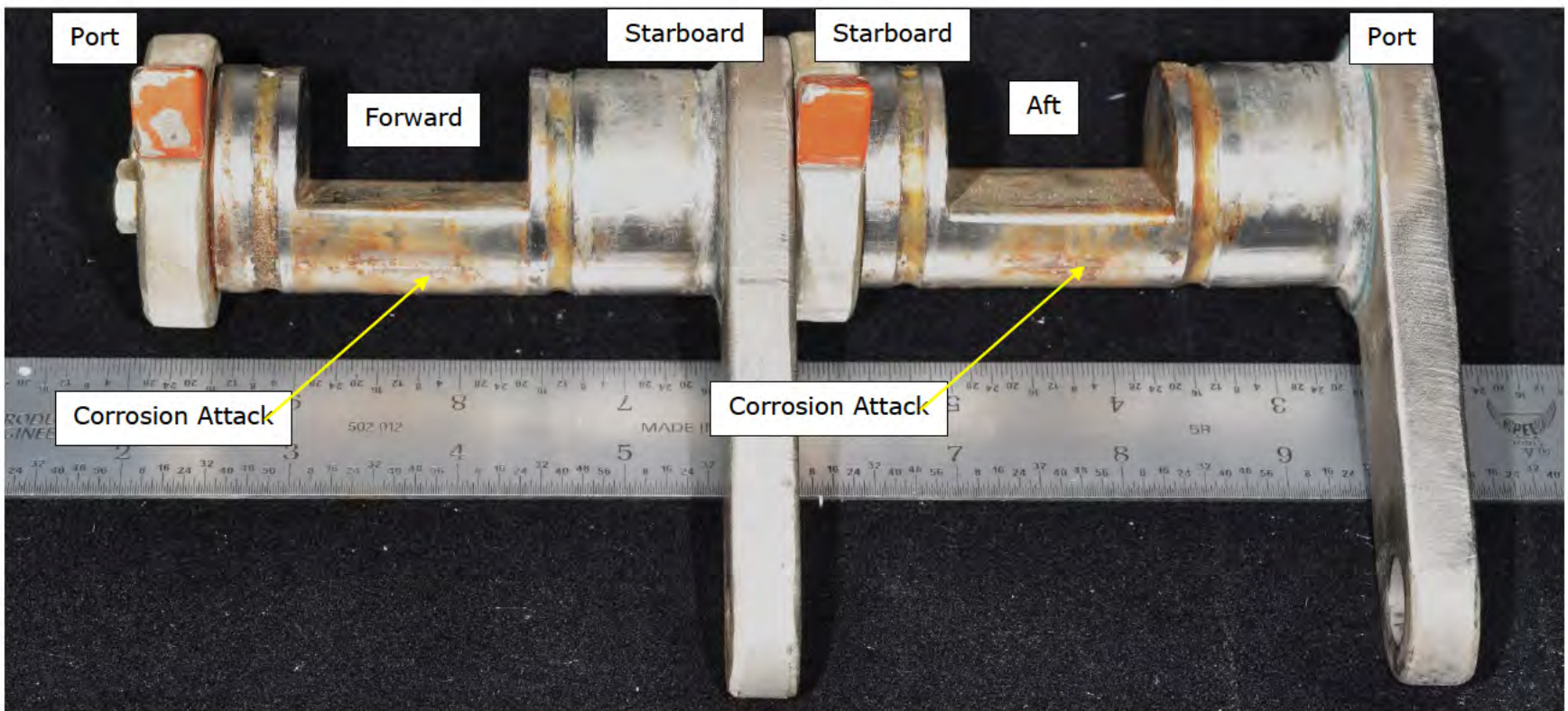


Figure 64. Photograph of the locking shaft from the Subject Forward and Aft Hooks comparing the areas of corrosion attack on the round of the locking shaft and comparing the overall geometry. Ruler is in inches.

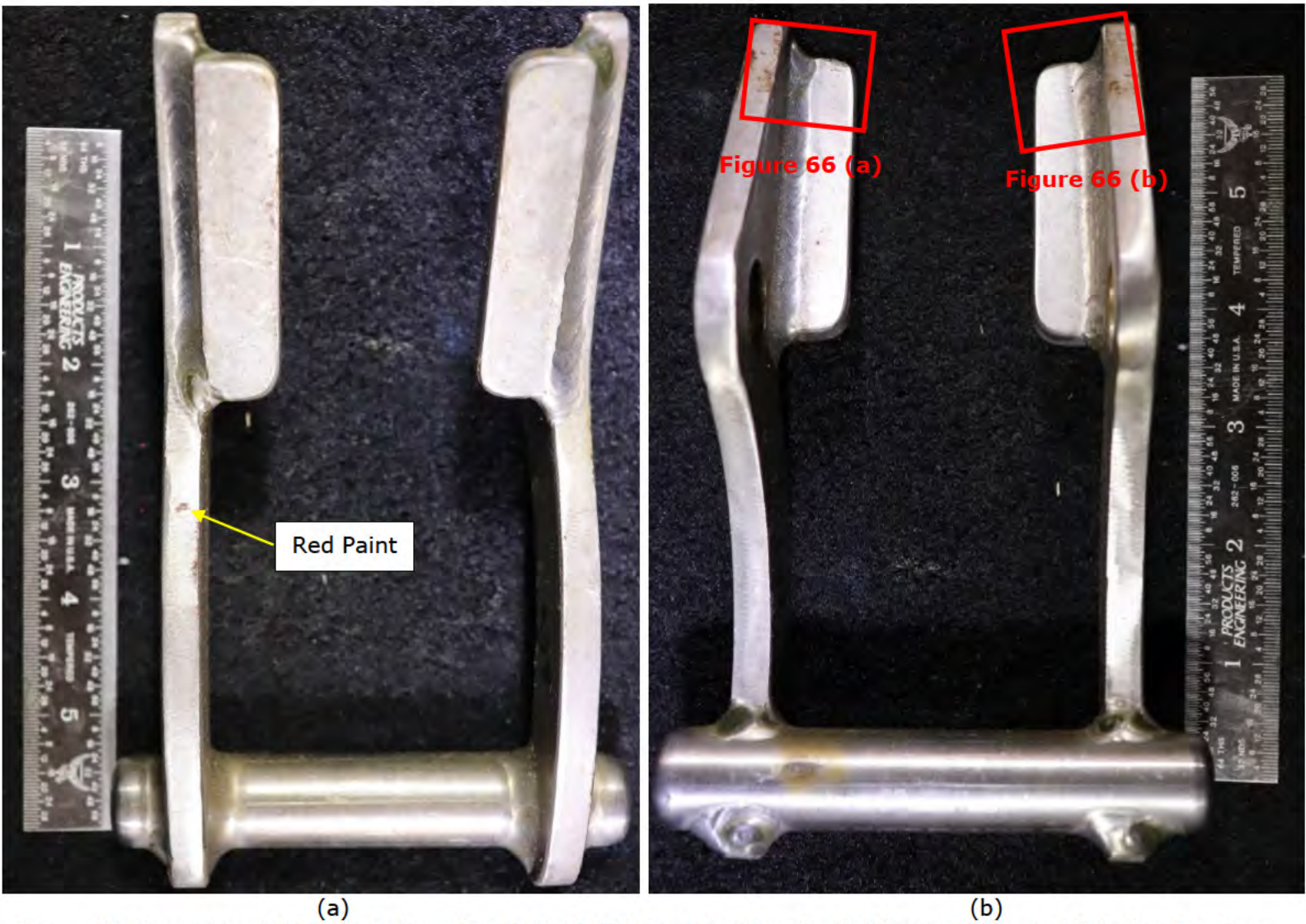


Figure 65. Photographs of the keeper from the Subject Aft Hook showing the (a) forward side and (b) aft side, after disassembly. Forward and aft refer to the orientation of the keeper relative to the lifeboat. Ruler is in inches.

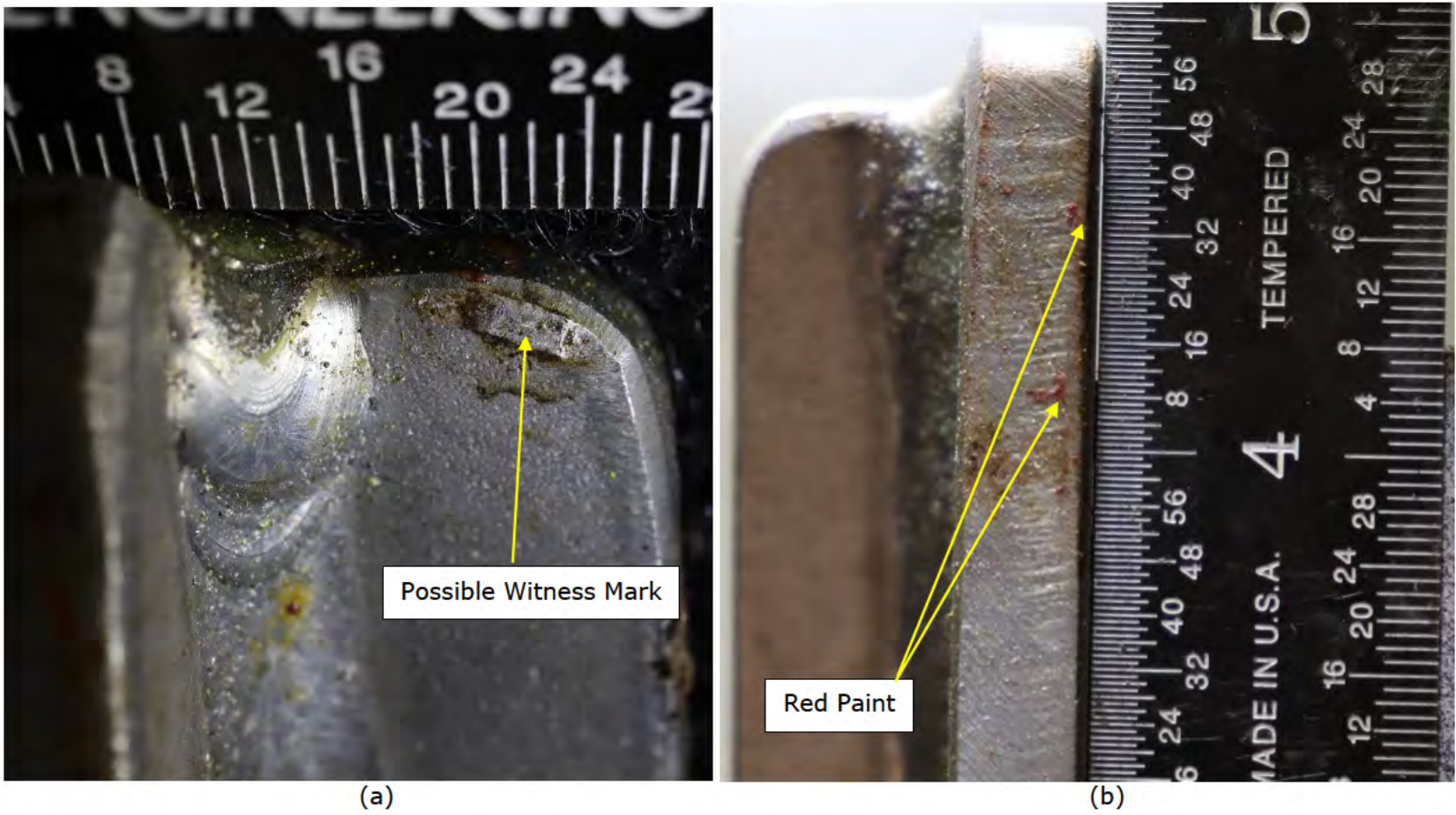


Figure 66. Photographs of the keeper from the Subject Aft Hook showing (a) a possible witness mark and (b) red paint; locations shown in Figure 65. Rulers are in inches.

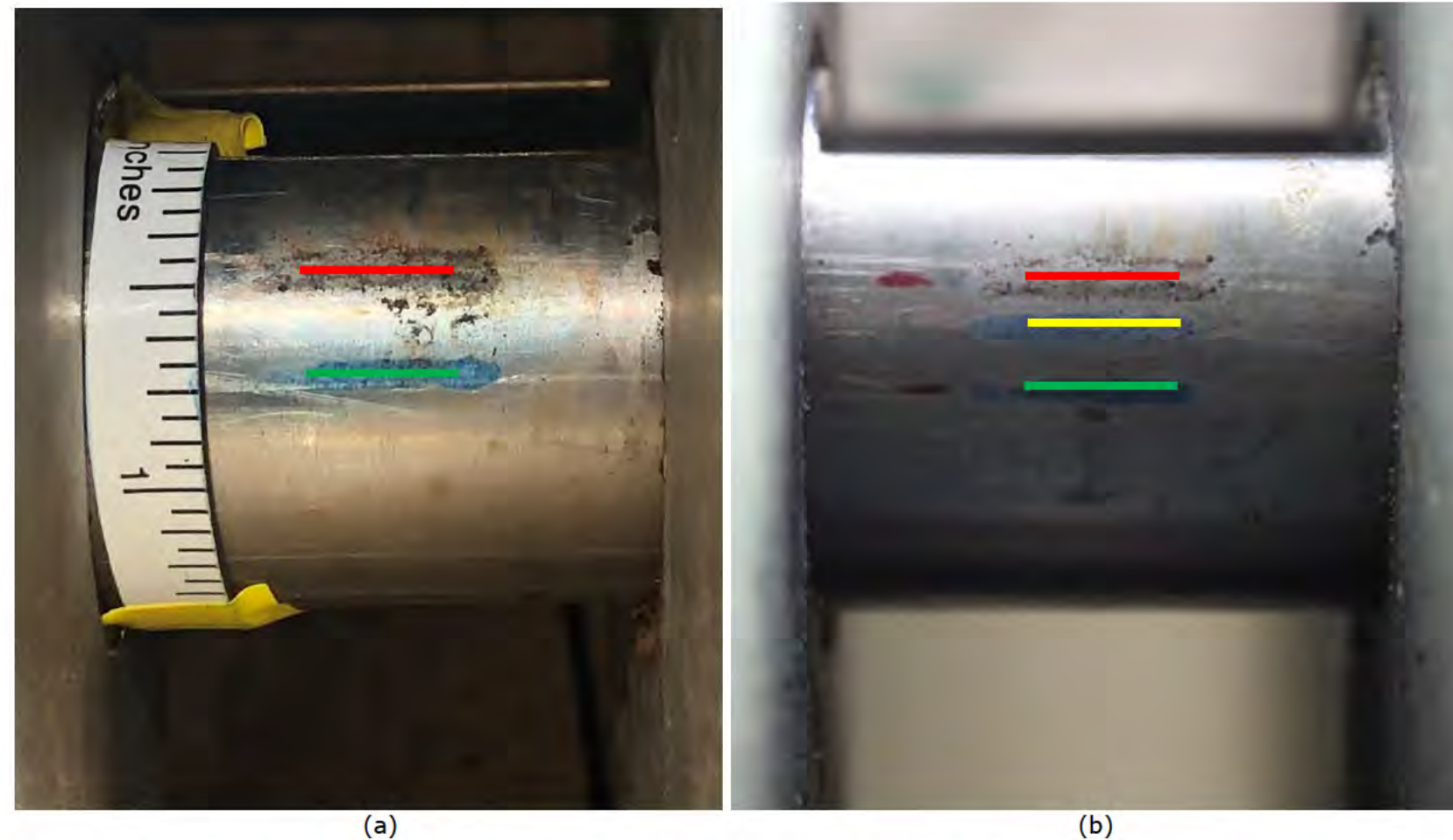


Figure 67. Photographs of the locking shaft from the Subject Aft Hook installed (a) in the Subject Aft Hook and (b) in the Exemplar Hook with the clevises and bulkhead nuts set to the as-found condition of the subject components. In both cases, the Subject Release Unit was in the closed position and the Exemplar Cable was used. The blue markings were produced by placing articulating paper between the hook roller and locking shaft contact location. The green line indicates the contact location between the hook roller and locking shaft when the locking shaft arm is fully closed. The red line is consistent with an area of corrosion and wear. The yellow line indicates the contact location between the hook roller and locking shaft when the release unit is closed, but the locking shaft arm is rotated as far as possible towards the open orientation. The red line is consistent with an area of corrosion and wear.

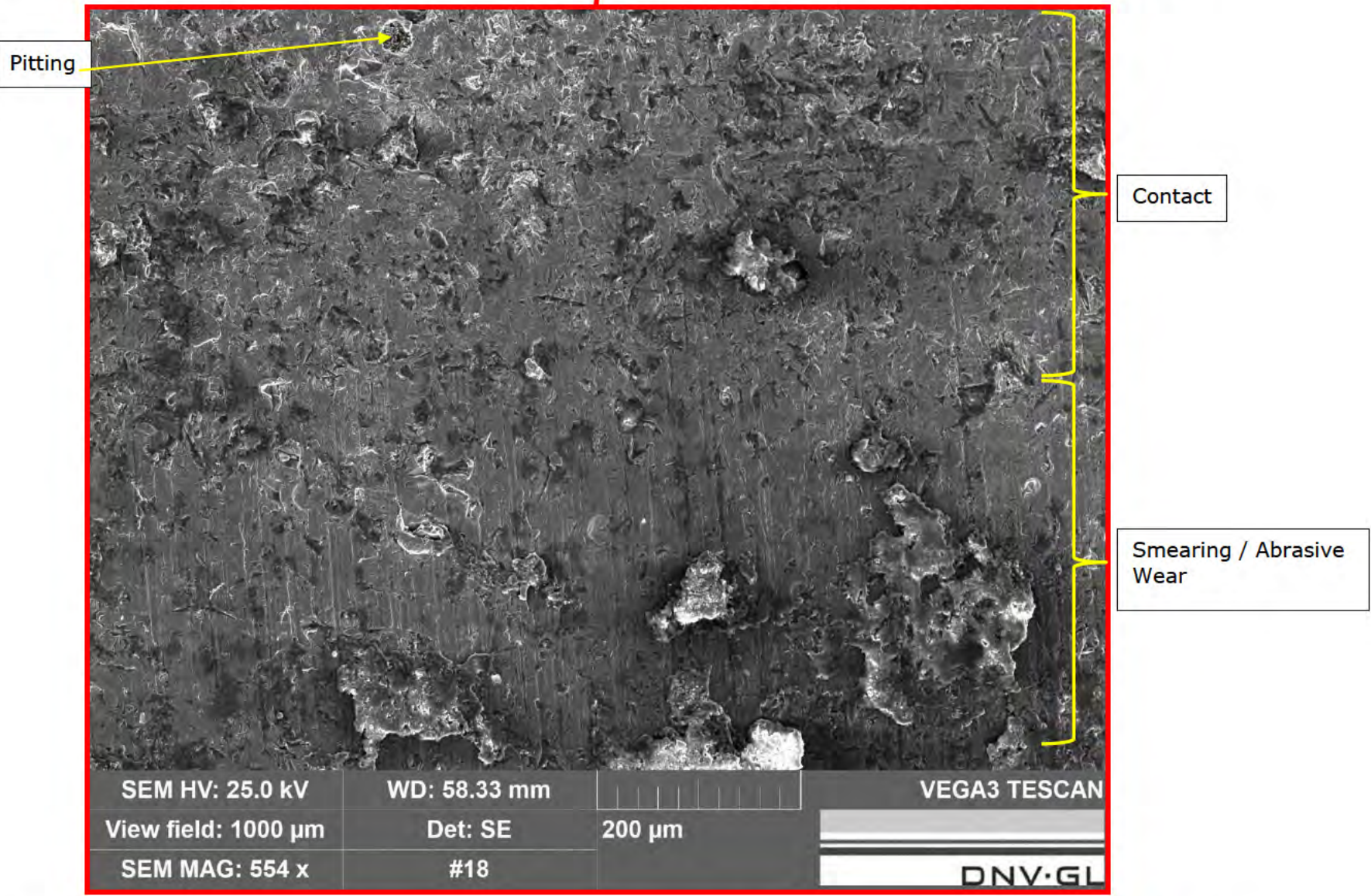
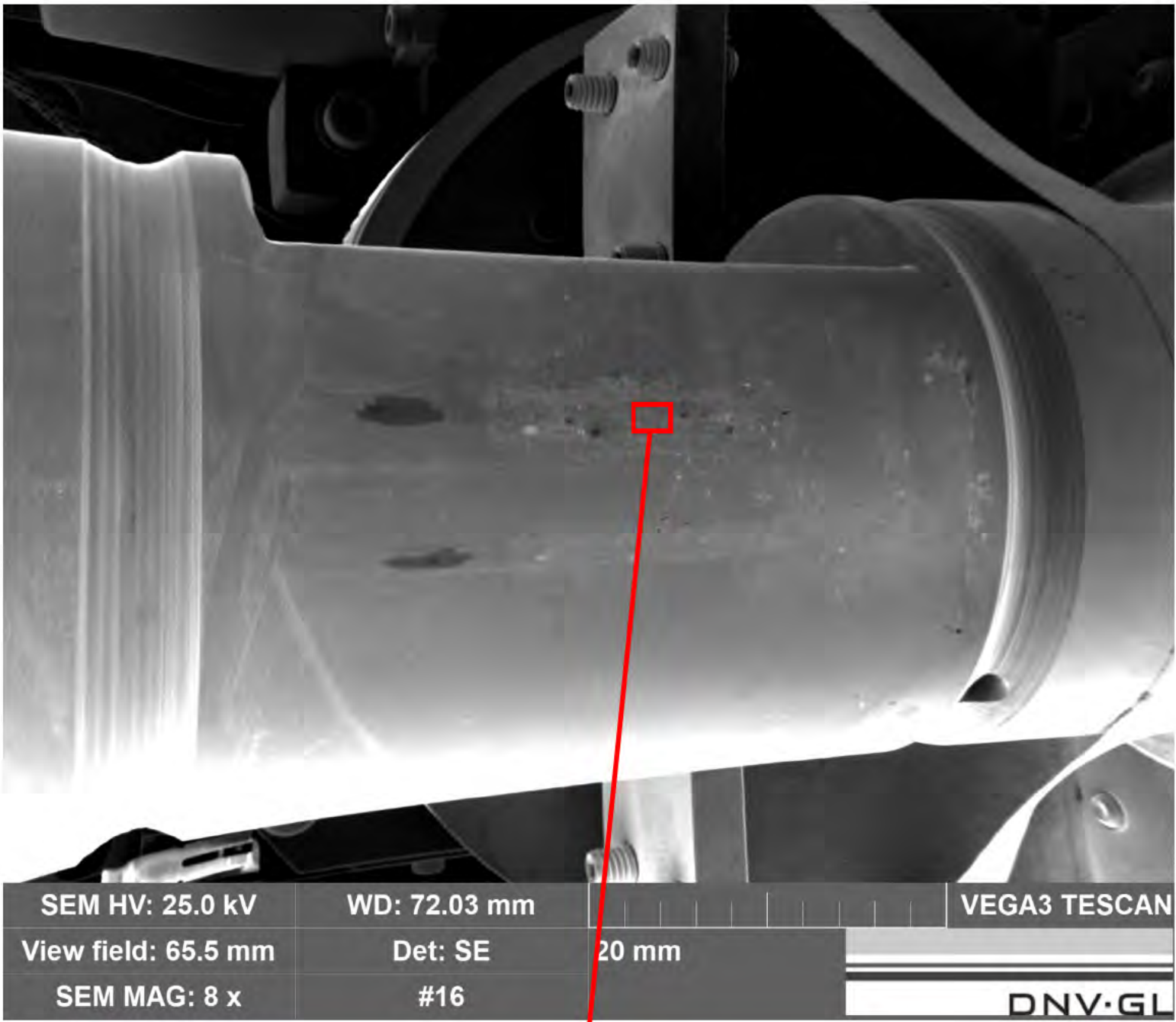


Figure 68. SEM images showing the detail for a suspected area of contact between the roller of the hook and locking shaft from the Subject Aft Hook.

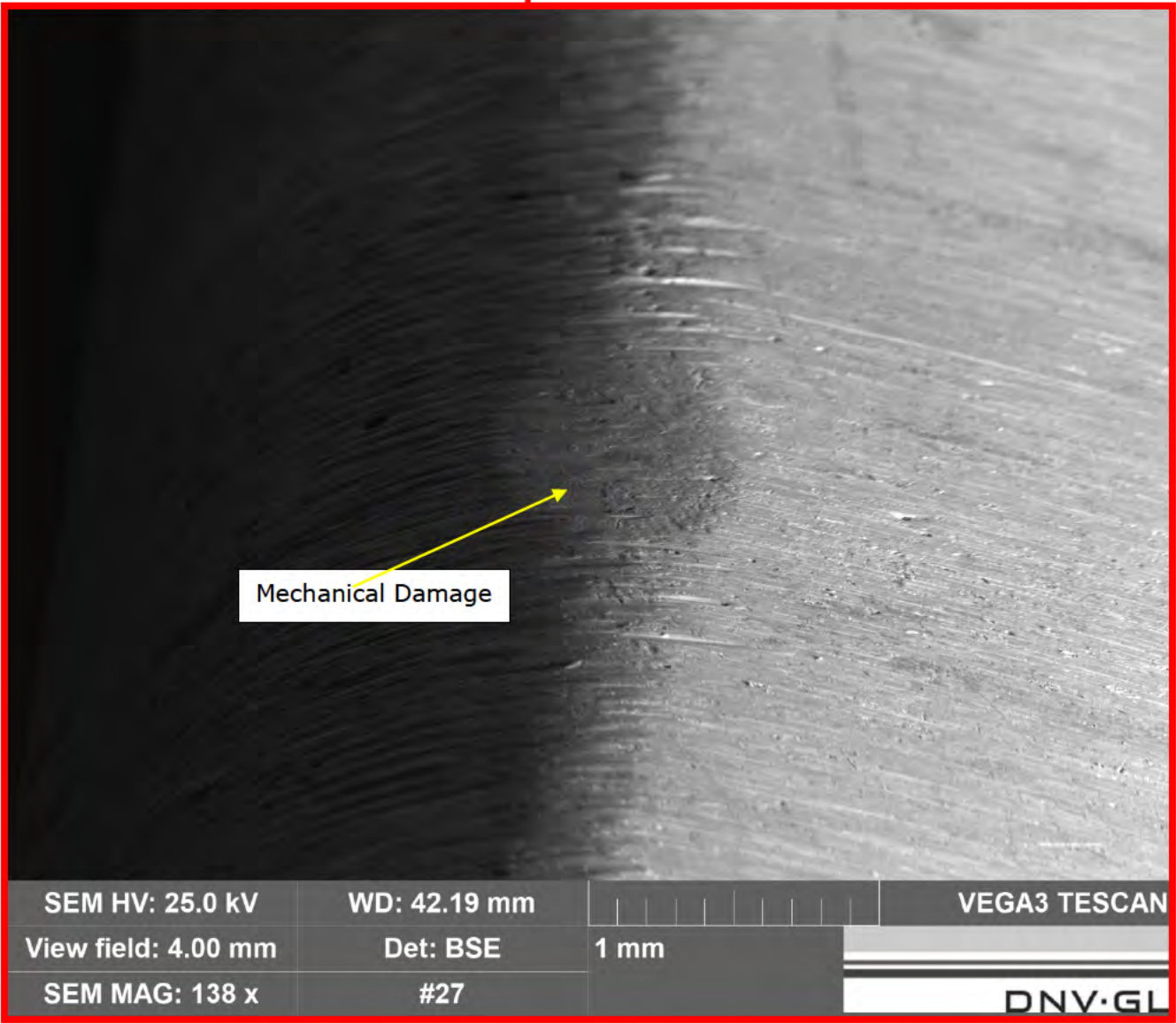
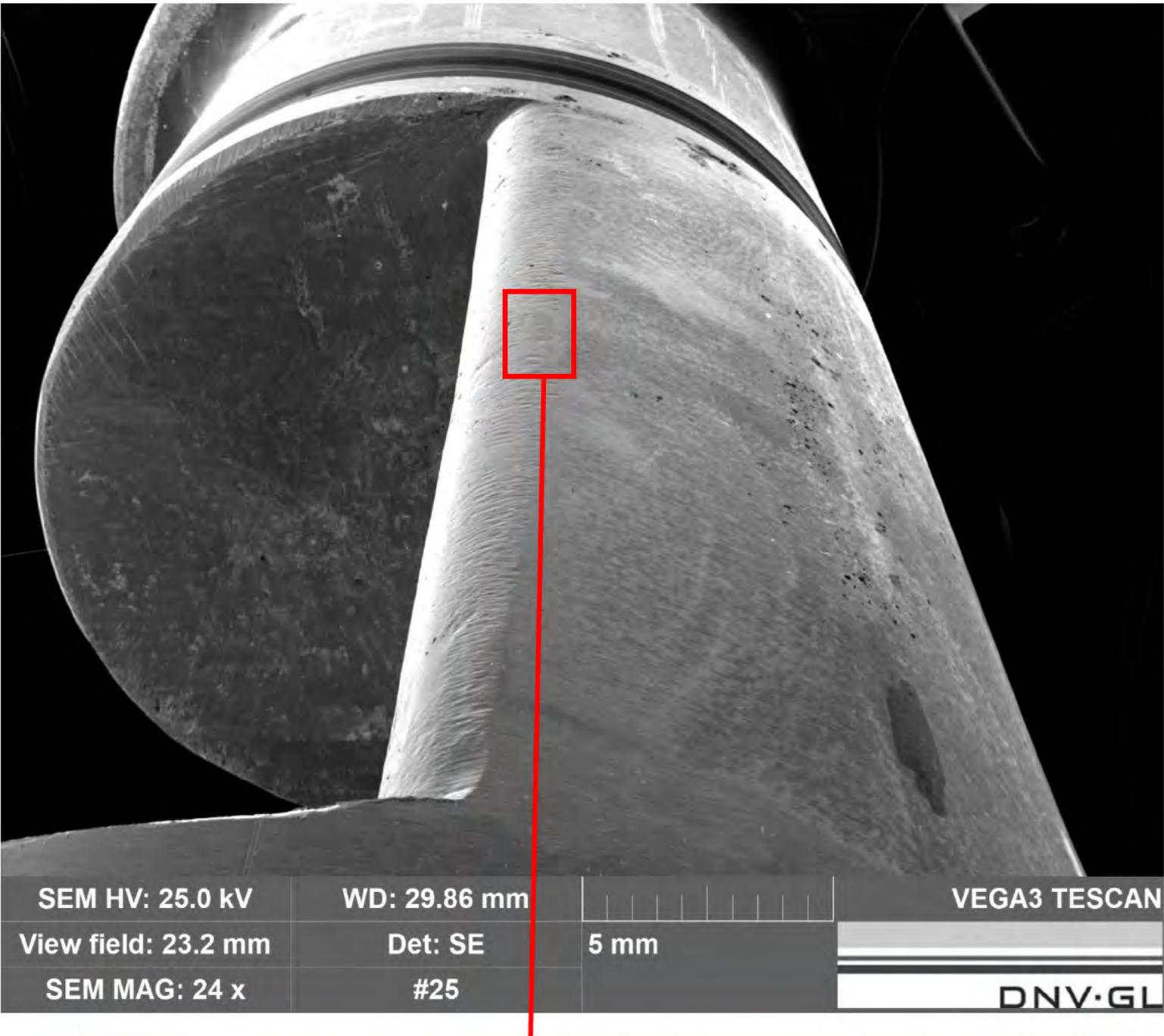


Figure 69. SEM images showing mechanical damage near the transition to the flat of the locking shaft from the Subject Aft Hook.

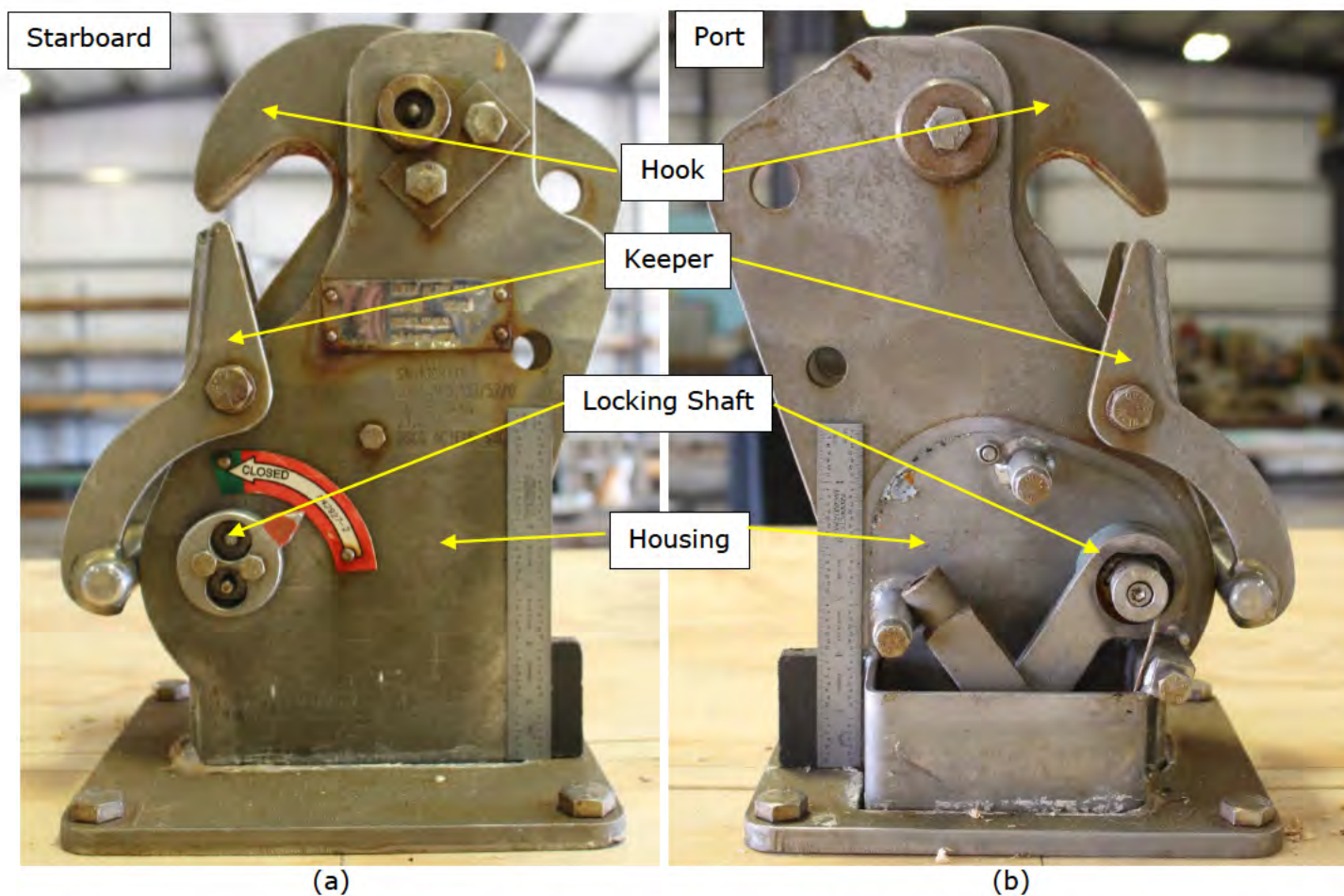
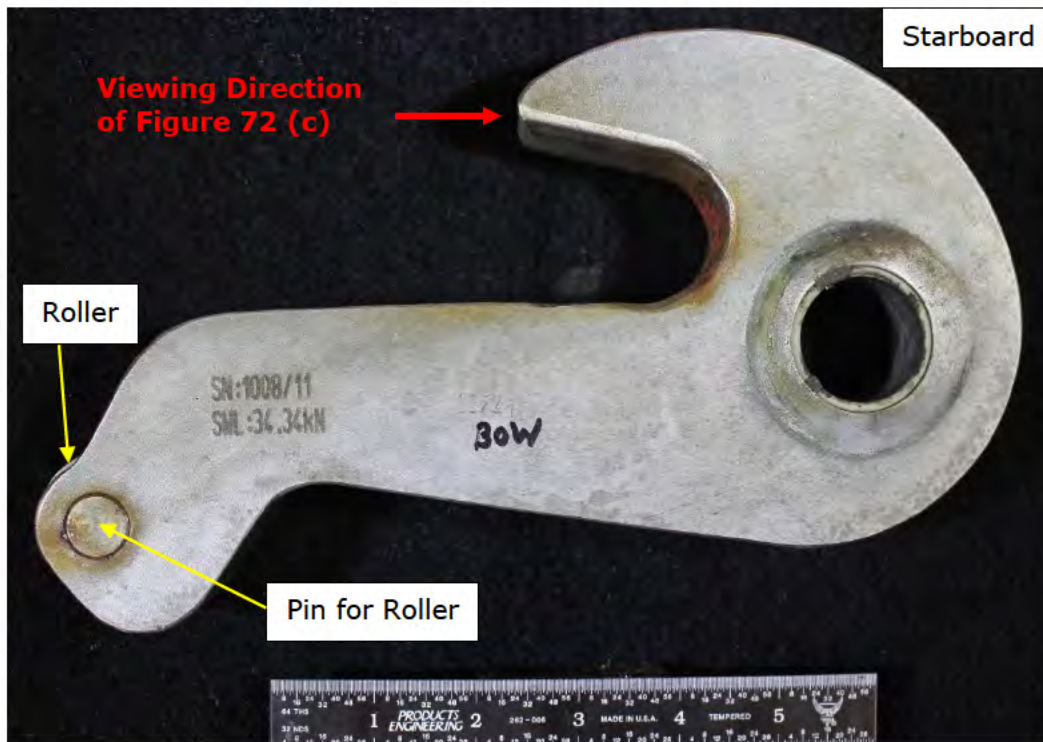
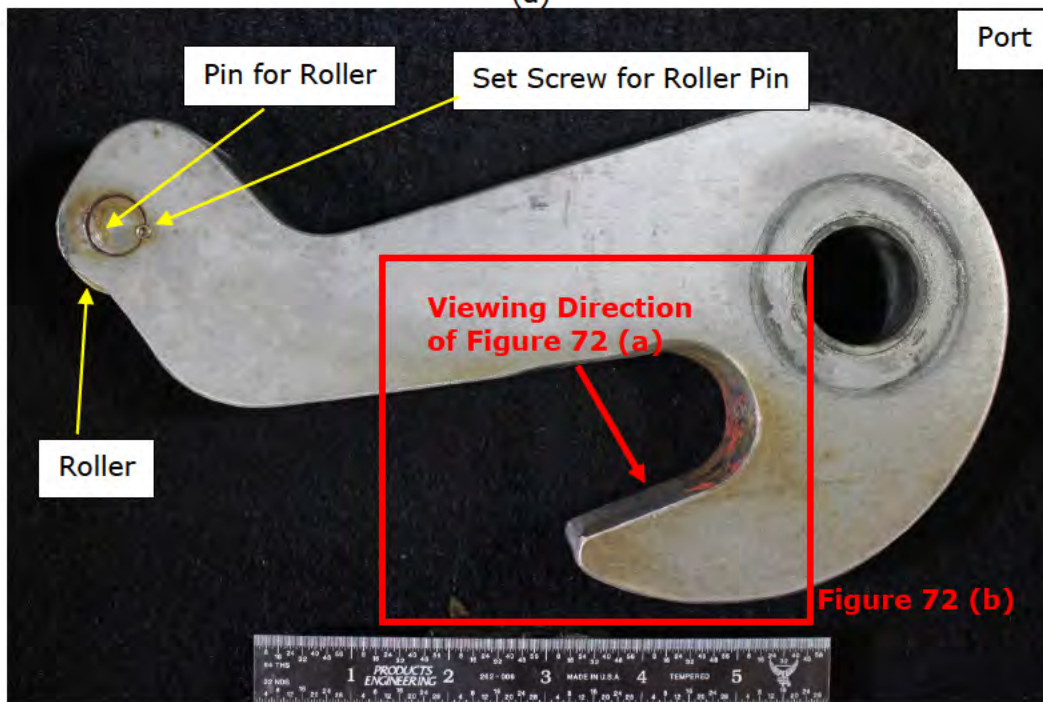


Figure 70. Photographs of the Subject Forward Hook with the locking shaft cover removed, viewed from (a) the starboard side and (b) the port side. Rulers are in inches.



(a)



(b)

Figure 71. Photographs of the hook from the Subject Forward Hook showing the (a) starboard side and (b) port side, after disassembly. Ruler is in inches.

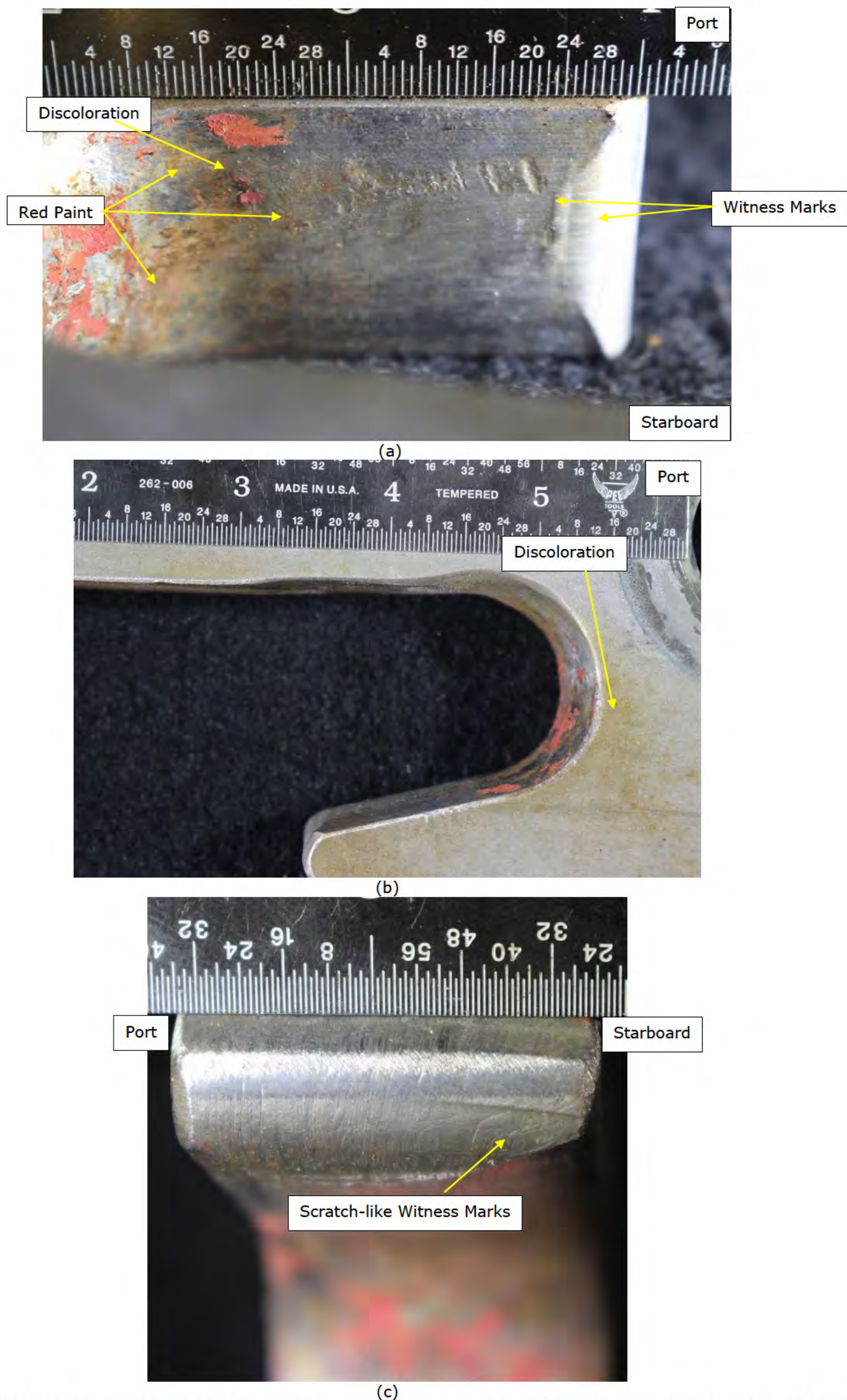


Figure 72. Photographs showing the details of witness marks identified on the Subject Forward Hook at (a) the inside bend of the hook, (b) the edge of the bend as viewed from the port side, and (c) the point of the hook; locations and viewing directions shown in Figure 58 (a) and (b). Rulers are in inches.

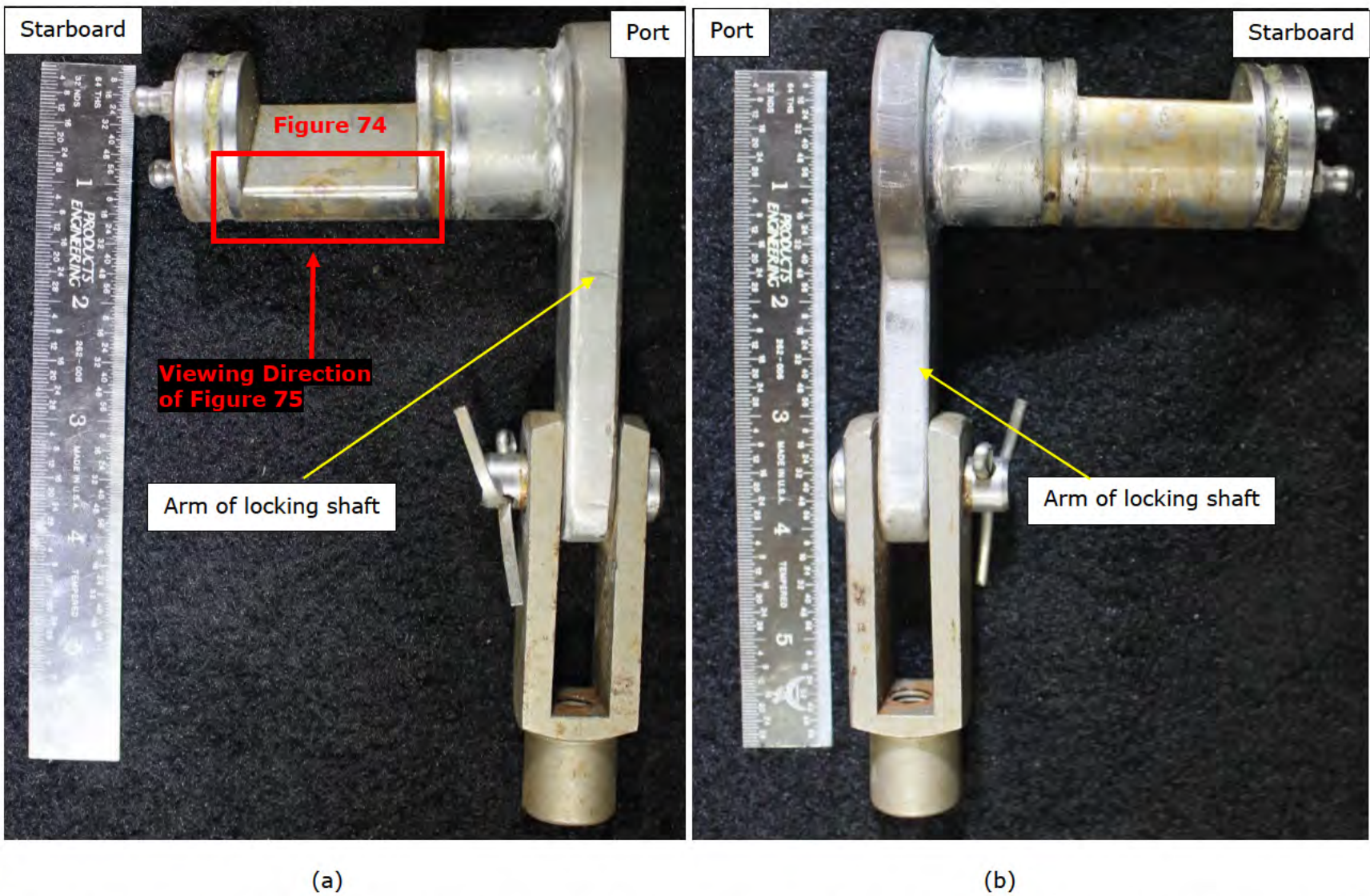


Figure 73. Photographs of the locking shaft from the Subject Forward Hook showing the (a) round side and (b) the flat, after disassembly. Rulers are in inches.



Figure 74. Photograph of the locking shaft from the Subject Forward Hook showing the edge between the round and flat of the locking shaft; area shown in Figure 73. Ruler is in inches.



Figure 75. Photograph of the locking shaft from the Subject Forward Hook showing an area with corrosion attack on the round of the locking shaft; area shown in Figure 73. Ruler is in inches.

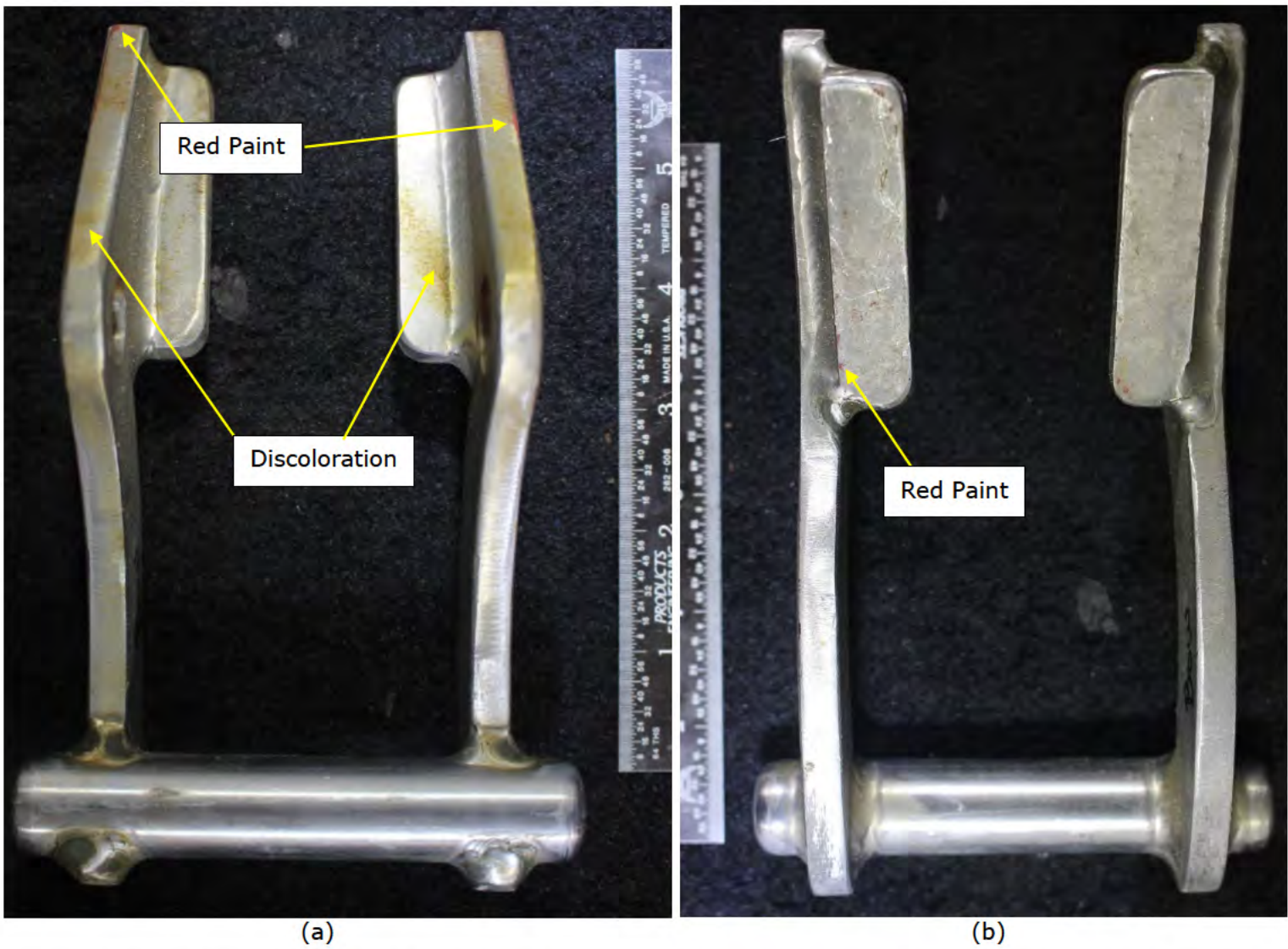


Figure 76. Photographs of the keeper from the Subject Forward Hook showing the (a) forward side and (b) aft side, after disassembly. Forward and aft refer to the orientation of the keeper relative to the lifeboat. Rulers are in inches.



Figure 77. Laser scans of Subject Aft Hook components displayed individually. From left to right: the locking shaft (gold), the keeper (yellow), the hook (orange), and the housing (purple). The Locations A, B, and C correlate to the centerlines of the components and their respective positions in the housing.

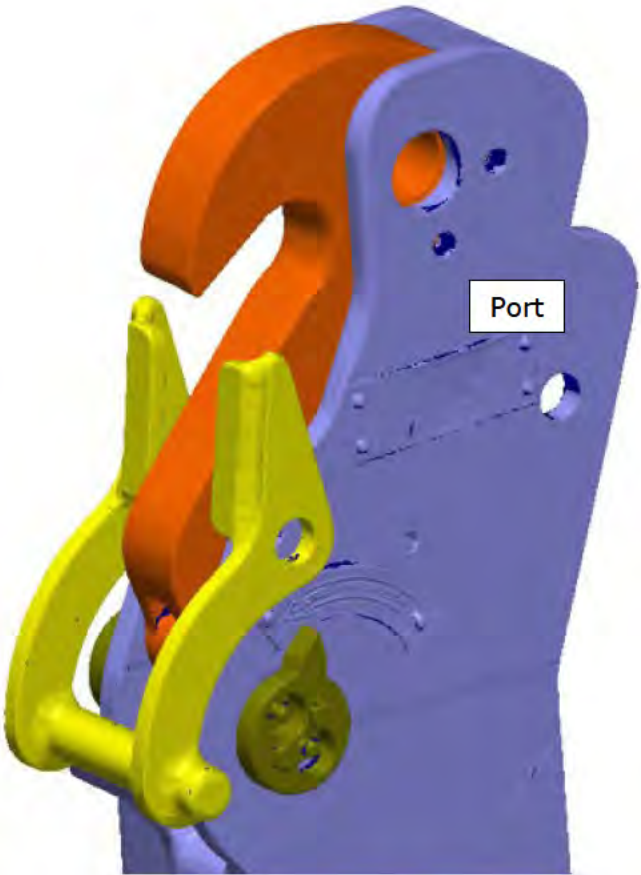


Figure 78. Laser scans of Subject Aft Hook components aligned to working positions.

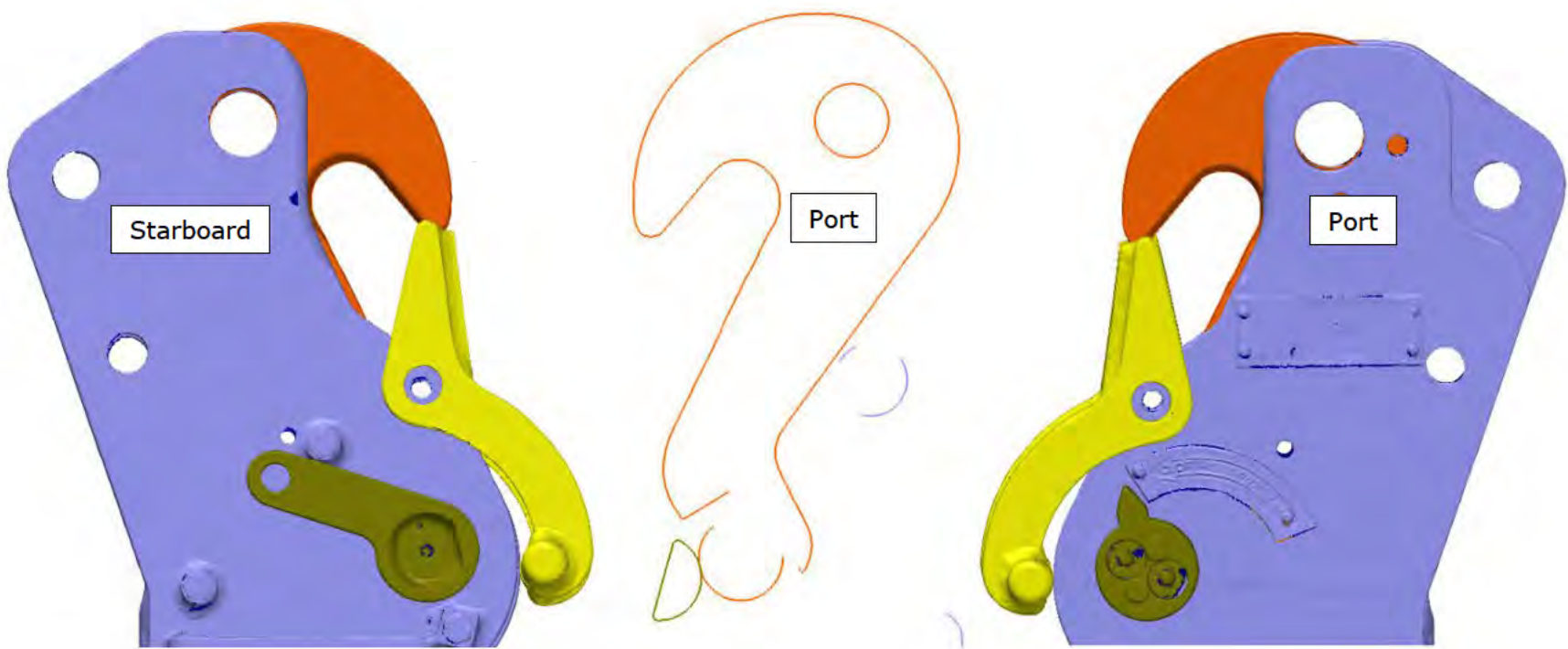


Figure 79. Laser scans of Subject Aft Hook components aligned to working positions with the locking shaft rotated into contact with the post of the hook body. An outline of the components shows the interacting locations of the hook and locking shaft.

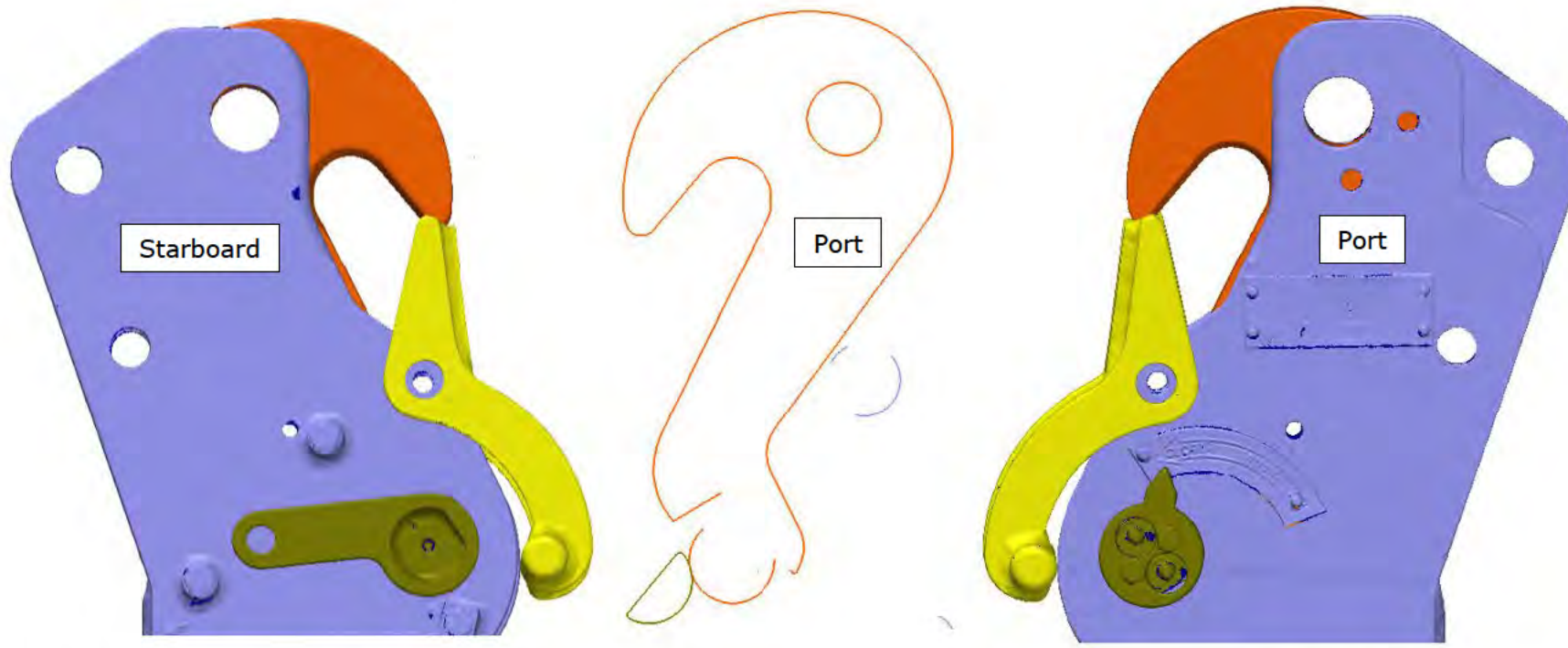


Figure 80. Laser scans of Subject Aft Hook showing the 3D assembly aligned assuming elongation of the liner equivalent to 2.58 inches. An outline of the components shows the interacting locations of the hook and locking shaft.

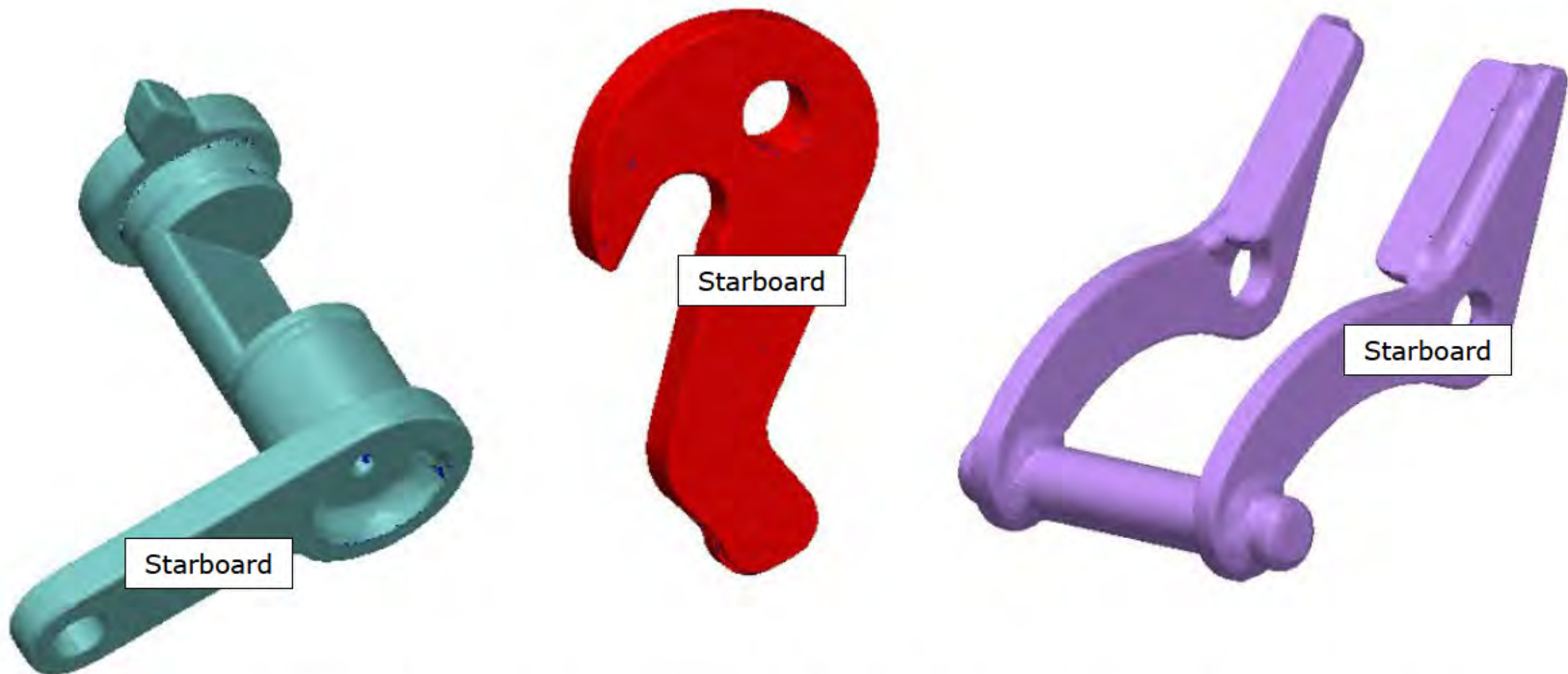
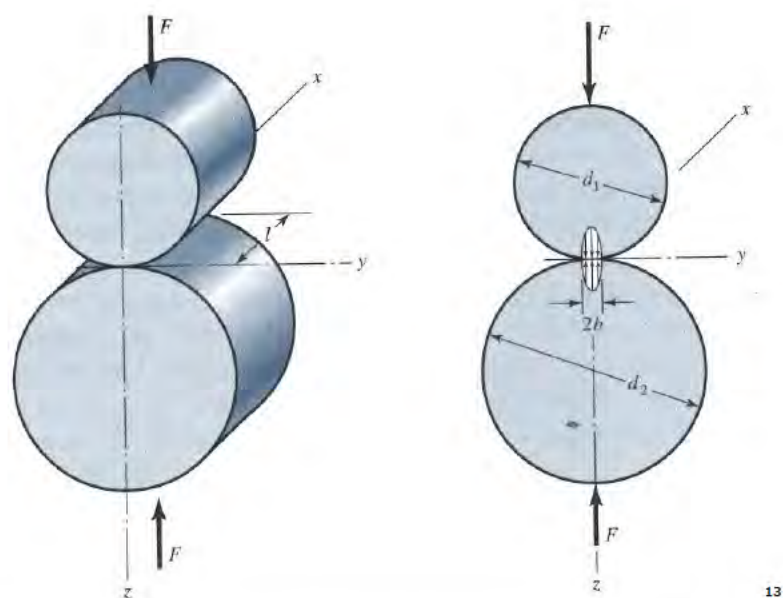


Figure 81. Laser scans of Subject Forward Hook components. From left to right: the locking shaft (teal), the hook (red), and the keeper (light purple).



| Variable | Value | Units | Notes |
|---------------------|------------|--------|--|
| F | 4,390.5 | lbs | 50% of boat weight (8,781 lbs) at time of incident estimated by USGC |
| l | 0.59 | inches | Hook roller width |
| ν_1 and ν_2 | 0.3 | — | Poisson's Ratio (assumed equal for both materials) |
| E_1 and E_2 | 29,000,000 | psi | Elastic Modulus (assumed equal for both materials) |
| d_1 , closed | 1.376 | inches | Locking shaft closed diameter measured with laser scan data |
| d_1 , edge | 0.169 | inches | Locking shaft edge diameter measured with laser scan data |
| d_2 | 0.59 | inches | Hook roller outer diameter measured with laser scan data |

Figure 82. Two right circular cylinders held in contact by forces F uniformly distributed along length l (Left). Elliptical contact stress distribution across contact area $2b$ (Right). Table of variables used in associated calculations (Bottom).

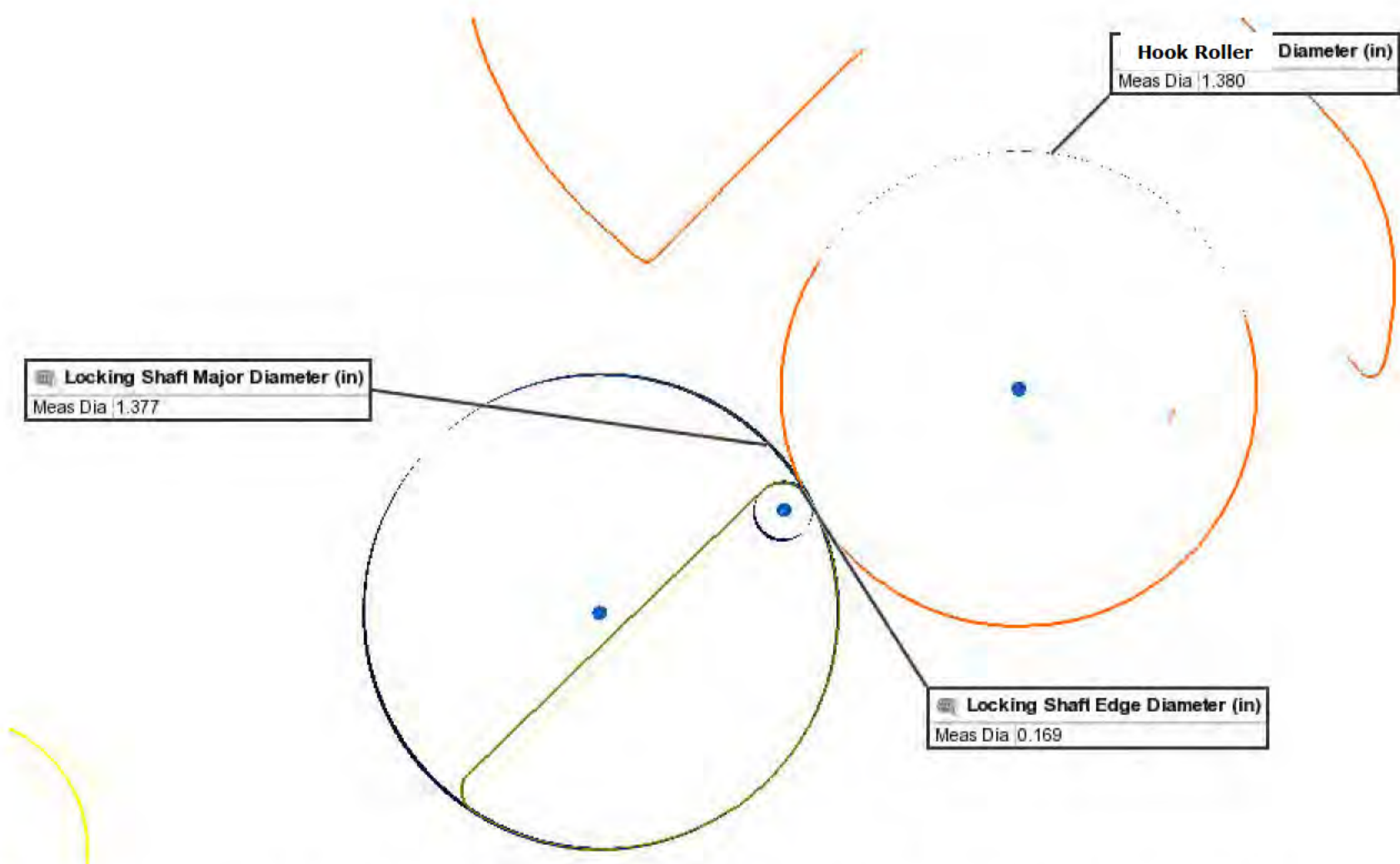


Figure 83. Locking shaft major diameter, locking shaft edge diameter and hook roller diameter illustrated by fitting nominal cylinders to the Subject Aft Locking Shaft (green) and Subject Aft Hook (Orange).

13 Budynas, R., Nisbett, K. (2008). Shigley's Mechanical Engineering Design. 8th edition. McGraw-Hill.

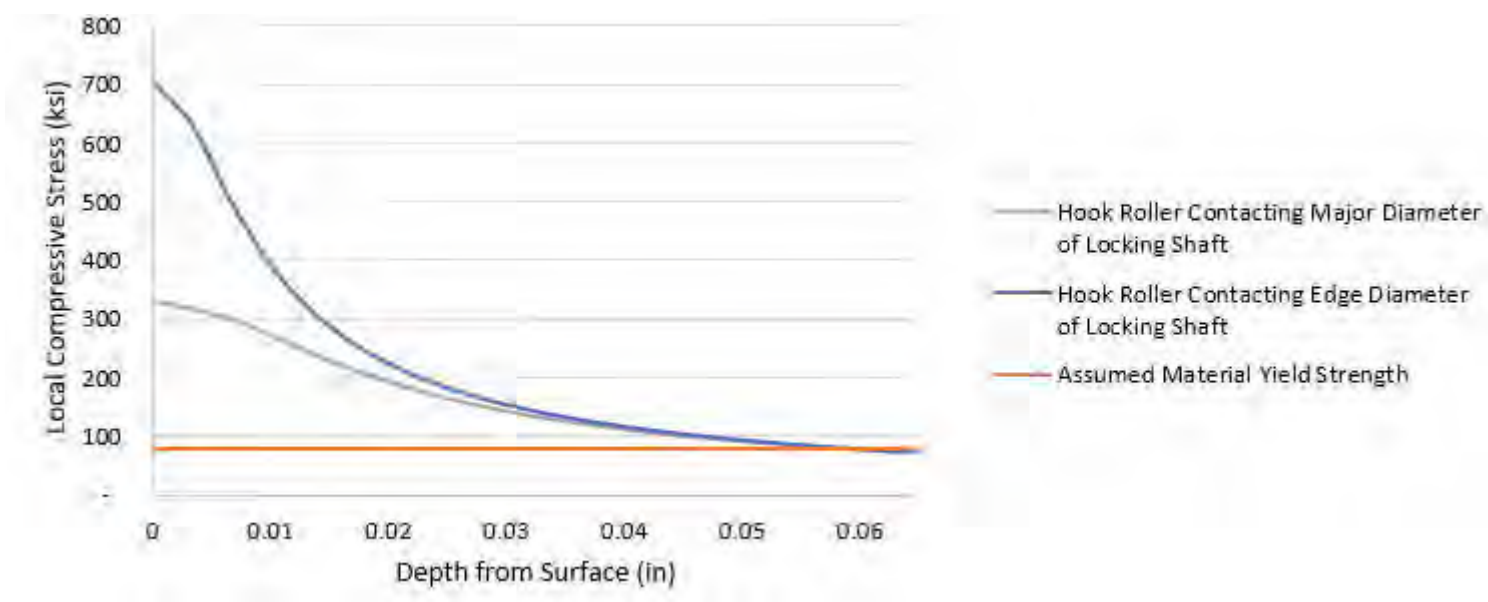


Figure 84. Local Compressive Stress vs. Depth into Material from Contact Surface.

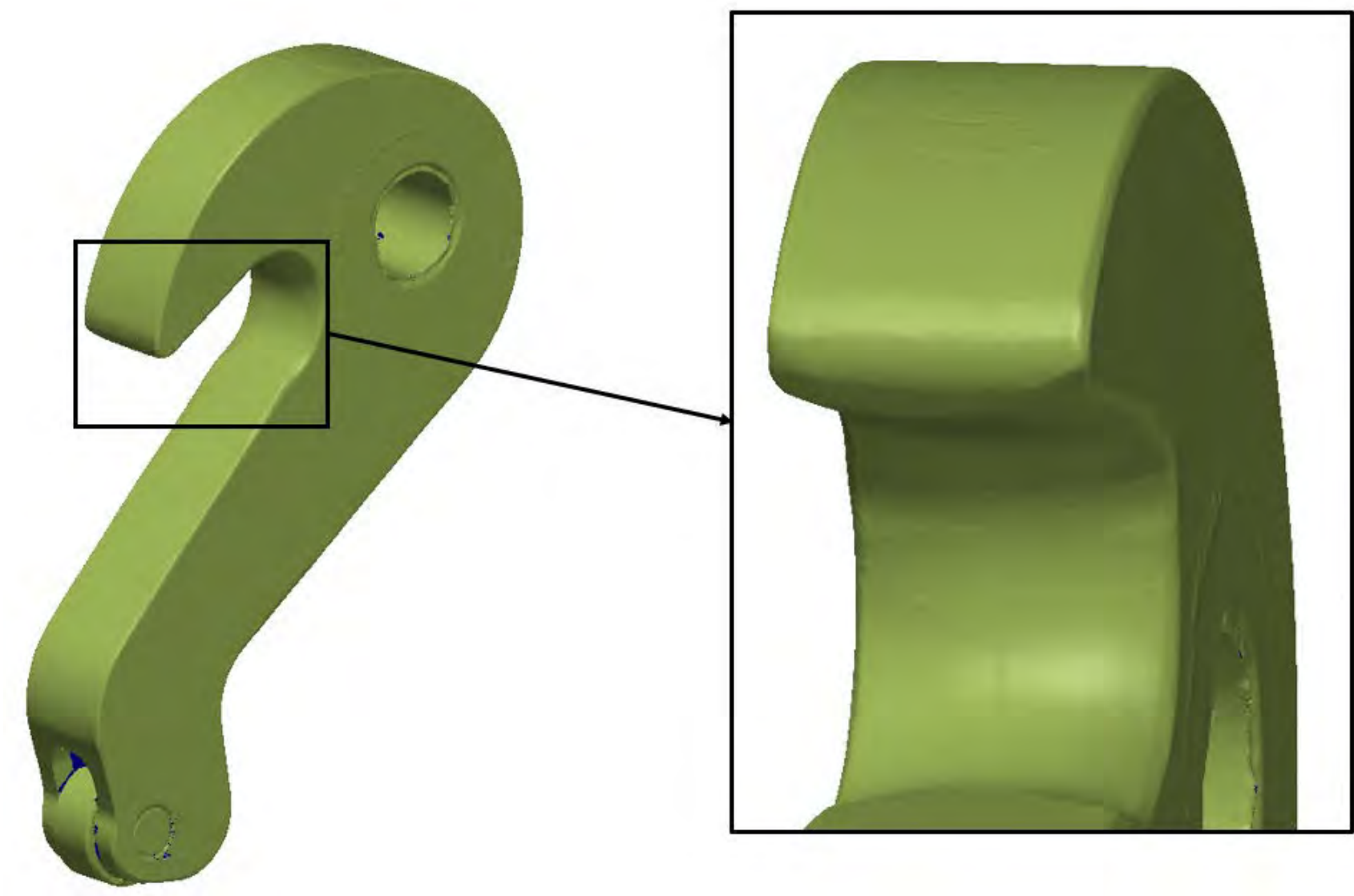


Figure 85. Laser scans of Exemplar Hook with a close-up image of the hook tip.

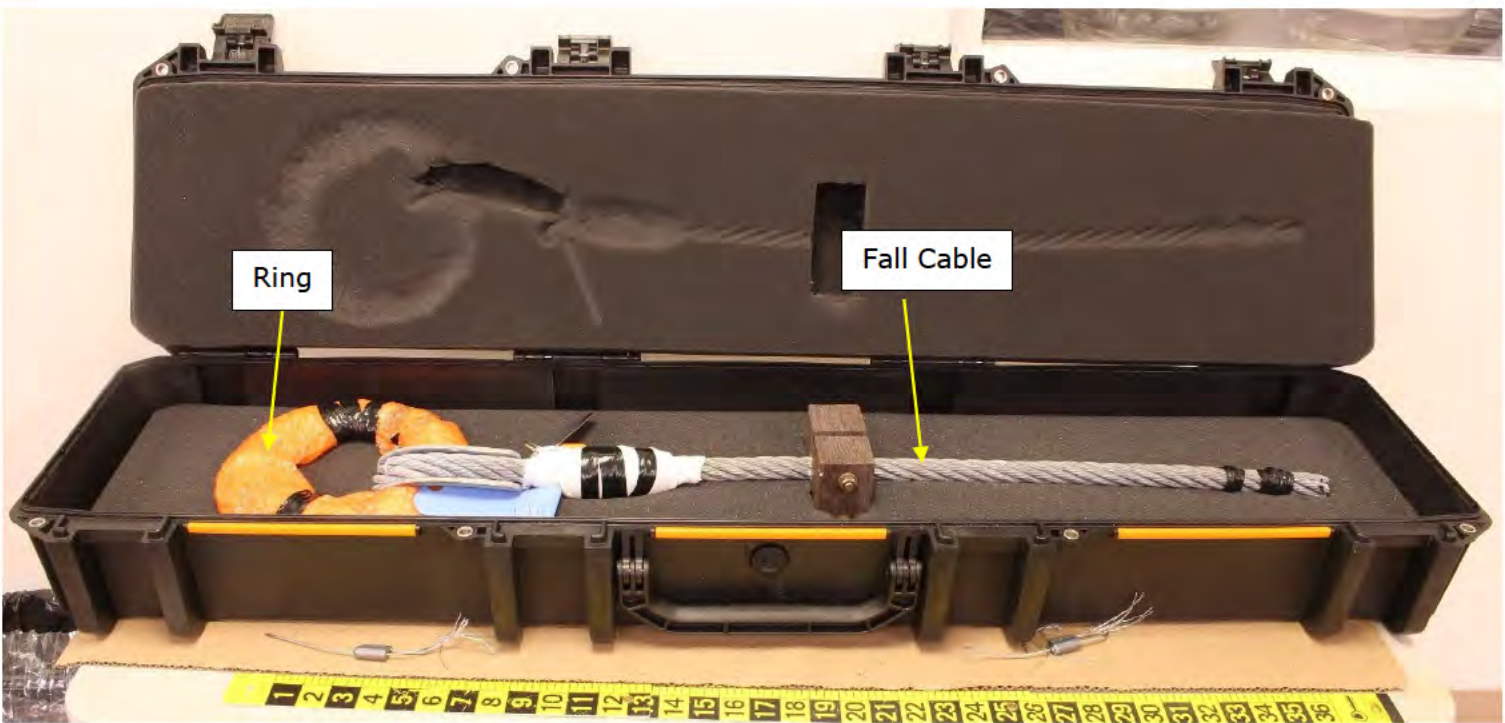
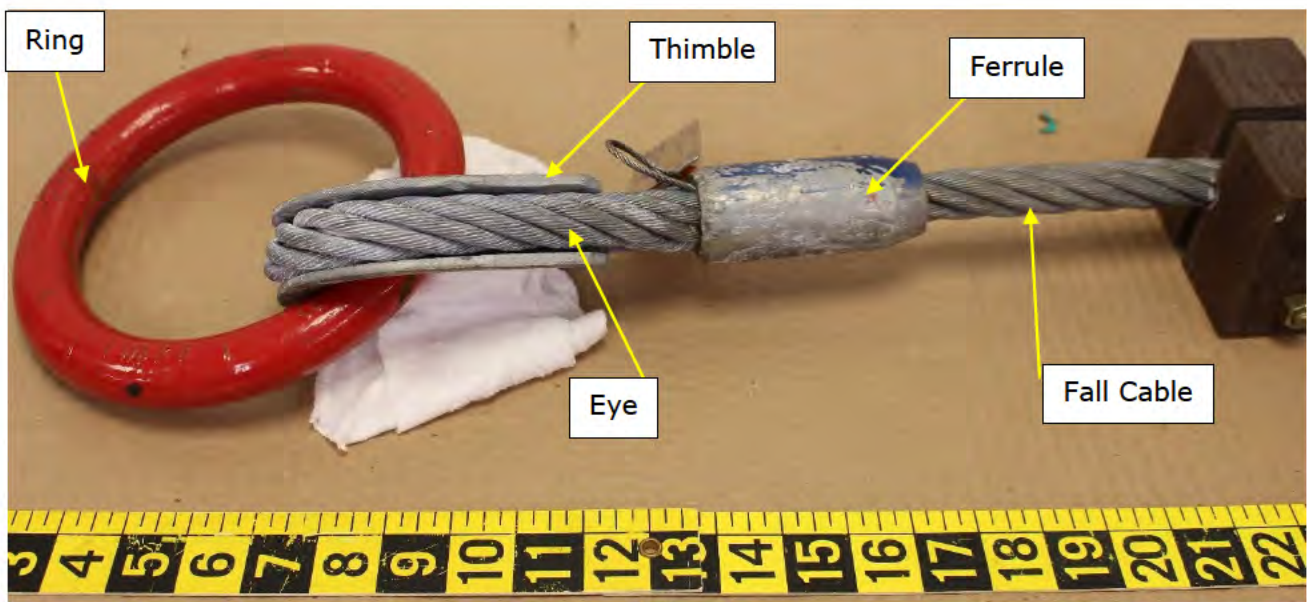
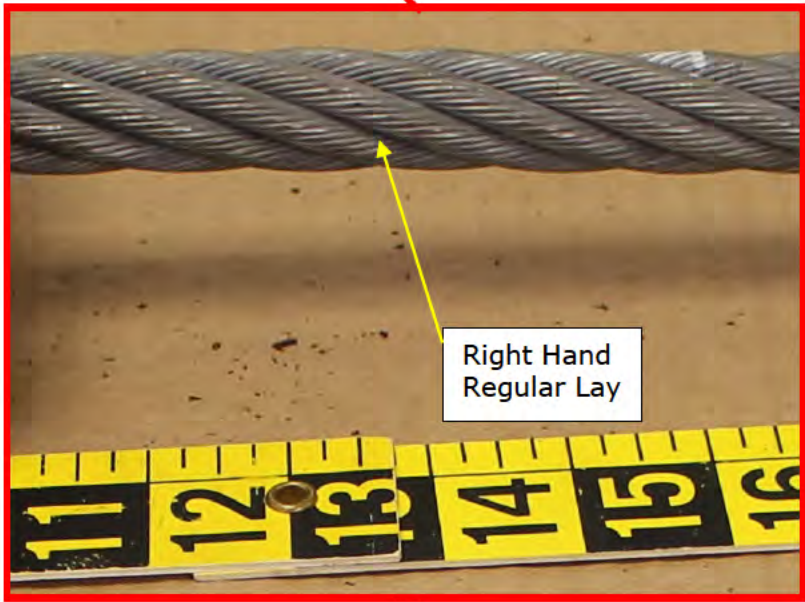
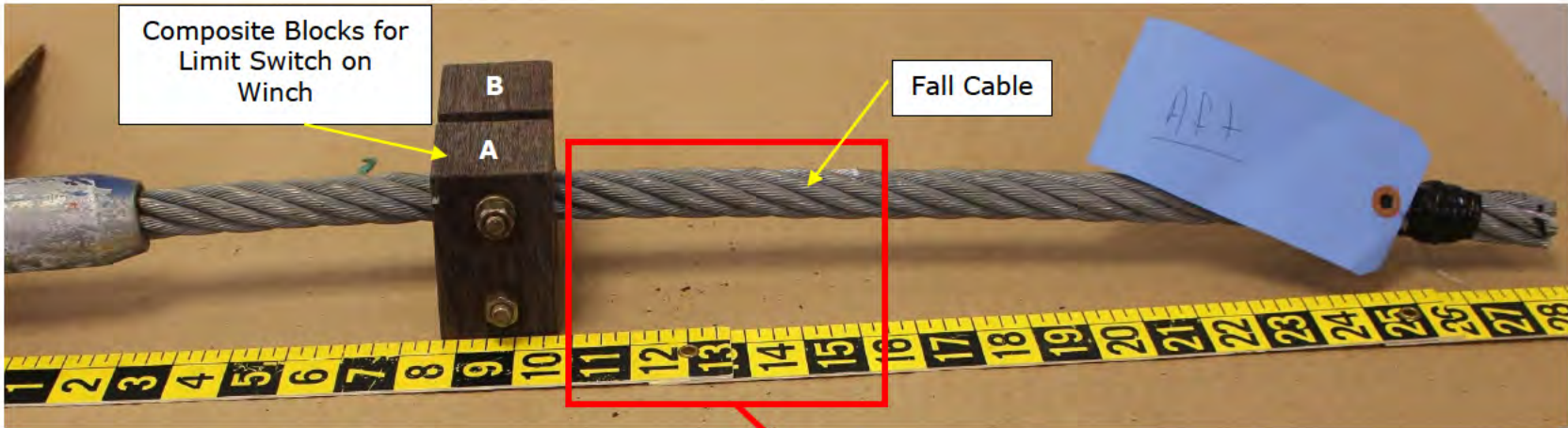


Figure 86. Photograph of the Subject Aft Ring and a section of the Subject Aft Fall Cable as received at DNV GL. Ruler is in inches.



(a)



(b)

Figure 87. Photographs of (a) the Subject Aft Ring and (b) the section of the Subject Aft Fall Cable after removal from shipping container. Rulers are in inches.

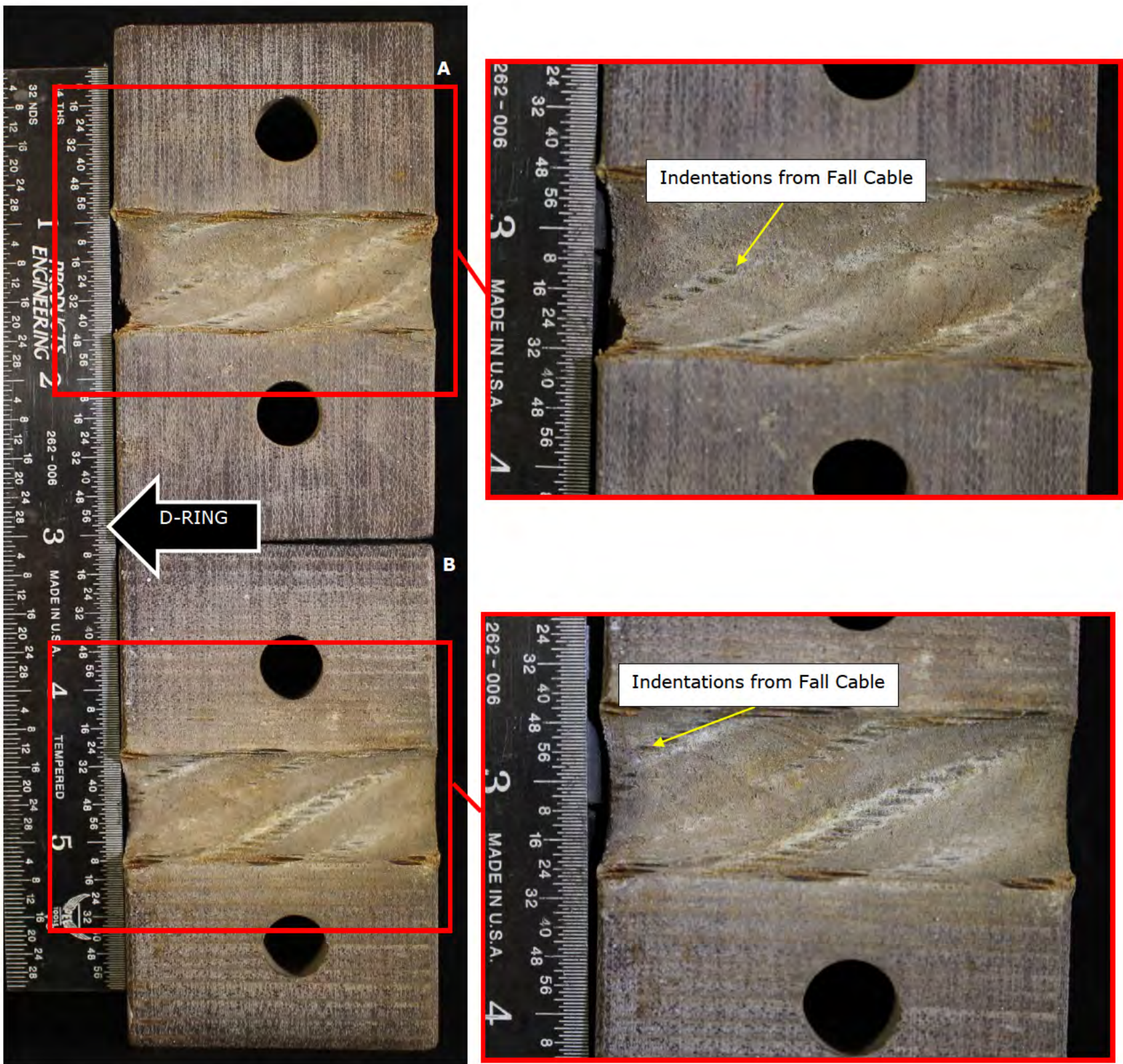


Figure 88. Photographs of composite block after removal from the section of the Subject Aft Fall Cable. The direction toward the Subject Aft Ring is shown. Rulers are in inches.

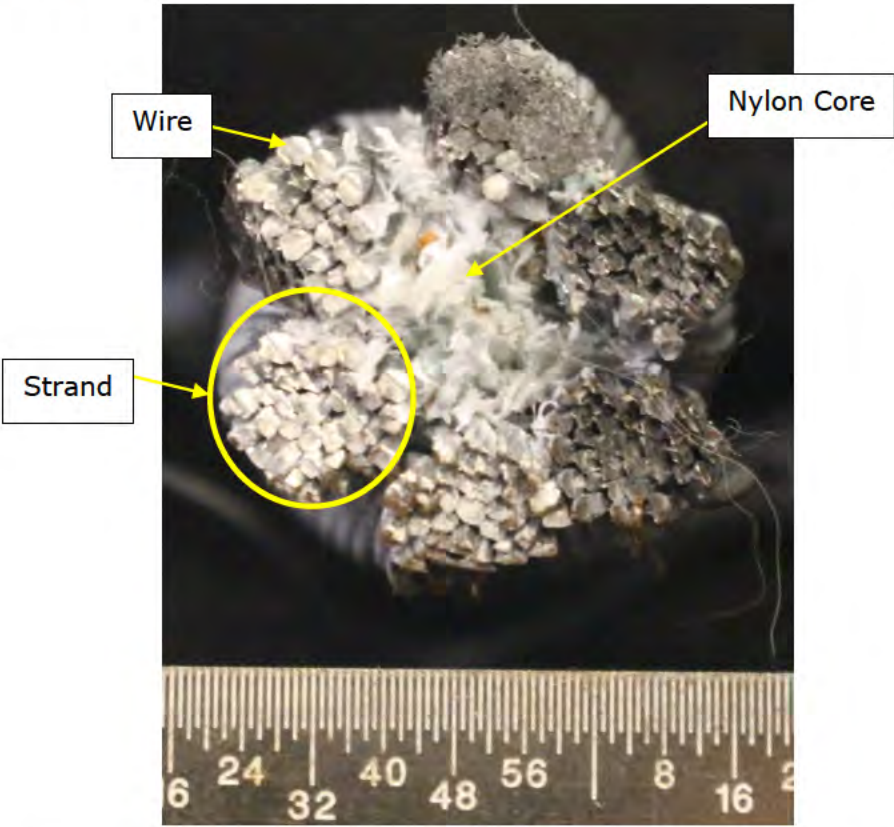


Figure 89. Photograph showing the cross-section of the Subject Aft Fall Cable. Ruler is in inches.

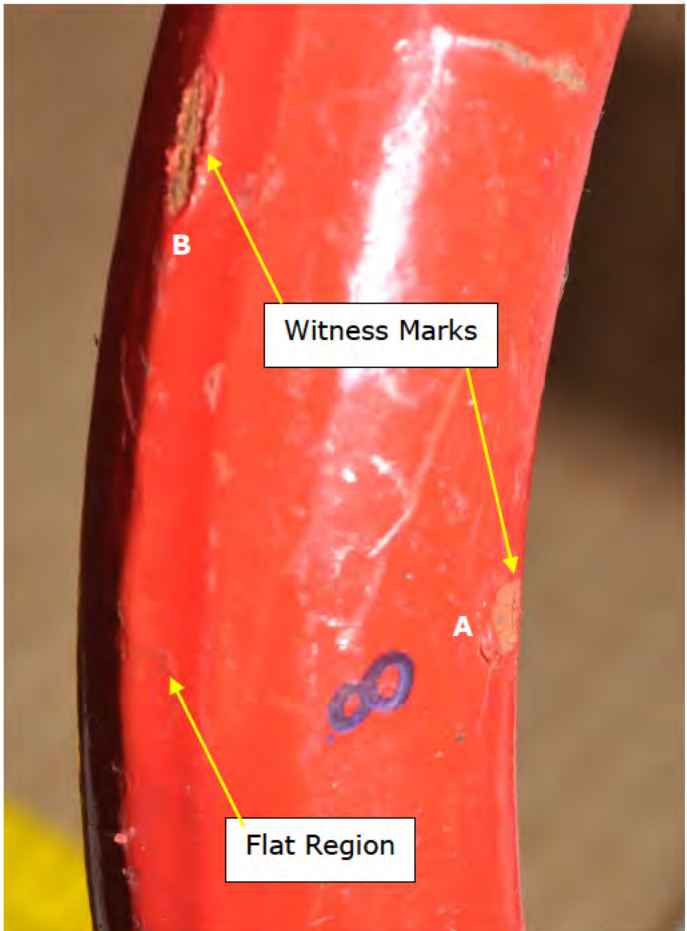


Figure 90. Photographs showing the Subject Aft Ring and locations where witness marks were identified. Ruler in top image is in inches and the ruler in the bottom image is in mm.

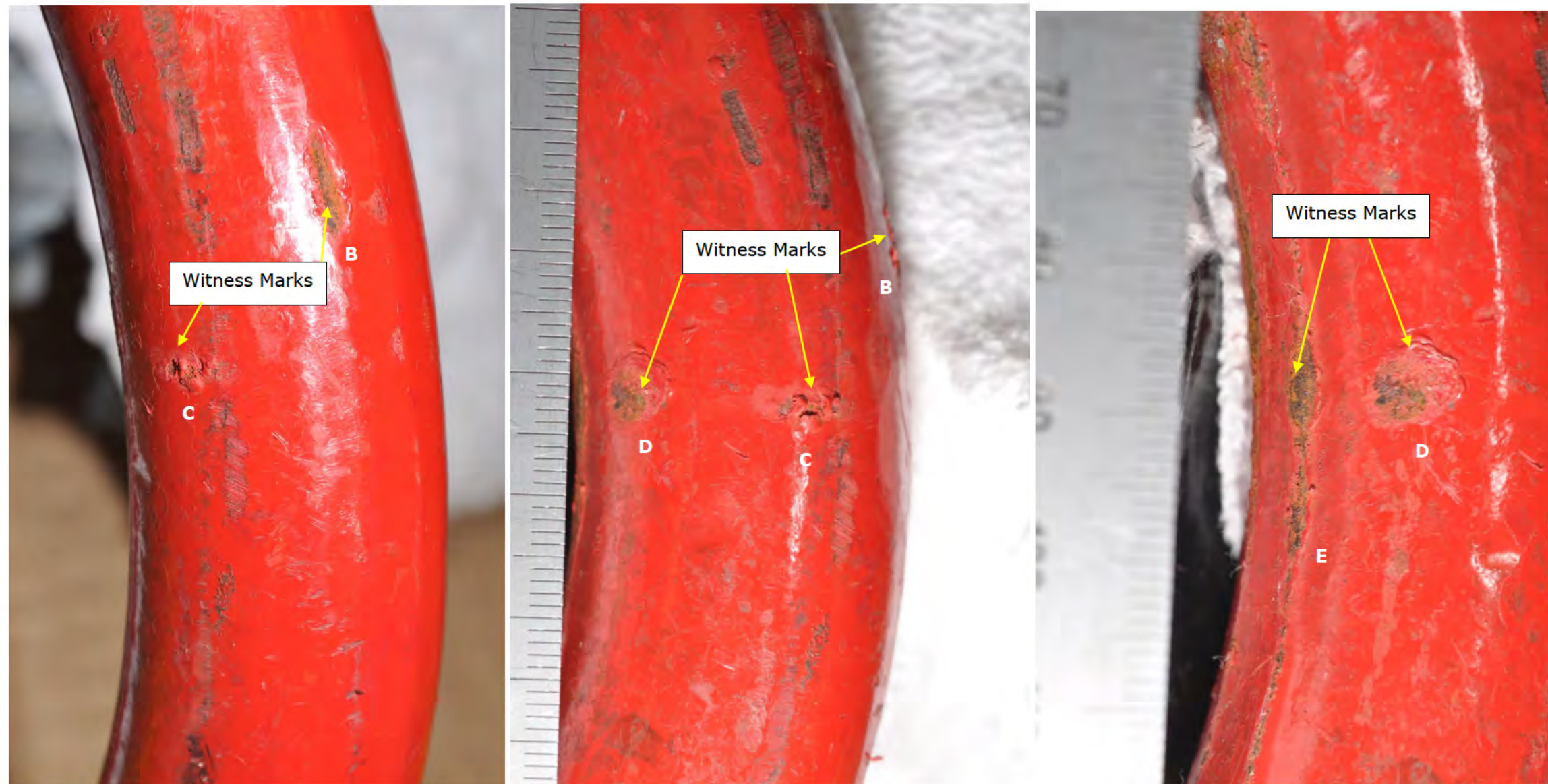


Figure 91. Photographs showing additional witness marks on the Subject Aft Ring; the location of witness mark "B" is shown in Figure 90. Ruler is in mm.

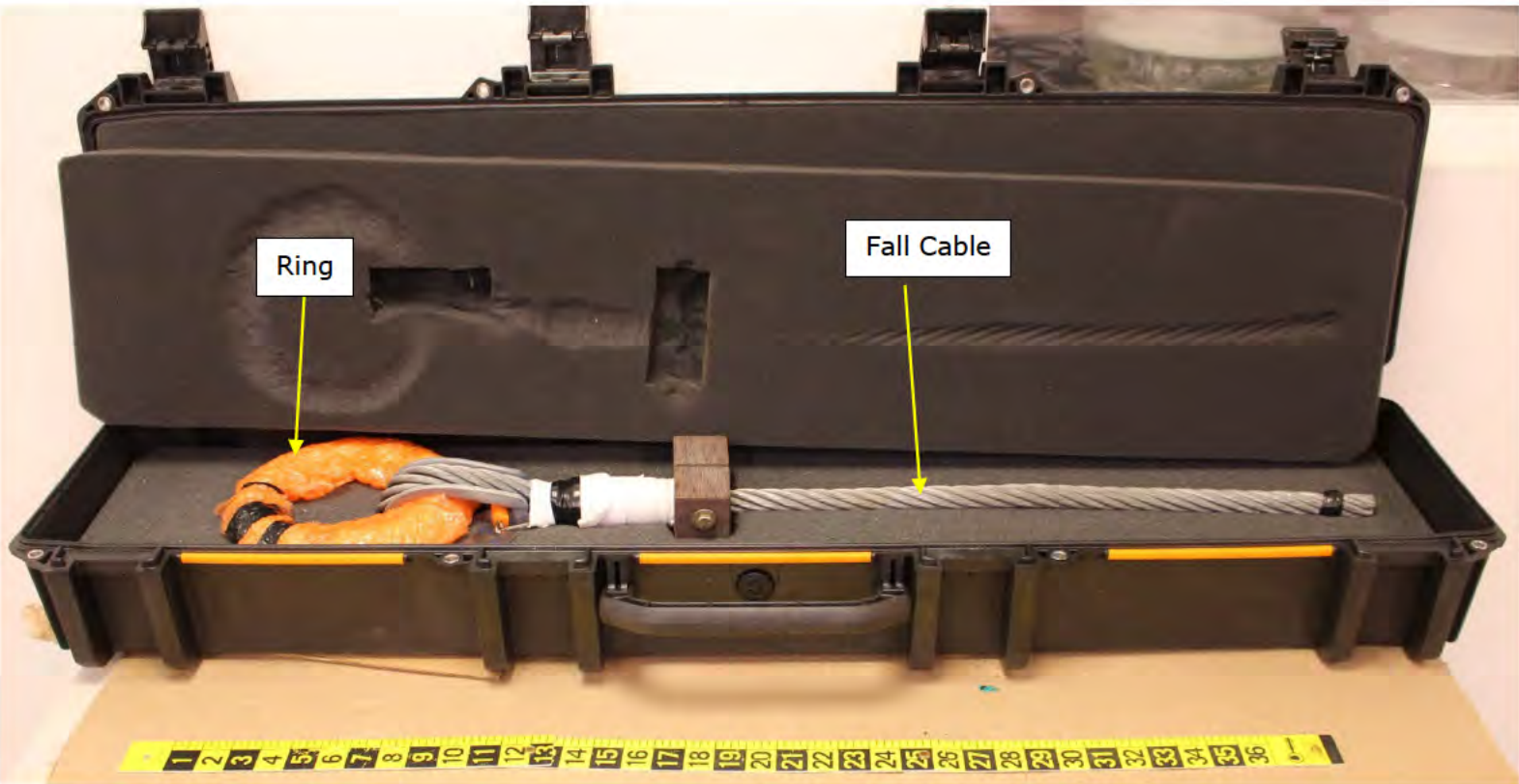


Figure 92. Photograph of the Subject Forward Ring and a section of the Subject Forward Fall Cable as received at DNV GL. Ruler is in inches.

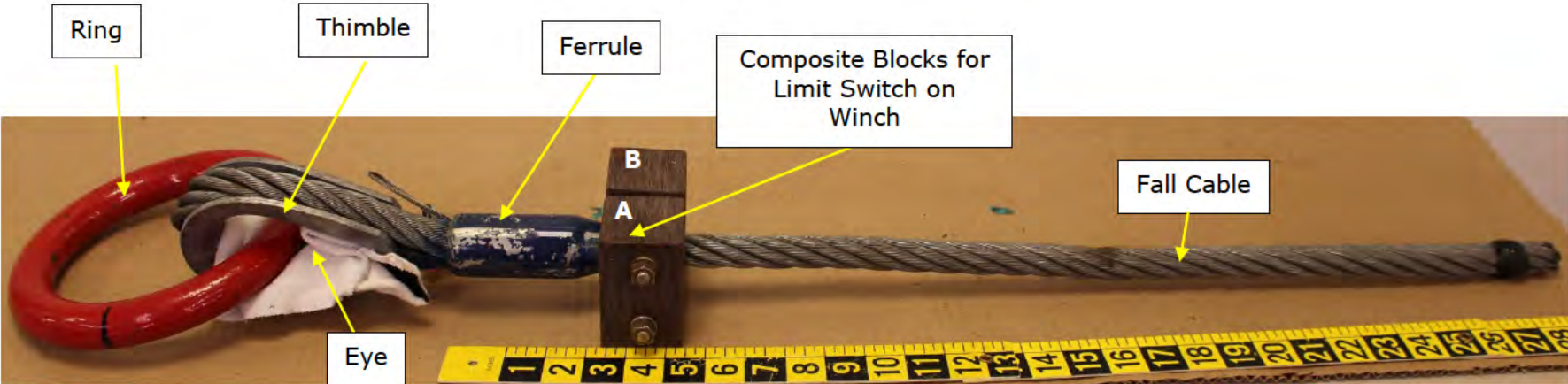


Figure 93. Photograph of the Subject Forward Ring and the section of the Subject Forward Fall Cable after removal from shipping container. Ruler is in inches.

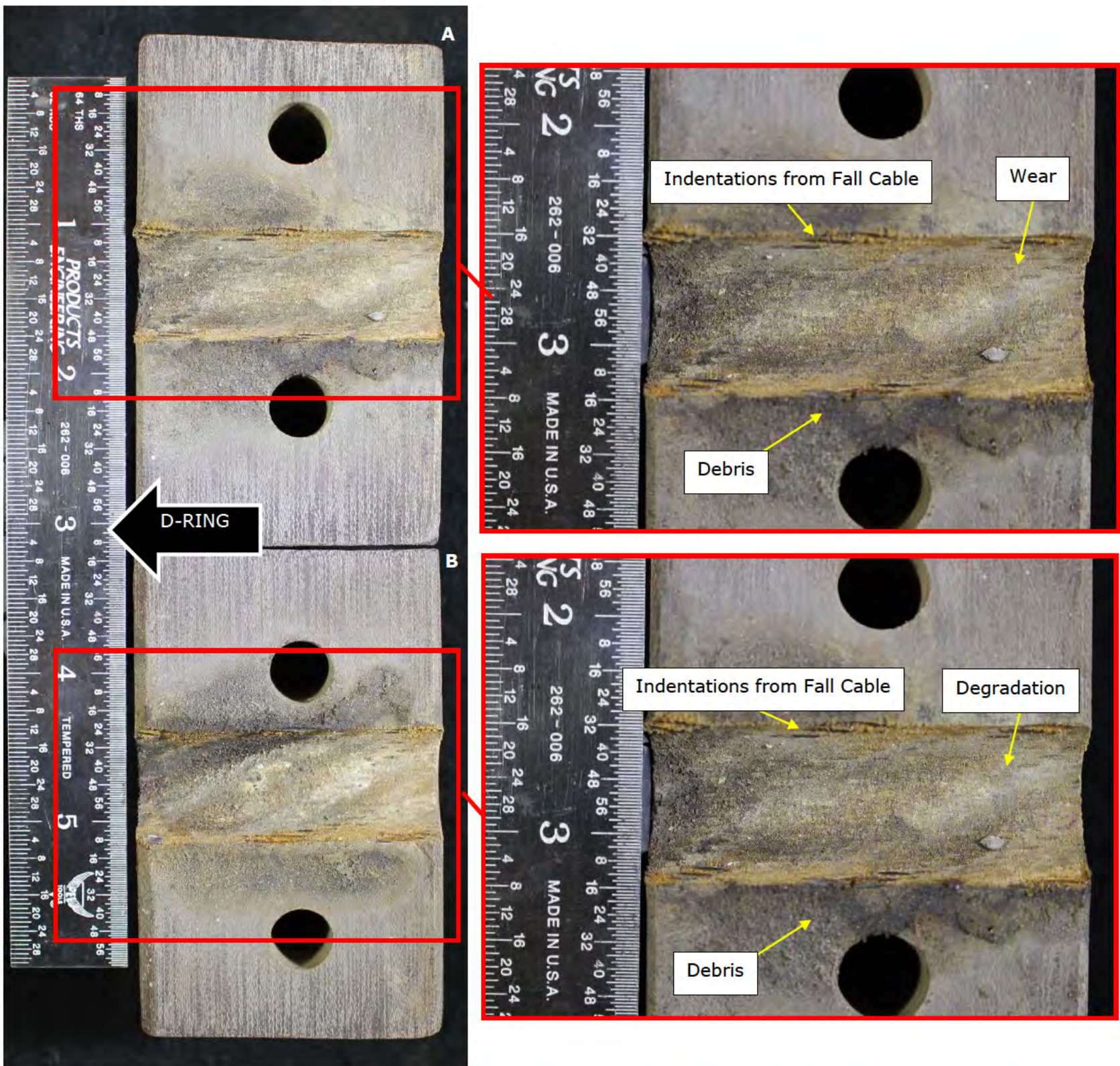


Figure 94. Photographs of composite block after removal from the section of the Subject Forward Fall Cable. The direction toward the Subject Forward Ring is shown. Ruler is in inches.

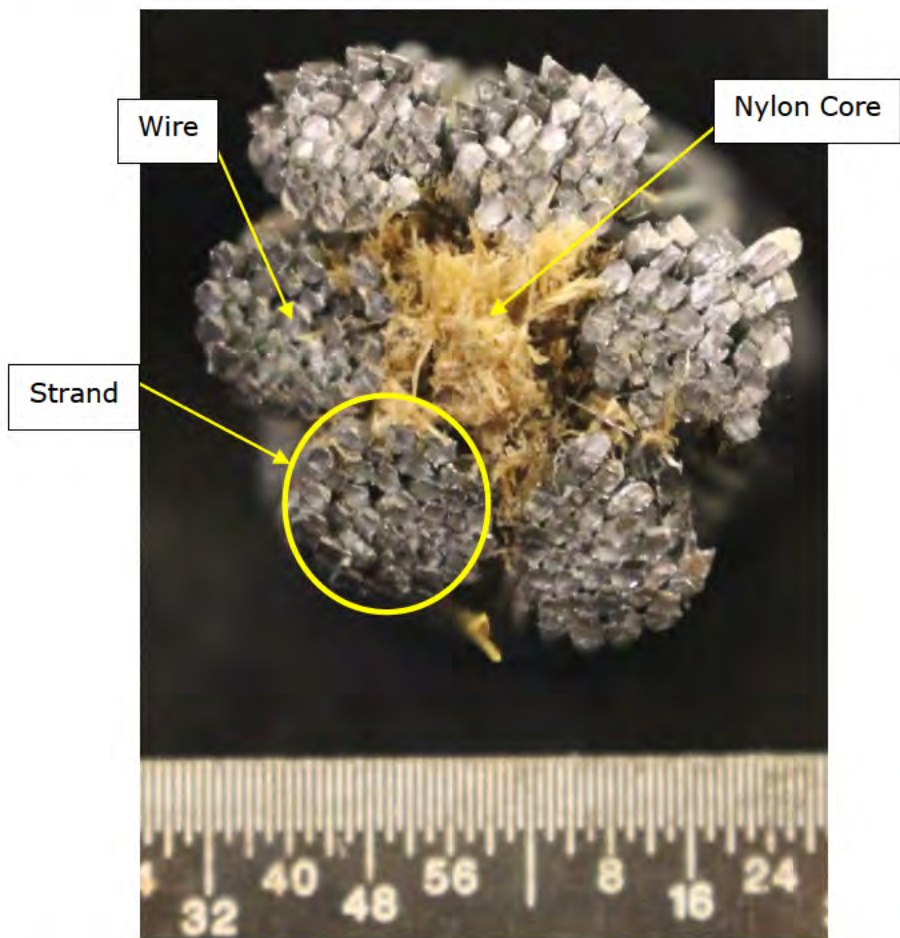


Figure 95. Photograph showing the cross-section of the Subject Forward Fall Cable. Ruler is in inches.

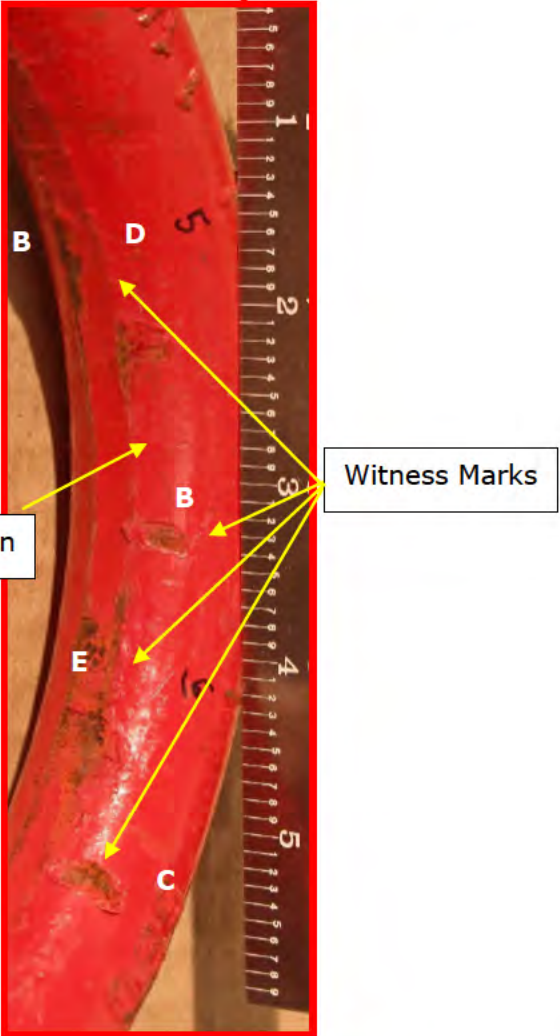
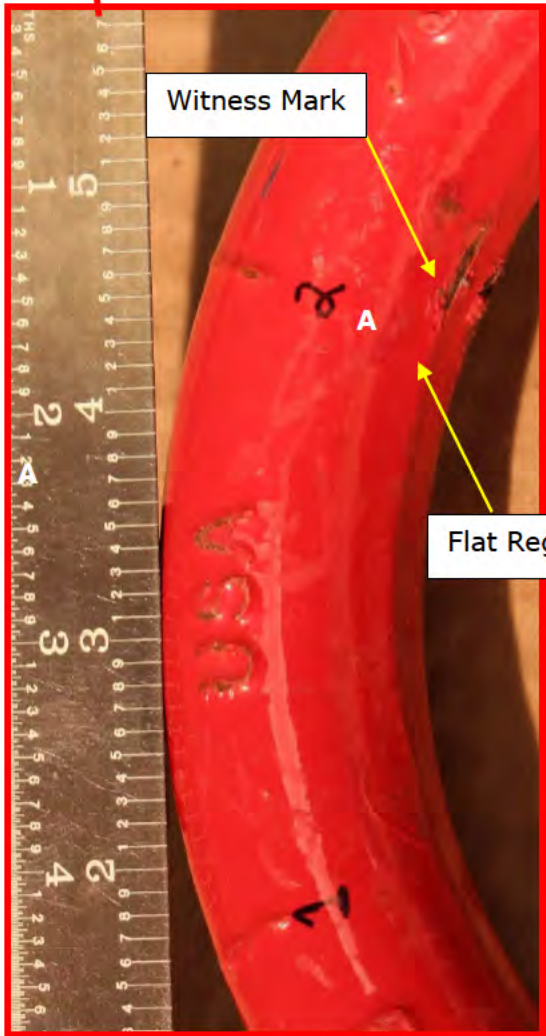


Figure 96. Photographs showing the Subject Forward Ring and locations where witness marks were identified. Rulers are in inches.



Figure 97. Laser scans of Subject Aft Ring.



Figure 98. Laser scans of Subject Aft Ring with the section of the Subject Aft Fall Cable.

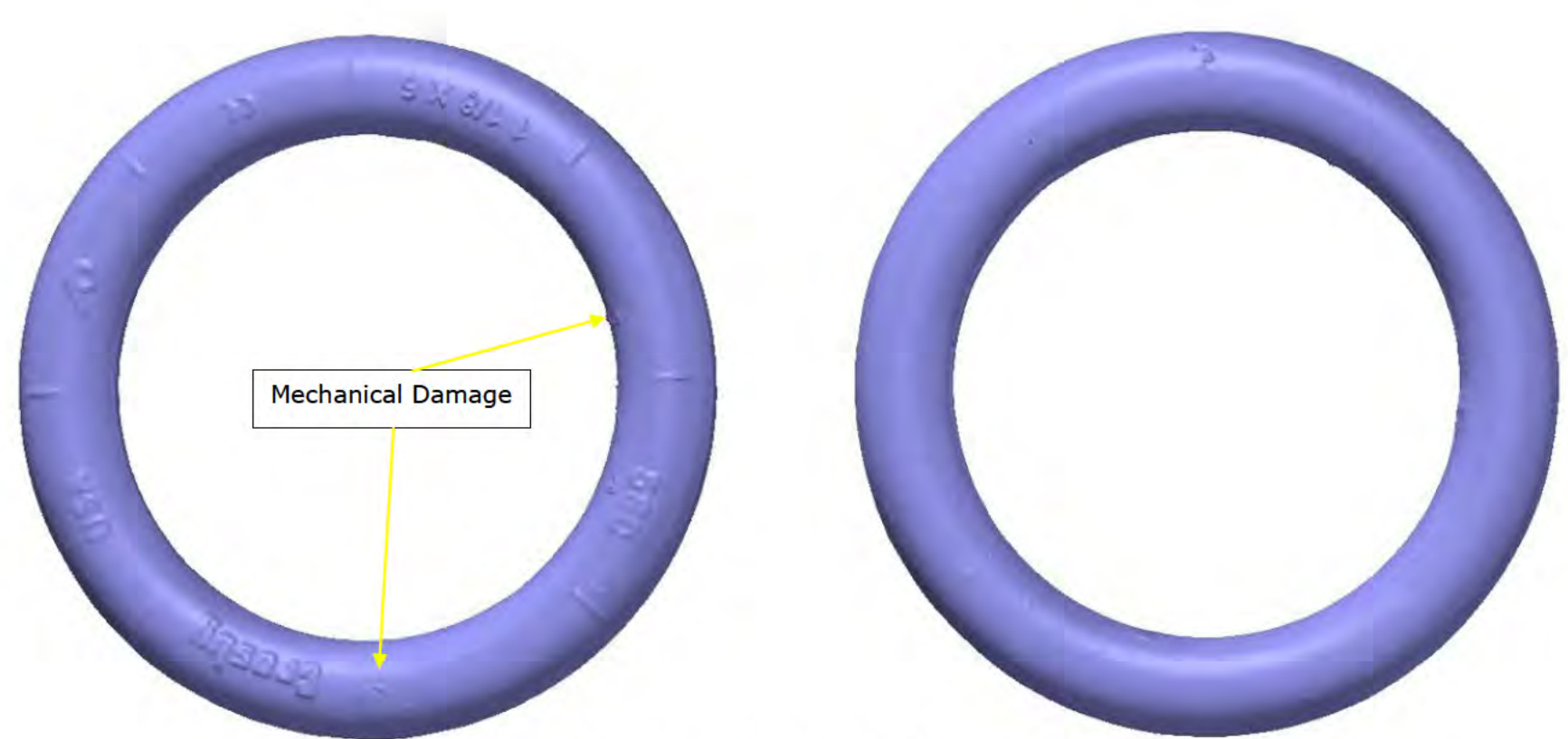


Figure 99. Laser scans of Subject Forward Ring.

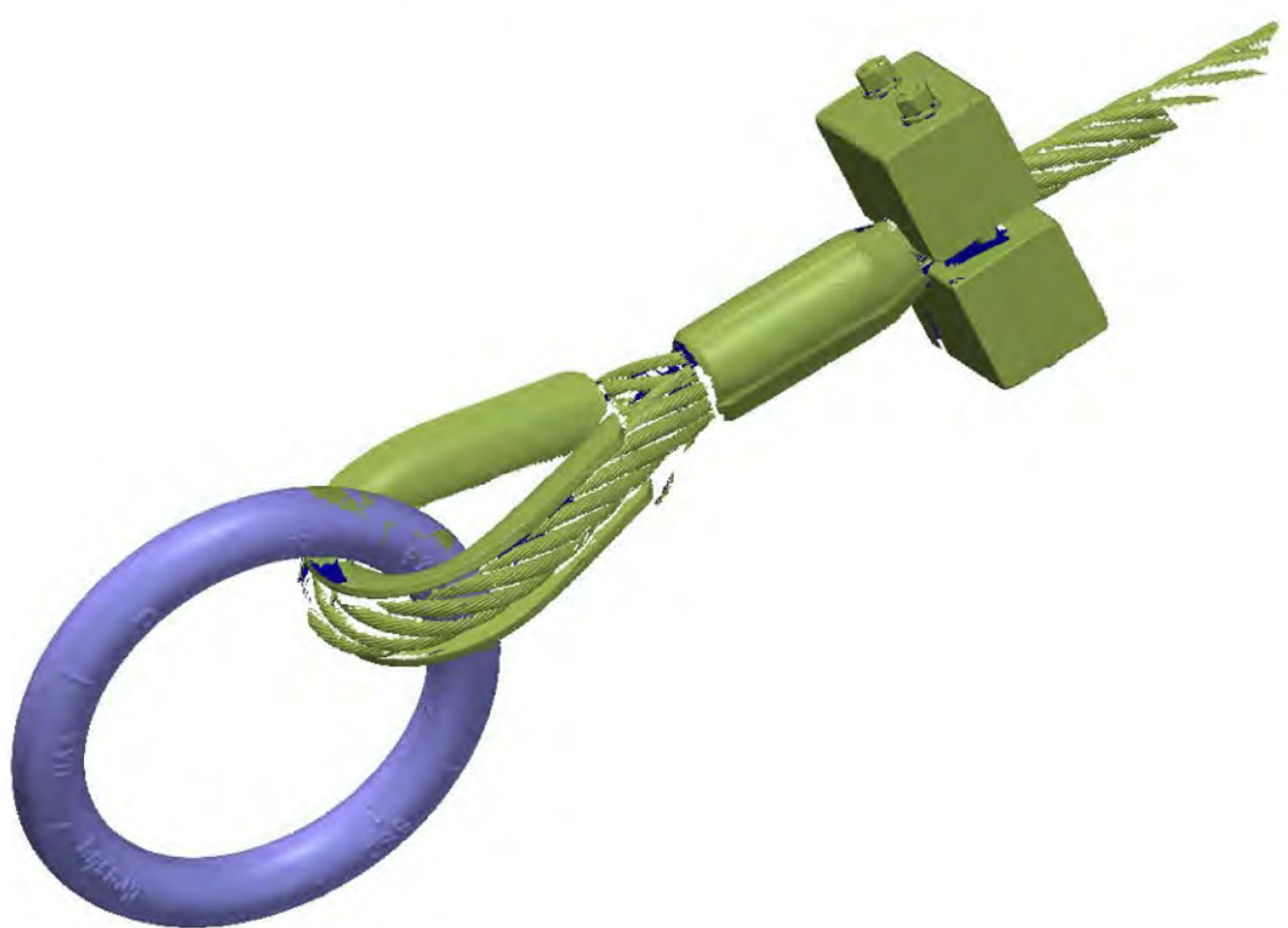


Figure 100. Laser scans of Subject Forward Ring with the section of the Subject Forward Fall Cable.

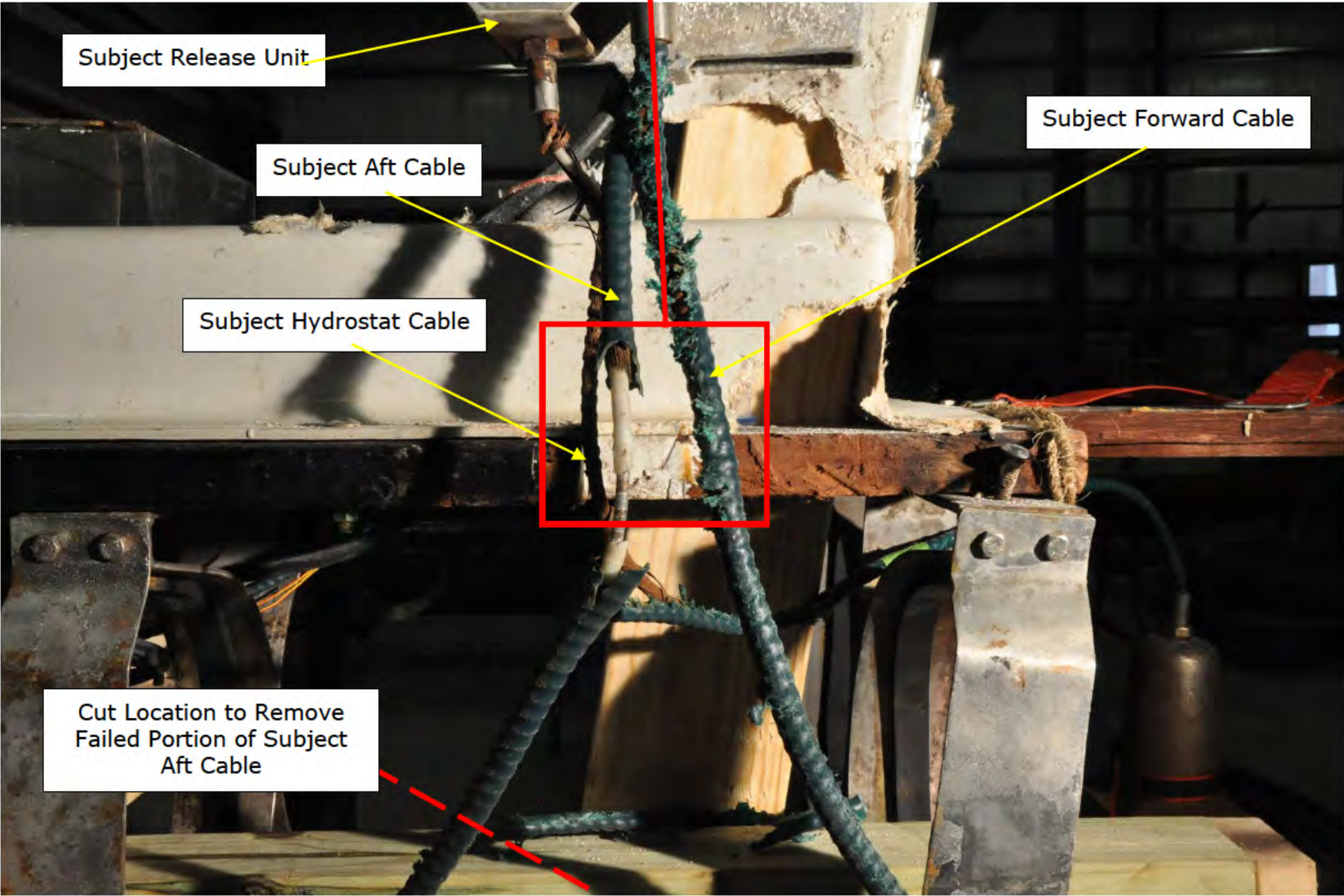
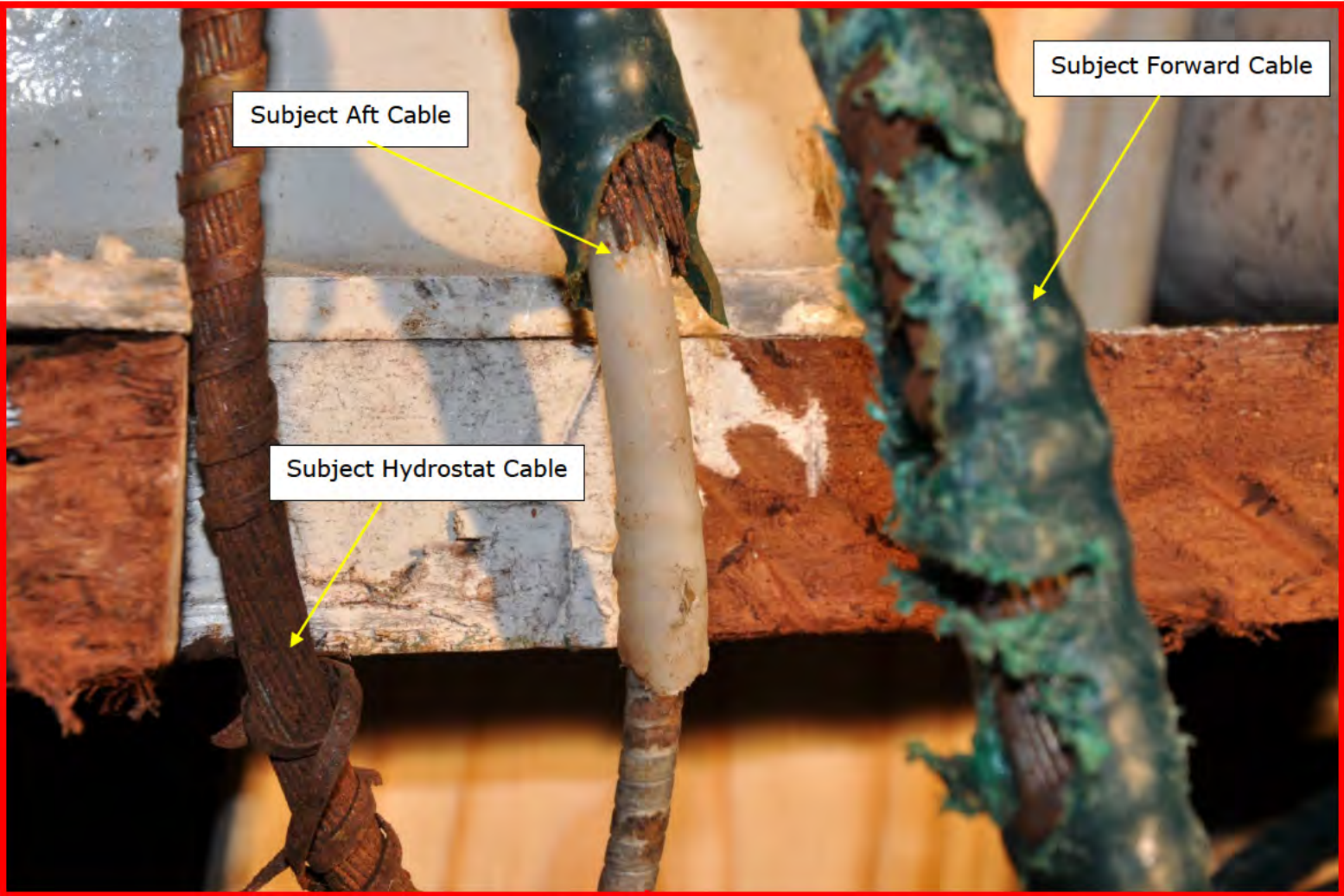
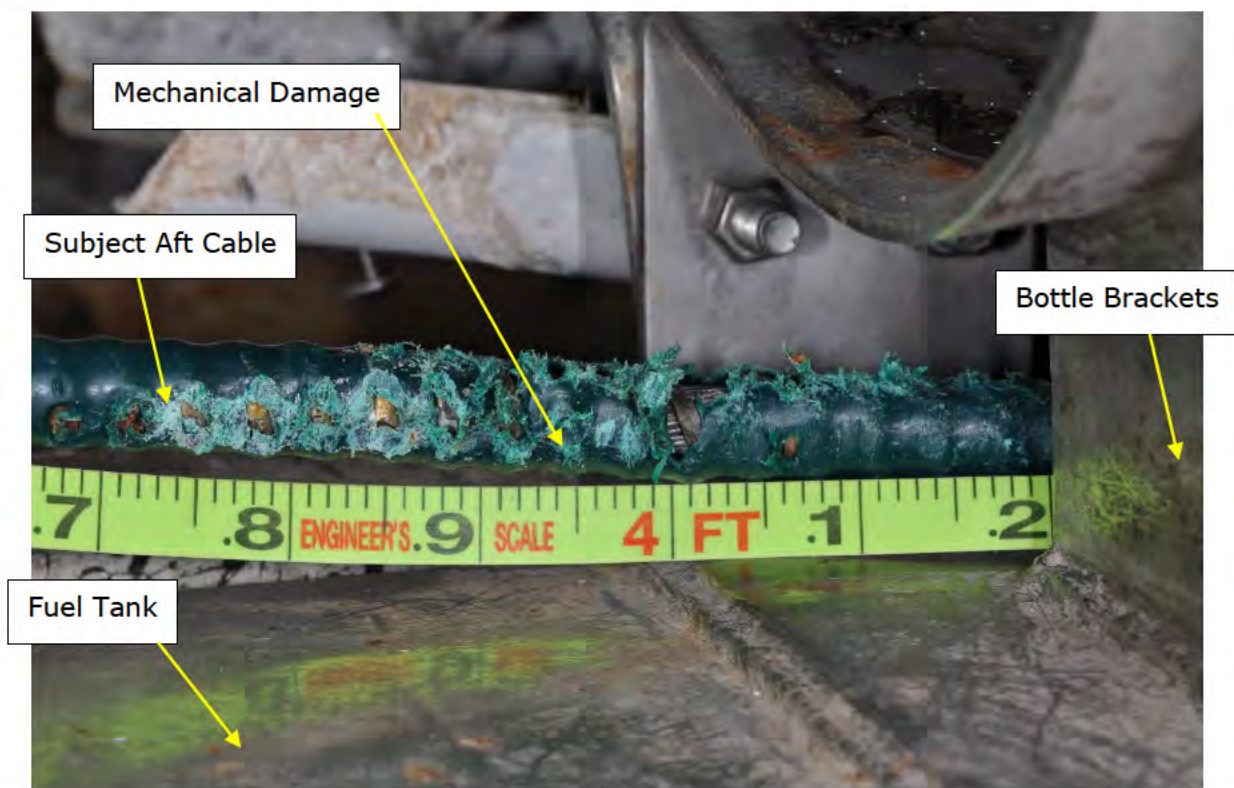


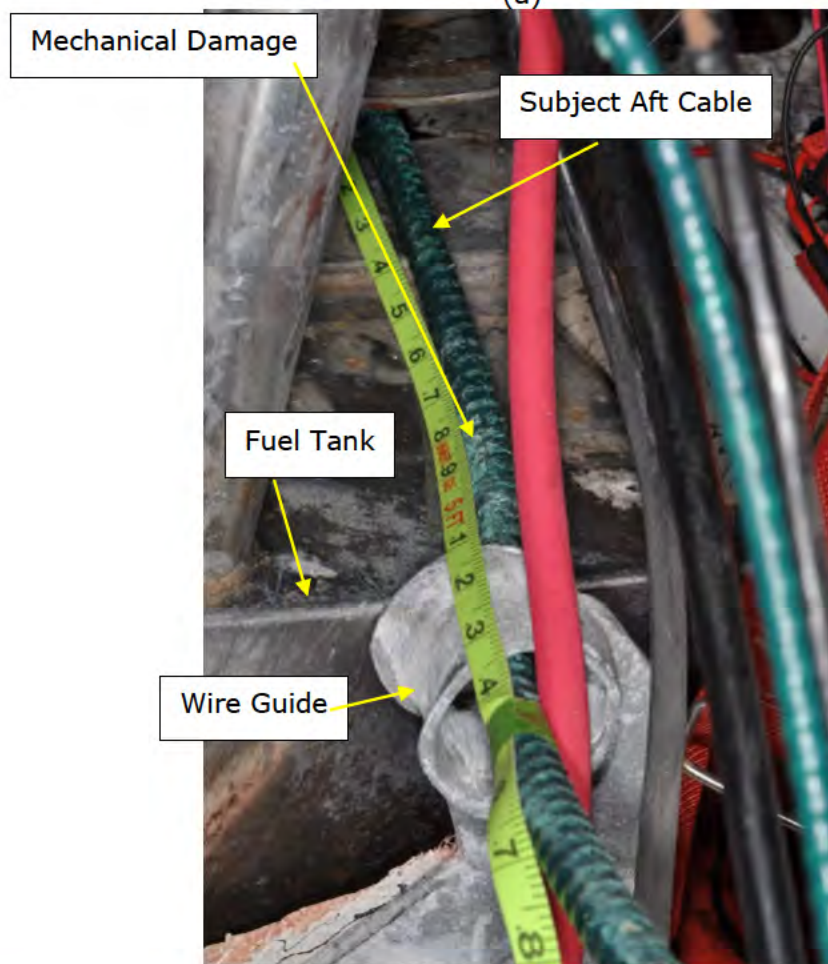
Figure 101. Photograph showing Subject Aft Cable, Subject Forward Cable, and Subject Hydrostat Cable at the Release Unit after reconstruction at DNV GL's facility.



Figure 102. Photographs showing (a) Subject Aft Cable and (b) Subject Forward Cable at the Subject Aft and Subject Forward Hooks, respectively.



(a)



(b)



(c)

Figure 103. Photographs showing mechanical damage to the cover of the Subject Aft Cable (a) 3.70 feet to 4.10 feet, (b) 4.70 feet to 5.70 feet, and (c) 8.10 feet to 8.60 feet from the conduit cap at the Subject Release Unit. These photographs were taken by DNV GL during a site visit to Harvey Terminal on July 31, 2019. Tape measures are in feet.

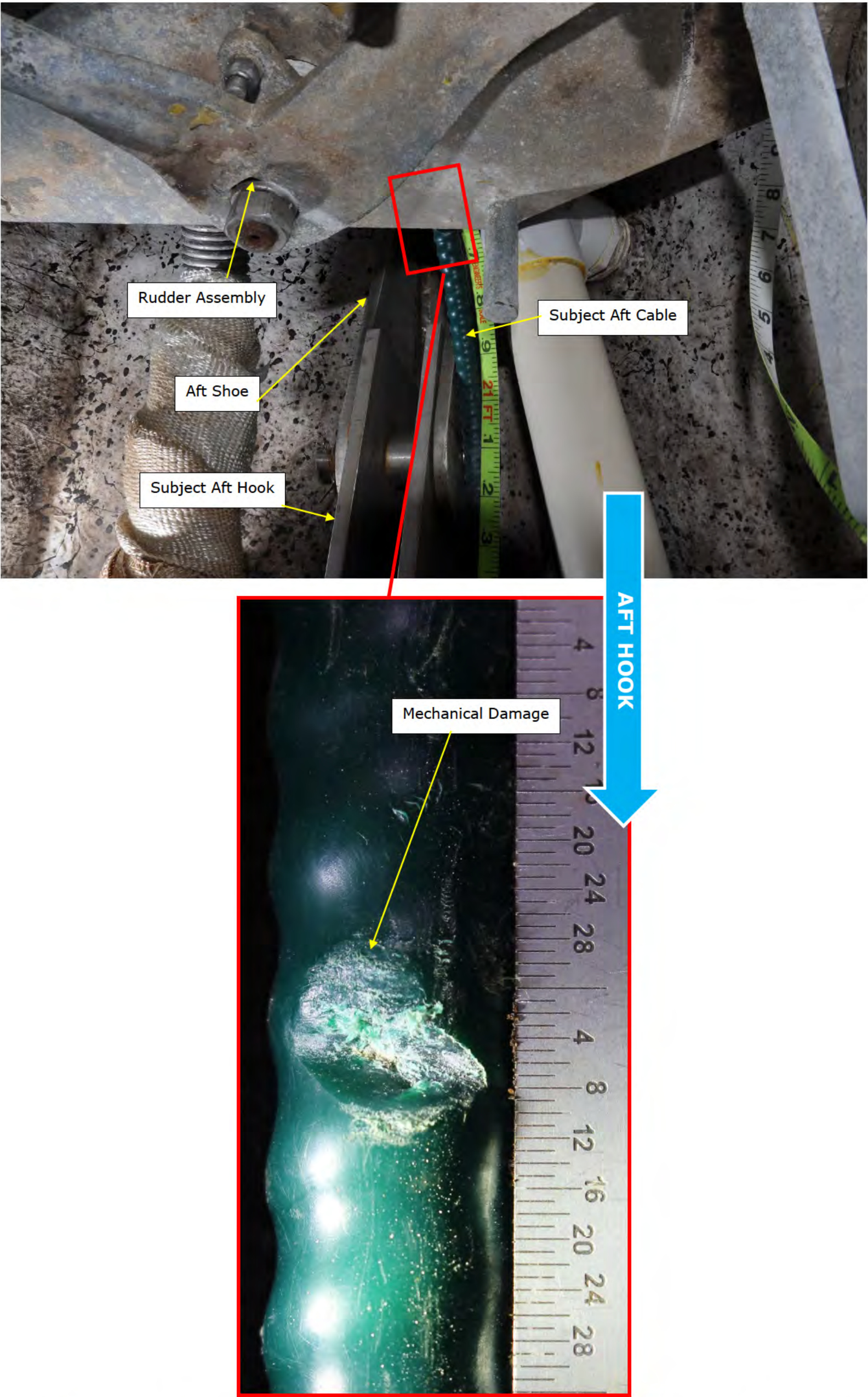


Figure 104. Photographs showing mechanical damage to the cover layer of the Subject Aft Cable 20.63 feet from the conduit cap at the Subject Release Unit. The top photograph was taken by DNV GL during a site visit to Harvey Terminal on July 31, 2019 and the lower photograph was taken at DNV GL's laboratory in Dublin, Ohio. The direction of the Subject Aft Hook is noted with the blue arrow. Tape measure is in feet and ruler is in inches.

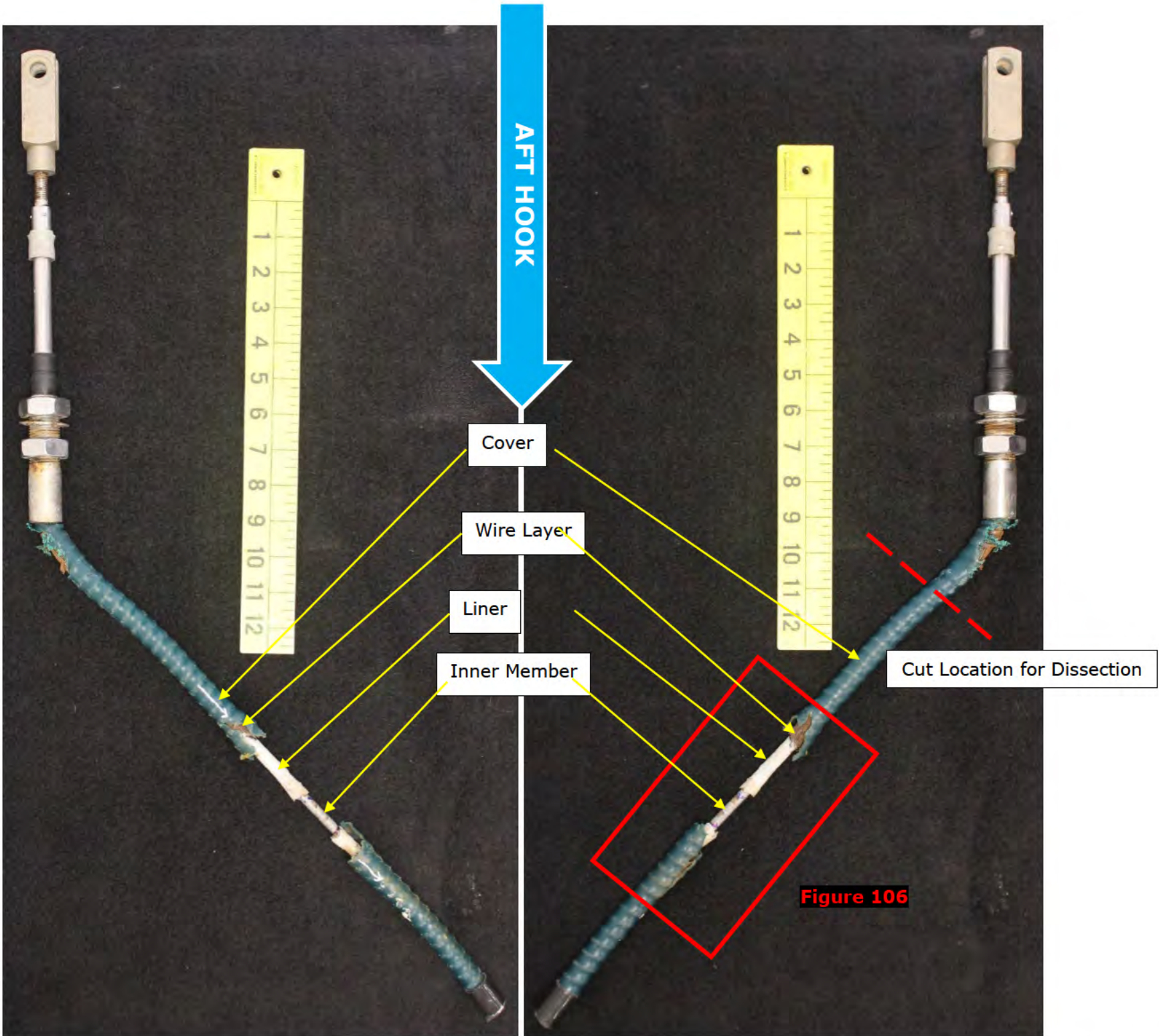


Figure 105. Photographs of the Subject Aft Cable after removing a section with the failure in the outer layers. The direction of the Subject Aft Hook is noted with the blue arrow. Rulers are in inches.

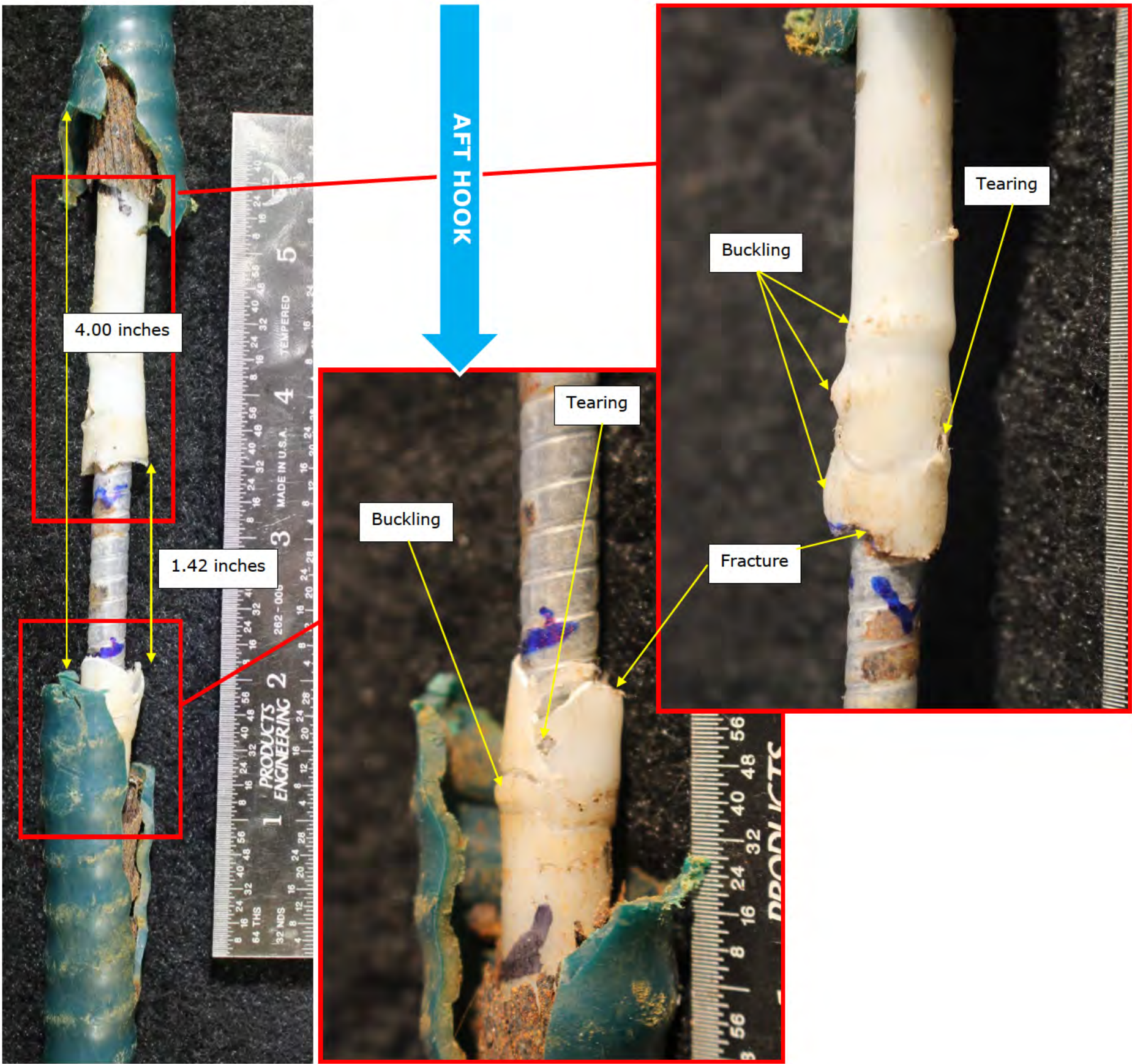


Figure 106. Photographs of the Subject Aft Cable showing the detail of the failure. The direction of the Subject Aft Hook is noted with the blue arrow. Rulers are in inches.

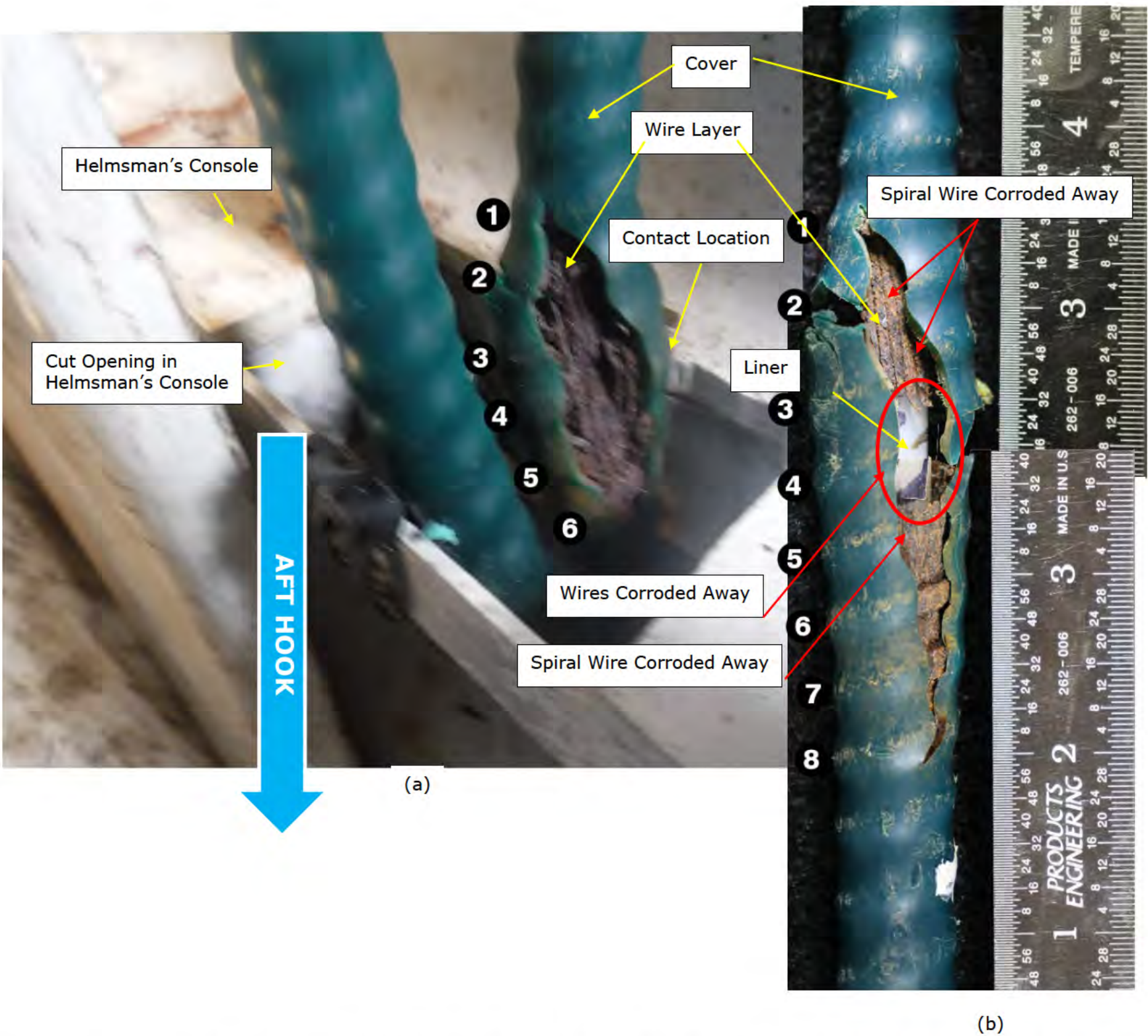


Figure 107. Photograph and montage of photographs of the Subject Aft Cable (a) taken in the field on June 6, 2019 by Palfinger and (b) taken in the laboratory by DNV GL, respectively. For the montage, the fracture surfaces of the cover were matched to generate an image similar to the photograph shown in Figure 107 (a). The numbers in Figure 107 (a) and (b) are corresponding locations along the length the control cable. The direction of the Subject Aft Hook is noted with the blue arrow. Ruler is in inches.

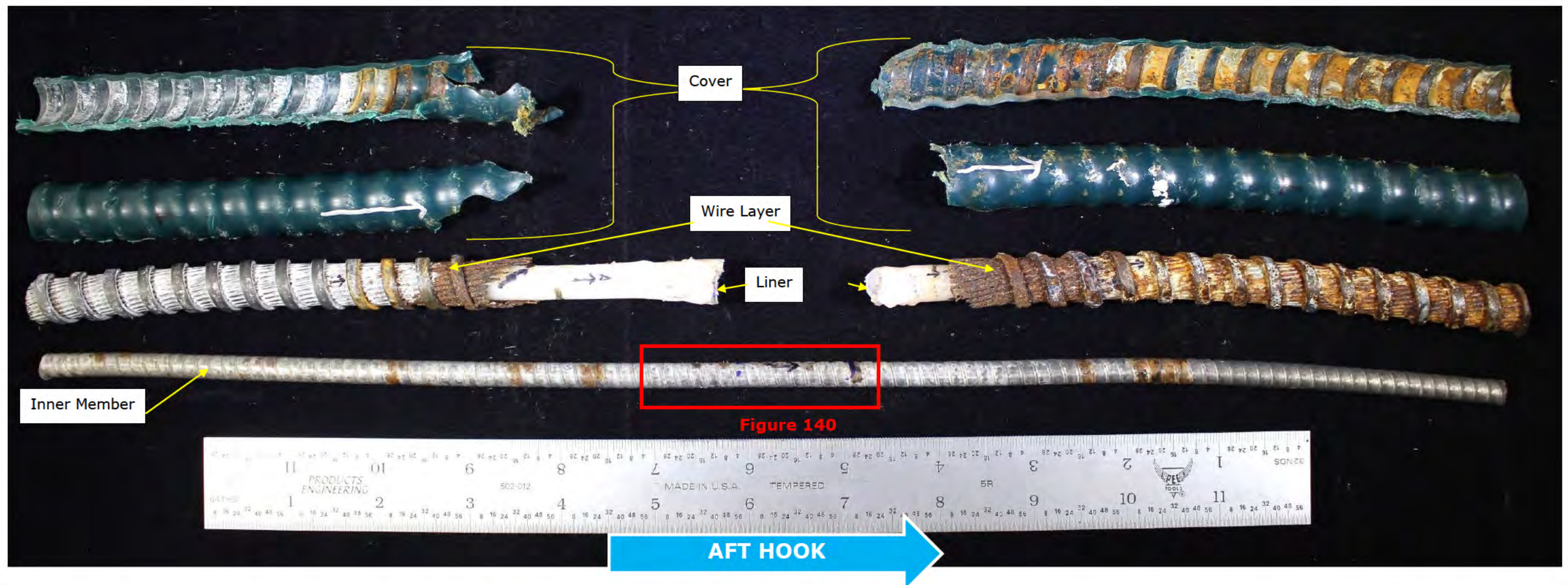


Figure 108. Photograph of the Subject Aft Cable showing the layers of the control cable after dissection near the location of failure. The direction of the Subject Aft Hook is noted with the blue arrow. Ruler is in inches.

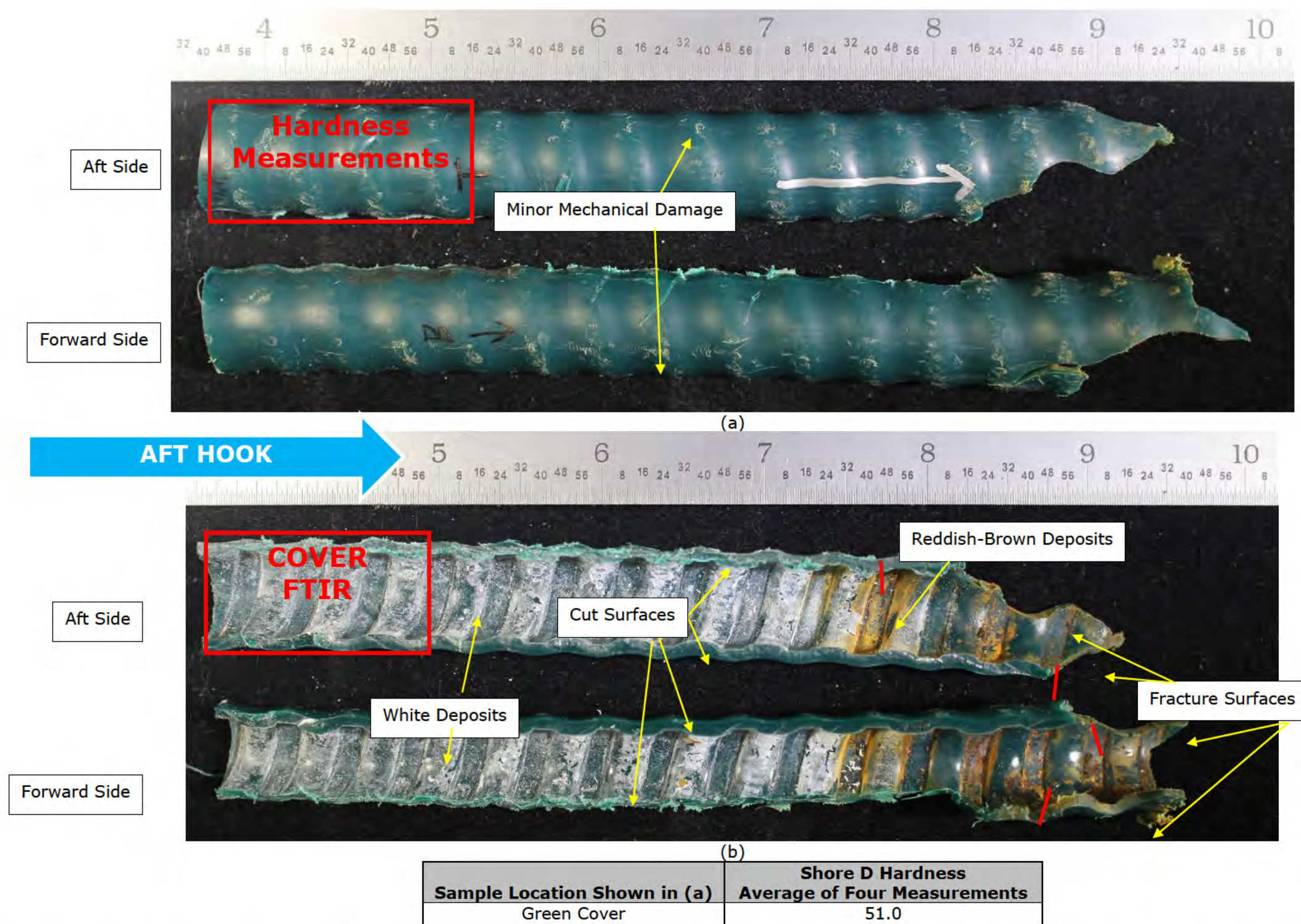


Figure 109. Photographs of the cover from the Subject Release Unit side of the failure in the Subject Aft Cable after dissection showing the (a) external surface and (b) internal surface; samples shown in Figure 108. Forward and aft refer to the orientation of the cover relative to the lifeboat. The direction of the Subject Aft Hook is noted with the blue arrow. Results of hardness measurements shown in table. Ruler is in inches.

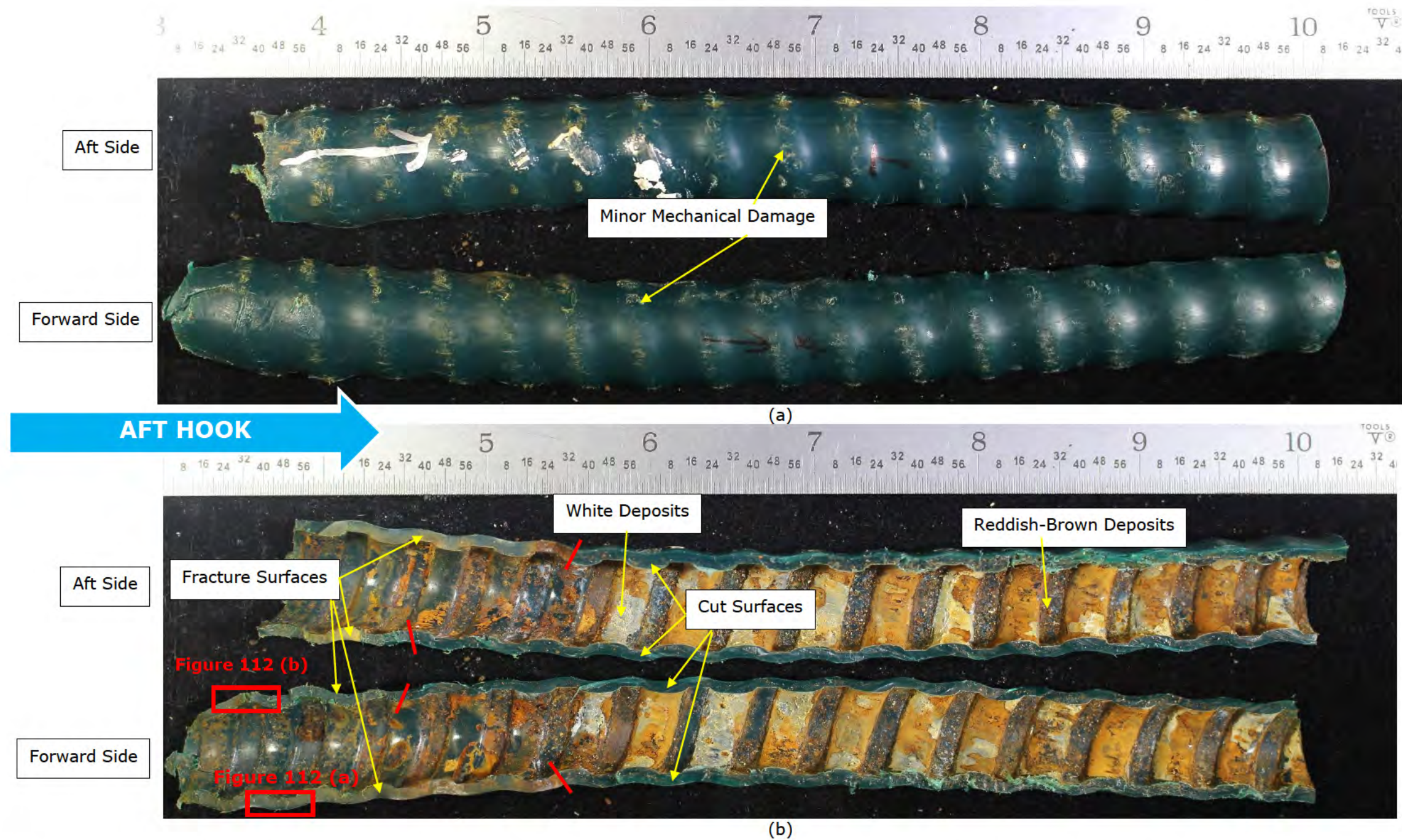


Figure 110. Photographs of the cover from the Subject Aft Hook side of the failure in the Subject Aft Cable after dissection showing the (a) external surface and (b) internal surface; samples shown in Figure 108. Forward and aft refer to the orientation of the cover relative to the lifeboat. The direction of the Subject Aft Hook is noted with the blue arrow. Ruler is in inches.

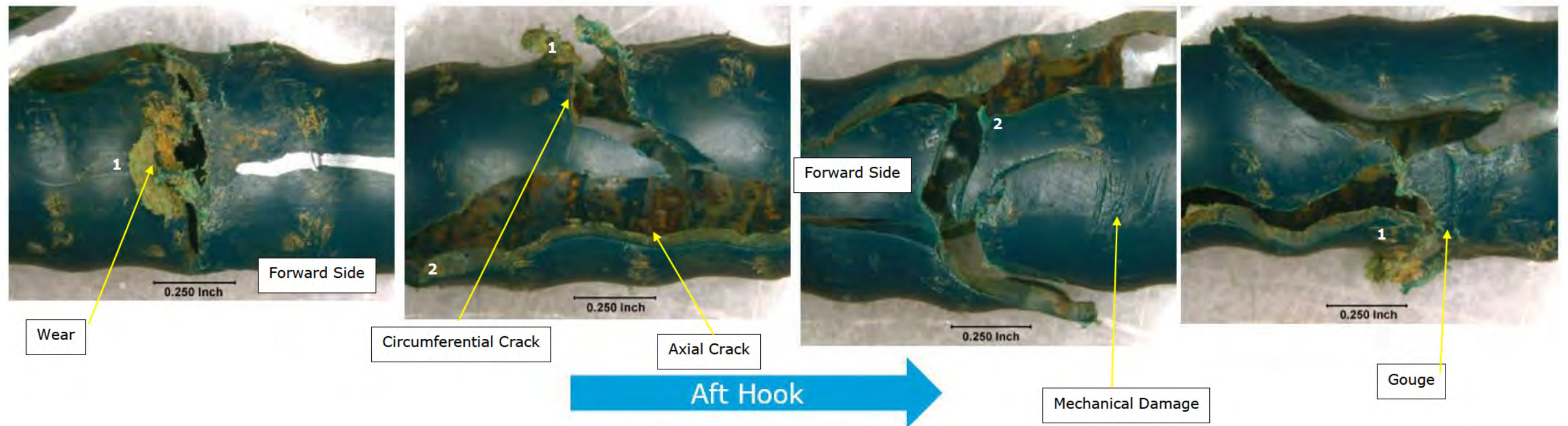


Figure 111. Light photomicrographs of the cover from the Subject Aft Cable after matching the fractures surfaces at the failure. The numbers "1" and "2" are reference locations. Forward and aft refer to the orientation of the cover relative to the lifeboat. The direction of the Subject Aft Hook is noted with the blue arrow.

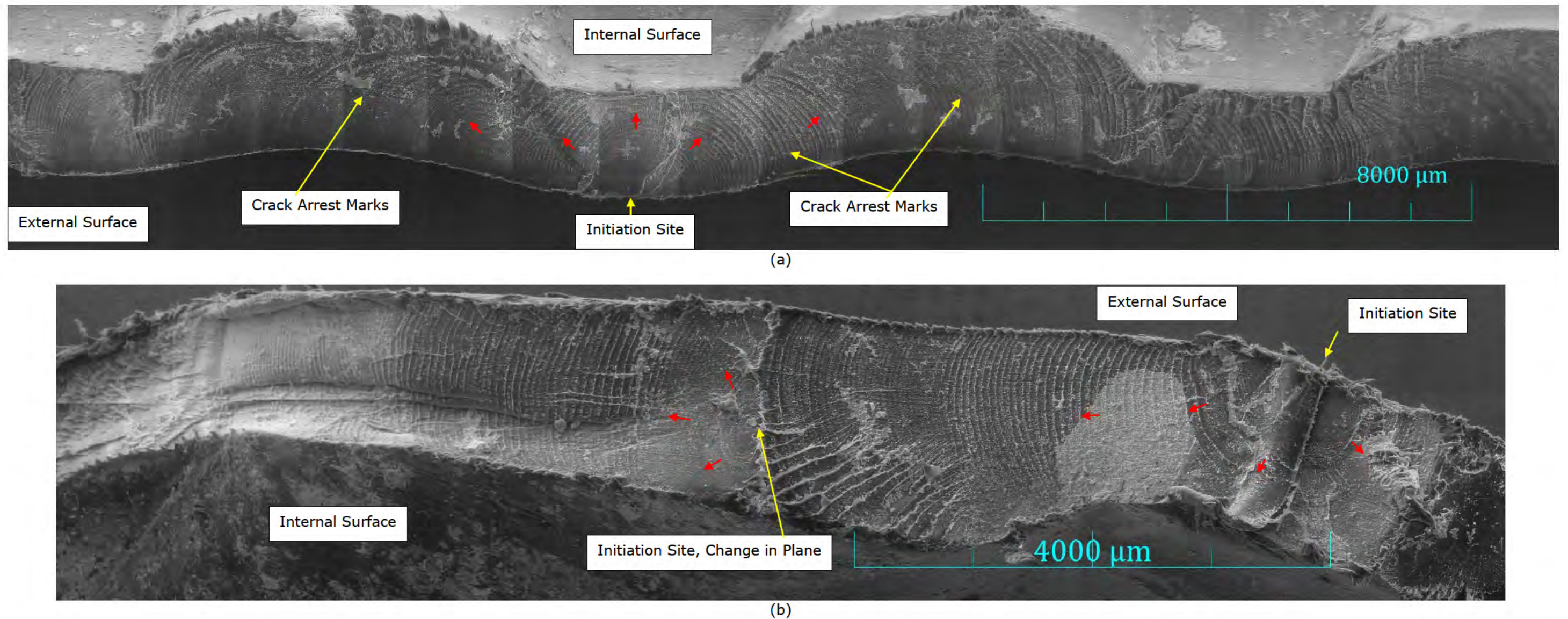


Figure 112. Montages of SEM images taken of the fracture surfaces from the cover of the Subject Aft Cable showing crack arrest marks and initiation sites; locations for (a) and (b) are shown in Figure 110. The red arrow indicated the direction of fatigue propagation.

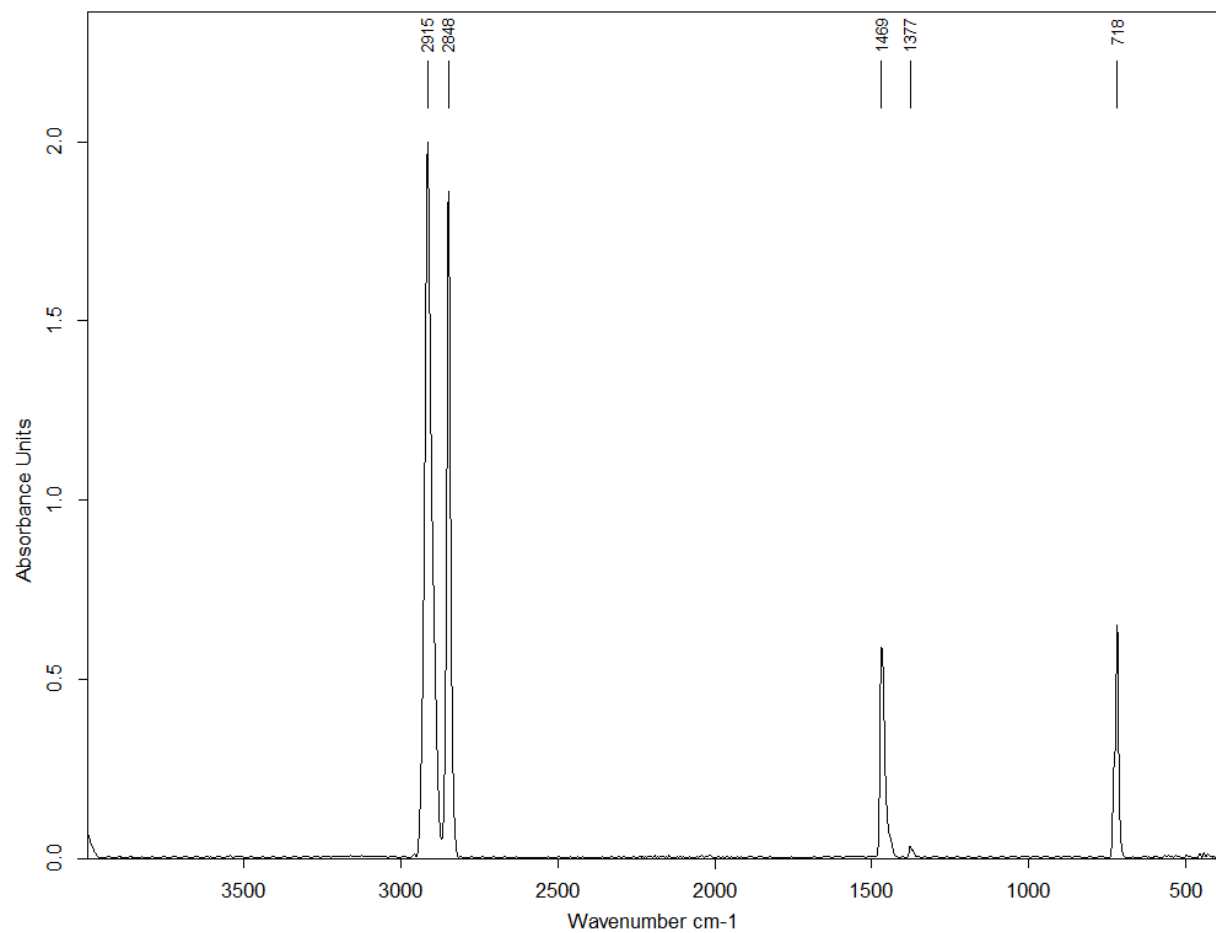


Figure 113. Fourier-transform Infrared Spectroscopy spectrum of the FTIR sample removed from the cover of the Subject Aft Cable; sample location shown in Figure 109.

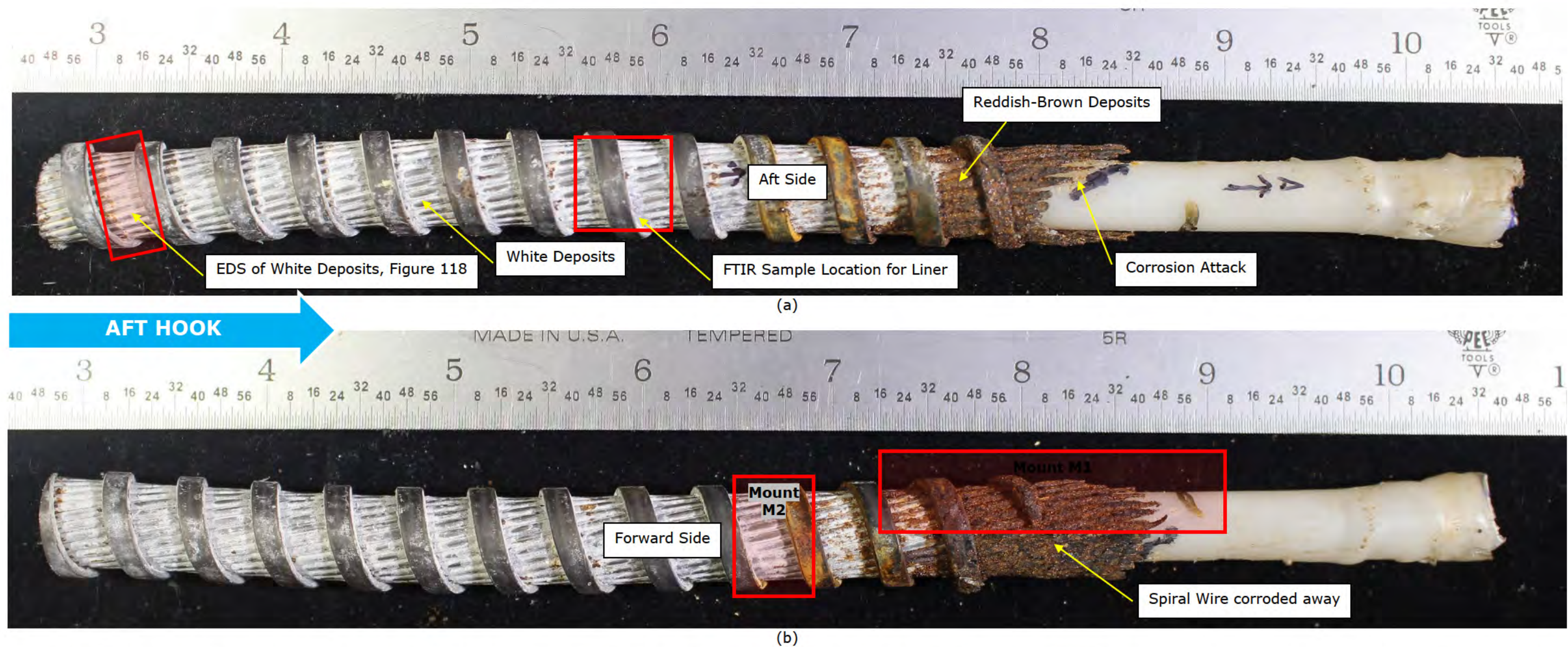
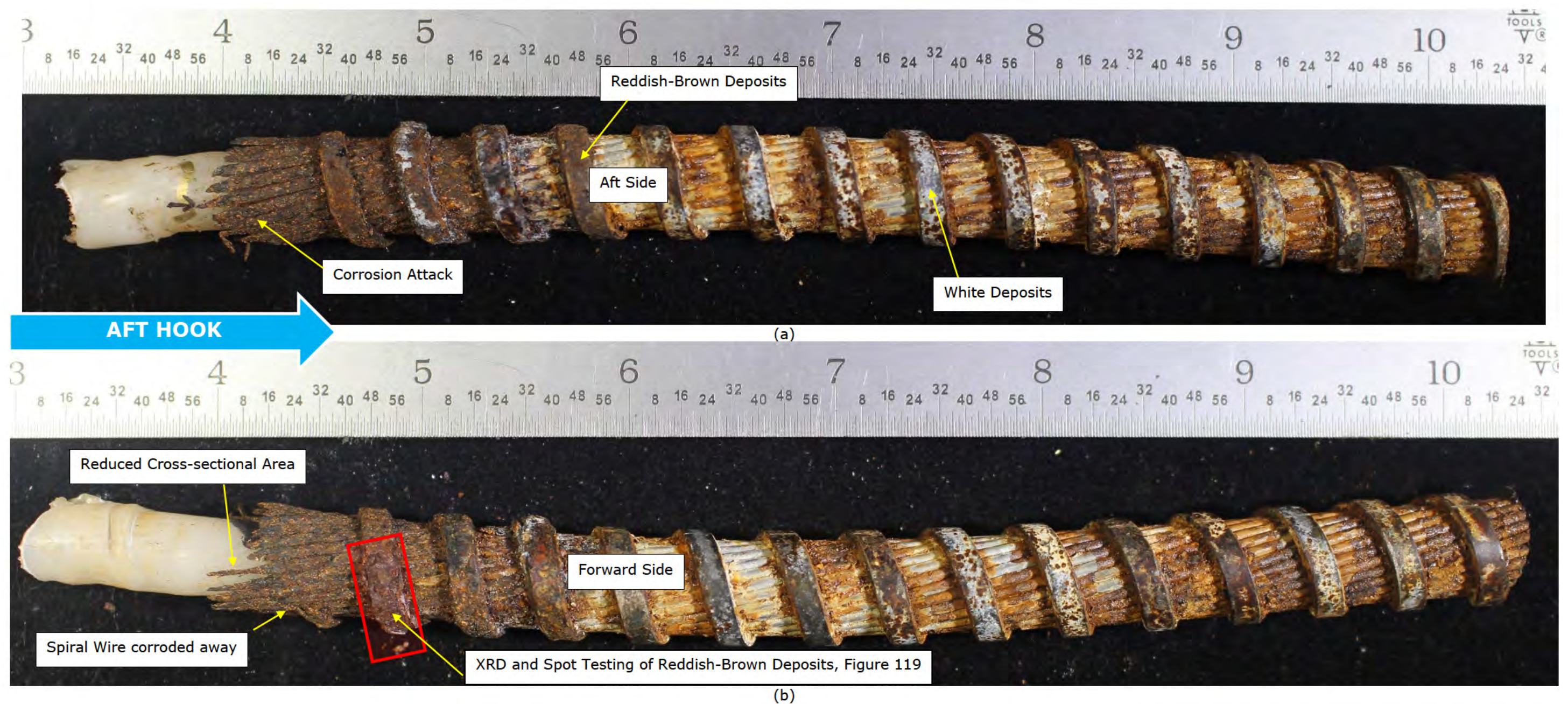


Figure 114. Photographs of the wire layer from the Subject Release Unit side of the failure in the Subject Aft Cable after dissection showing the (a) aft side and (b) forward side; samples shown in Figure 108. Forward and aft refer to the orientation of the keeper relative to the lifeboat. The direction of the Subject Aft Hook is noted with the blue arrow. Rulers are in inches.



| Deposits | Sulfides | Carbonates |
|-------------------------------|----------|------------|
| Reddish-Brown from Wire Layer | N | N |

Figure 115. Photographs of the wire layer from the Subject Aft Hook side of the failure in the Subject Aft Cable after dissection showing the (a) aft side and (b) forward side; samples shown in Figure 108. The direction of the Subject Aft Hook is noted with the blue arrow. Forward and aft refer to the orientation of the keeper relative to the lifeboat. Rulers are in inches.

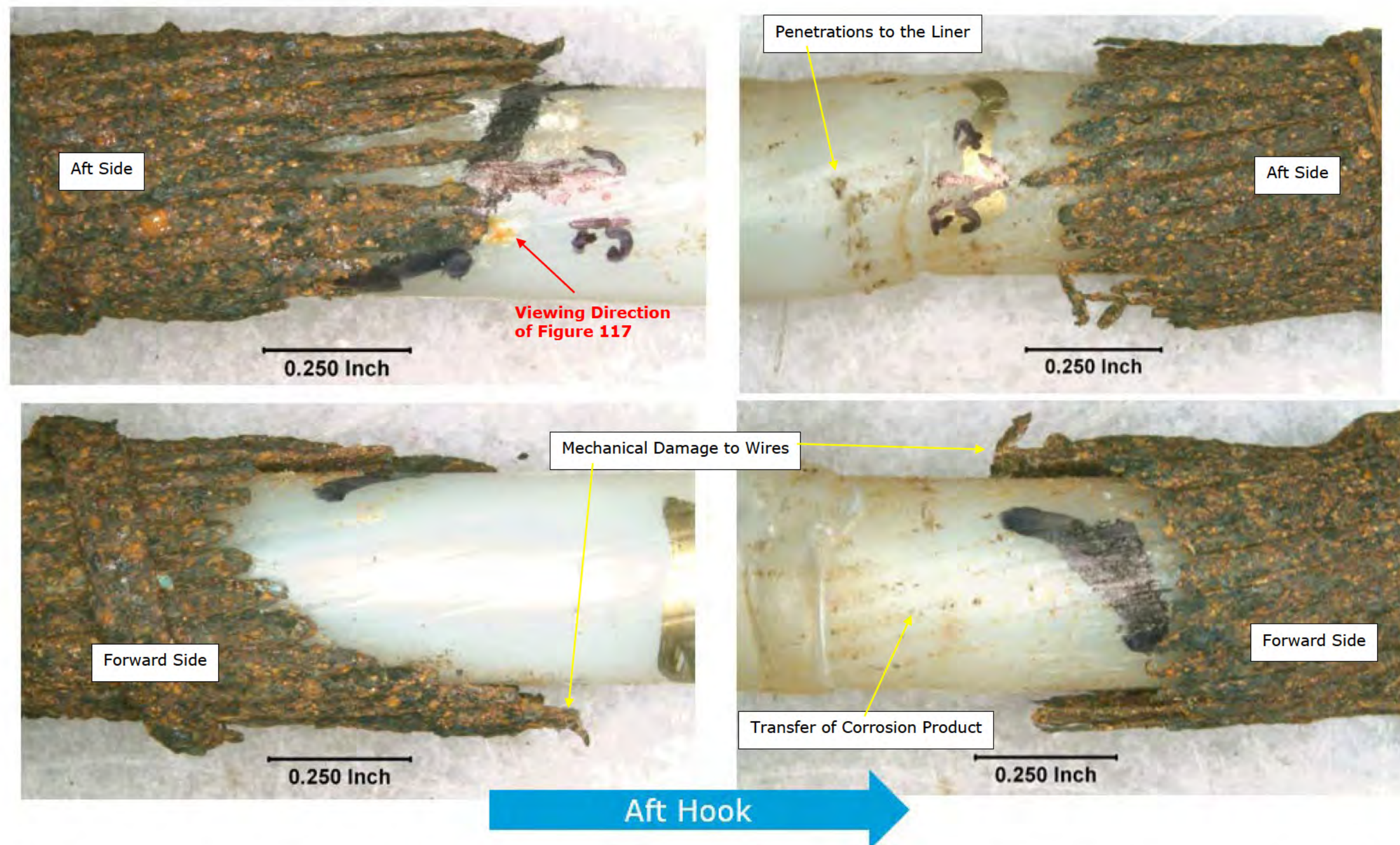


Figure 116. Light photomicrographs of the wire layer from the Subject Aft Cable showing the corrosion damage at the failure. The direction of the Subject Aft Hook is noted with the blue arrow.

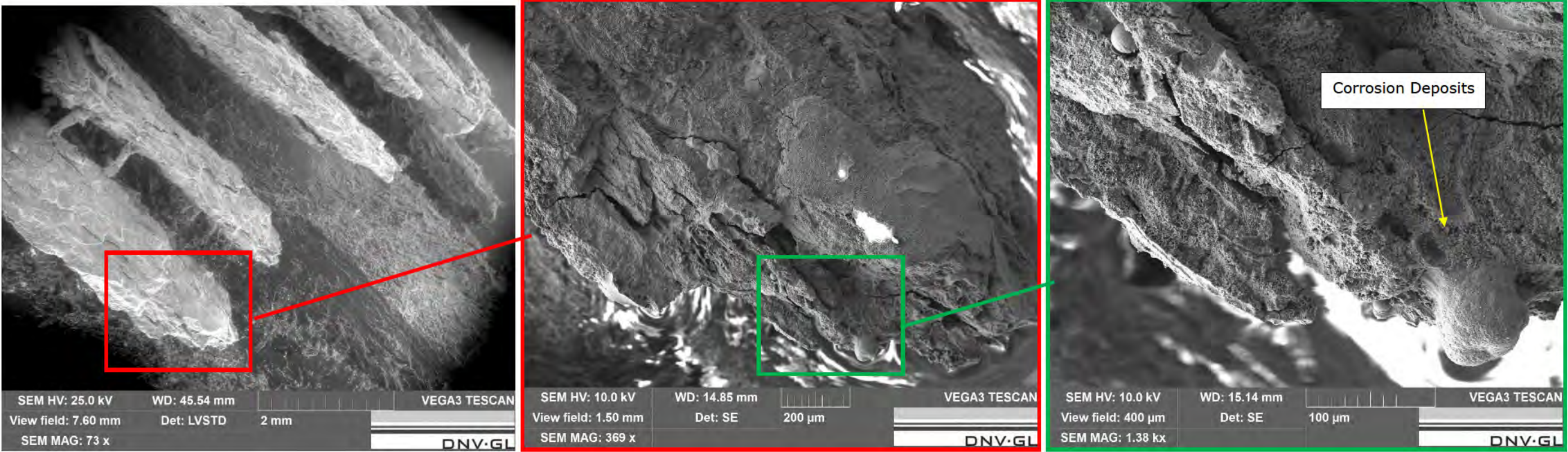
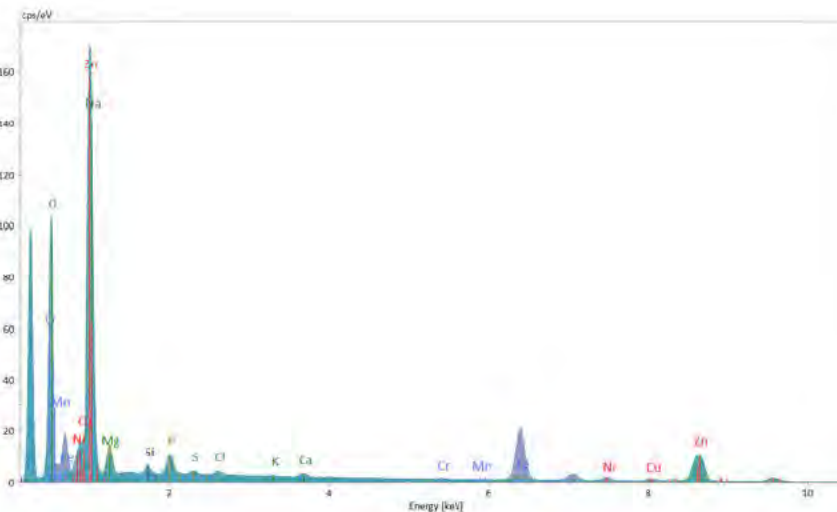
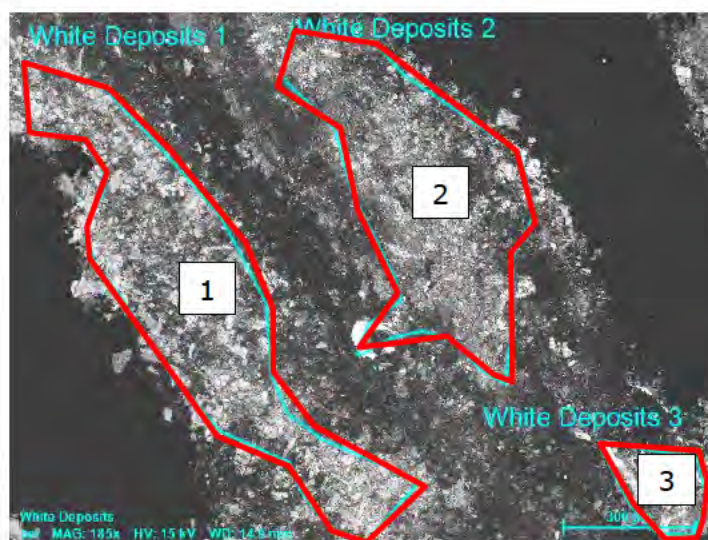


Figure 117. SEM images taken of the strand wires from the wire layer of the Subject Aft Cable showing corrosion damage; viewing direction is shown in Figure 116.



| Location | Oxygen (O) | Sodium (Na) | Magnesium (Mg) | Silicon (Si) | Phosphorus (P) | Sulfur (S) | Chlorine (Cl) | Potassium (K) | Calcium (Ca) | Chromium (Cr) | Manganese (Mn) | Iron (Fe) | Nickel (Ni) | Copper (Cu) | Zinc (Zn) |
|----------|------------|-------------|----------------|--------------|----------------|------------|---------------|---------------|--------------|---------------|----------------|-----------|-------------|-------------|-----------|
| | Wt% | | | | | | | | | | | | | | |
| 1 | 35.0 | 14.0 | 3.0 | 0.8 | 1.7 | 0.3 | 0.3 | 0.1 | 0.5 | | | 1.0 | | | 43.3 |
| 2 | 34.4 | 13.8 | 4.8 | 0.8 | 1.7 | 0.3 | 0.3 | 0.1 | 0.8 | | | 3.2 | | | 39.8 |
| 3 | 19.8 | 10.5 | 2.1 | 0.7 | 1.4 | 0.2 | 0.4 | 0.1 | 0.6 | 0.2 | 0.1 | 26.8 | 2.9 | 2.5 | 31.8 |

Figure 118. SEM image, EDS spectra, and table of results for white deposits removed from the external surface of the wire layer of the Subject Aft Cable; location shown in Figure 114.

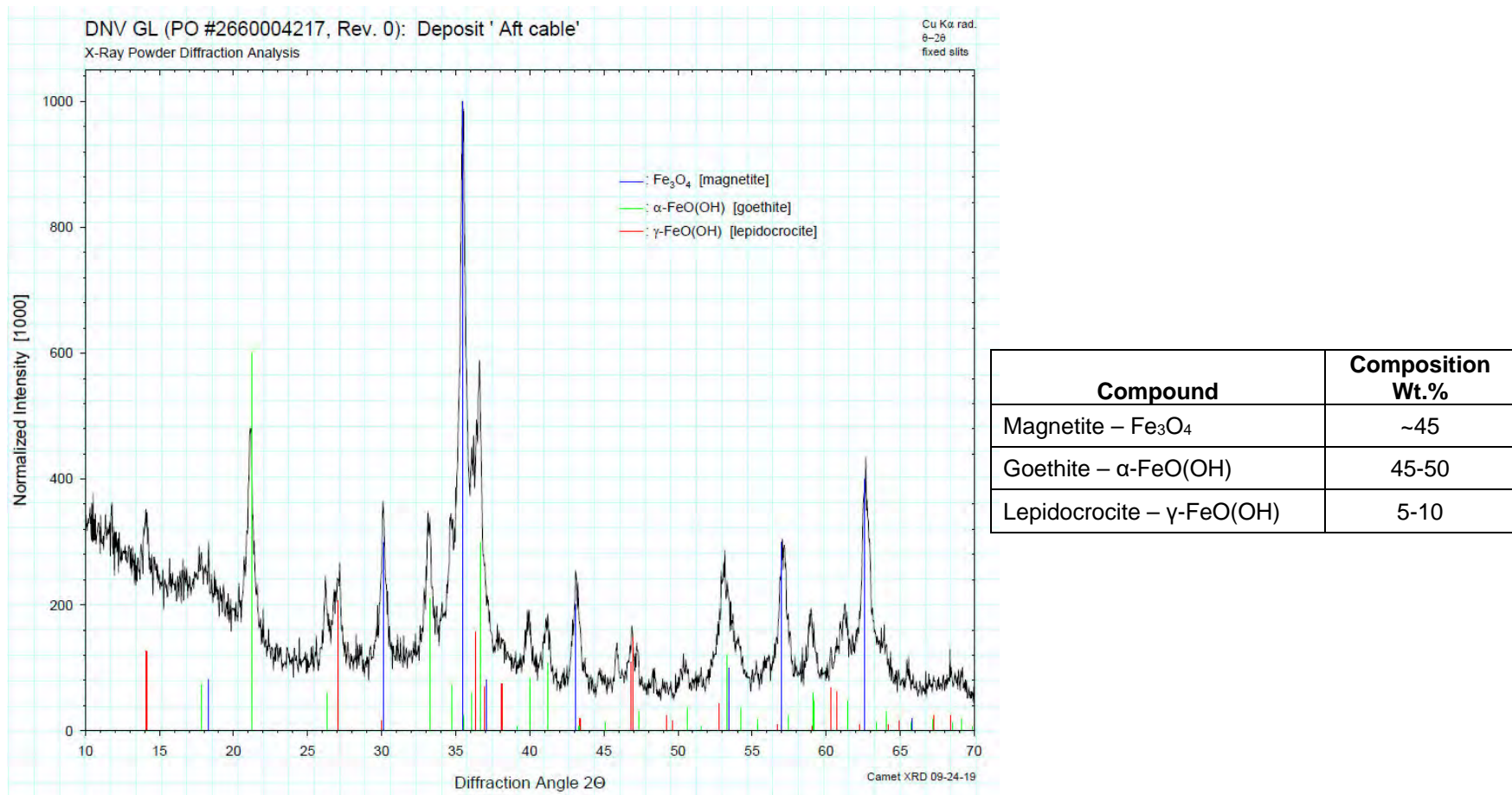


Figure 119. Spectrum and table summarizing the results of an XRD analysis performed on reddish-brown deposits that were removed from the wire layer of Subject Aft Cable near the failure; location shown in Figure 115.

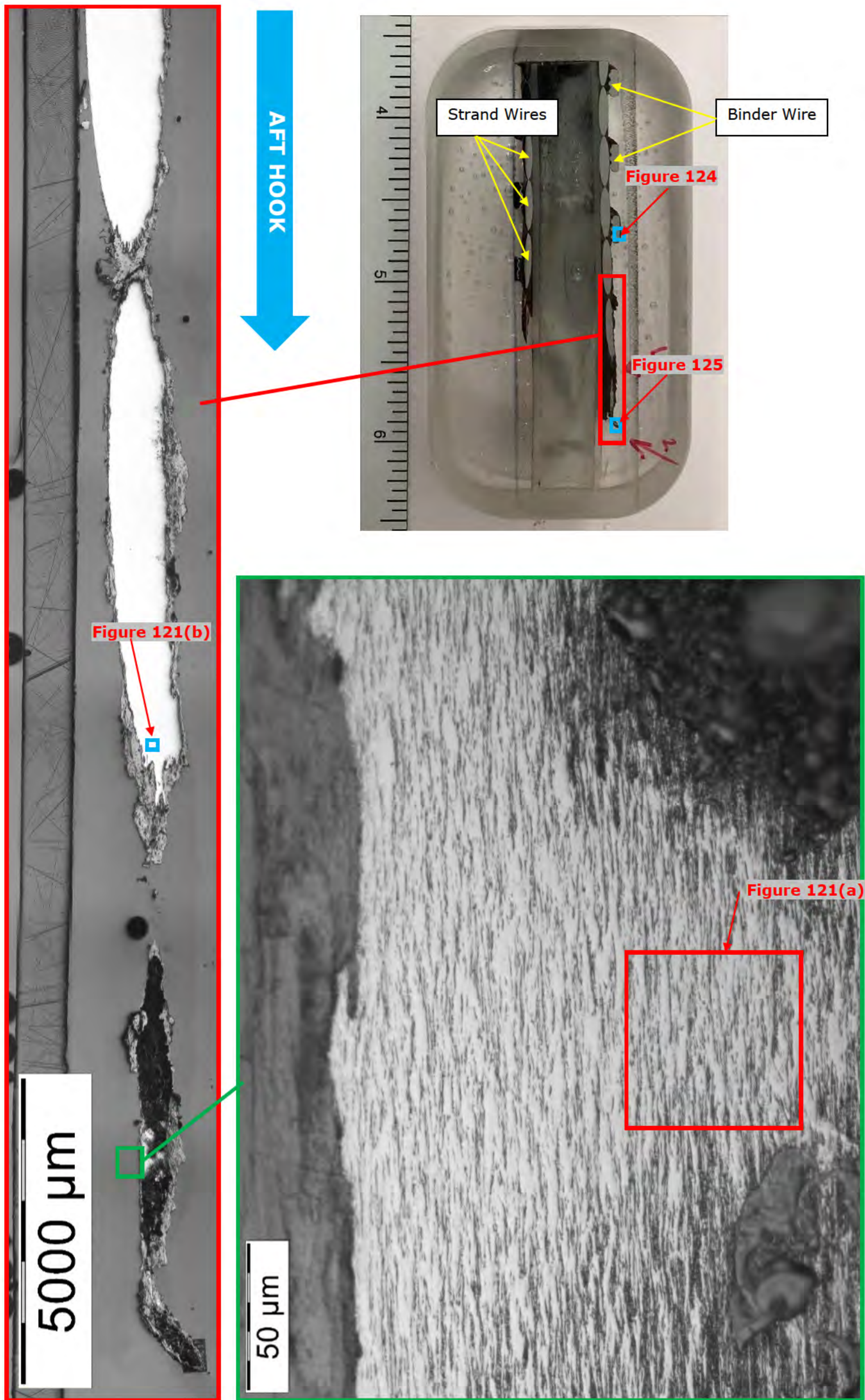


Figure 120. Photograph and photomicrographs of a longitudinal metallographic mount, Mount M1, showing the corrosion attack of the strand wires from the wire layer of the Subject Aft Cable; mount removed from location shown in Figure 114. The direction of the Subject Aft Hook is noted with the blue arrow. The ruler in the upper right photograph is in inches.

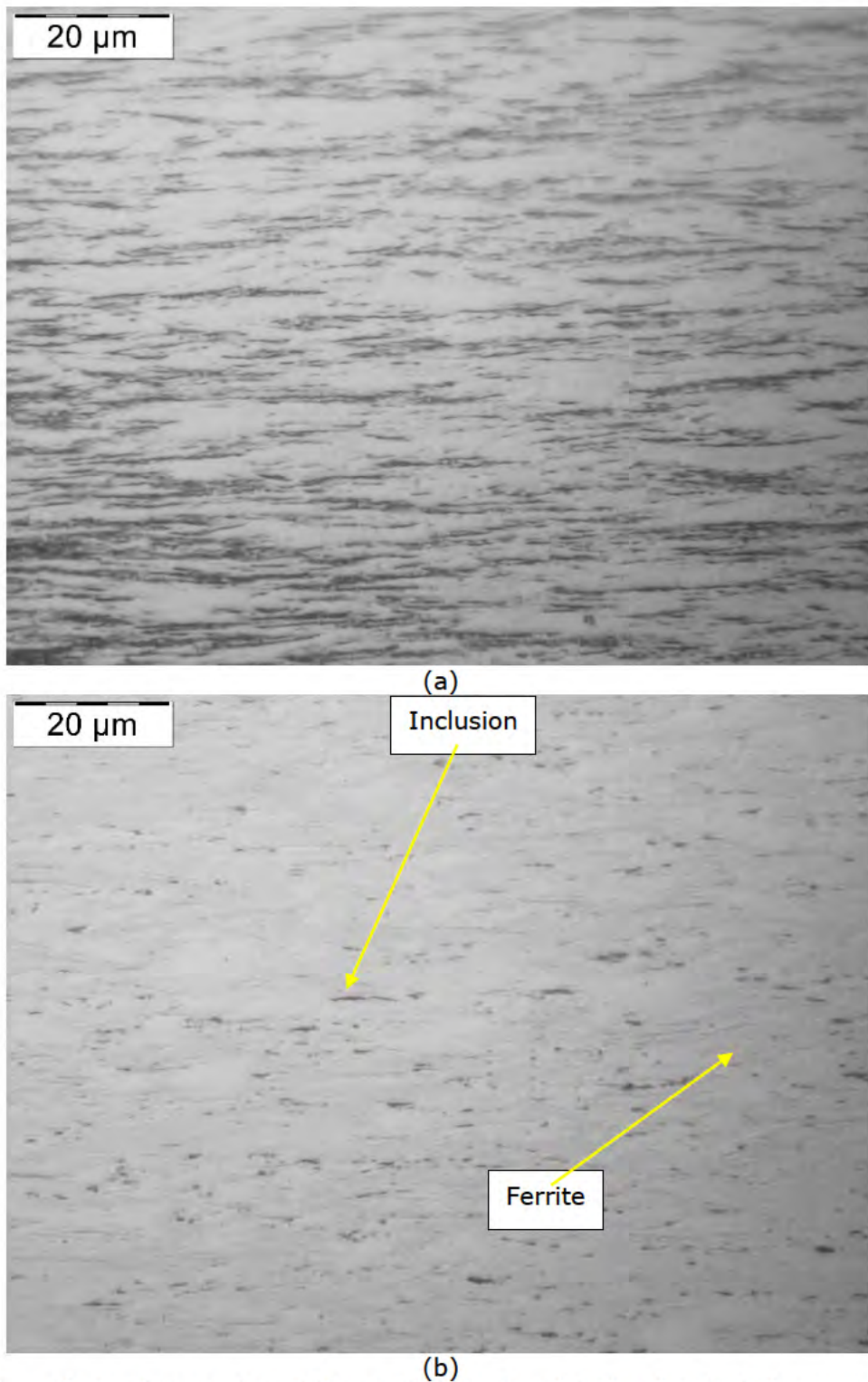


Figure 121. Photomicrographs of Mount M1 showing (a) the detail of the corrosion attack and (b) the microstructure of the strand wires from the wire layer of the Subject Aft Cable; locations shown in Figure 120.

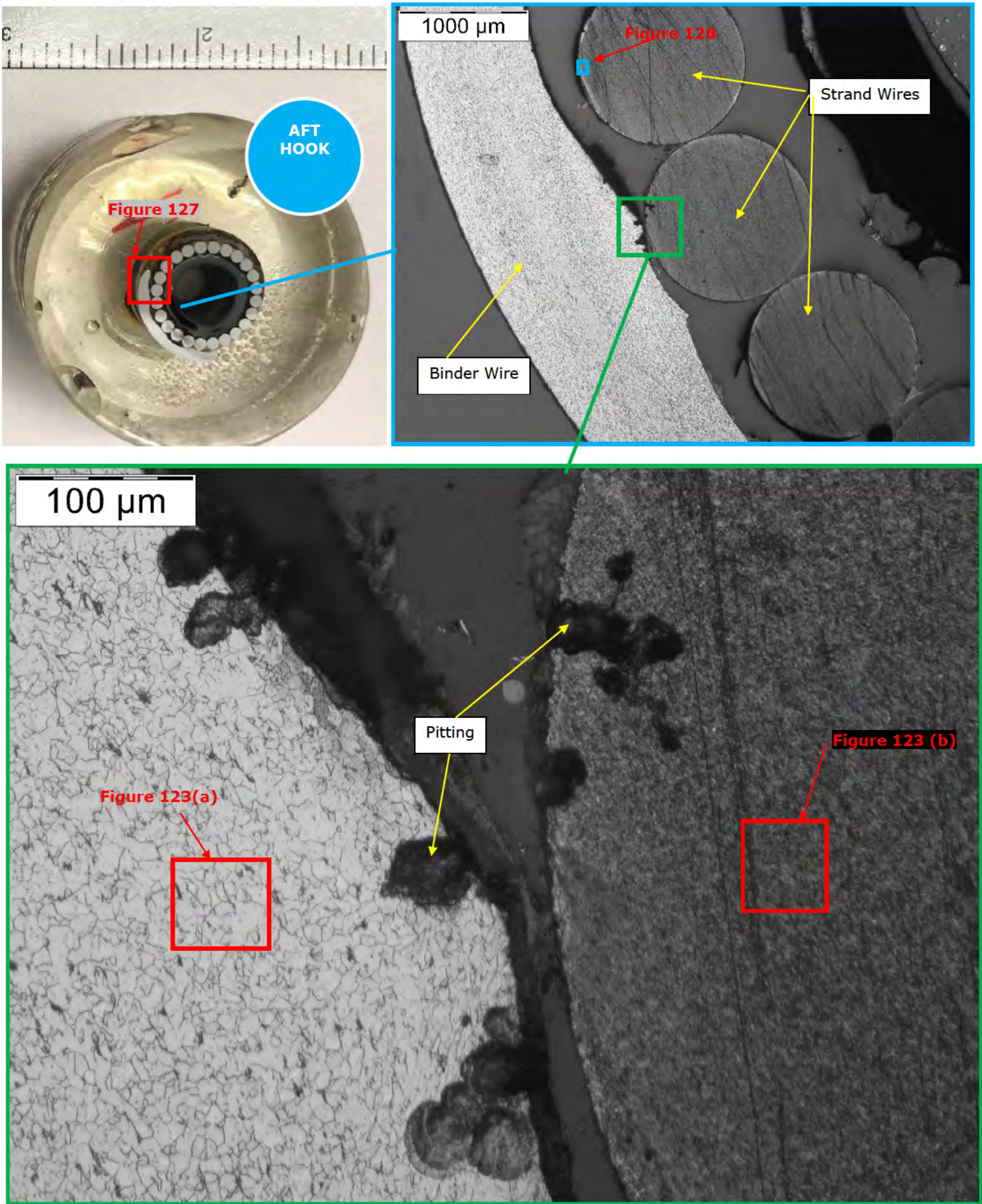


Figure 122. Photograph and photomicrographs of a transverse metallographic mount, Mount M2, showing the corrosion attack of the binder and strand wires from the wire layer of the Subject Aft Cable; mount removed from location shown in Figure 114. The blue circle indicates that the direction toward the Subject Aft Hook is out of the paper. The ruler in the upper left photograph is in inches.

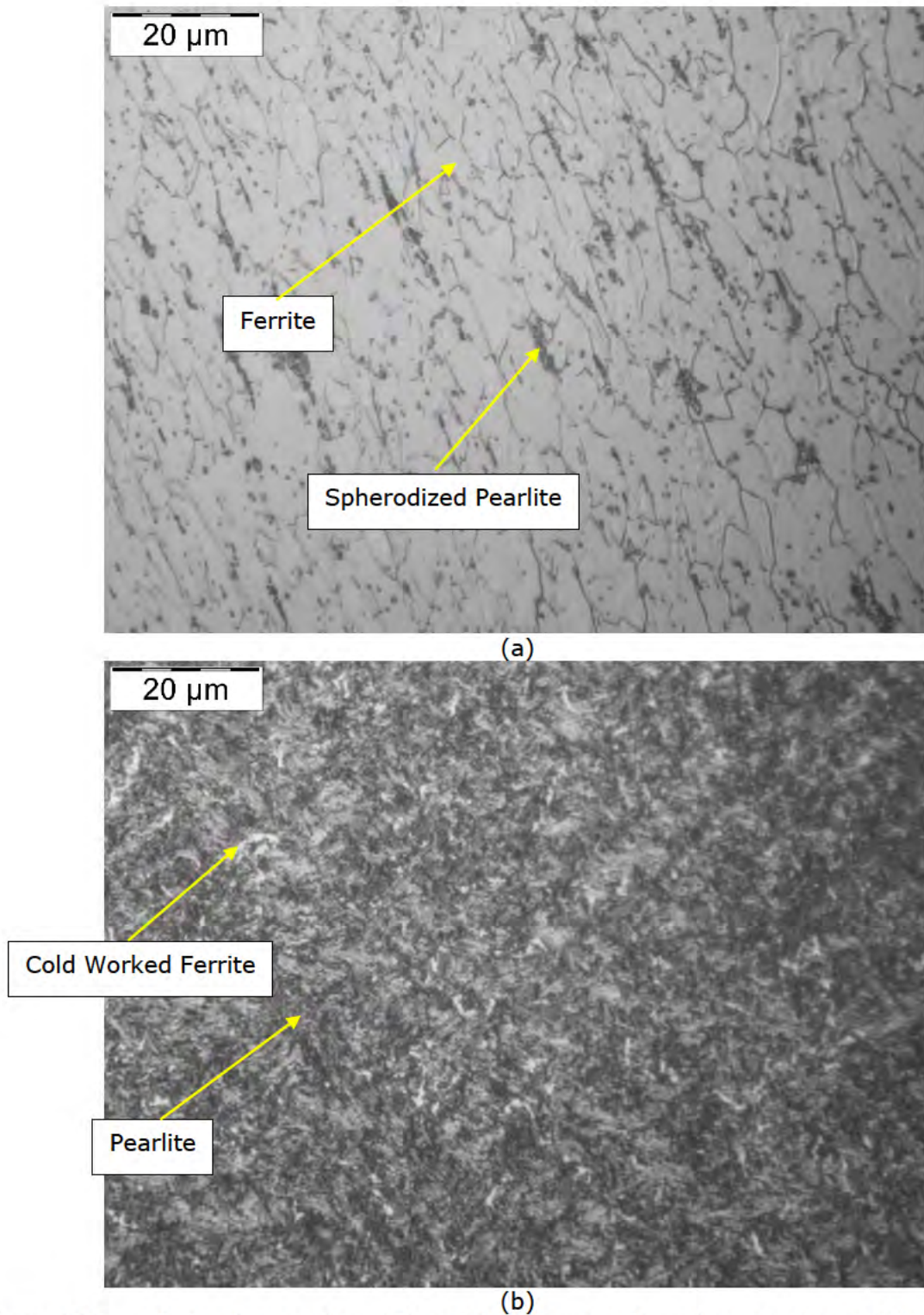
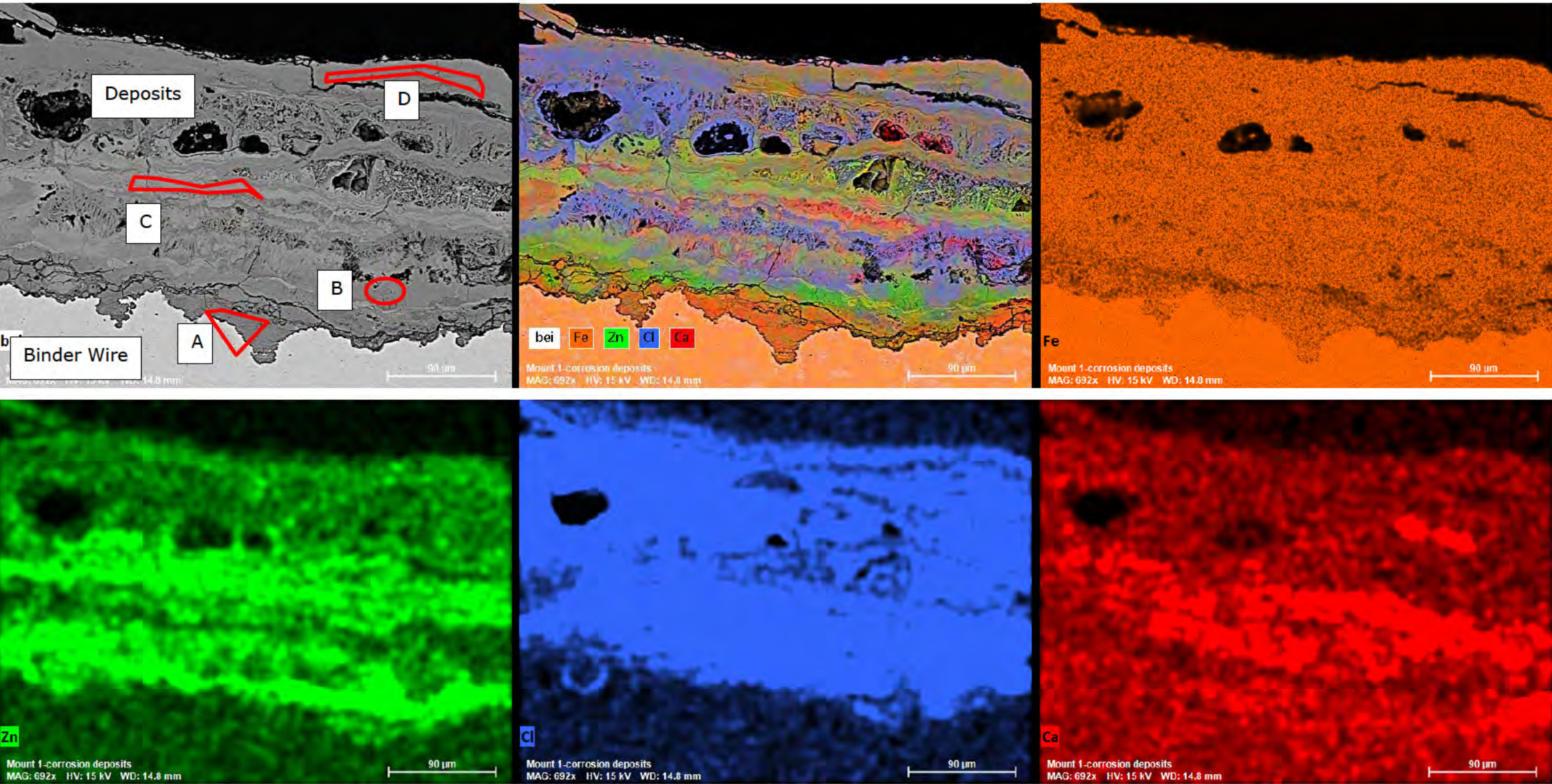


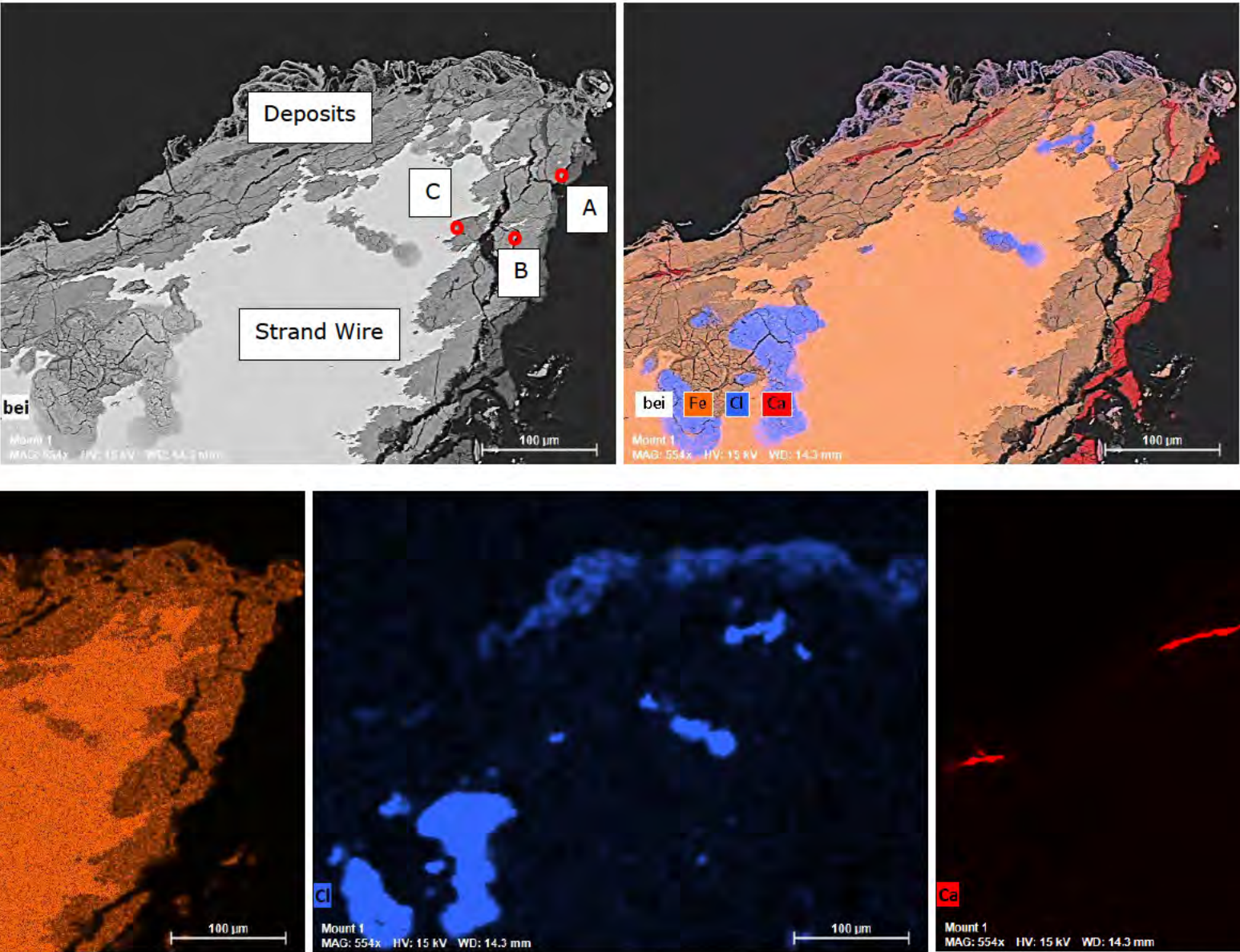
Figure 123. Photomicrographs of Mount M2 showing the microstructure of the (a) binder wire and (b) strand wires from the wire layer of the Subject Aft Cable in the transverse orientation; locations shown in Figure 122.



| Location | Oxygen (O) | Sodium (Na) | Magnesium (Mg) | Aluminum (Al) | Silicon (Si) | Sulfur (S) | Chlorine (Cl) | Calcium (Ca) | Chromium (Cr) | Manganese (Mn) | Iron (Fe) | Copper (Cu) | Zinc (Zn) |
|----------|------------|-------------|----------------|---------------|--------------|------------|---------------|--------------|---------------|----------------|-----------|-------------|-----------|
| A | 29.2 | 0.5 | 0.8 | 0.0 | 0.2 | <0.05 | 0.1 | 0.3 | 0.1 | 0.2 | 66.5 | 0.6 | 1.3 |
| B | 32.9 | 1.7 | 0.3 | 0.1 | 0.1 | 0.1 | 2.0 | 0.1 | <0.05 | 0.3 | 47.3 | 0.6 | 14.5 |
| C | 26.5 | 1.4 | 0.4 | 0.1 | 0.1 | 0.2 | 1.7 | 0.2 | <0.05 | 0.1 | 57.1 | ND | 12.2 |
| D | 33.1 | 0.5 | ND | 0.2 | <0.05 | 0.1 | 1.1 | ND | ND | 0.1 | 60.0 | ND | 4.9 |

ND: Not Detected

Figure 124. SEM images, SEM-EDS elemental maps, and EDS results of deposits present on the binder wire from the Subject Aft Cable showing the distribution of iron (Fe), zinc (Zn), chlorine (Cl), and calcium (Ca); area of Mount M1 shown in Figure 120 (rotated 90°).



| Spectrum | Oxygen (O) | Sodium (Na) | Magnesium (Mg) | Aluminum (Al) | Silicon (Si) | Sulfur (S) | Chlorine (Cl) | Potassium (K) | Calcium (Ca) | Chromium (Cr) | Manganese (Mn) | Iron (Fe) | Strontium (Sr) |
|----------|------------|-------------|----------------|---------------|--------------|------------|---------------|---------------|--------------|---------------|----------------|-----------|----------------|
| A | 47.0 | 0.9 | 0.6 | ND | <0.05 | 0.3 | 0.1 | ND | 46.0 | ND | ND | 4.2 | 1.0 |
| B | 31.7 | 0.3 | 1.3 | ND | 0.4 | 0.1 | <0.05 | ND | 0.4 | 0.2 | 0.2 | 65.4 | <0.05 |
| C | 29.5 | 0.7 | 0.4 | <0.05 | 0.3 | 0.1 | <0.05 | <0.05 | 0.2 | 0.2 | 0.2 | 68.3 | ND |

ND: Not Detected

Figure 125. SEM images, SEM-EDS elemental maps, and EDS results of deposits present on the strand wire from the Subject Aft Cable showing the distribution of iron (Fe), chlorine (Cl), and calcium (Ca); area of Mount M1 shown in Figure 120 (rotated 90°).

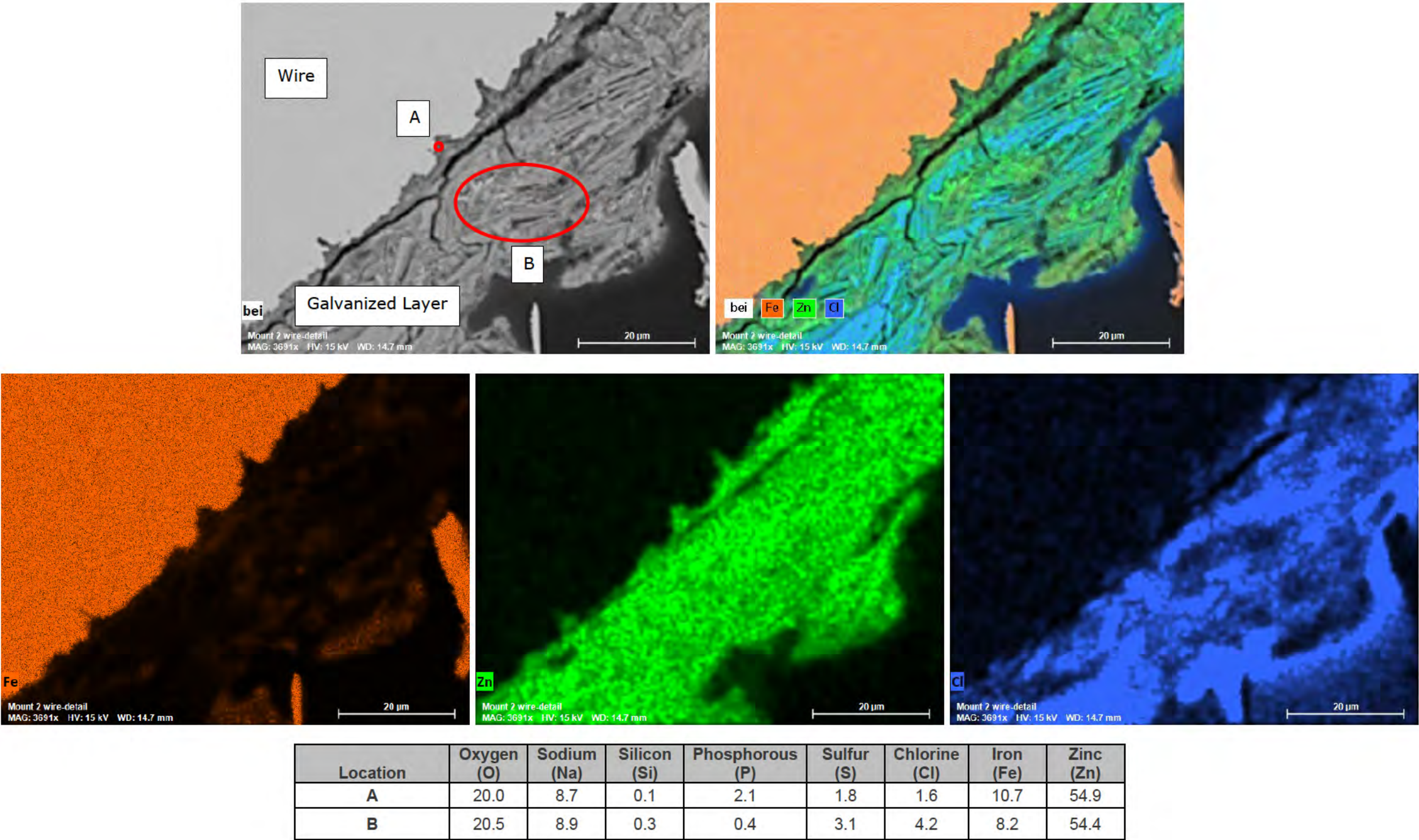
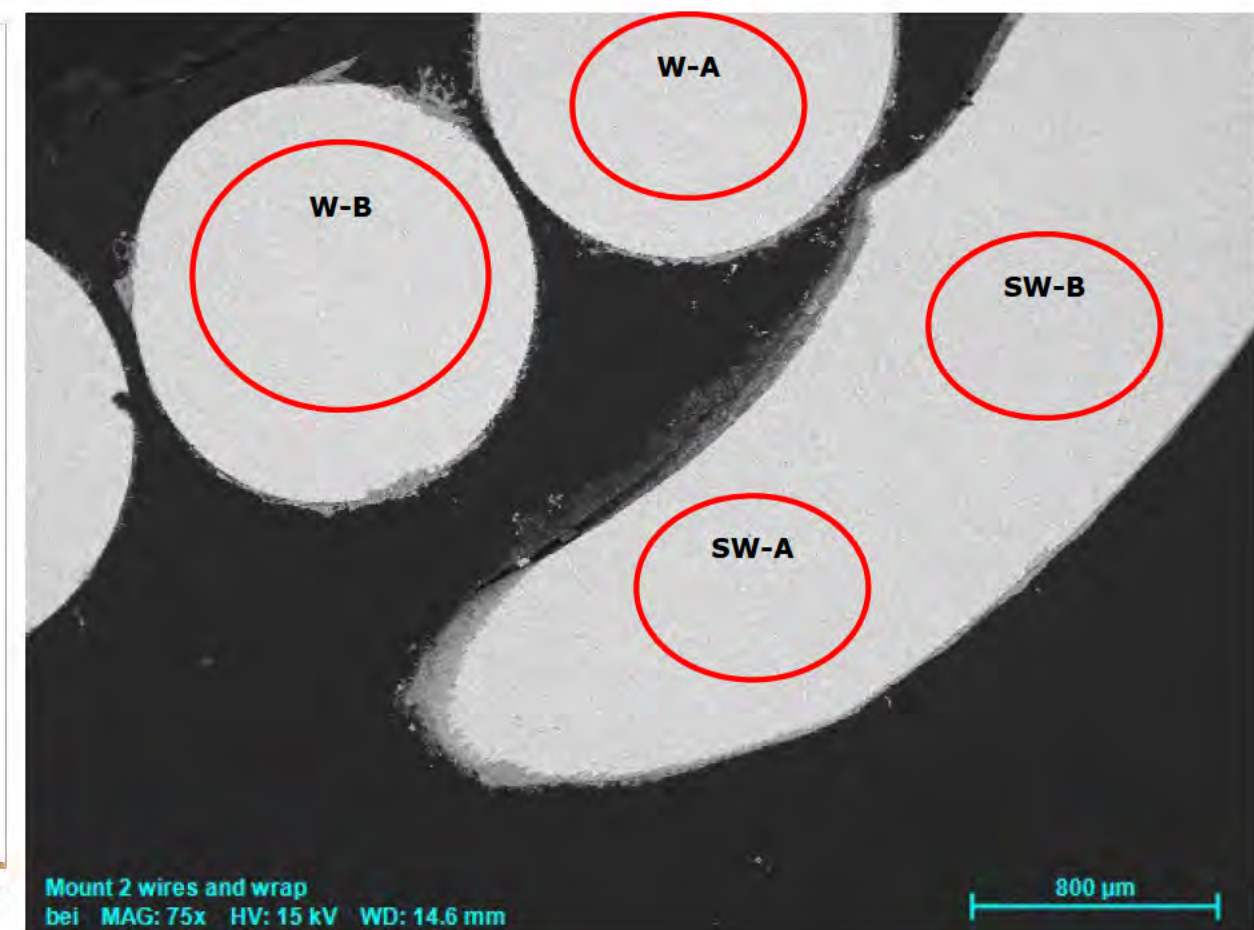
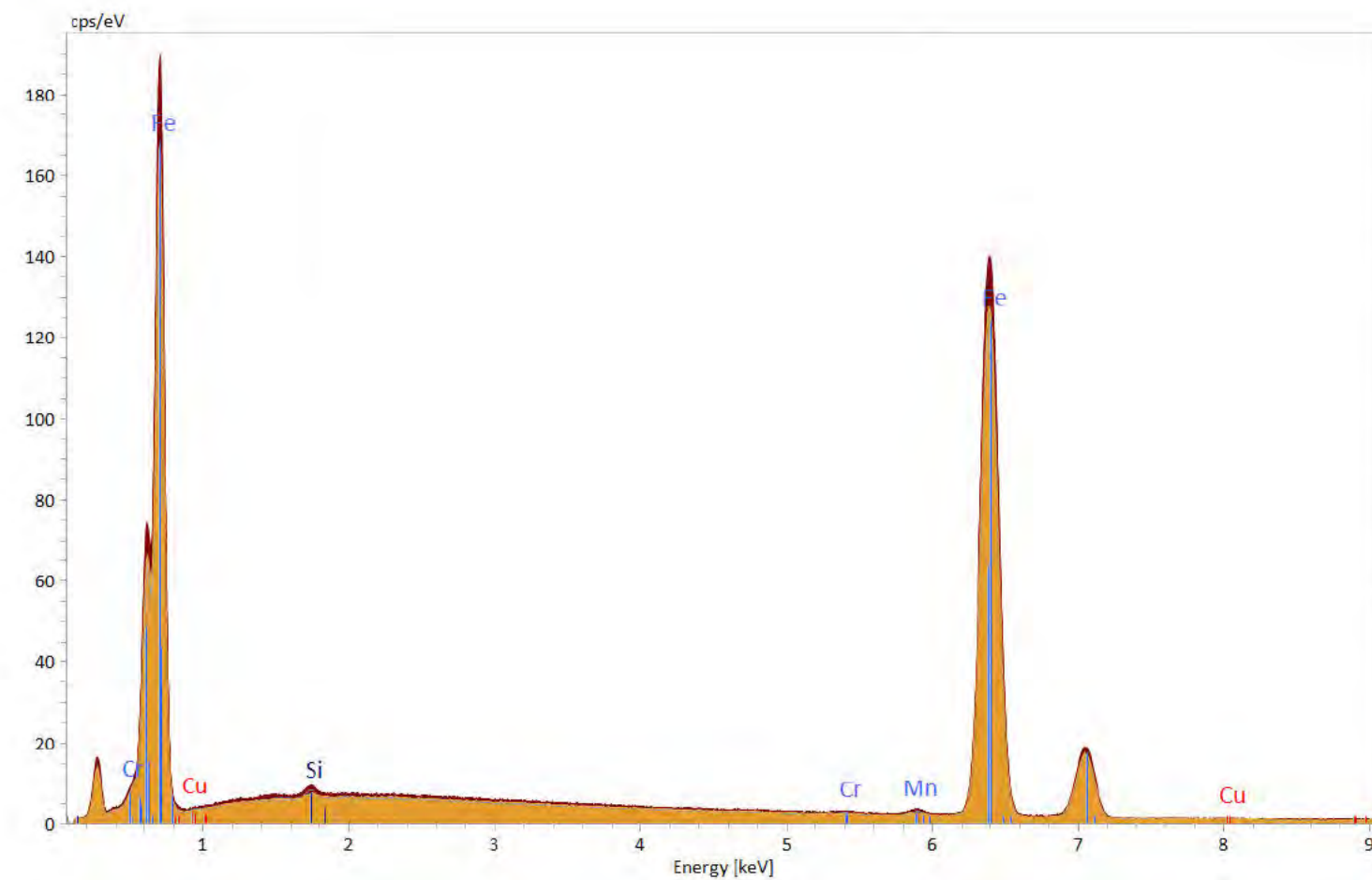


Figure 126. SEM images and SEM-EDS elemental maps of deposits present on the binder wire from the Subject Aft Cable showing the distribution of iron (Fe), zinc (Zn), and chlorine (Cl); area of Mount M2 shown in Figure 122 (rotated 90° counter clockwise).



| Locations | Si | Cr | Mn | Fe | Cu |
|-----------|-----|-------|-----|------|-----|
| W-A | 0.2 | 0.1 | 0.5 | 99.0 | 0.2 |
| W-B | 0.2 | 0.1 | 0.5 | 98.9 | 0.2 |
| | | | | | |
| SW-A | 0.1 | <0.05 | 0.3 | 99.4 | 0.1 |
| SW-B | 0.1 | <0.05 | 0.4 | 99.2 | 0.3 |

Figure 127. EDS Spectra, SEM image, and EDS results for wire and binder wire from the Subject Aft Cable; area shown in Figure 122 (rotated 90°).

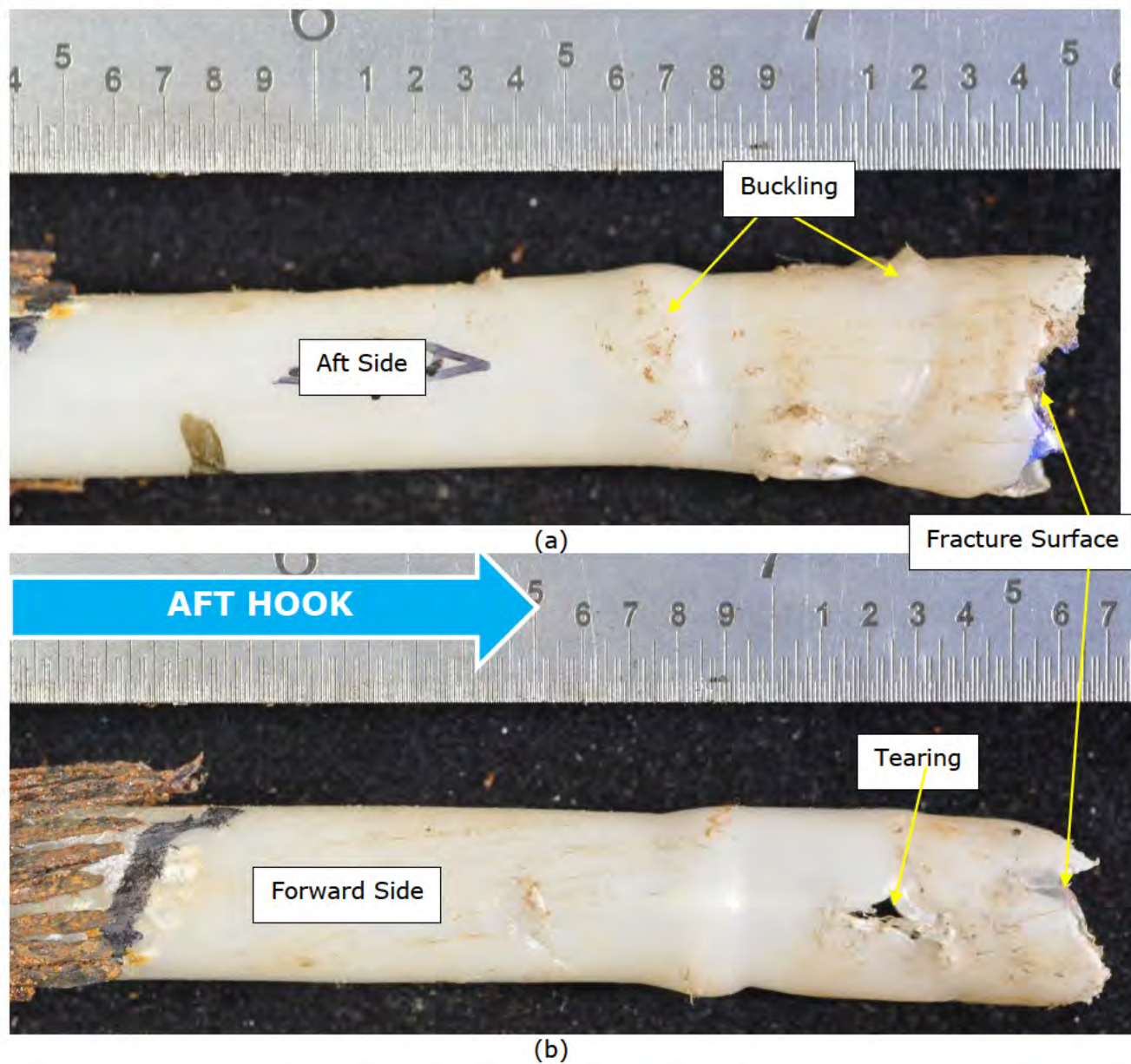


Figure 128. Photographs of the one failed liner from the Subject Release Unit side after dissection showing the (a) aft side and (b) forward side; samples shown in Figure 108. The mating half of the failed liner is shown in Figure 129. Forward and aft refer to the orientation of the keeper relative to the lifeboat. The direction of the Subject Aft Hook is noted with the blue arrow. Rulers are in inches.

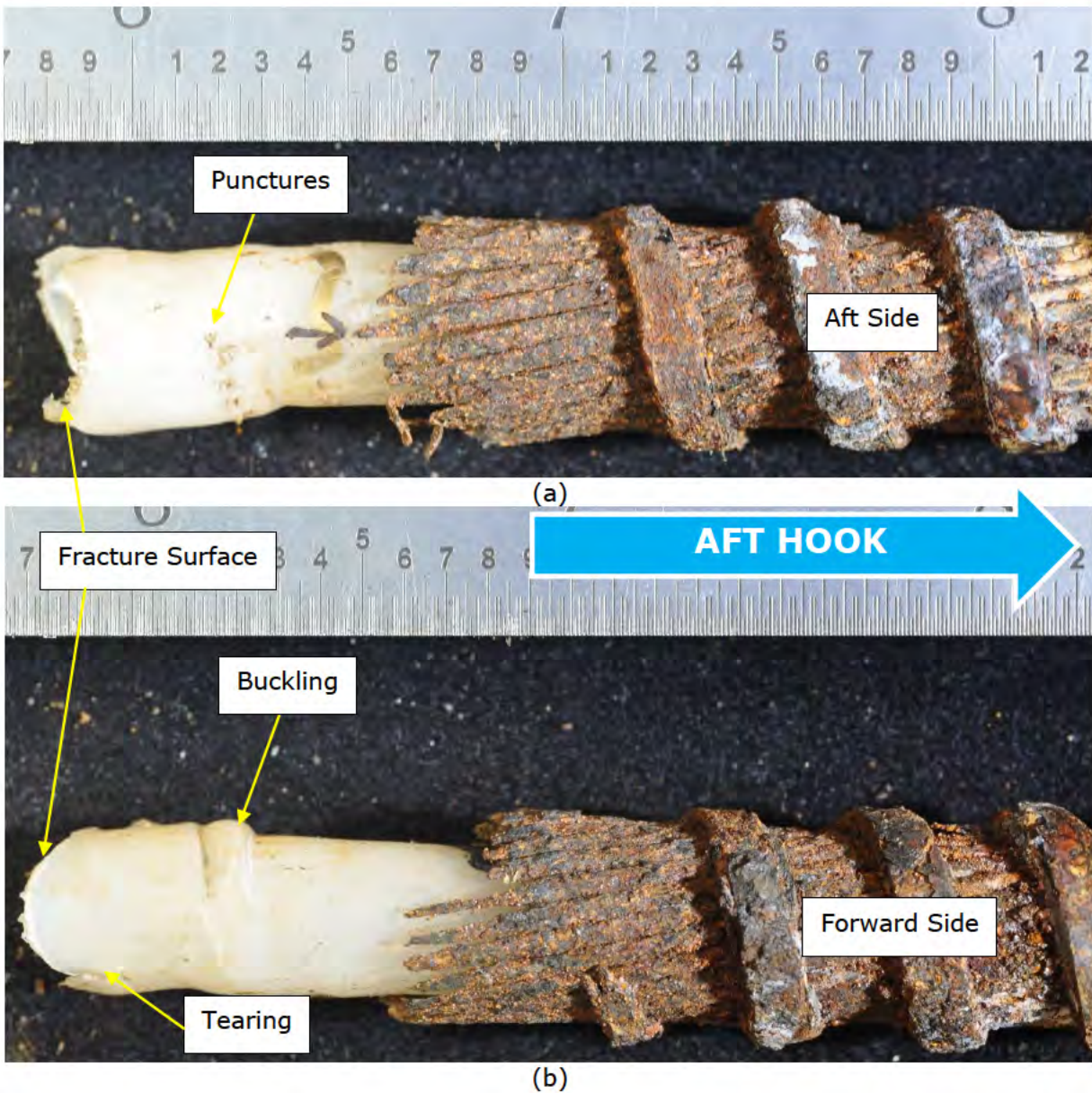
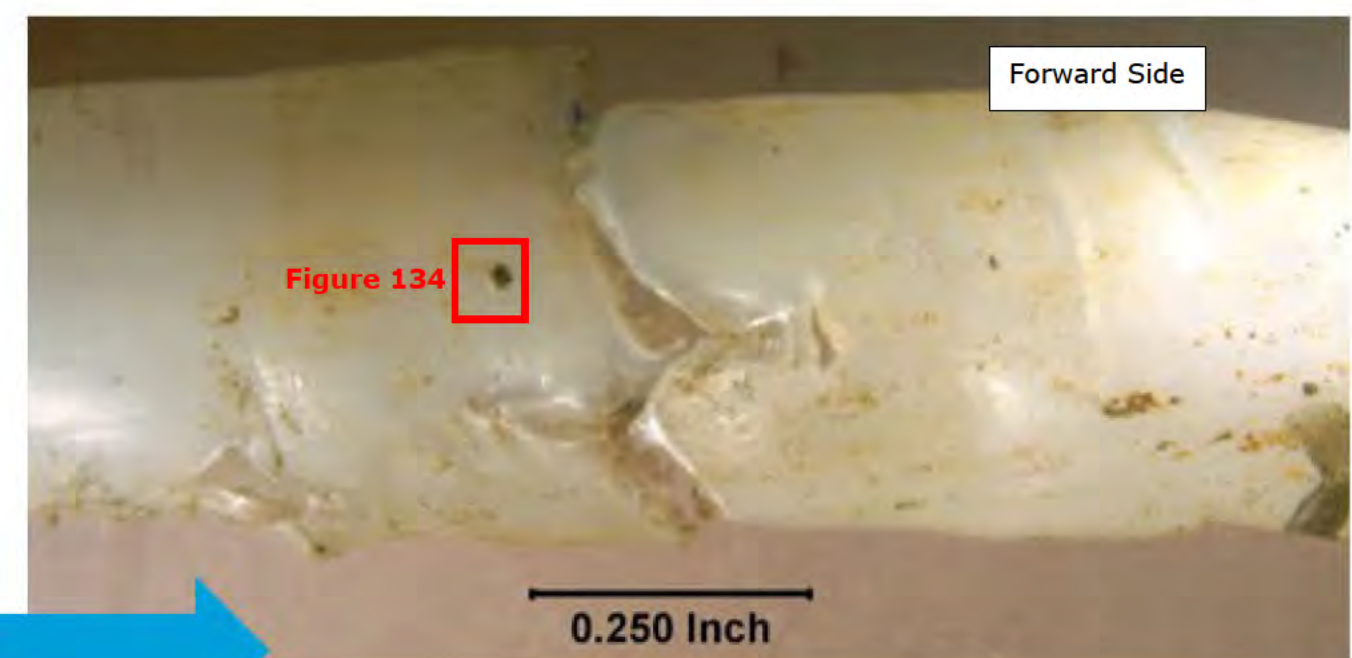
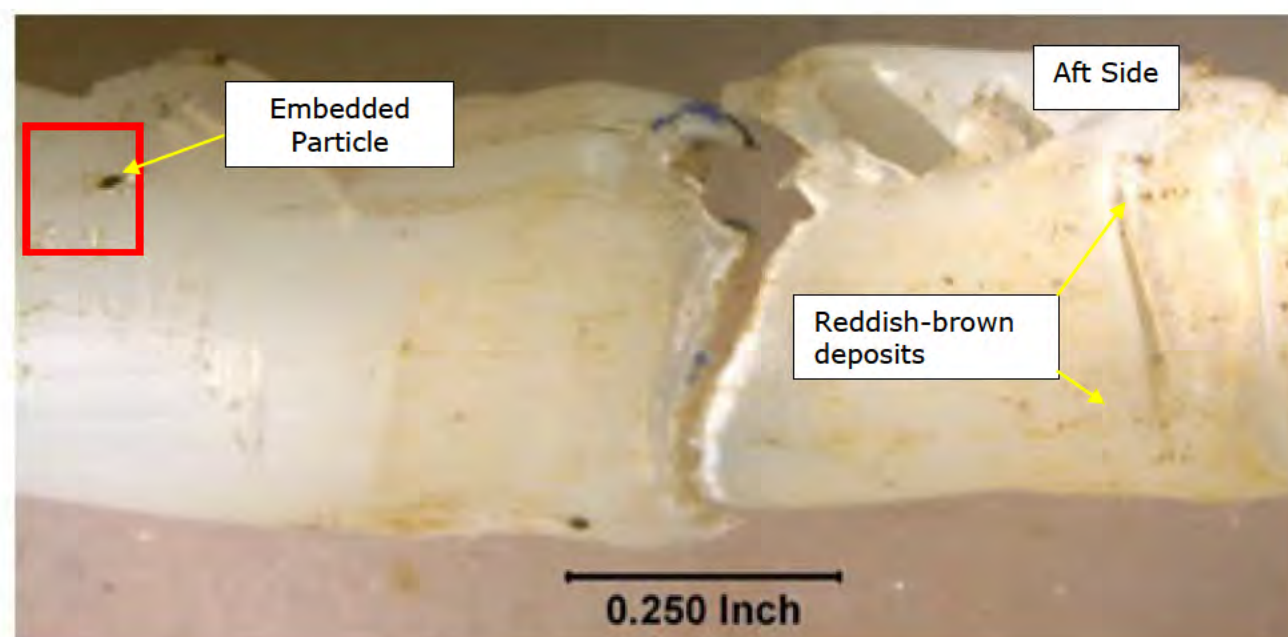
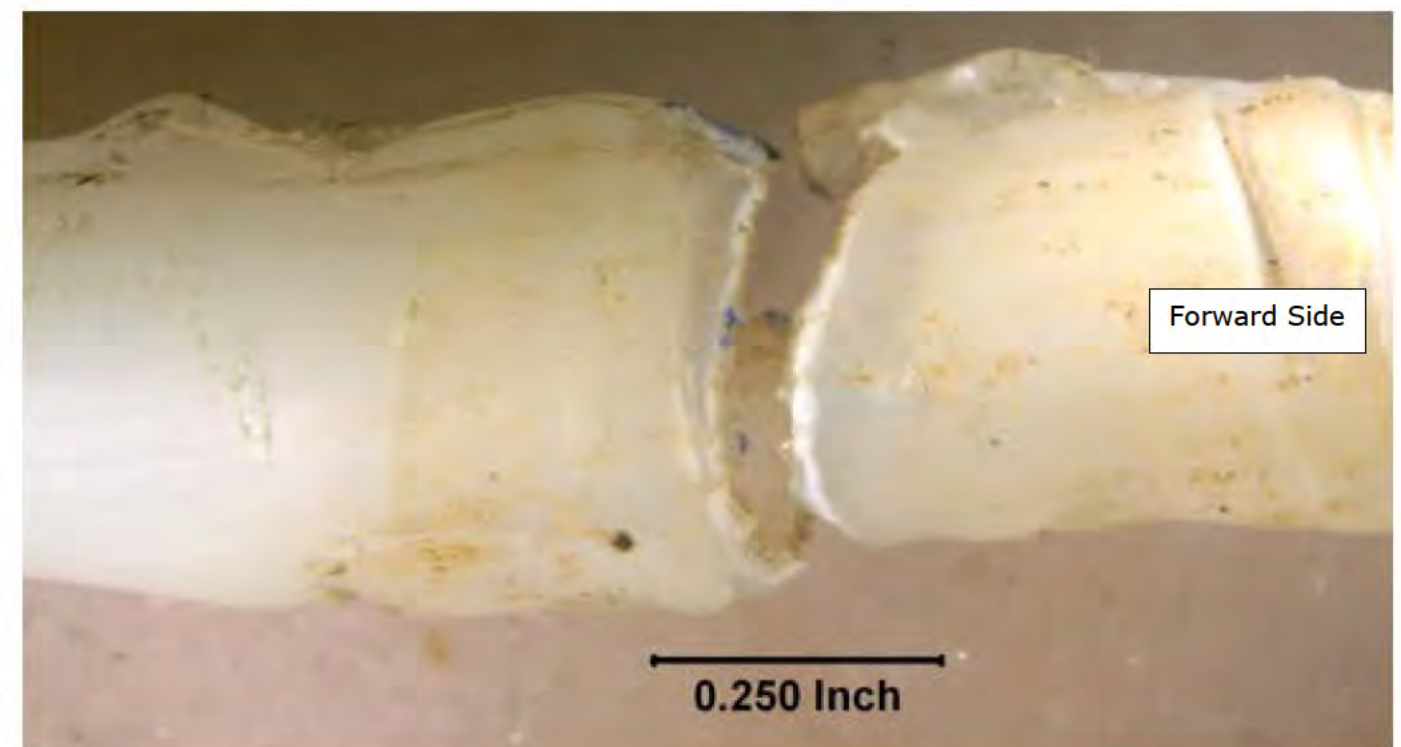
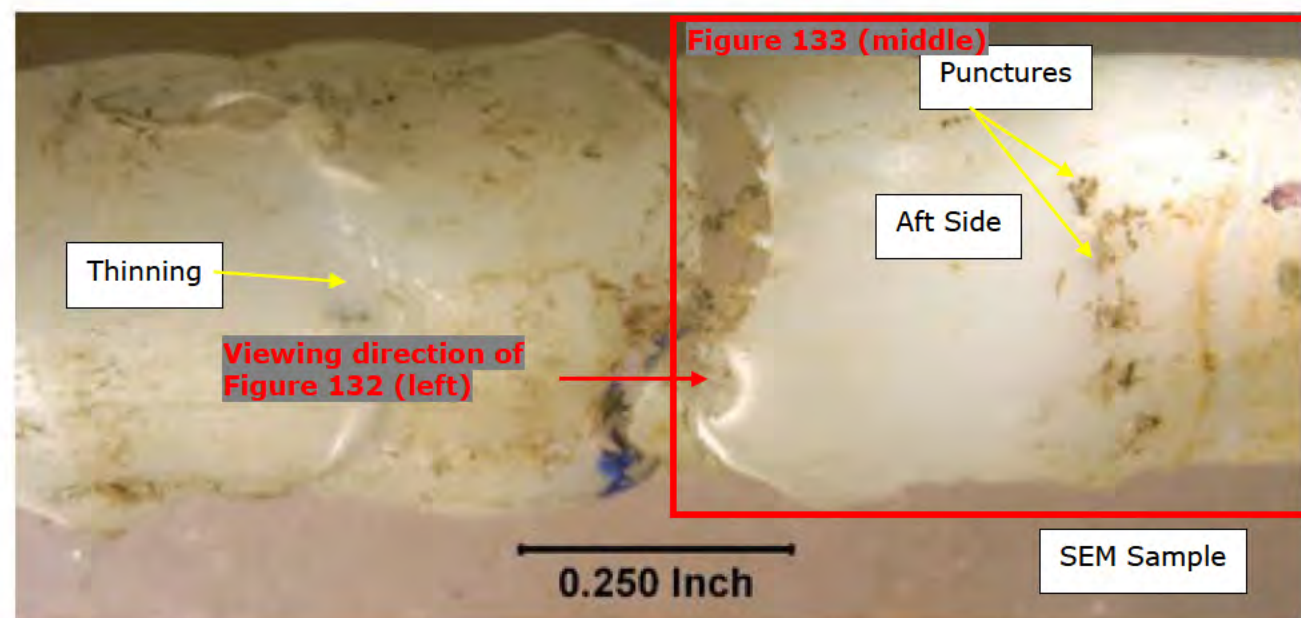


Figure 129. Photographs of the failed liner from the Subject Aft Hook side after dissection showing the (a) aft side and (b) forward side; samples shown in Figure 108. The mating half of the failed liner is shown in Figure 128. Forward and aft refer to the orientation of the keeper relative to the lifeboat. The direction of the Subject Aft Hook is noted with the blue arrow. Rulers are in inches.



| Sample location shown in (a) | Shore D Hardness Average of Four Measurements |
|------------------------------|--|
| White Liner | 51.0 |

Figure 130. Photograph showing the liner from the Subject Release Unit side after removing the wire layer; sample shown in Figure 108. The direction of the Subject Aft Hook is noted with the blue arrow. The results of the hardness testing of the white liner layer are shown in the table.



Aft Hook

Figure 131. Light photomicrographs of the liner from the Subject Aft Cable showing the failure. The direction of the Subject Aft Hook is noted with the blue arrow.

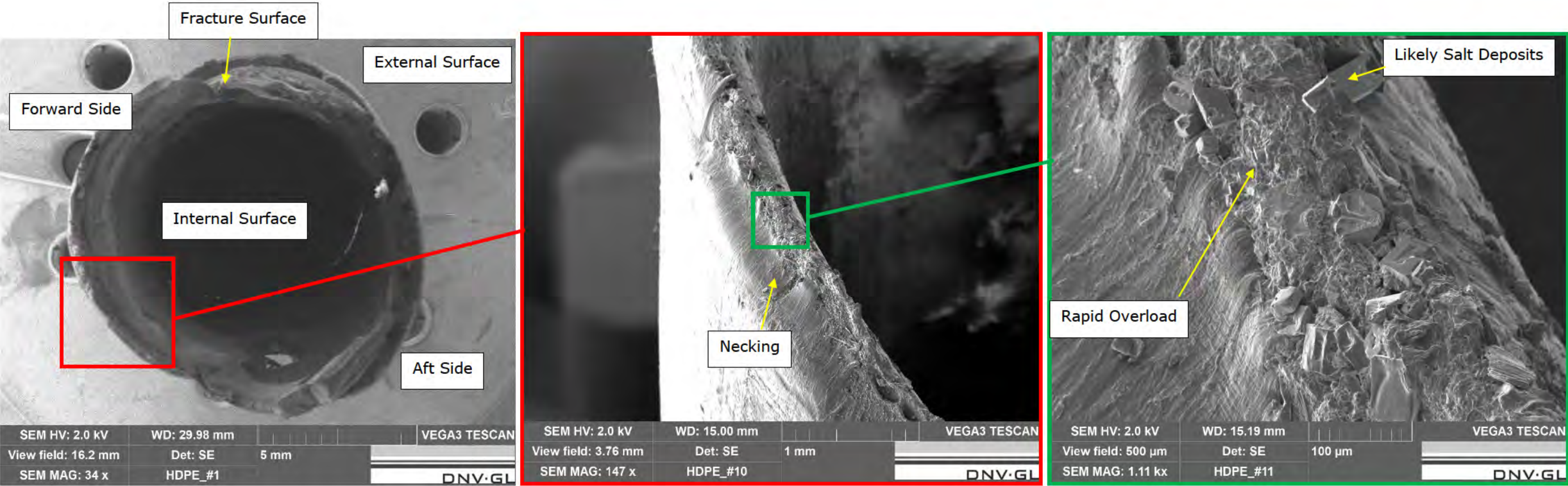


Figure 132. SEM images of the liner from the Subject Aft Hook side of the Subject Aft Cable showing the fracture surface; sample location is shown in Figure 131.

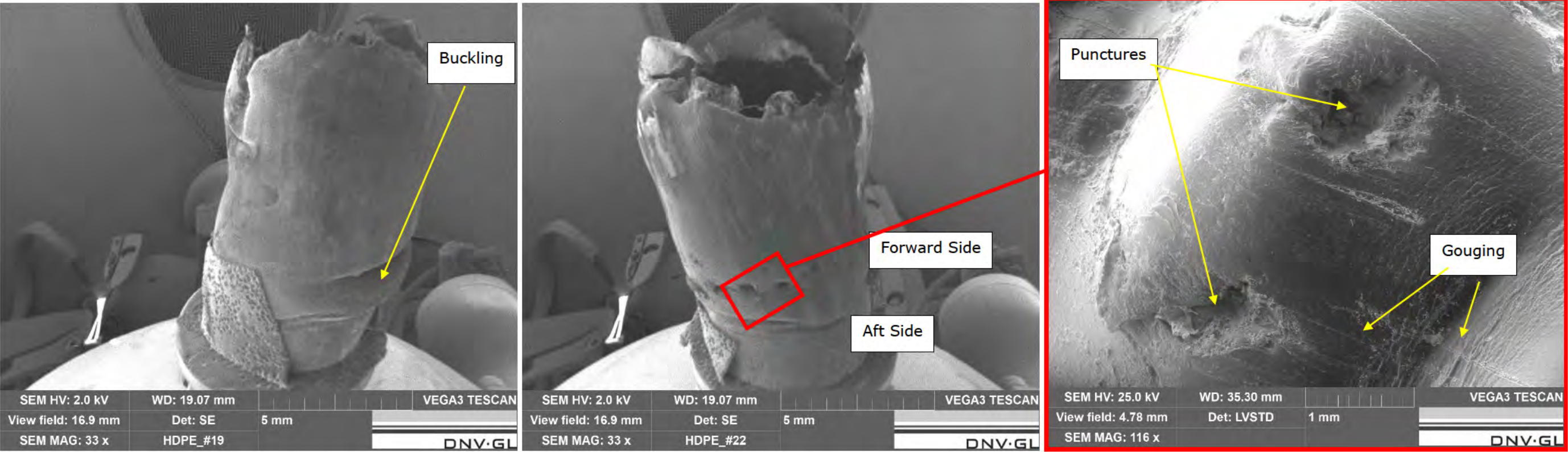
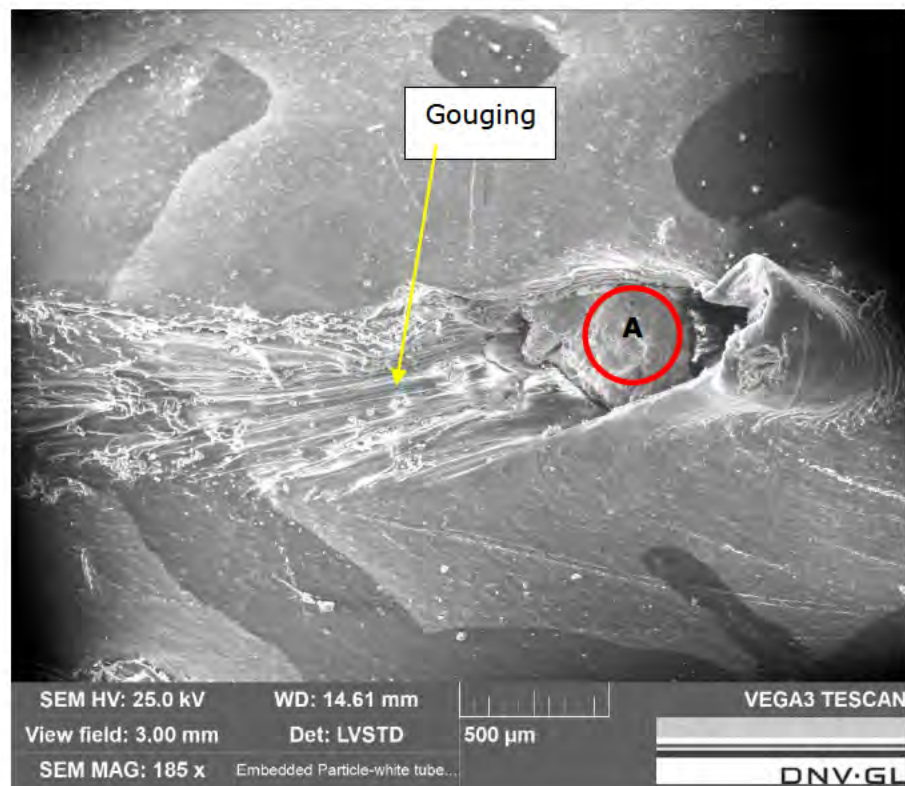


Figure 133. SEM images of the liner from the Subject Aft Hook side of the Subject Aft Cable showing the external surface; sample location is shown in Figure 131.



| Location | Oxygen (O) | Sodium (Na) | Magnesium (Mg) | Aluminum (Al) | Silicon (Si) | Sulfur (S) | Chlorine (Cl) | Potassium (K) | Calcium (Ca) | Iron (Fe) |
|----------|------------|-------------|----------------|---------------|--------------|------------|---------------|---------------|--------------|-----------|
| A | 7.3 | 38.5 | 0.5 | 0.2 | 0.3 | 0.3 | 44.8 | 0.2 | 0.3 | 7.7 |

Figure 134. SEM image and EDS Results of the embedded particle in the external surface of the liner of the Subject Aft Cable; location is shown in Figure 131.

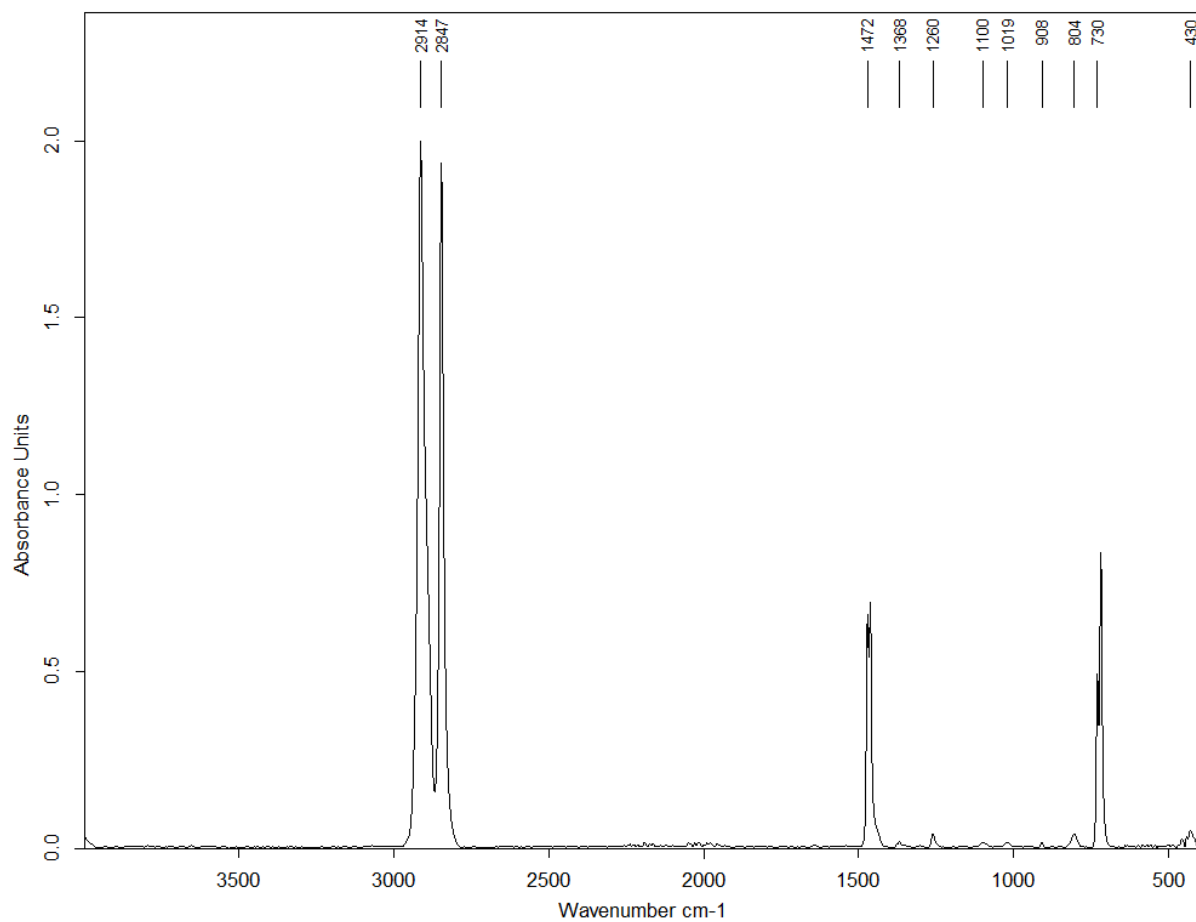


Figure 135. Fourier-transform Infrared Spectroscopy spectrum of a sample removed from the liner of the Subject Aft Cable; sample location shown in Figure 114. The wire layer was removed to gain access to the liner layer underneath.

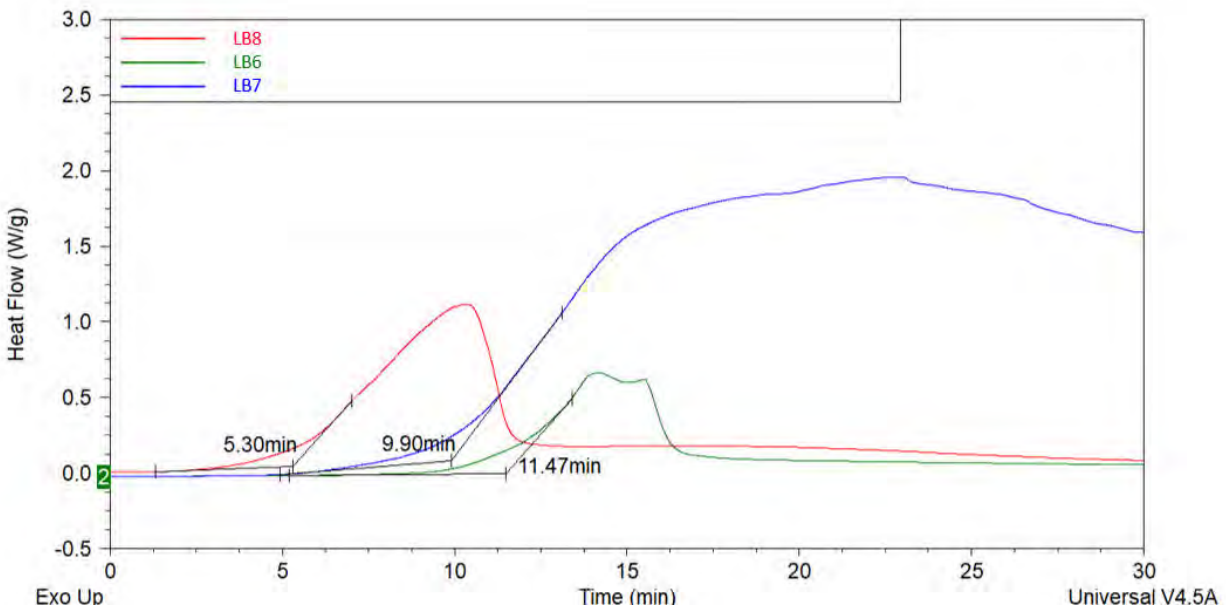


Figure 136. Results of Differential Scanning Calorimetry (DSC) analysis for Oxidative Induction Time (OIT). Samples from liners of Lifeboat 6 (LB6), Lifeboat 7 (LB7), and Lifeboat 8 (LB8) were removed from the aft control cables and tested.

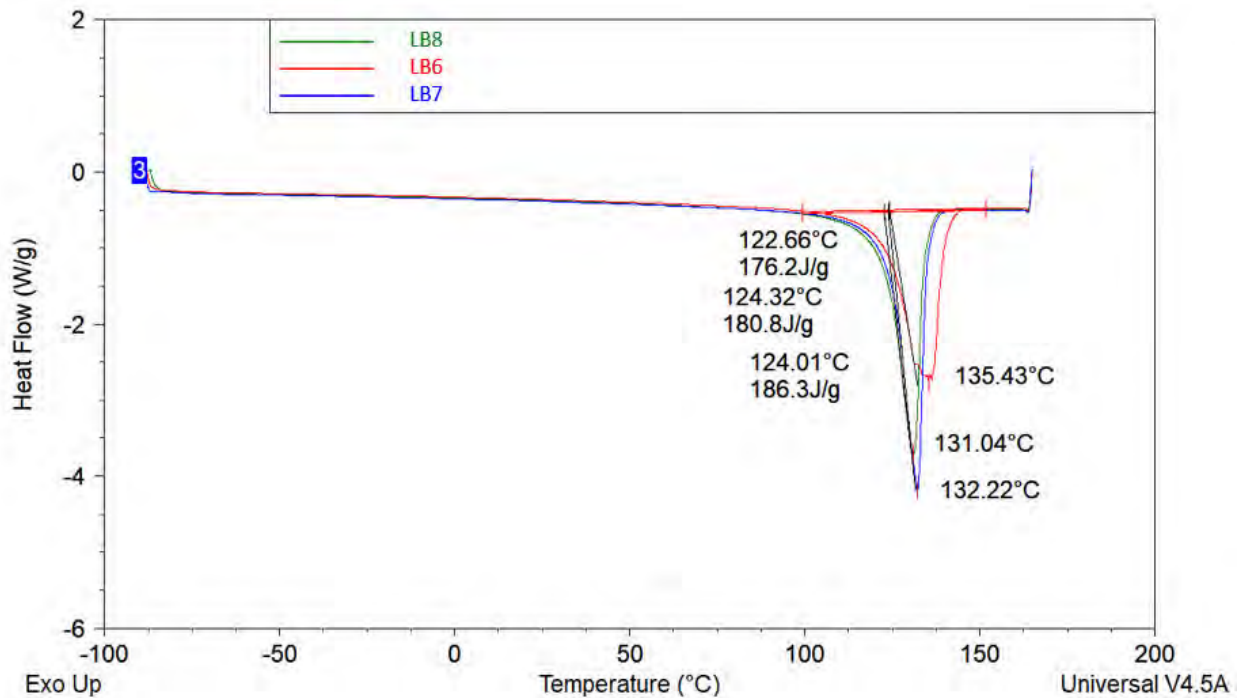


Figure 137. Results of Differential Scanning Calorimetry (DSC) analysis for Glass Transition Temperature (Tg). Samples from liners of Lifeboat 6 (LB6), Lifeboat 7 (LB7), and Lifeboat 8 (LB8) were removed from the aft control cables and tested.

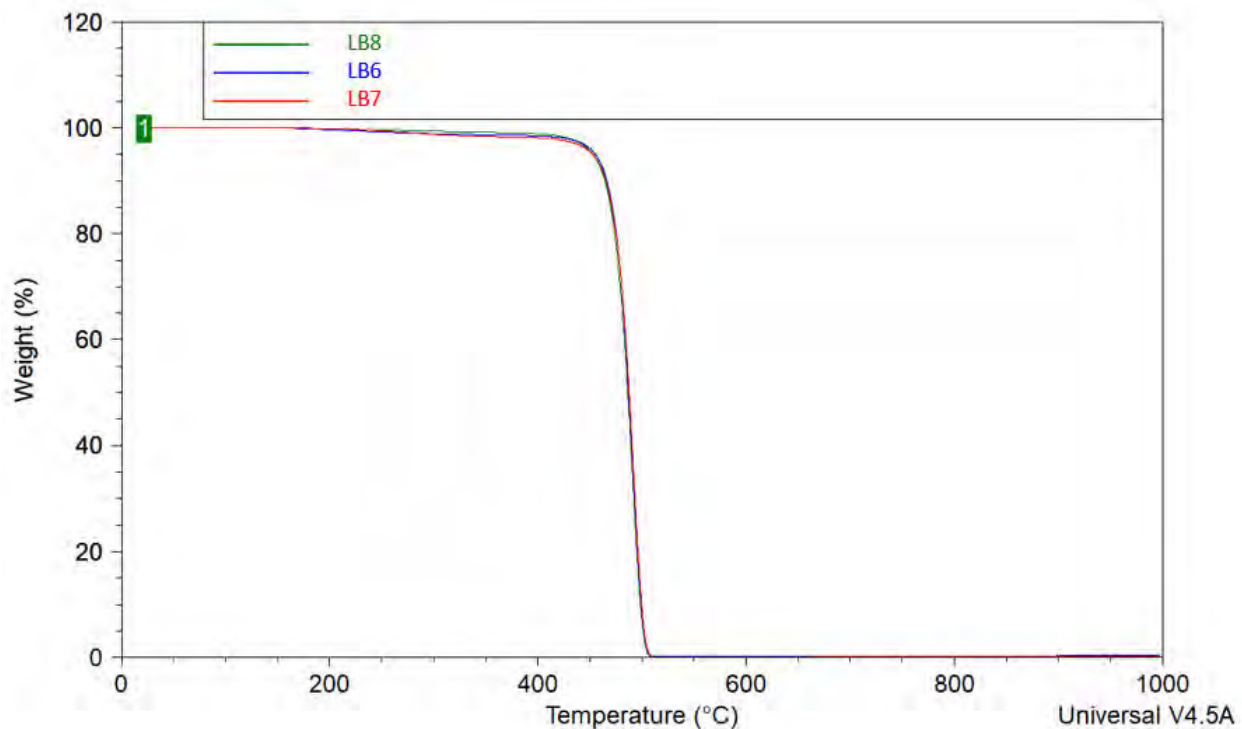


Figure 138. Schematic showing the results of the Thermogravimetric Analysis (TGA). Samples from the liners of Lifeboat 6 (LB6), Lifeboat 7 (LB7), and Lifeboat 8 (LB8) were removed from the aft control cables and tested.



| Material | Tensile Strength (psi) | Strain at Yield (%) | Break Stress (psi) | Break Strain (%) | Tensile Modulus (psi) |
|------------------------|------------------------|---------------------|--------------------|------------------|-----------------------|
| LB6 Liner – 0.2 in/min | 2,800 | 8.40 | 3,022 | 557.3 | 110,300 |
| LB7 Liner – 0.2 in/min | 2,730 | 8.62 | 3,321 | 834.5 | 87,340 |
| LB8 Liner – 0.2 in/min | 2,490 | 8.60 | 3,101 | 527.8 | 92,500 |
| LB6 Liner – 2 in/min | 3,212 | 7.12 | 2,839 | 330.8 | 136,600 |
| LB7 Liner – 2 in/min | 3,196 | 7.23 | 4,313 | 594.4 | 124,300 |
| LB8 Liner – 2 in/min | 2,870 | 6.60 | 3,141 | 437.2 | 118,900. |
| LB6 Liner – 20 in/min | 3,637 | 6.74 | 2,018 | 27.13 | 98,930 |
| LB7 Liner – 20 in/min | 3,665 | 6.13 | 1,912 | 25.08 | 123,300 |
| LB8 Liner – 20 in/min | 3,400 | 6.05 | 1,875 | 37.73 | 114,800 |

Figure 139. Photograph showing the geometry of tensile specimens extracted from the liners of the aft control cables from of Lifeboat 6 (LB6), Lifeboat 7 (LB7), and Lifeboat 8 (LB8) and a summary table of results of testing. The tests were performed at strain rates of 0.2 in/min, 2 in/min, and 20 in/min.

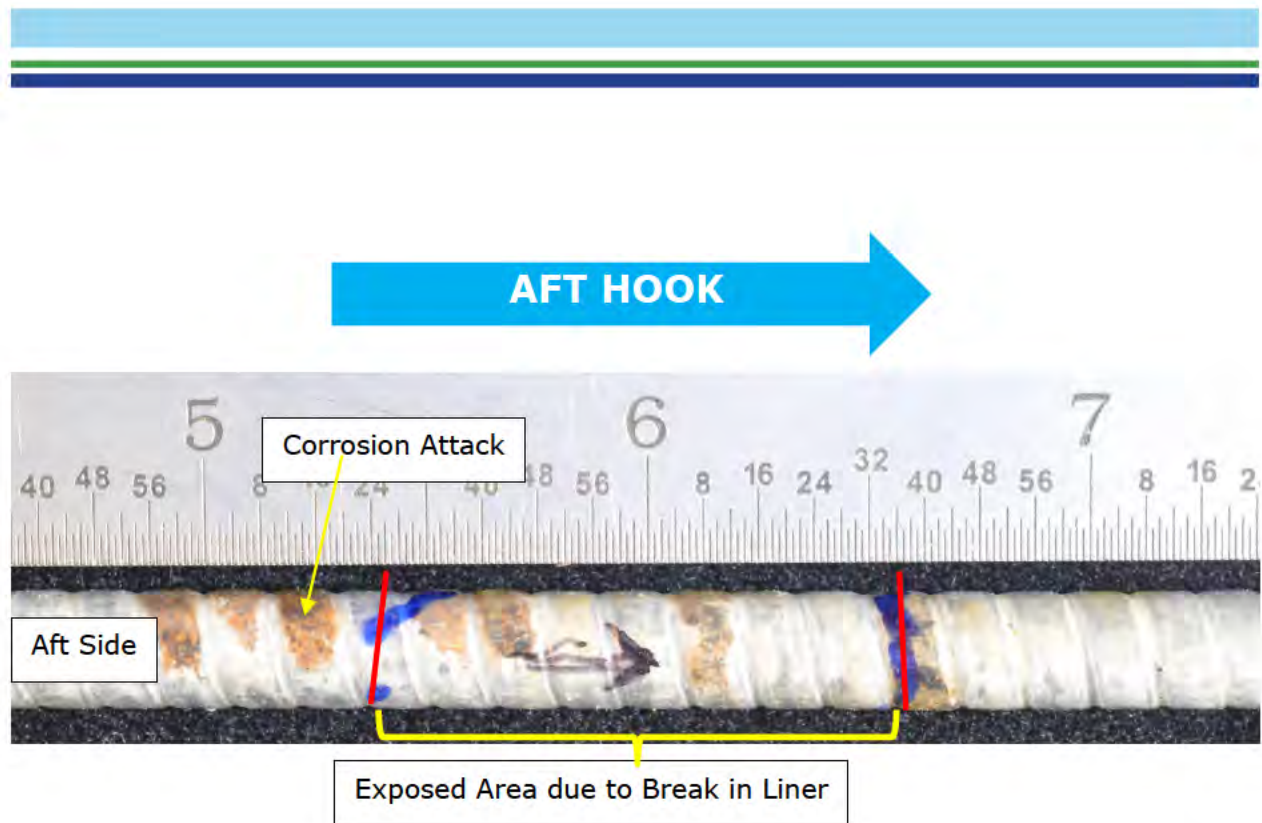
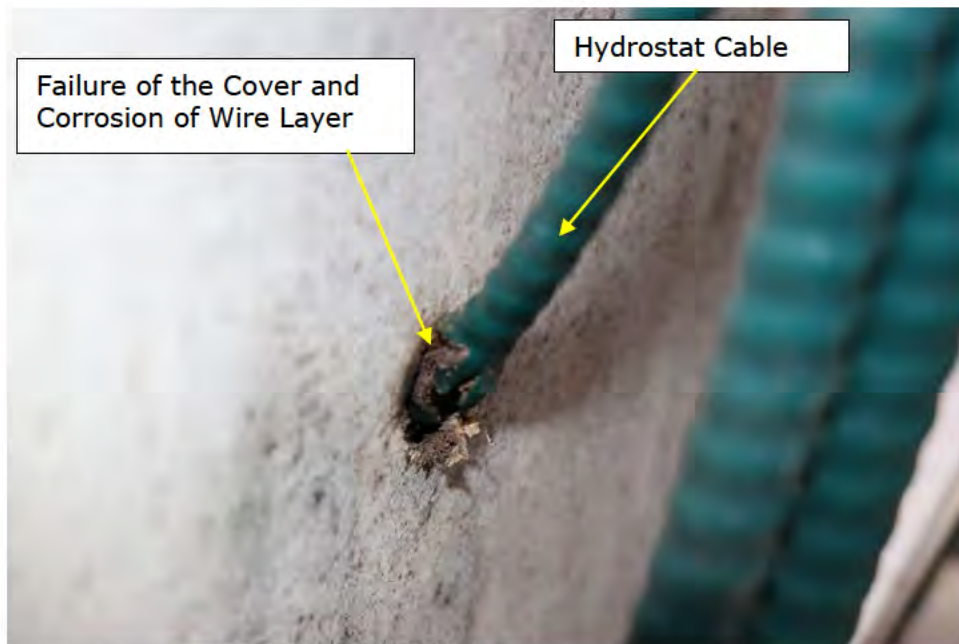


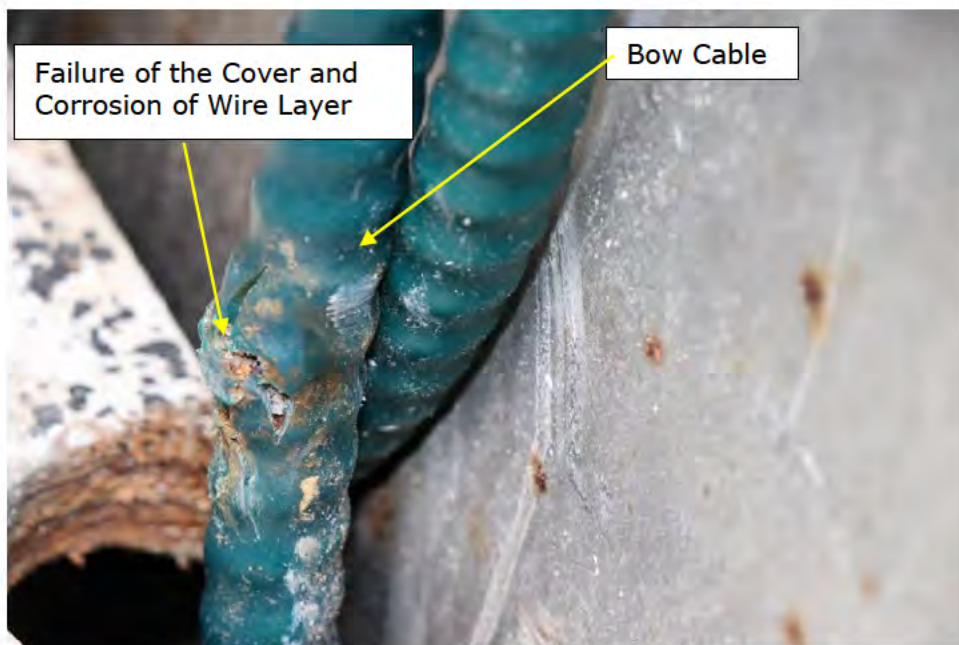
Figure 140. Photograph of the inner member from the Subject Aft Cable after dissection showing the aft side; samples shown in Figure 108. Aft refers to the orientation of the keeper relative to the lifeboat. The direction of the Subject Aft Hook is noted with the blue arrow. Ruler is in inches.



Figure 141. Light micrographs of the inner member of the Subject Aft Cable showing the detail of the minor corrosion attack to the binder wire and damage to the sheath layer of the inner member. The direction of the Subject Aft Hook is noted with the blue arrow.



(a)



(b)

Figure 142. Photographs of the (a) hydrostat cable from Lifeboat 7 and (b) the forward control cable from Lifeboat 8 showing evidence of degradation. Photographs were provided by SOI.

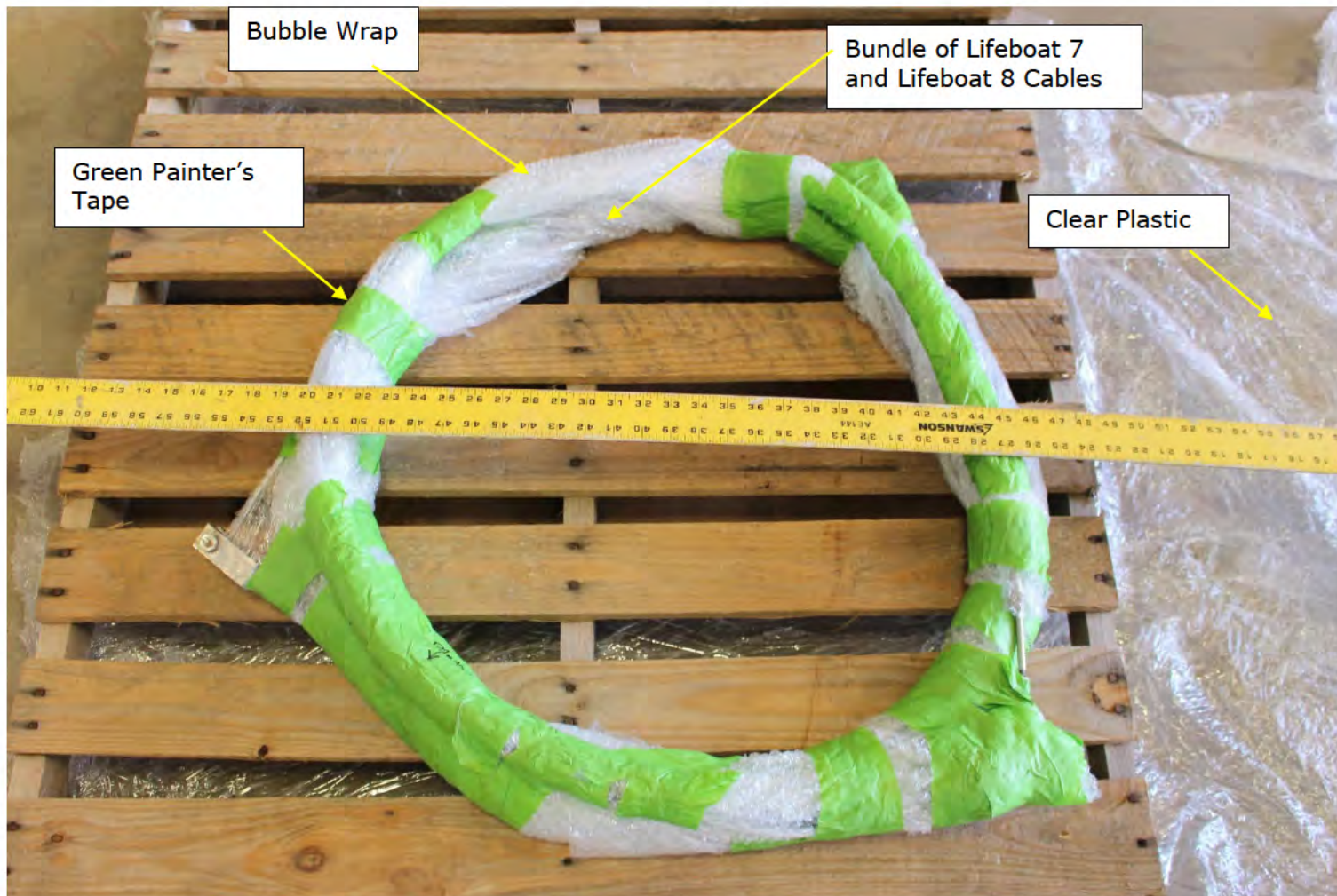


Figure 143. Photograph of the hydrostat cable from Lifeboat 7 and the forward control cable from Lifeboat 8, at DNV GL, after partially removing the wrappings from shipment. Ruler is in inches.

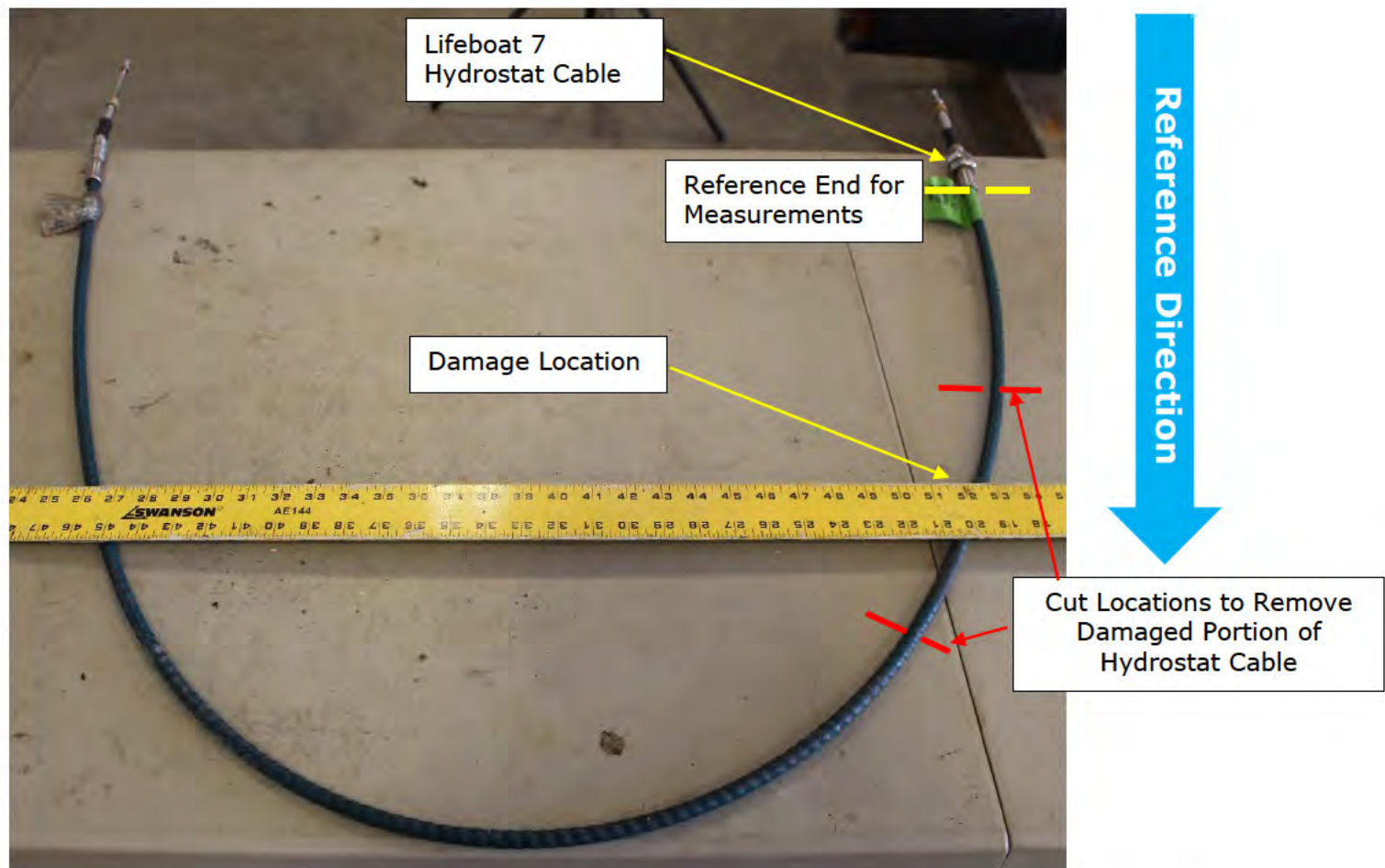


Figure 144. Photograph of the hydrostat cable from Lifeboat 7 after removing the wrappings. Ruler is in inches.

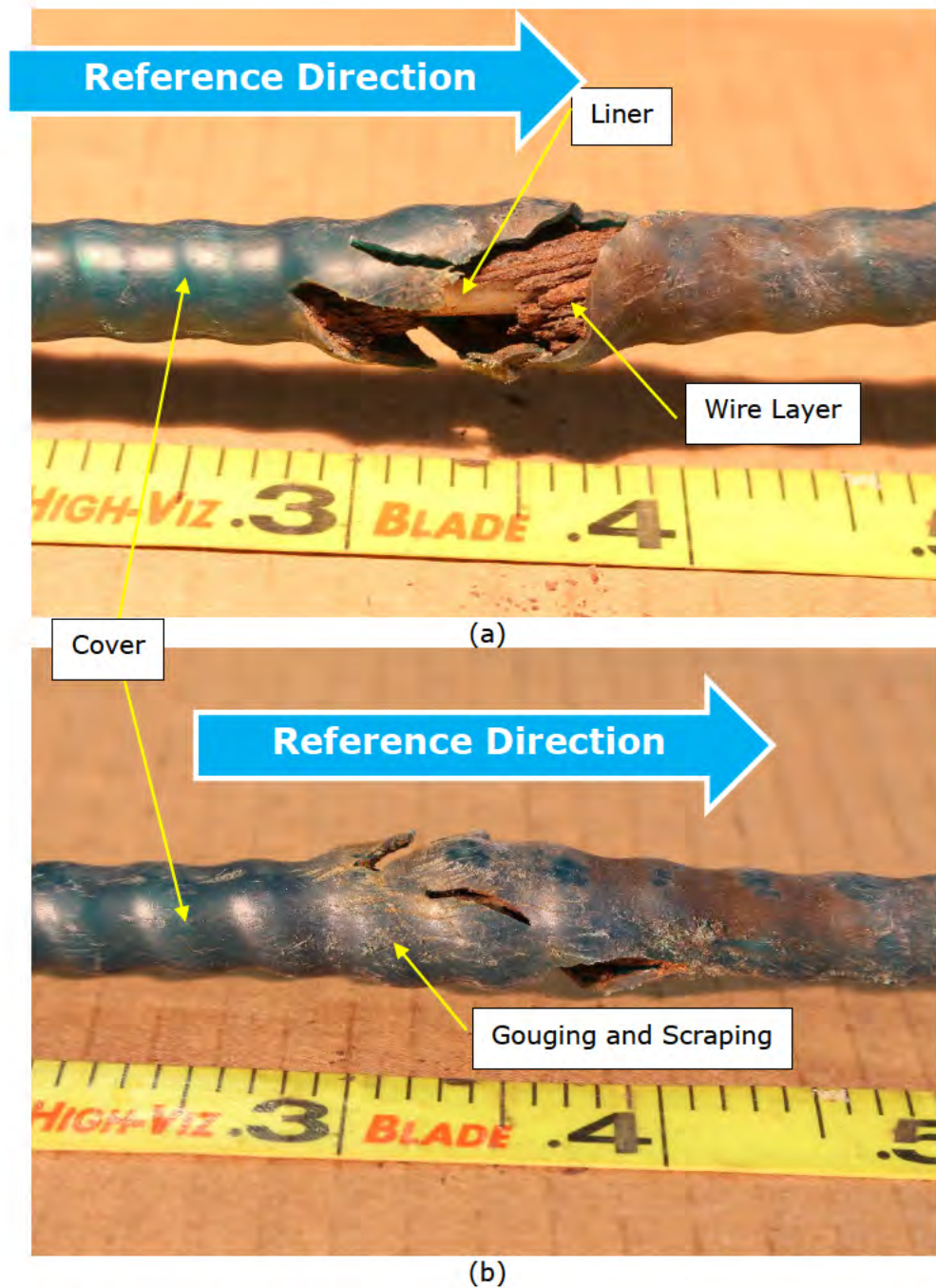


Figure 145. Photographs of the hydrostat cable from Lifeboat 7 showing damage at (a) the assumed top orientation and (b) the assumed bottom orientation. Measuring tape is in feet.

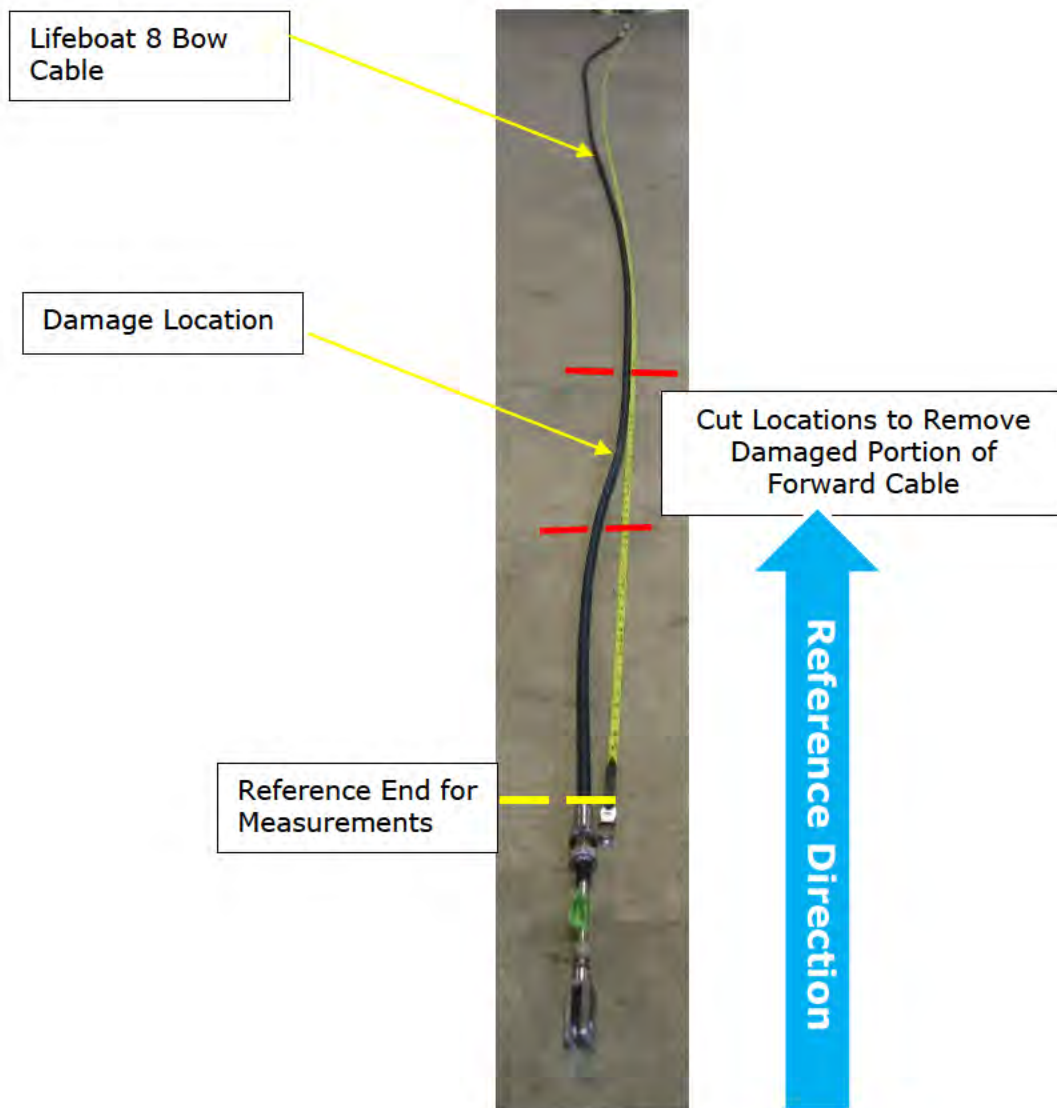


Figure 146. Photograph of the forward control cable from Lifeboat 8 after removing the wrappings. Measuring tape is in feet.

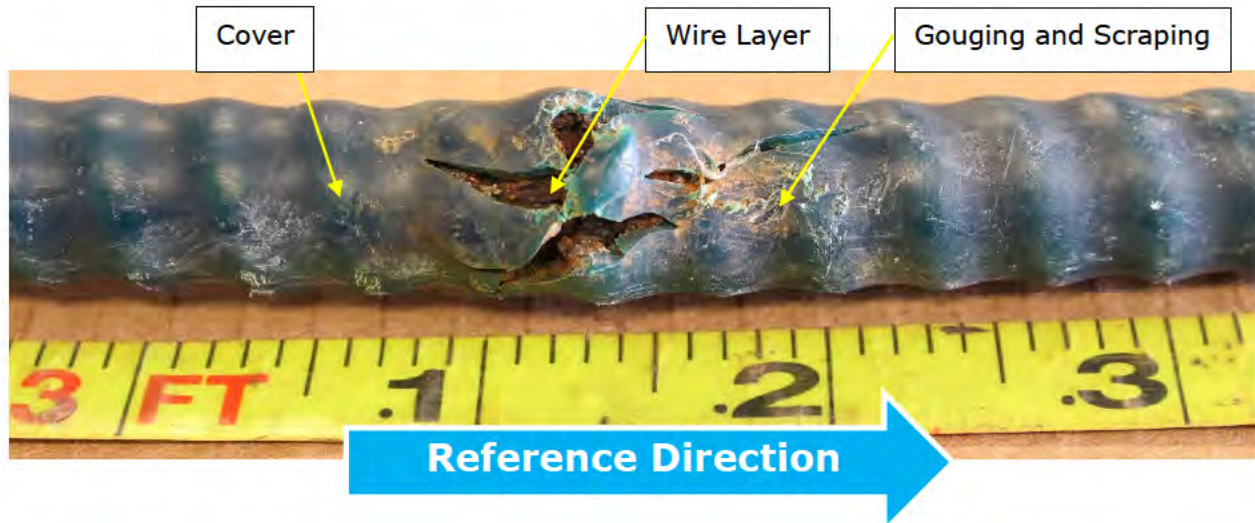


Figure 147. Photograph of the forward control cable from Lifeboat 8 showing damage at the assumed top orientation. Measuring tape is in feet.

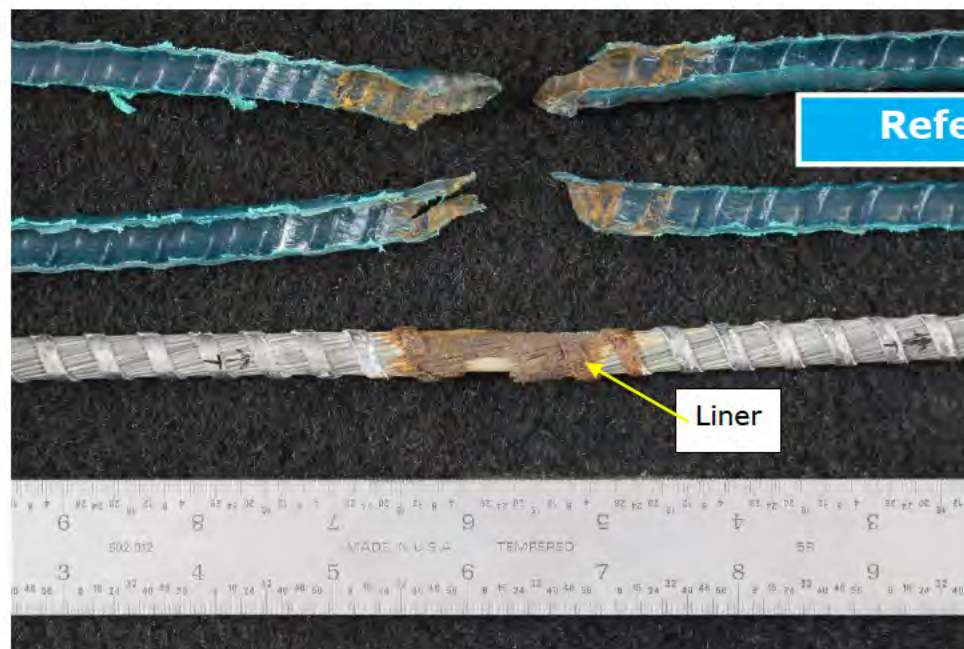
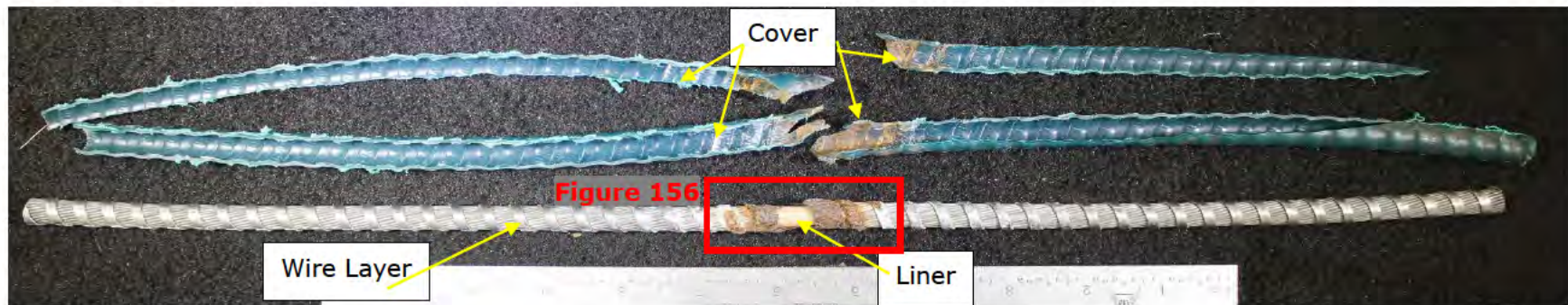


Figure 148. Photograph of the Lifeboat 7 hydrostat cable after dissection near the damaged location. Ruler is in inches.

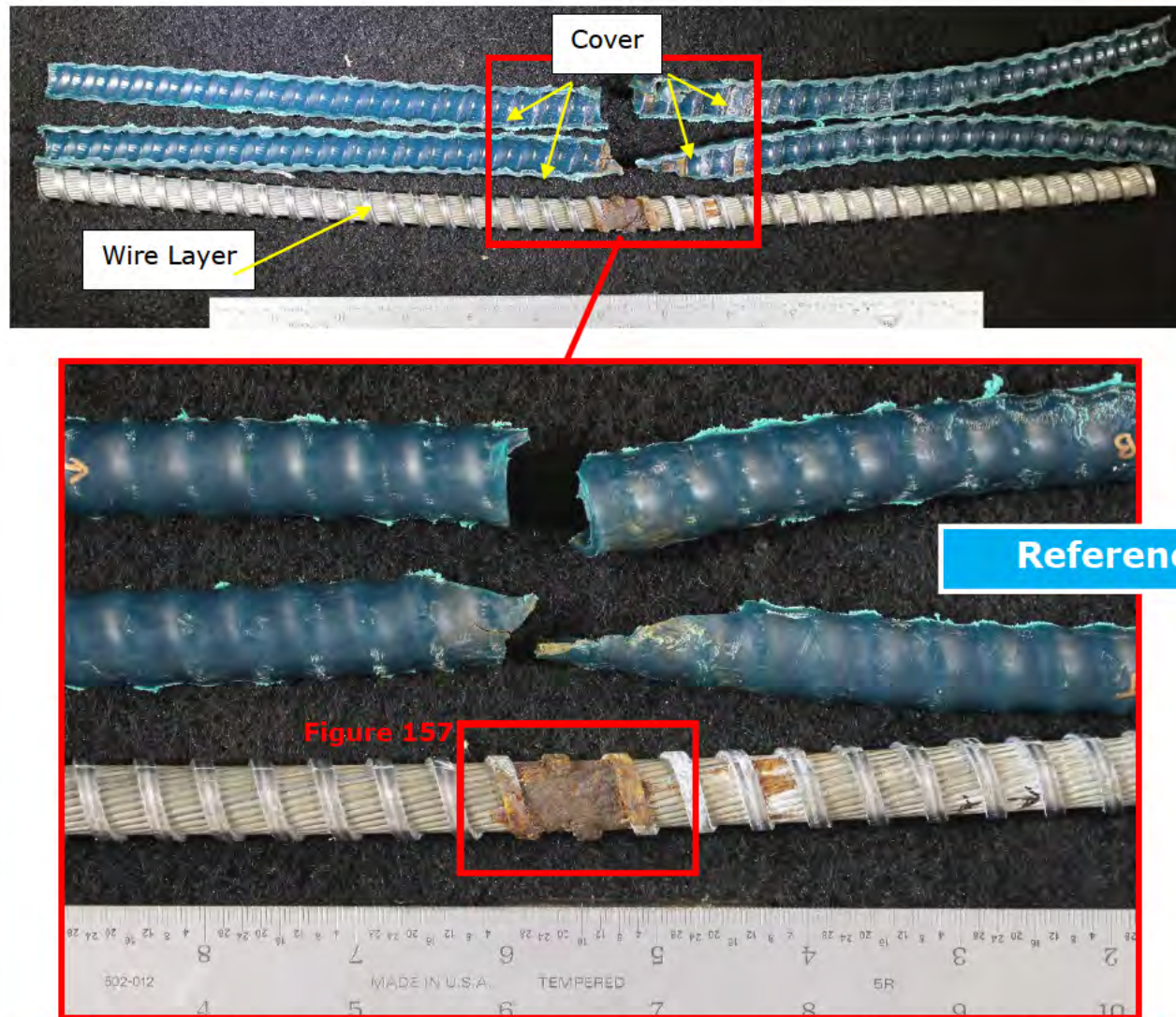


Figure 149. Photograph of the Lifeboat 8 forward control cable after dissection near the damaged location. Rulers are in inches.

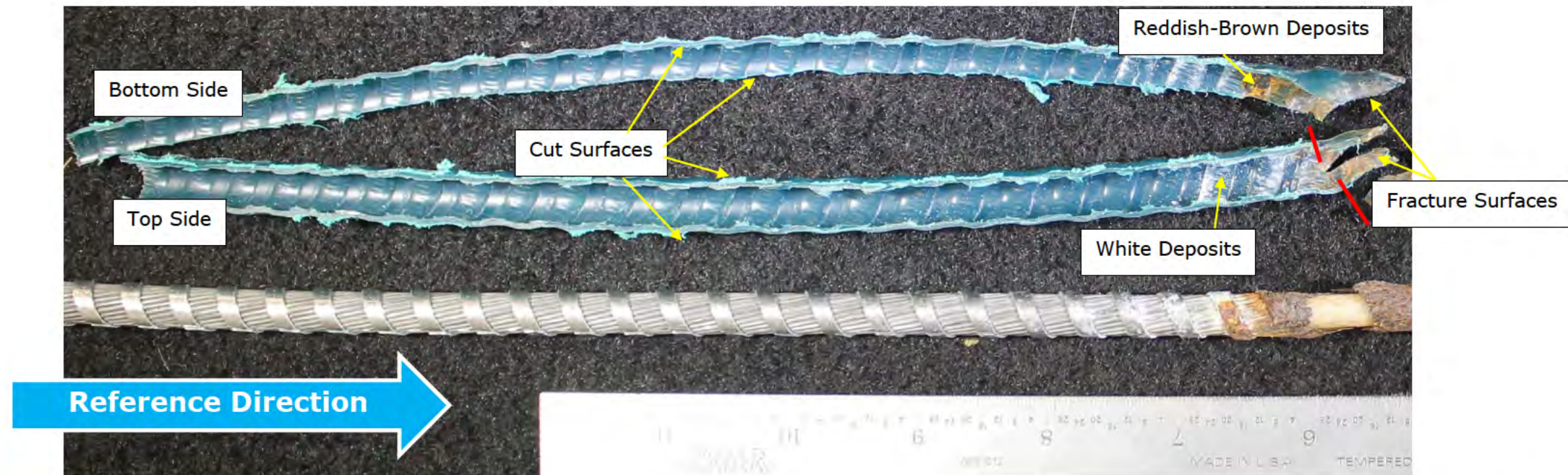


Figure 150. Photographs of the half the cover from the Lifeboat 7 hydrostat cable after dissection showing the internal surface near the damaged location; samples shown in Figure 148. The reference direction is noted with the blue arrow. Rulers are in inches.

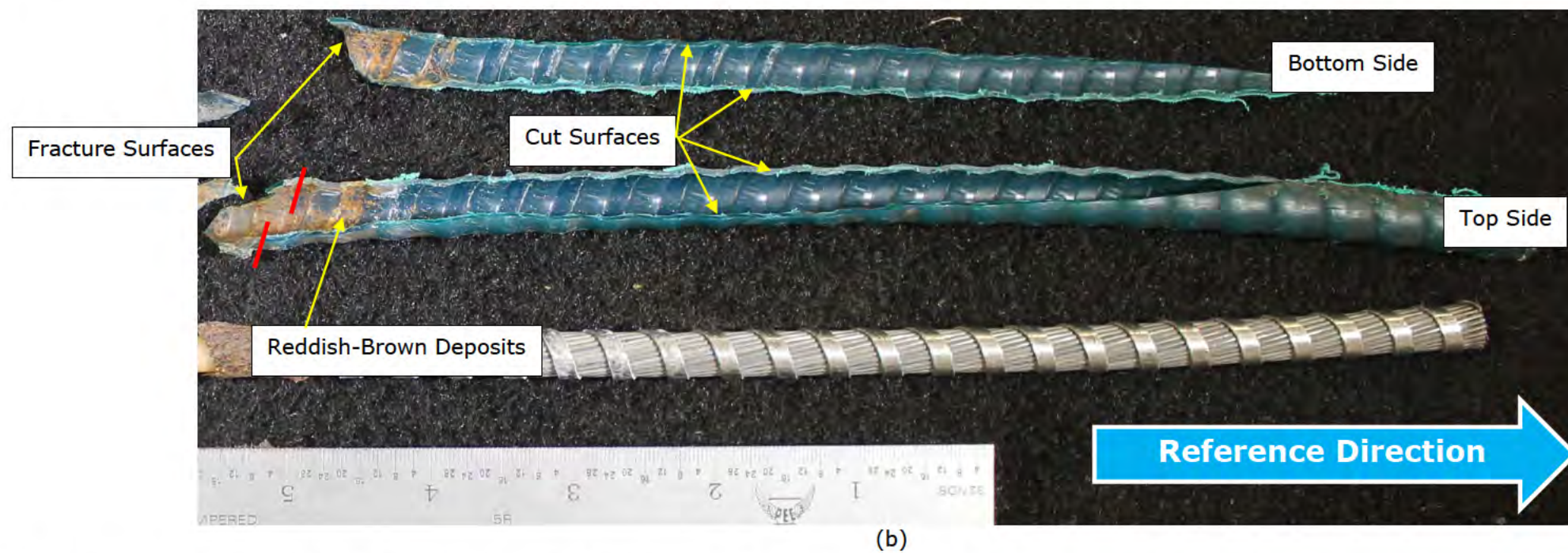


Figure 151. Photographs of the cover from the Lifeboat 7 hydrostat cable after dissection showing the internal surface near the damaged location; samples shown in Figure 148. The reference direction is noted with the blue arrow. Rulers are in inches.

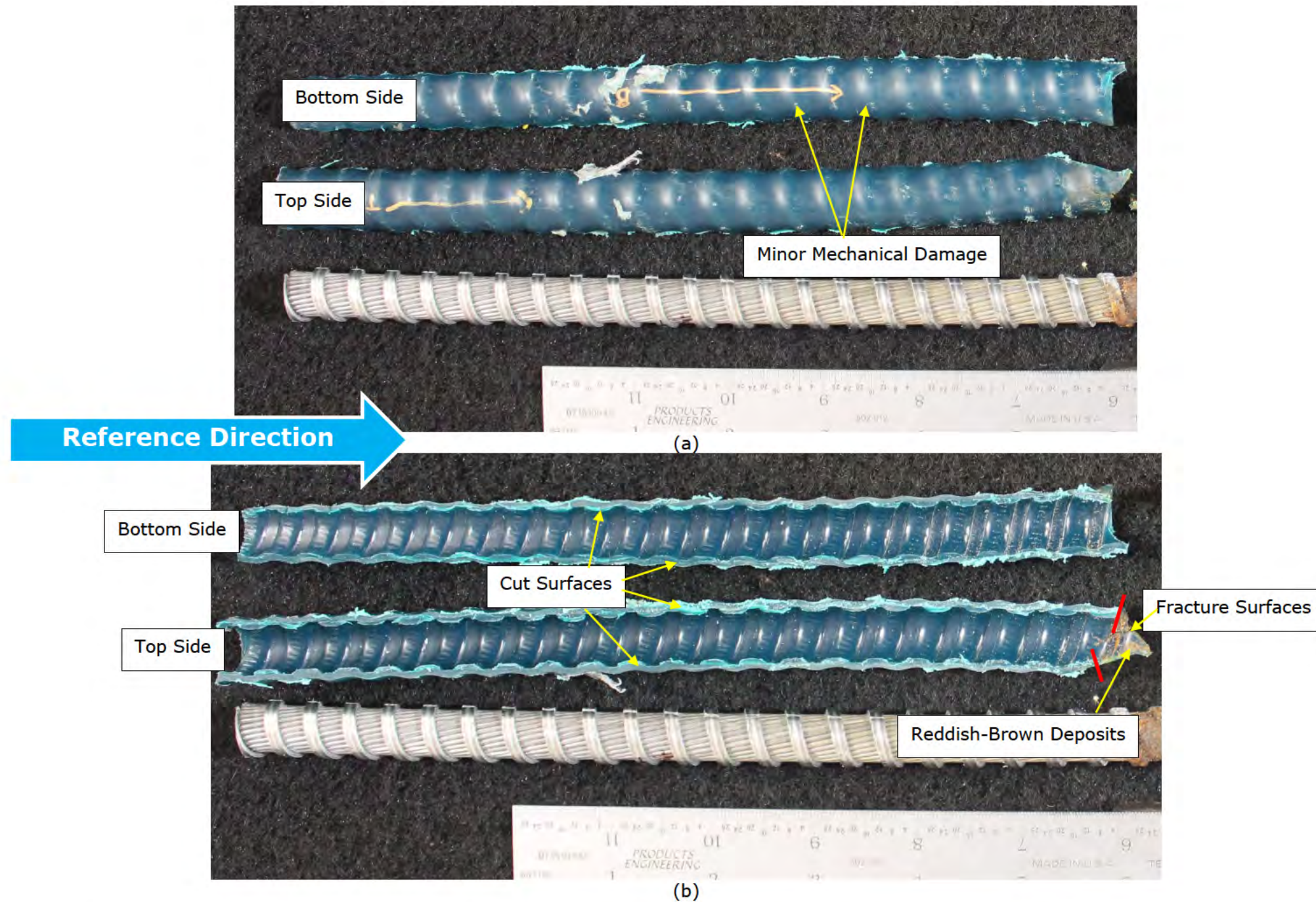


Figure 152. Photographs of the cover from the Lifeboat 8 forward control cable after dissection showing the (a) external surface and (b) internal surface near the damaged location; samples shown in Figure 149 (top). The reference direction is noted with the blue arrow. Rulers are in inches.

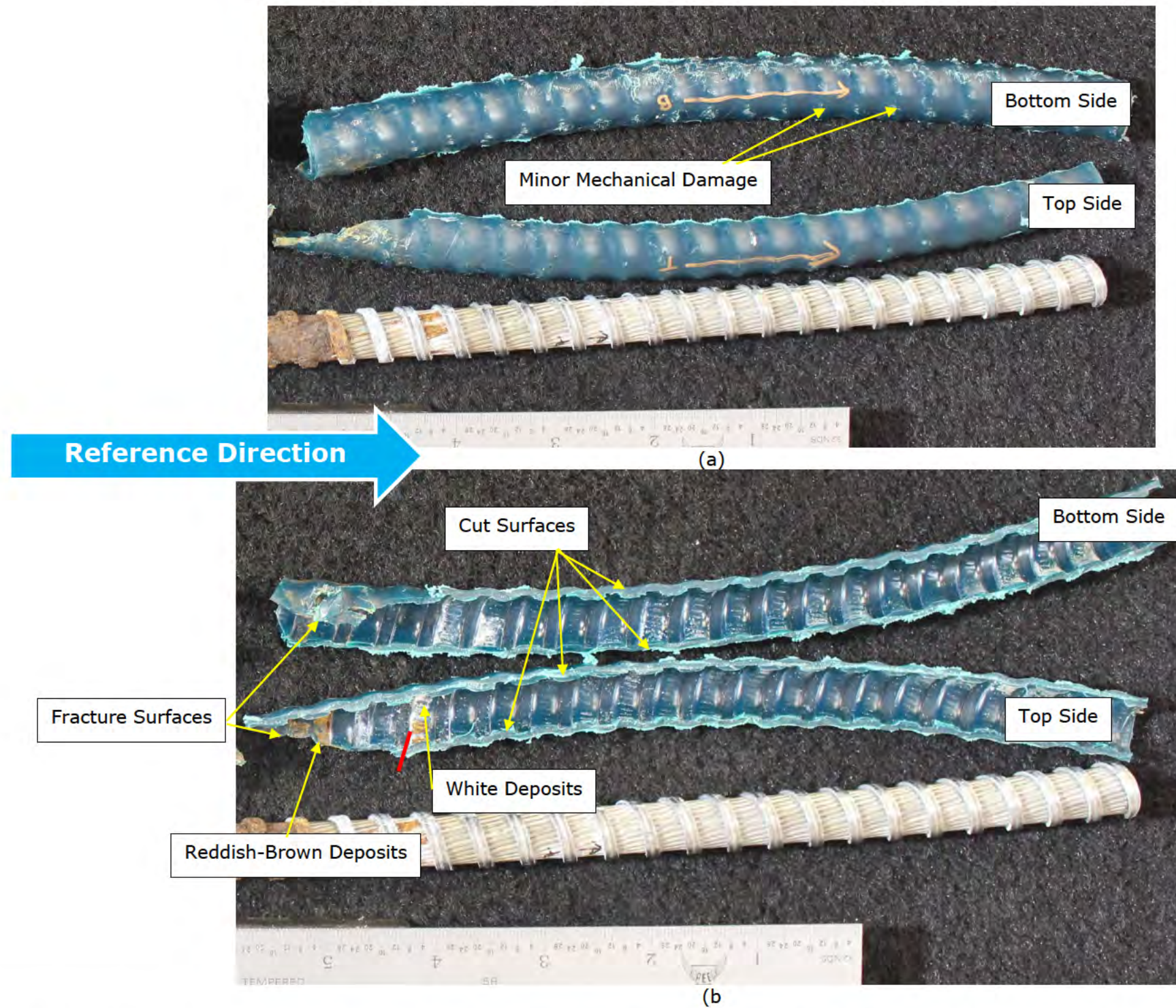


Figure 153. Photographs of the cover from the Lifeboat 8 forward control cable after dissection showing the (a) external surface and (b) internal surface near the damaged location; samples shown in Figure 149 (top). The reference direction is noted with the blue arrow. Rulers are in inches.

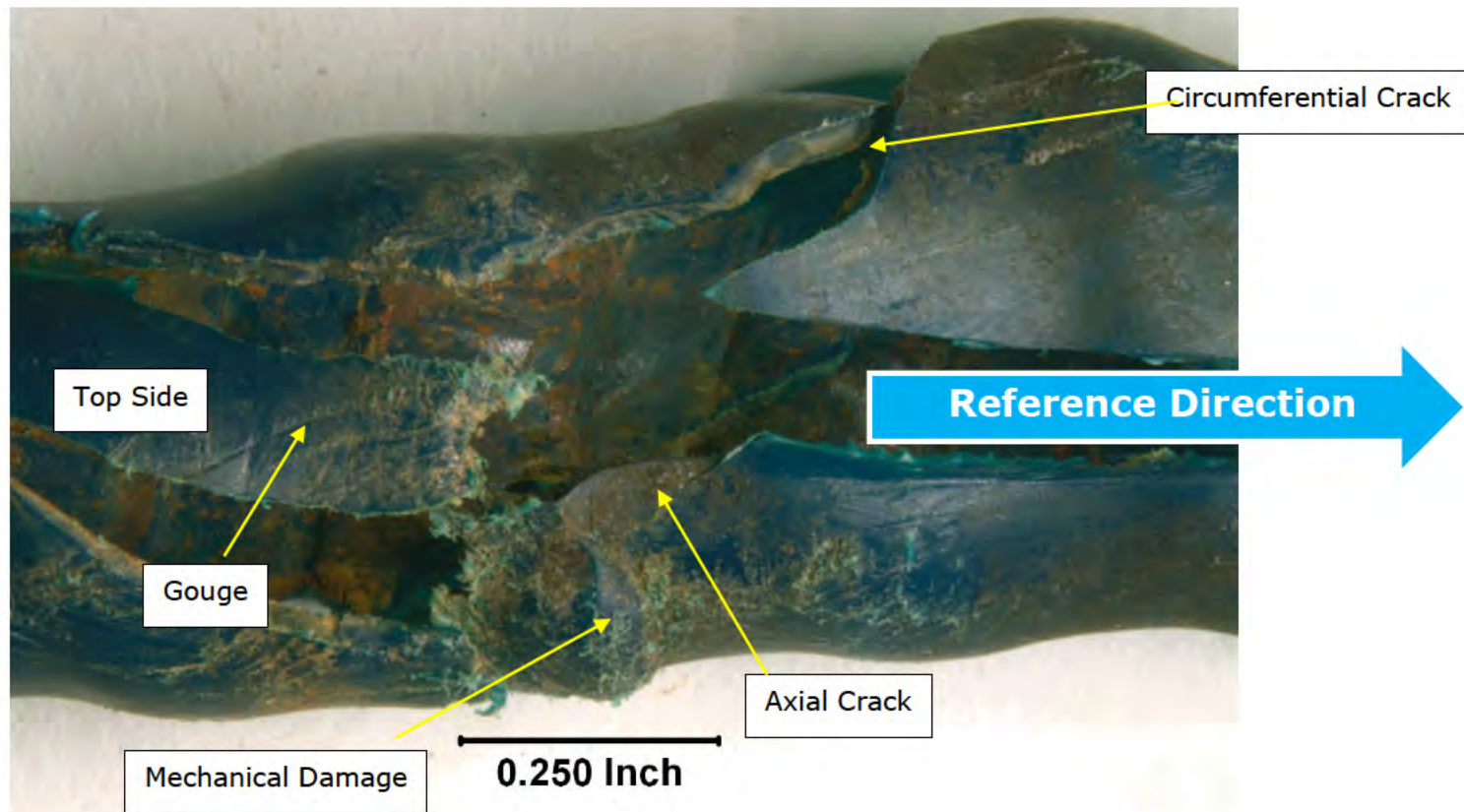


Figure 154. Light photomicrographs of the cover from the Lifeboat 7 hydrostat cable after matching the fractures surfaces. The reference direction is noted with the blue arrow.

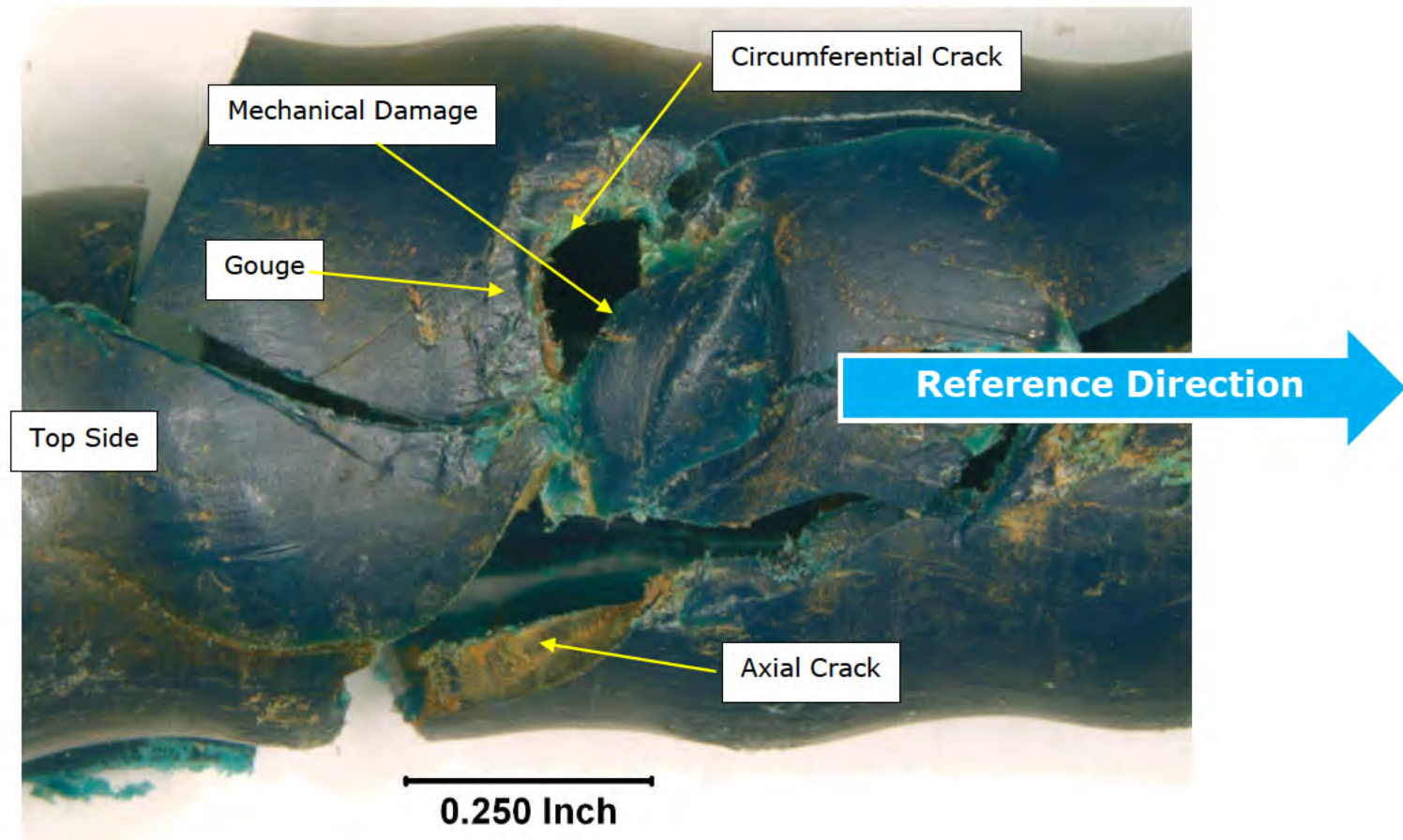


Figure 155. Light photomicrographs of the cover from the Lifeboat 8 forward control cable after matching the fractures surfaces. The reference direction is noted with the blue arrow.



Reference Direction

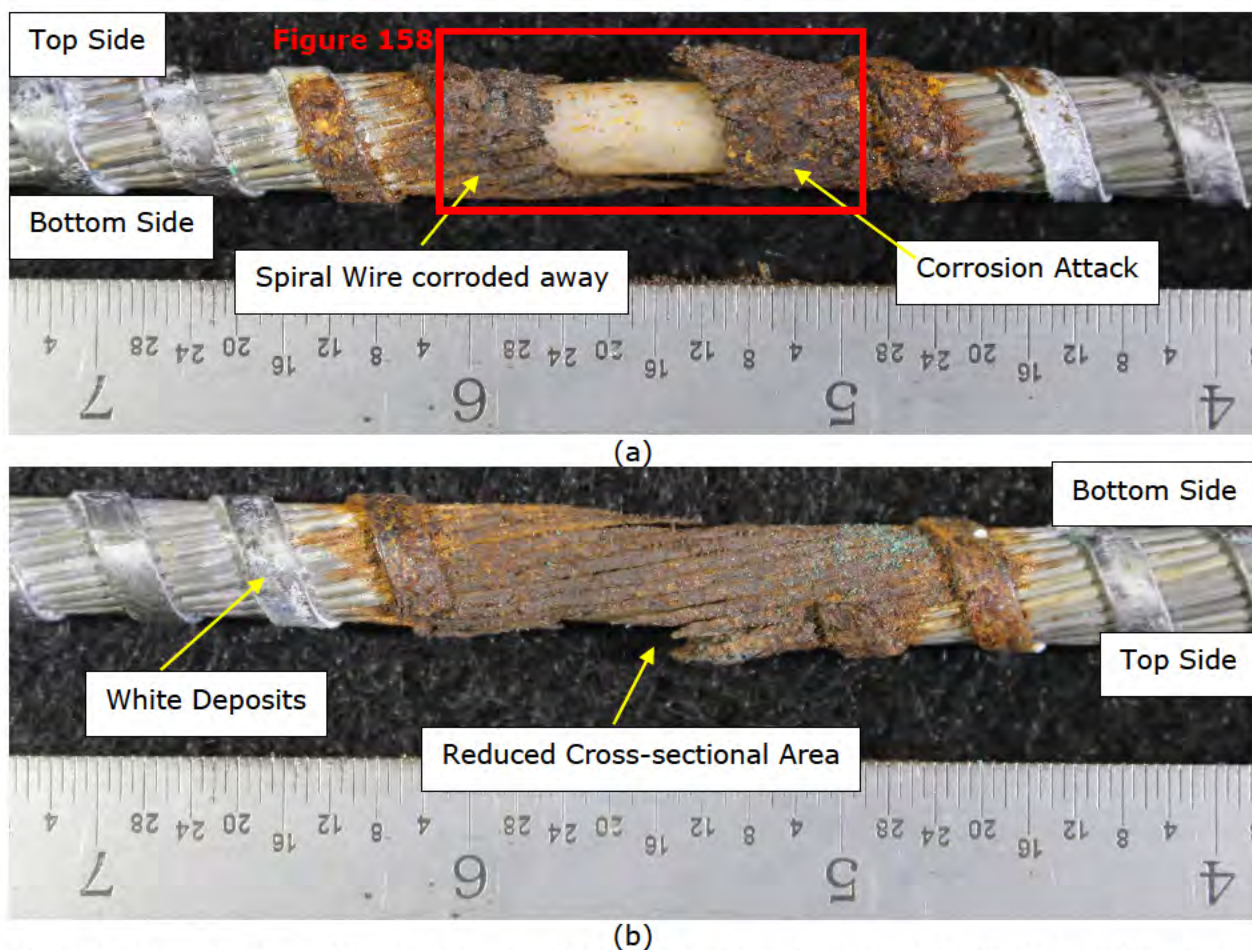


Figure 156. Photographs of the wire layer from the Lifeboat 7 hydrostat cable at the damaged location showing the (a) side exposing the liner and (b) the side with some wires intact; sample location shown in Figure 148 (top). The reference direction is noted with the blue arrow. Rulers are in inches.

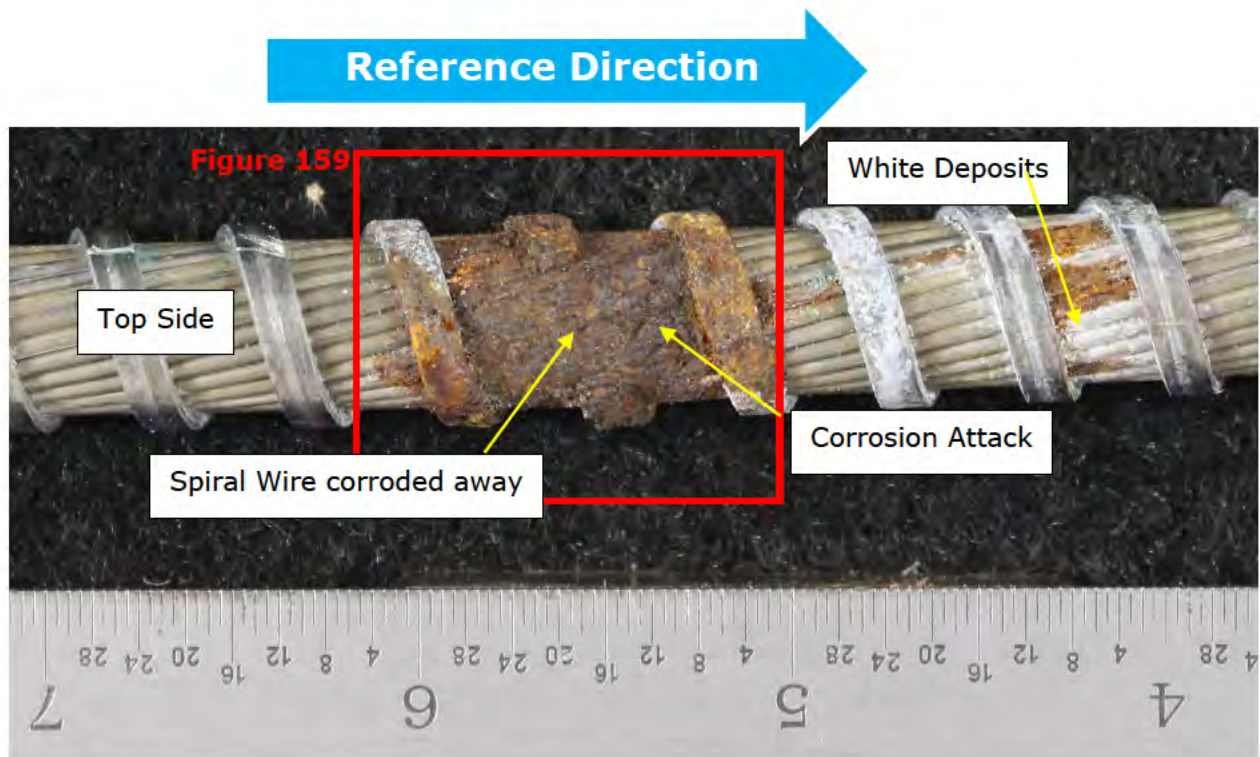


Figure 157. Photograph of the wire layer from the Lifeboat 8 forward control cable at the damaged location showing the corrosion attack to the wire layer; sample location shown in Figure 149. The reference direction is noted with the blue arrow. Ruler is in inches.

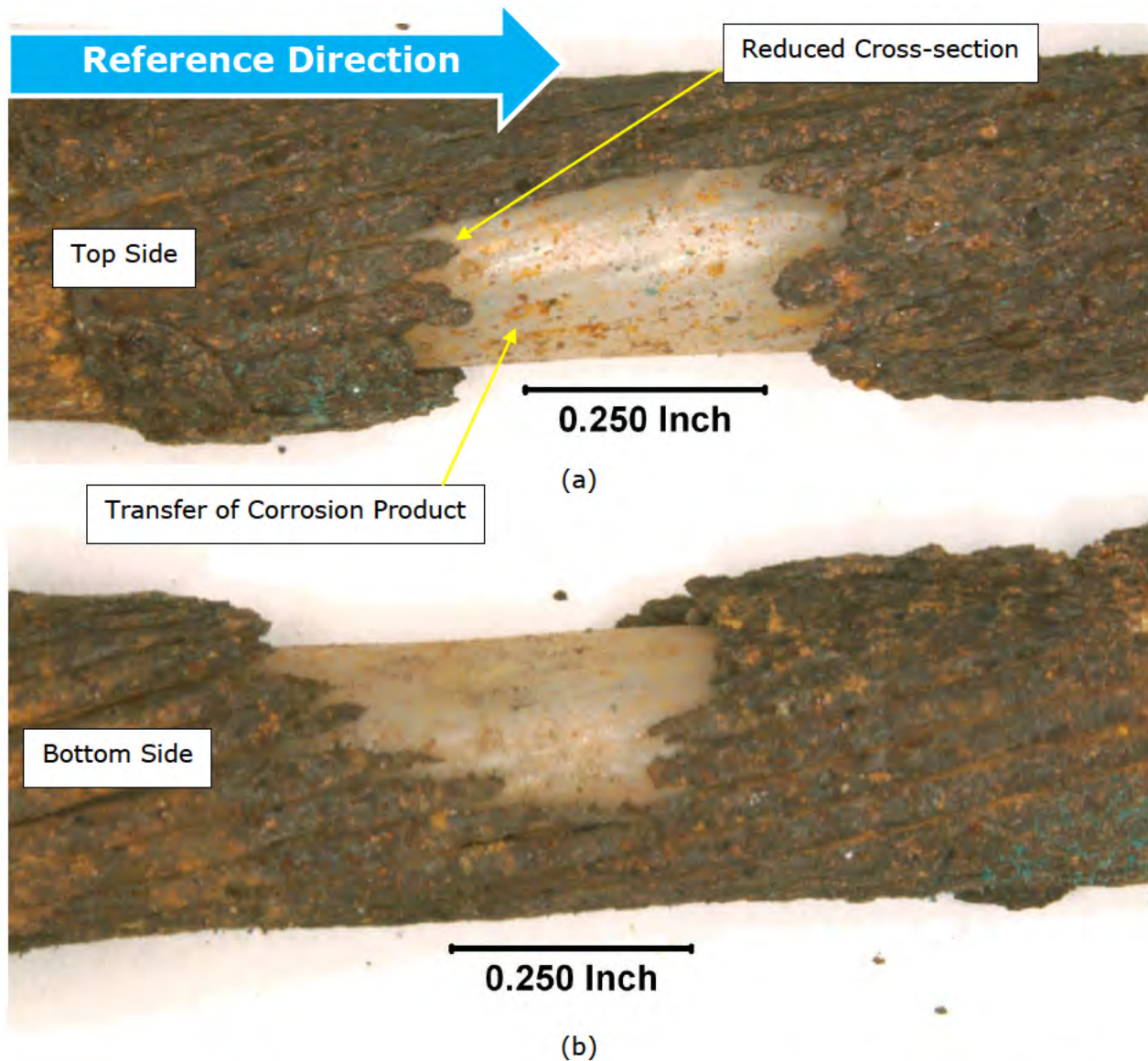
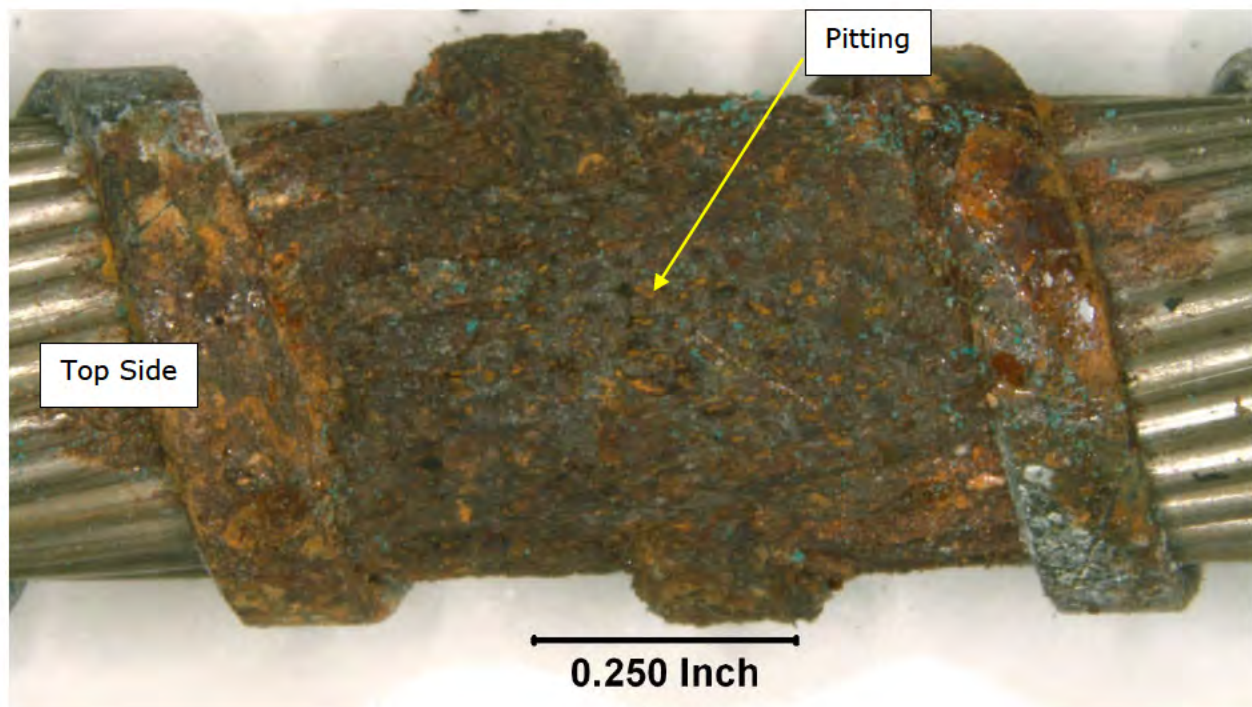
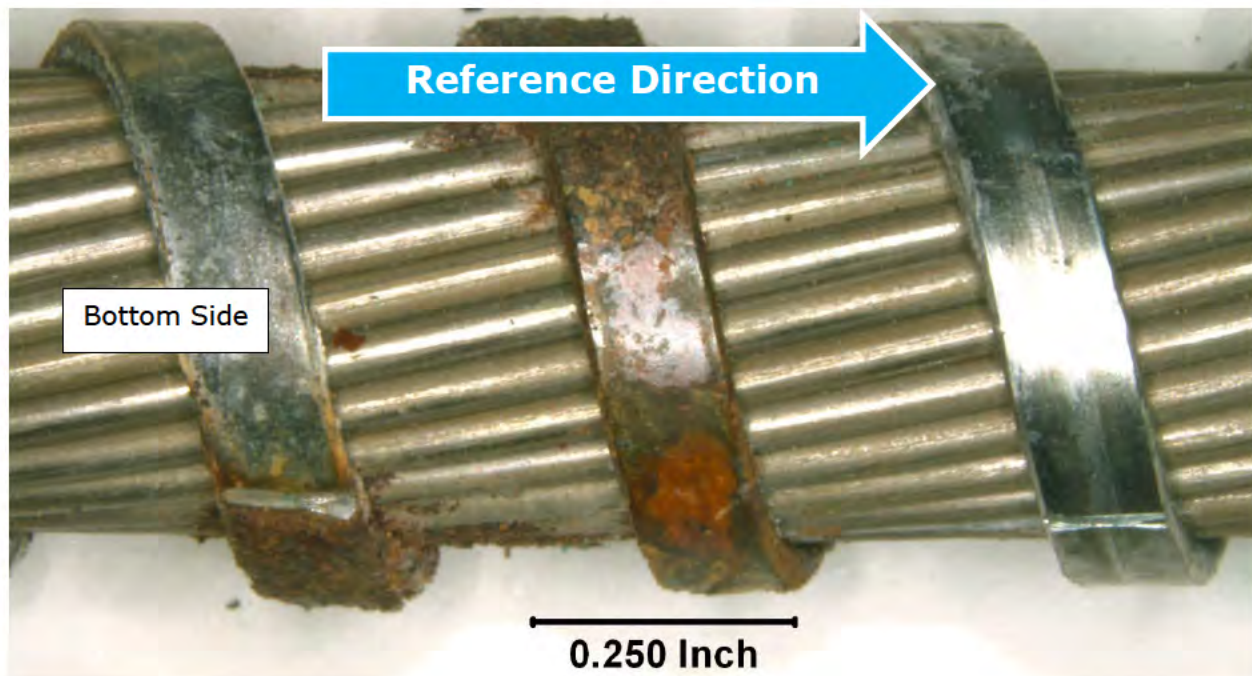


Figure 158. Light photomicrographs showing the (a) top and (b) bottom of the wire layer from the Lifeboat 7 hydrostat cable showing the corrosion damage; location shown in Figure 156. The reference direction is noted with the blue arrow.



(a)



(b)

Figure 159. Light photomicrographs showing the (a) top and (b) bottom of the wire layer from the Lifeboat 8 forward control cable showing the corrosion damage; location shown in Figure 157. The reference direction is noted with the blue arrow.

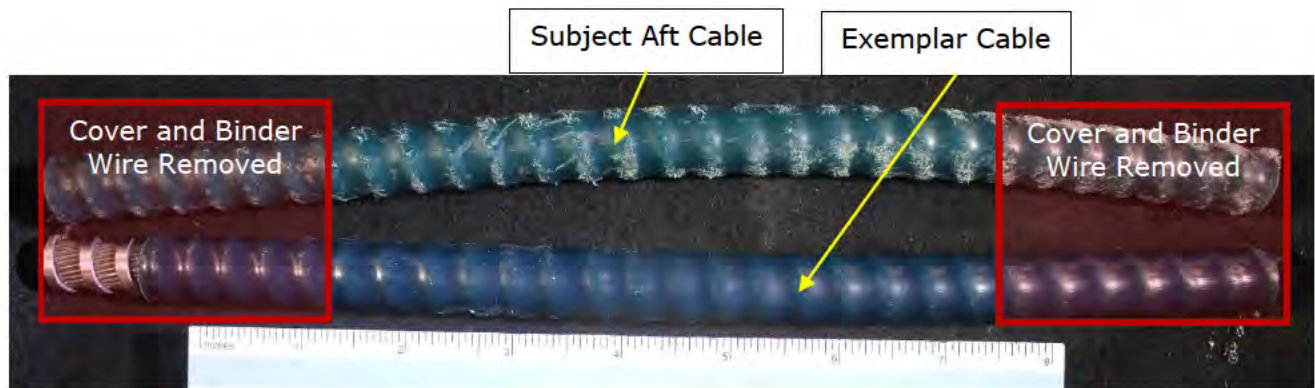
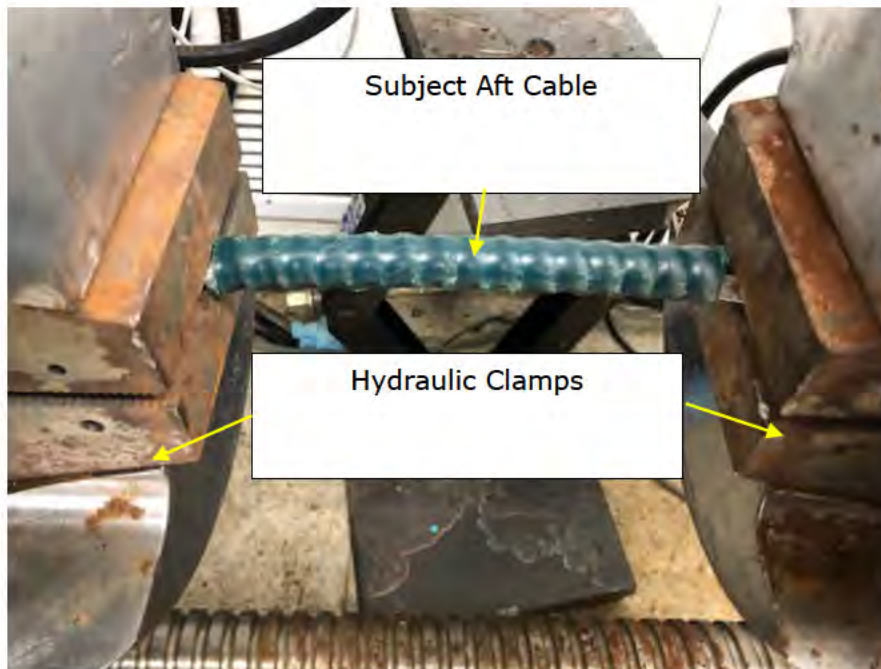
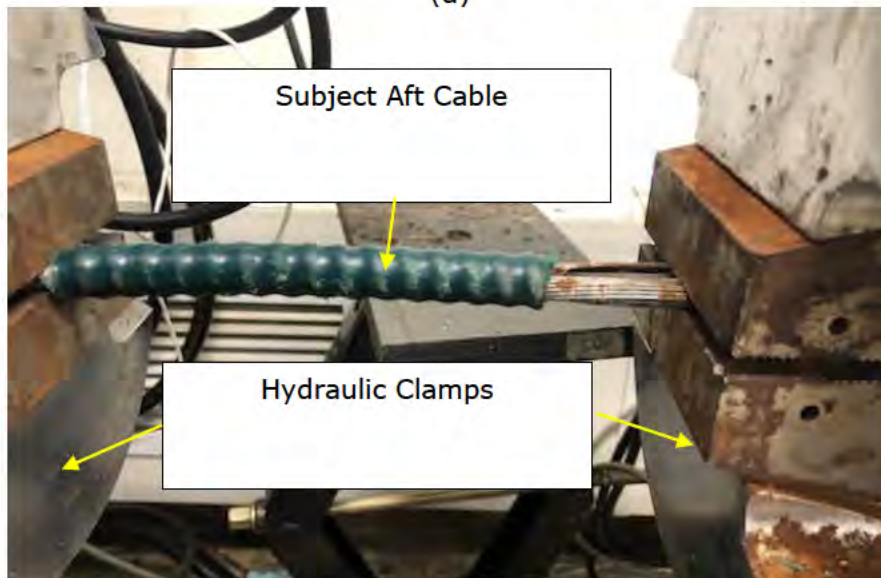


Figure 160. Photograph showing the 12-inch lengths of Subject Aft Cable and Exemplar Cable used for mechanical testing. The cover and binder wire were removed from the locations shown. Ruler is in inches.



(a)



(b)

| Sample Identification | Maximum Load (lbs) | Maximum Extension (inches) |
|-----------------------|--------------------|----------------------------|
| Subject Aft Cable | 2175 | 1.10 * |
| Exemplar Cable | 6622 | 2.65 ** |

*: Measured using measuring tape.

***: Displacement measured in test rig.

Figure 161. Photographs showing the Subject Aft Cable in the hydraulic clamps (a) before and (b) after mechanical testing as well as a table summarizing the results of the mechanical testing of the Subject Aft Cable and Exemplar Cable.

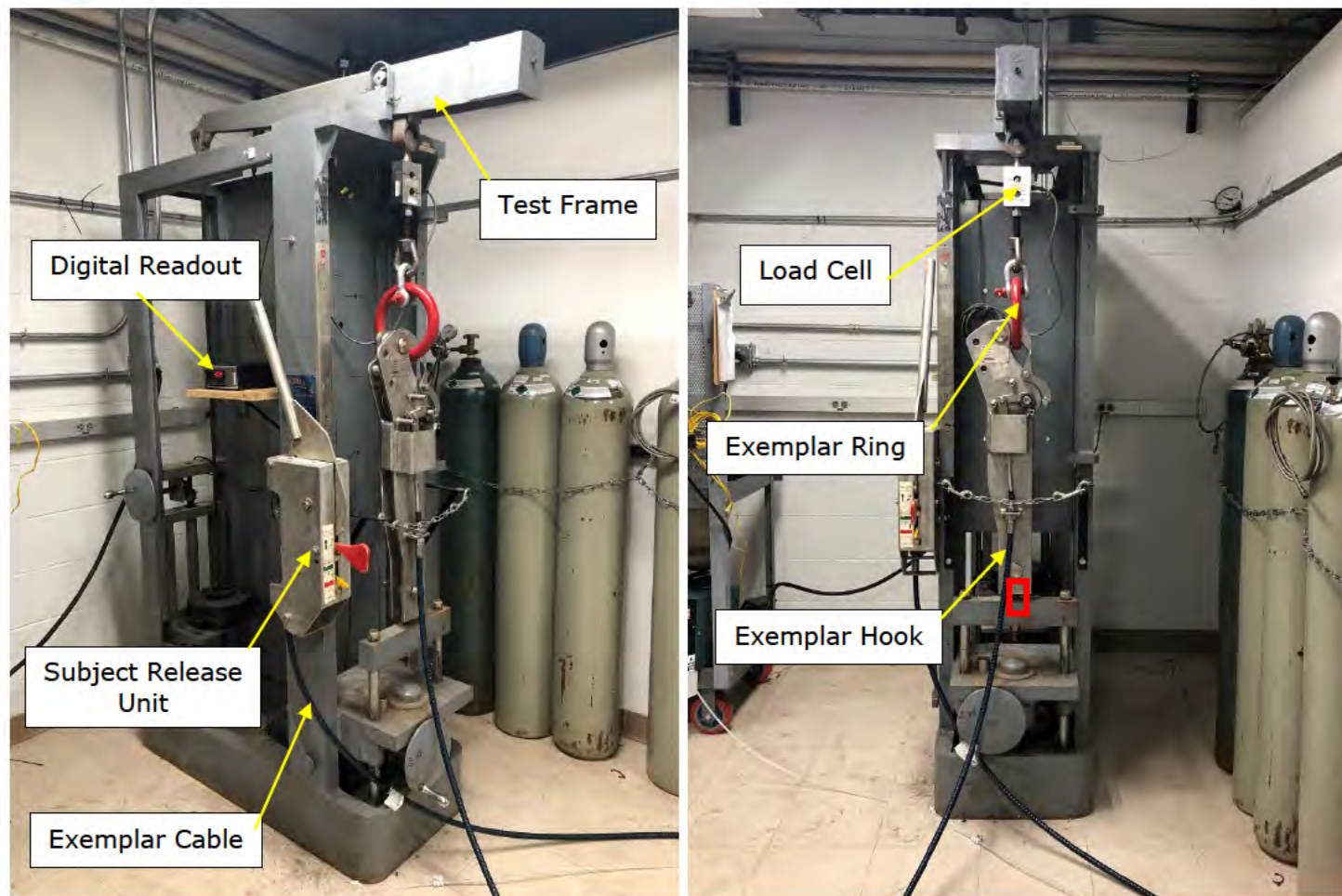


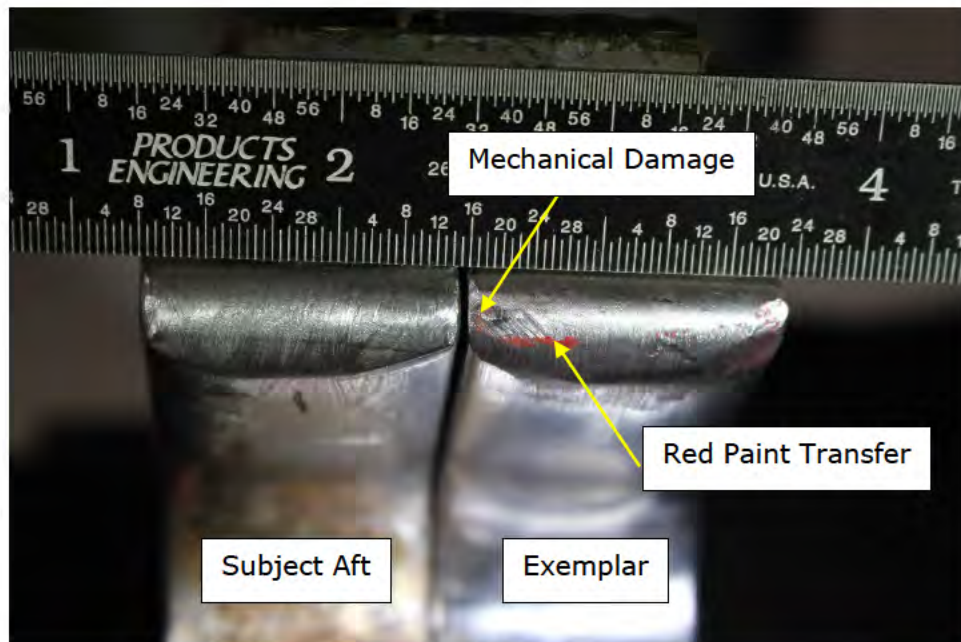
Figure 162. Photographs showing the test rig for the load testing with the Exemplar Cable, Exemplar Hook, Exemplar Ring, and Subject Release Unit.



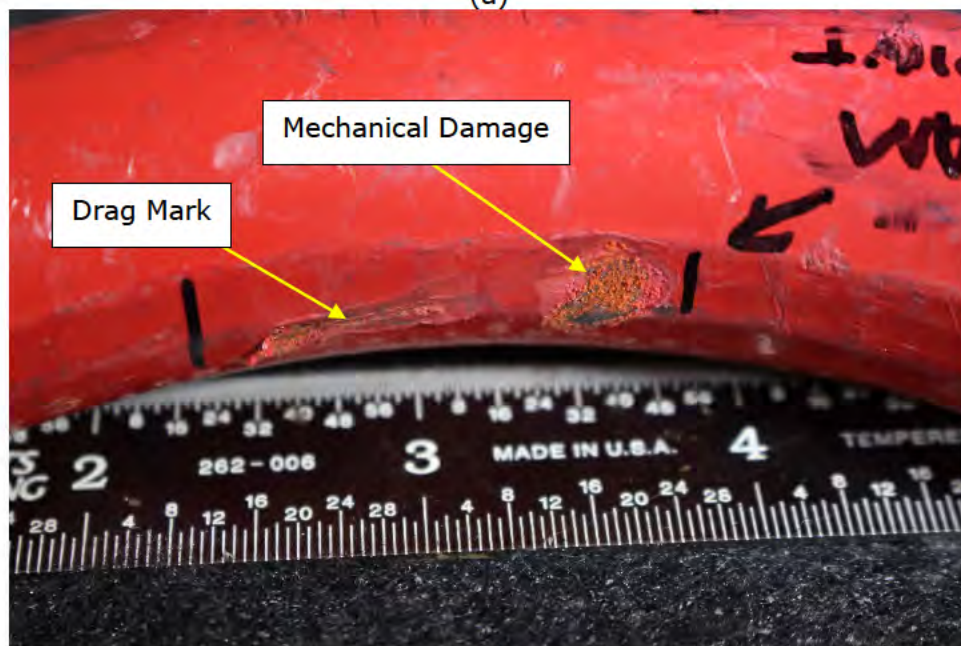
| Scenario | Maximum Load Measured (lbs) |
|----------|-----------------------------|
| 1 | 4391 * |
| 2 | 4391 * |
| 3 | 3400 |

*Maximum load applied.

Figure 163. Photographs showing (a) Scenario 1, (b) Scenario 2, and (c) Scenario 3 of the ring resting on the point of the Exemplar Hook and a table summarizing the results of the load testing. In Scenario 1 and 2, the ring did not move, but in Scenario 3 the ring slipped off the hook point.

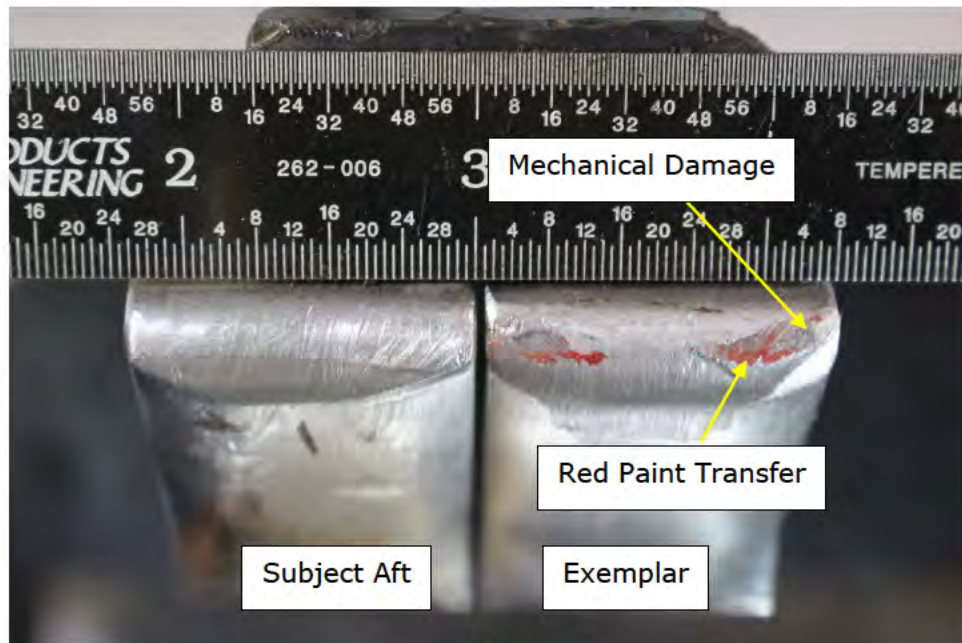


(a)



(b)

Figure 164. Photographs showing (a) the point of the Exemplar Hook compared to the Subject Aft Hook and (b) the mechanical damage to the ring after testing Scenario 1. Rulers are in inches.

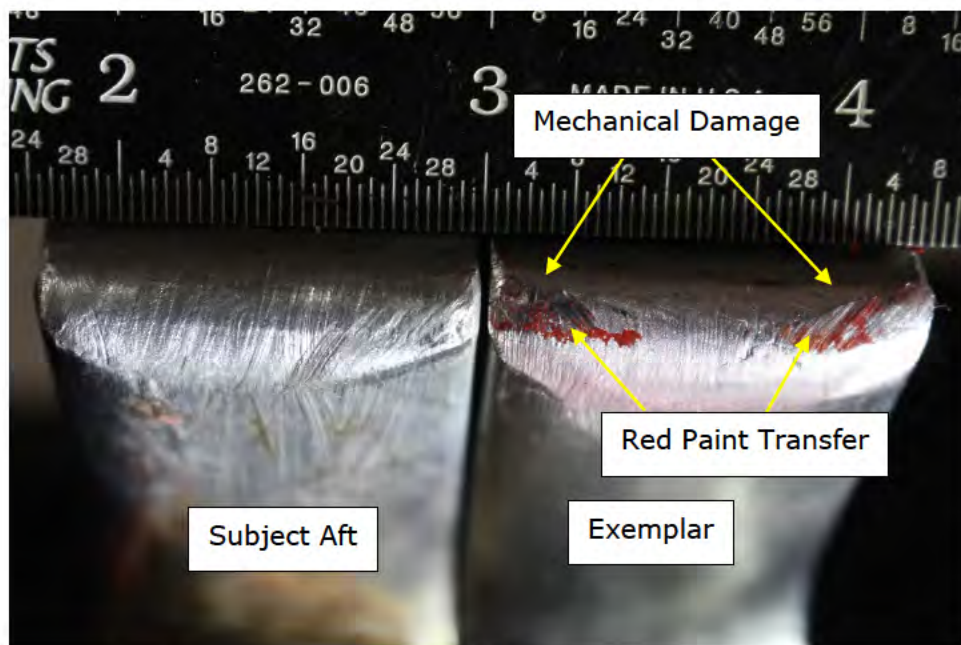


(a)

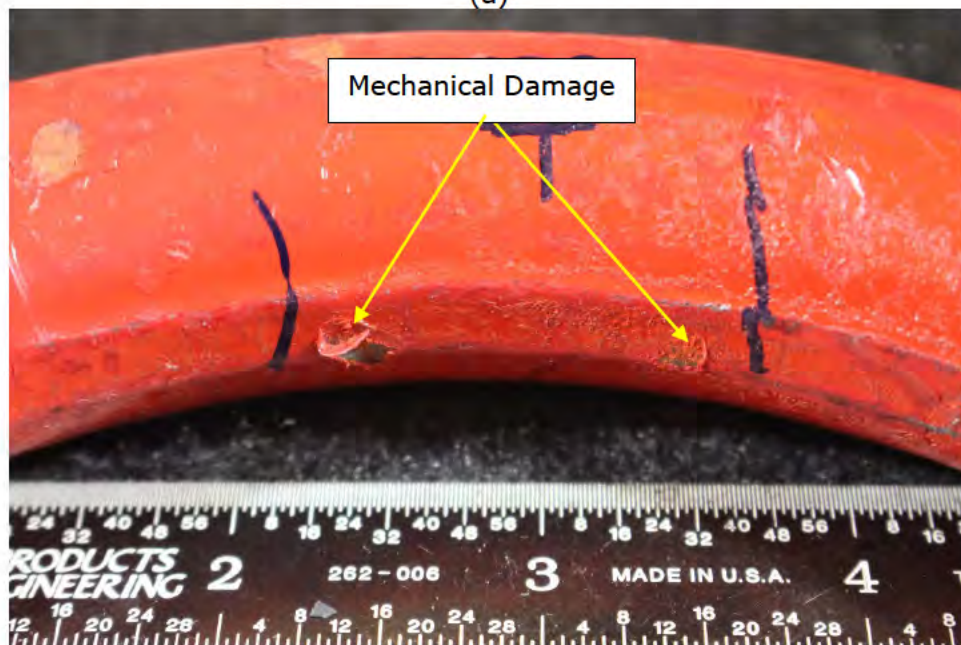


(b)

Figure 165. Photographs showing (a) the point of the Exemplar Hook compared to the Subject Aft Hook and (b) the mechanical damage to the ring after testing Scenario 2. Rulers are in inches.



(a)



(b)

Figure 166. Photographs showing (a) the point of the Exemplar Hook compared to the Subject Aft Hook and (b) the mechanical damage to the ring after testing Scenario 3. Rulers are in inches.

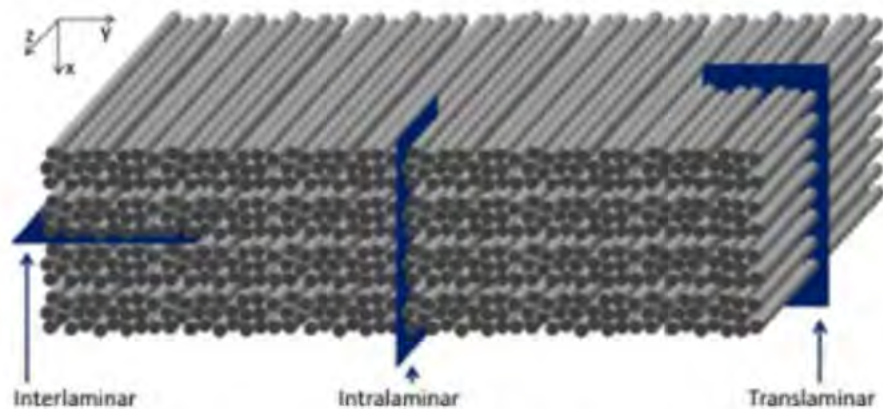


Figure 167. Schematic showing the three failure modes, interlaminar, intralaminar, and translaminar for fiberglass materials.¹⁴

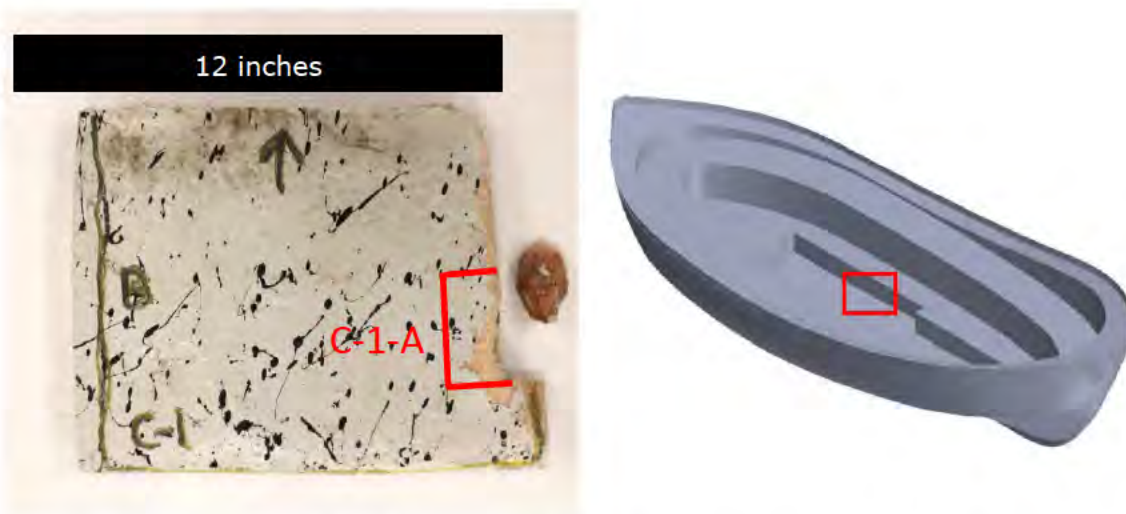


Figure 168. Photograph of Sample C-1 and schematic showing the location where the sample was removed from the inner hull. Sample C-1 was located near the engine mount. The location of the sample examined in the SEM, Sample C-1-A, is shown. Ruler is in inches.

¹⁴ G. Frossard, J. Cugnoli, T. Gmür, J. Botsis, Composites Part A: Applied Science and Manufacturing, Volume 109, June 2018, p. 95-104.

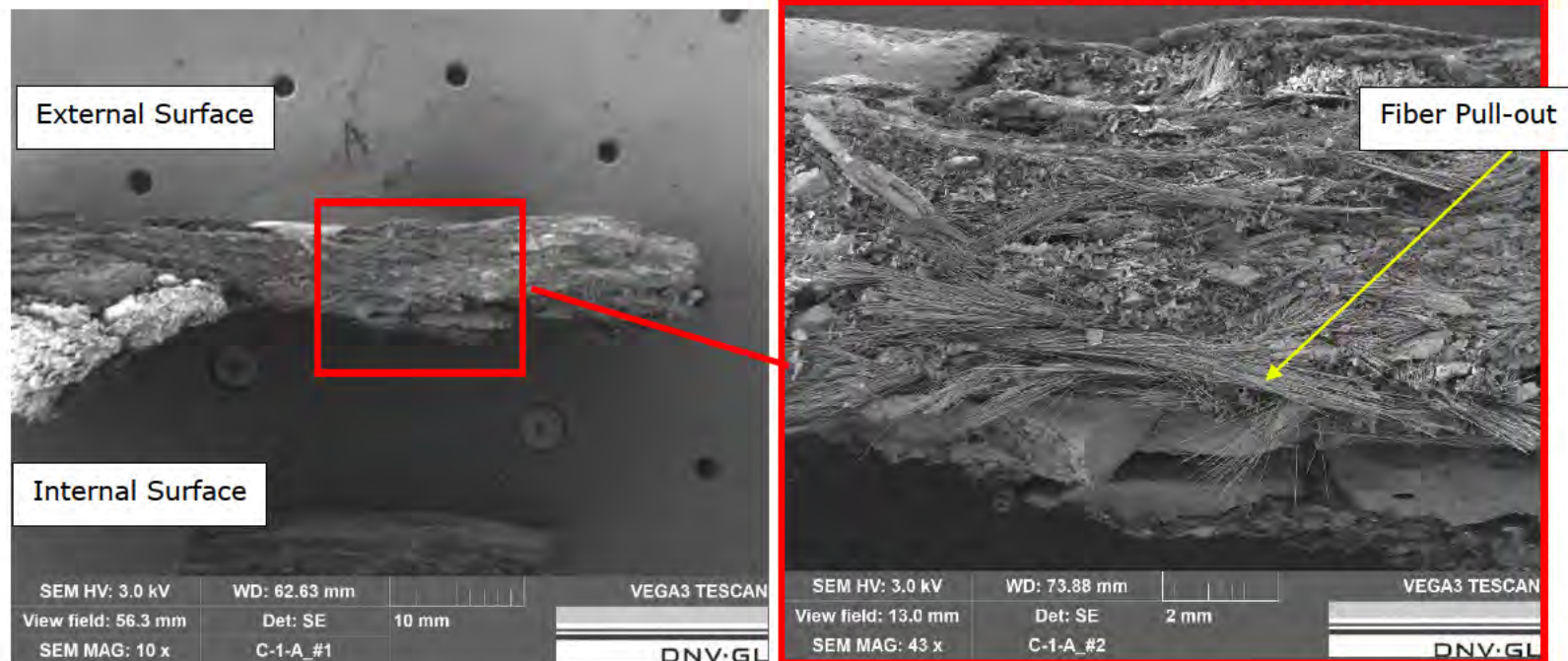


Figure 169. SEM images of Sample C-1-A and schematic showing the fracture surface at a low magnification. Fiber pull-out from the resin matrix is visible near the internal surface. Sample location is shown in Figure 168.

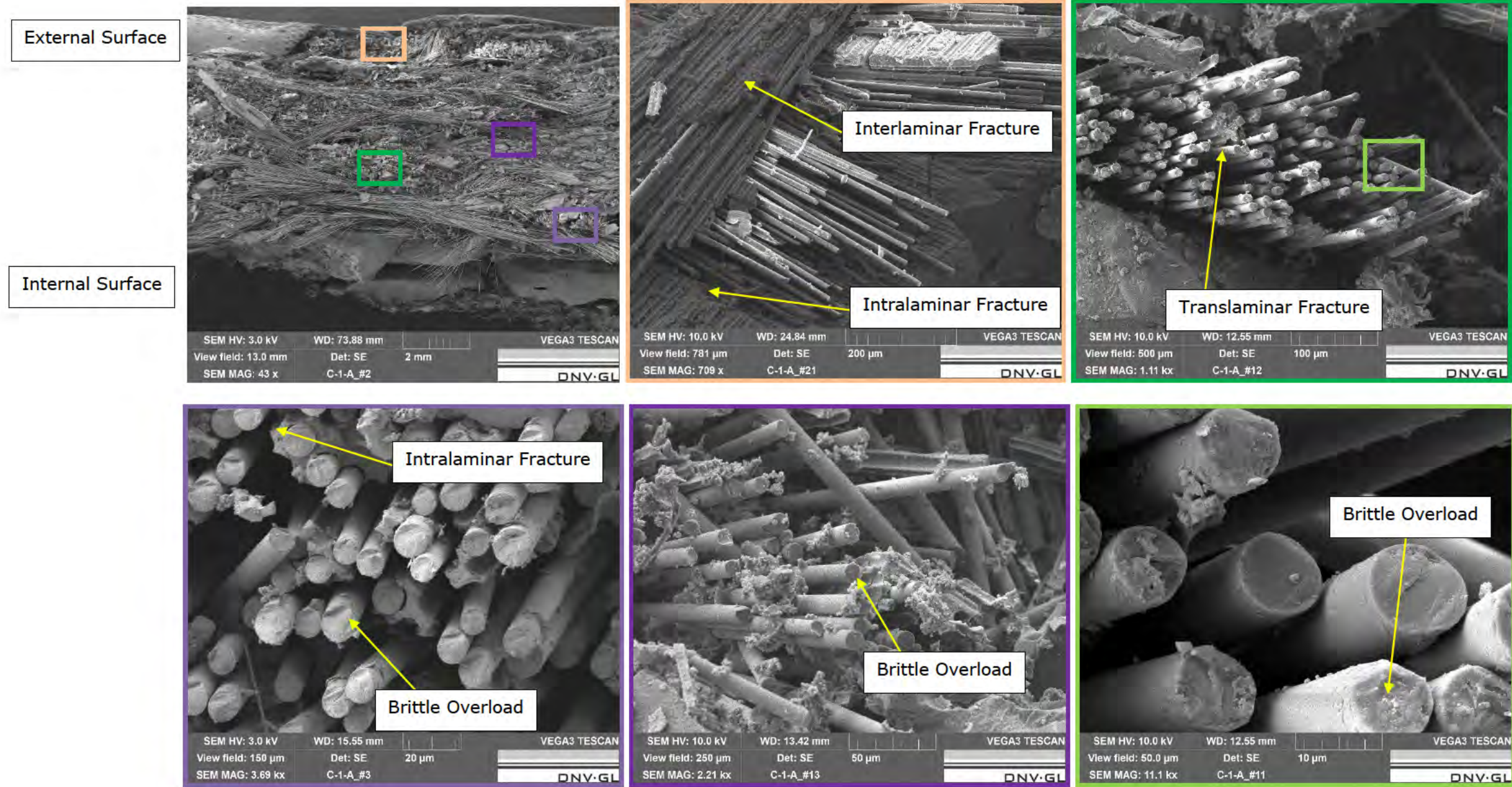


Figure 170. SEM images of Sample C-1-A showing notable fractures of glass fibers. Location of upper left image shown in Figure 169 (right).



Figure 171. Photographs of Sample C-2 and schematic showing the location where the sample was removed from the inner hull. Sample C-2 was located near a crack in the keel. The location of the sample examined in the SEM, Sample C-2-3, is shown.

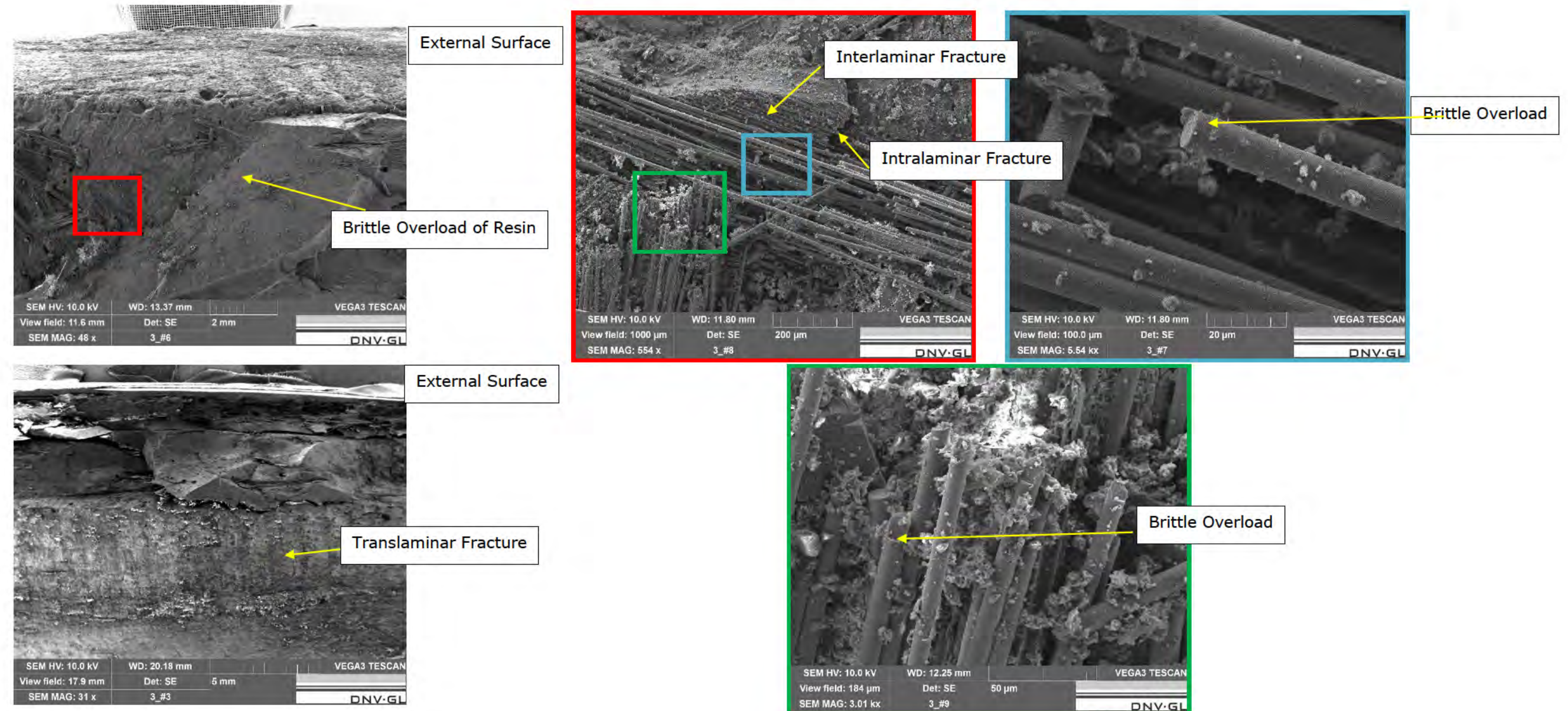
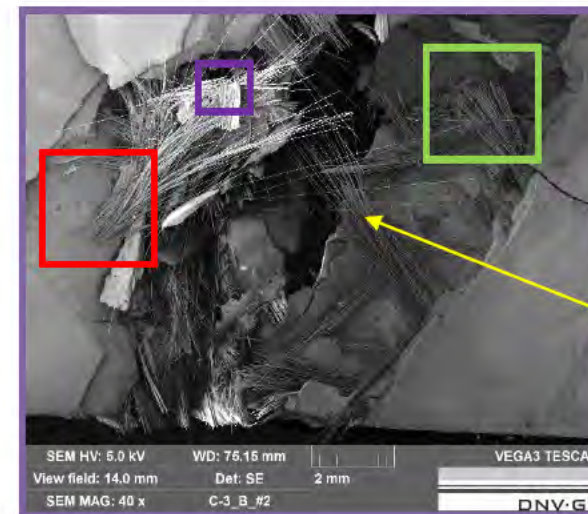


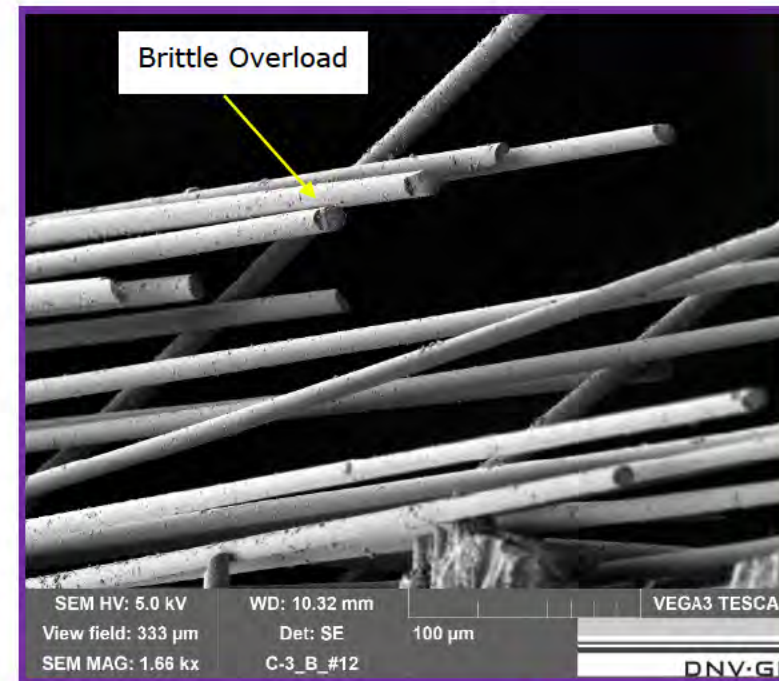
Figure 172. SEM images of Sample C-2-3 showing notable fractures of glass fibers.



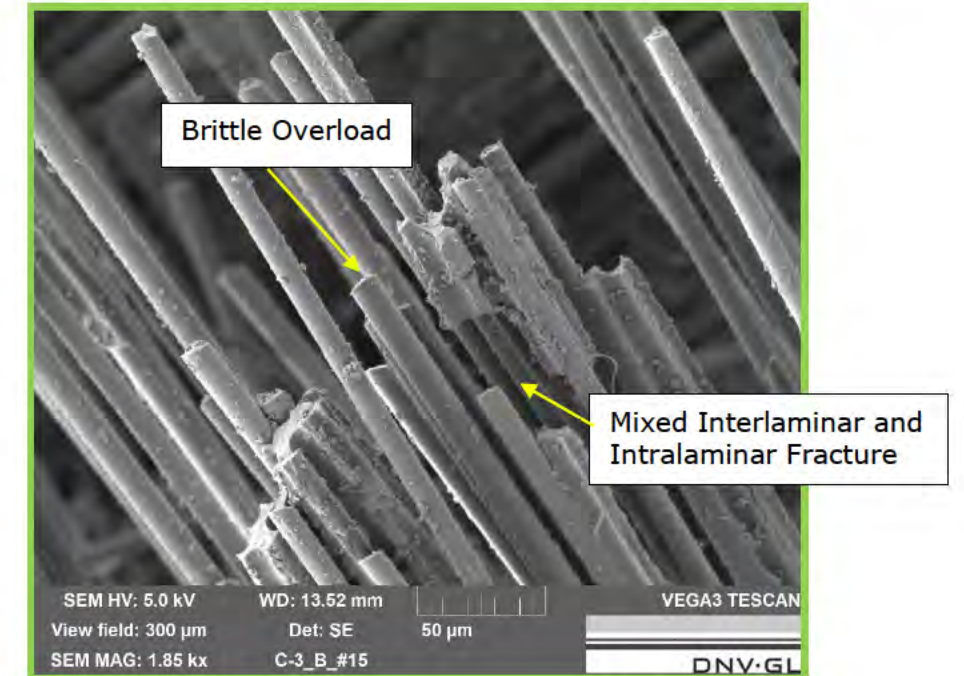
Figure 173. Photograph of Sample C-3 and schematic showing the location where the sample was removed from the outer hull. Sample C-3 was located 11.4 feet from the aft of Lifeboat 6. The location of the sample examined in the SEM, Sample C-3-B, is shown. Ruler are in inches.



Fiber pull-out

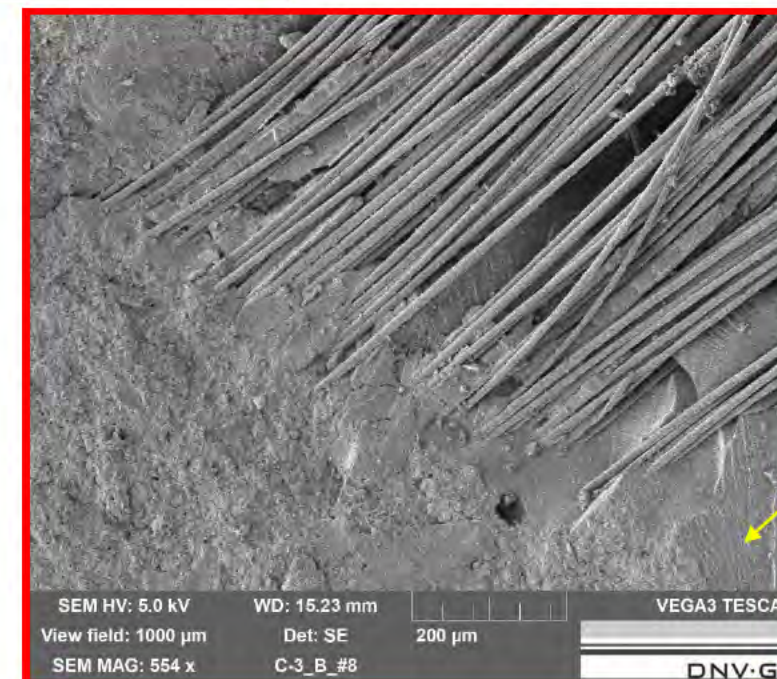


Brittle Overload



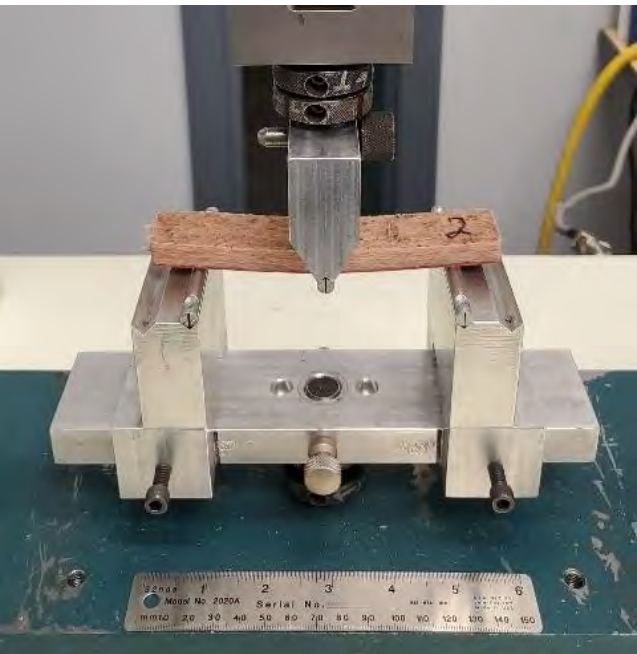
Brittle Overload

Mixed Interlaminar and Intralaminar Fracture



Brittle Overload of Resin

Figure 174. SEM images of Sample C-3-B showing notable fractures of glass fibers.



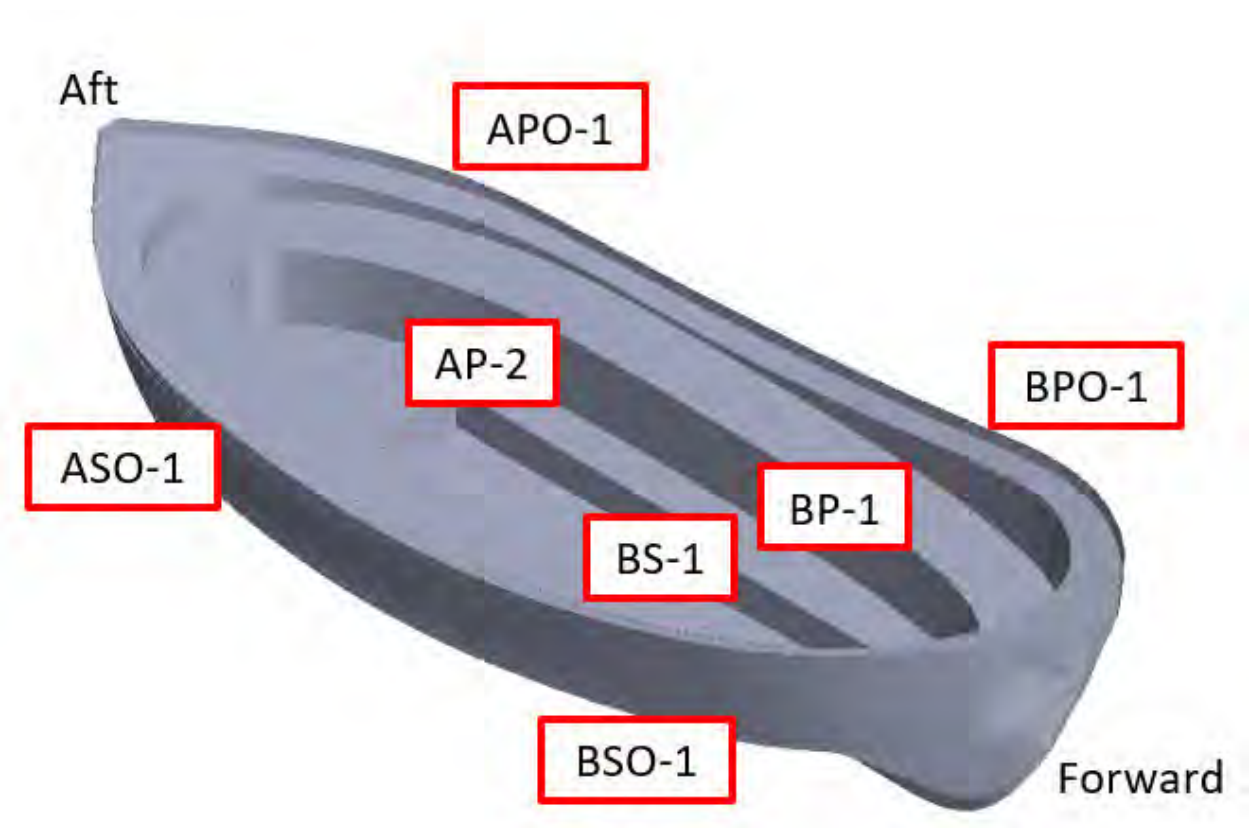
| Sample | Flexural Modulus (psi) | Ultimate Stress (psi) | Ultimate Strain (%) |
|-------------|------------------------|-----------------------|---------------------|
| ASO-1 0° | 558,400 | 11,160 | 2.89 |
| ASO-1 90° | 657,700 | 13,290 | 2.44 |
| APO-1 0° | 586,200 | 12,110 | 2.48 |
| APO-1 90° | 538,300 | 11,550 | 2.62 |
| BSO-1 0° | 578,800 | 13,730 | 2.89 |
| BSO-1 90° | 590,800 | 13,820 | 2.85 |
| BPO-1 0° | 490,000 | 11,980 | 3.27 |
| BPO-1 90° | 624,200 | 11,170 | 2.14 |
| Average 0° | 553,400 | 12,250 | 2.88 |
| Average 90° | 602,800 | 12,460 | 2.51 |
| Average All | 578,050 | 12,355 | 2.70 |

(a)

| Sample | Flexural Modulus (psi) | Ultimate Stress (psi) | Ultimate Strain (%) |
|-------------|------------------------|-----------------------|---------------------|
| AP-2 0° | 572,200 | 11,830 | 2.80 |
| AP-2 90° | 757,400 | 13,720 | 2.35 |
| BS-1 0° | 360,200 | 9,060 | 3.30 |
| BS-1 90° | 438,700 | 10,920 | 2.97 |
| Average 0° | 466,100 | 10,450 | 3.05 |
| Average 90° | 598,100 | 12,320 | 2.66 |
| Average All | 532,100 | 11,390 | 2.86 |

(b)

Figure 176. Photograph of the flexural testing setup on universal testing machine and tables of results for flexural testing of panels extracted from the locations shown in Figure 43.



| Sample | Ash % | | |
|--------|-------|---|------|
| ASO-1 | 40.17 | ± | 0.30 |
| BPO-1 | 35.91 | ± | 0.28 |
| APO-1 | 39.93 | ± | 0.42 |
| BSO-1 | 37.00 | ± | 0.11 |
| AP-2 | 34.23 | ± | 0.65 |
| BS-1 | 28.03 | ± | 0.20 |

Figure 177. Photograph showing the sample locations and a table summarizing the results of glass fiber content analysis via ash testing.

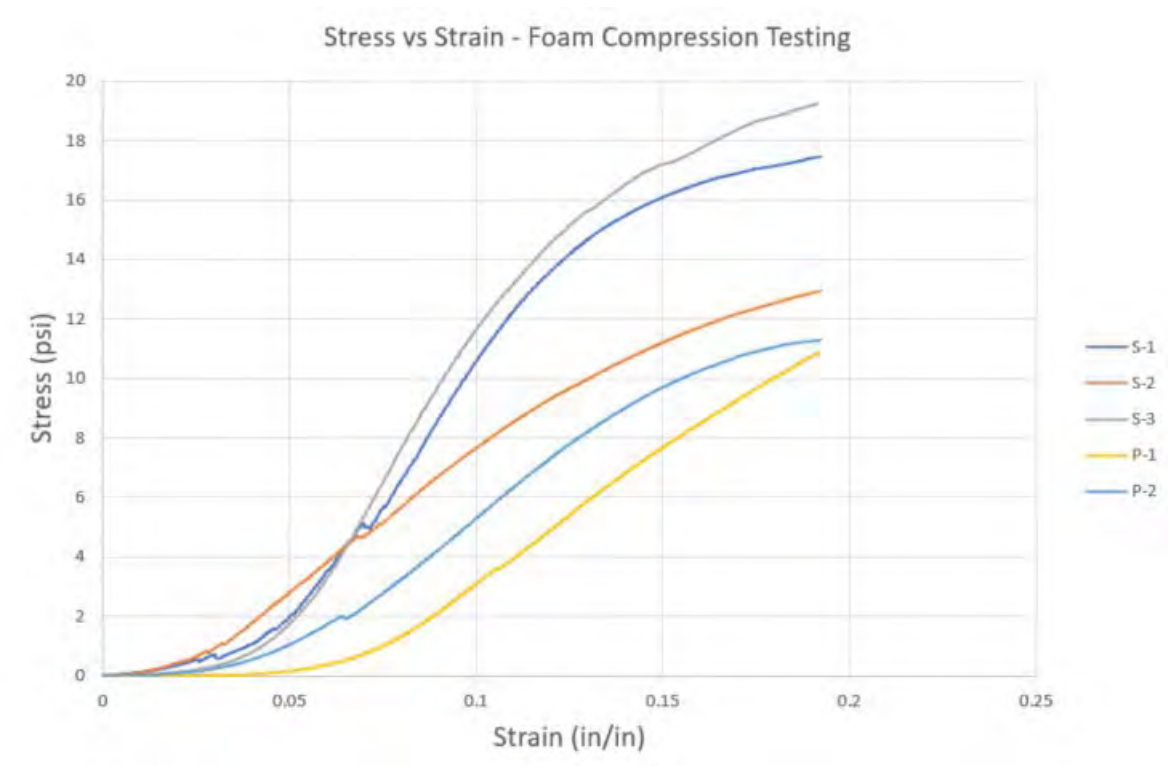


Figure 178. Schematic showing the stress-strain curves generated through compression testing foam from the Lifeboat. Samples with “S” refer to starboard and were removed from under location BS-1 and the samples with “P” refer to port and were removed from under location BP-1; locations of BS-1 and BP-1 are shown in Figure 43.

| Section Name | Color | Thickness |
|----------------------|-------|-----------|
| Bumper | | N/A |
| Canopy_1-4 | | 0.25" |
| Canopy_3-8 | | 0.375" |
| Canopy_5-16 | | 0.3125" |
| Foam | | N/A |
| FoamSkin01875 | | 0.1875" |
| FoamSkin_3-8 | | 0.375" |
| Hull_3-4 | | 0.75" |
| Hull_3-8 | | 0.375" |
| Int_3-8 | | 0.375" |
| LiftShoe-Ply | | |
| Ply 1: Steel | | 0.375" |
| Ply 2: Fiberglass | | 0.375" |
| Ply 3: Steel | | 0.375" |
| RudderAttachment-Ply | | |
| Ply 1: Fiberglass | | 0.375" |
| Ply 2: Steel | | 0.5" |
| SteelPlate_1-2 | | 0.5" |
| SteelPlate_3-8 | | 0.375" |
| SteelPlate_12GA | | 0.11" |

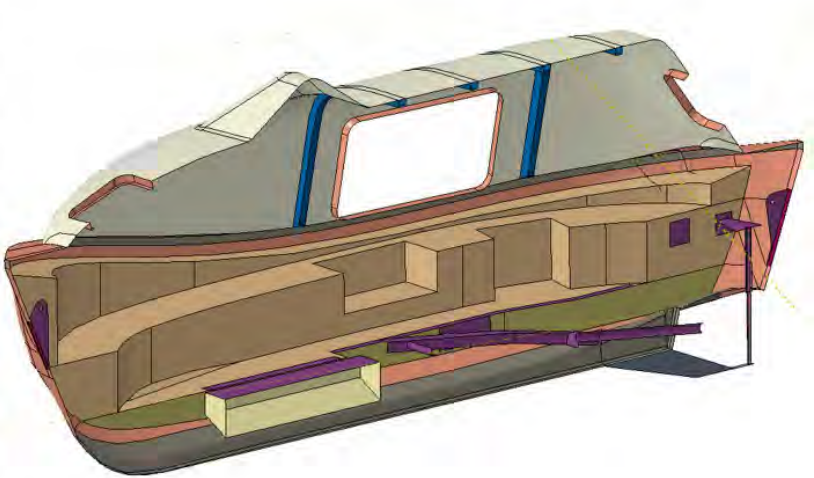


Figure 179. Schematic showing the material sections assigned to surface regions of the Lifeboat 6 model as viewed from the interior.

| Section Name | Color | Thickness |
|----------------------|-------|-----------|
| Bumper | | N/A |
| Canopy_1-4 | | 0.25" |
| Canopy_3-8 | | 0.375" |
| Canopy_5-16 | | 0.3125" |
| Foam | | N/A |
| FoamSkin01875 | | 0.1875" |
| FoamSkin_3-8 | | 0.375" |
| Hull_3-4 | | 0.75" |
| Hull_3-8 | | 0.375" |
| Int_3-8 | | 0.375" |
| LiftShoe-Ply | | |
| Ply 1: Steel | | 0.375" |
| Ply 2: Fiberglass | | 0.375" |
| Ply 3: Steel | | 0.375" |
| RudderAttachment-Ply | | |
| Ply 1: Fiberglass | | 0.375" |
| Ply 2: Steel | | 0.5" |
| SteelPlate_1-2 | | 0.5" |
| SteelPlate_3-8 | | 0.375" |
| SteelPlate_12GA | | 0.11" |

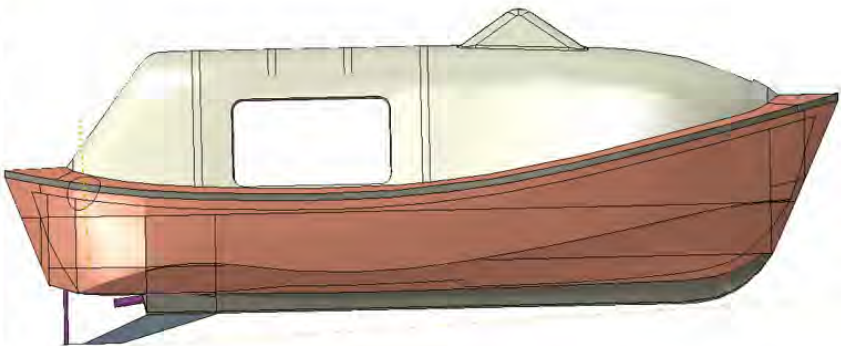


Figure 180. Schematic showing the material sections assigned to surface regions of the Lifeboat 6 model as viewed from the exterior.

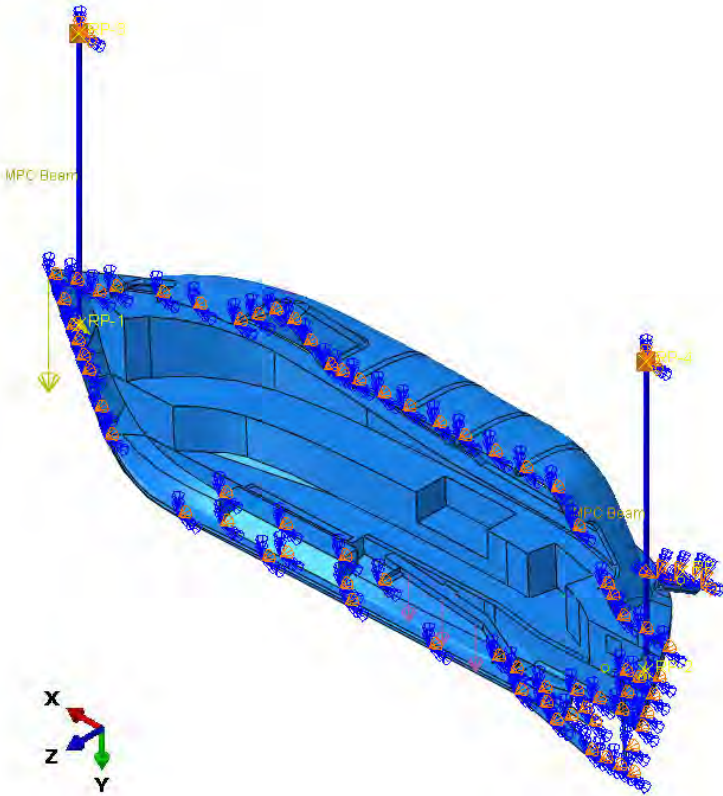


Figure 181. Schematic showing boundary conditions applied in model: XY symmetry, gravity, engine weight, and vertical displacements.

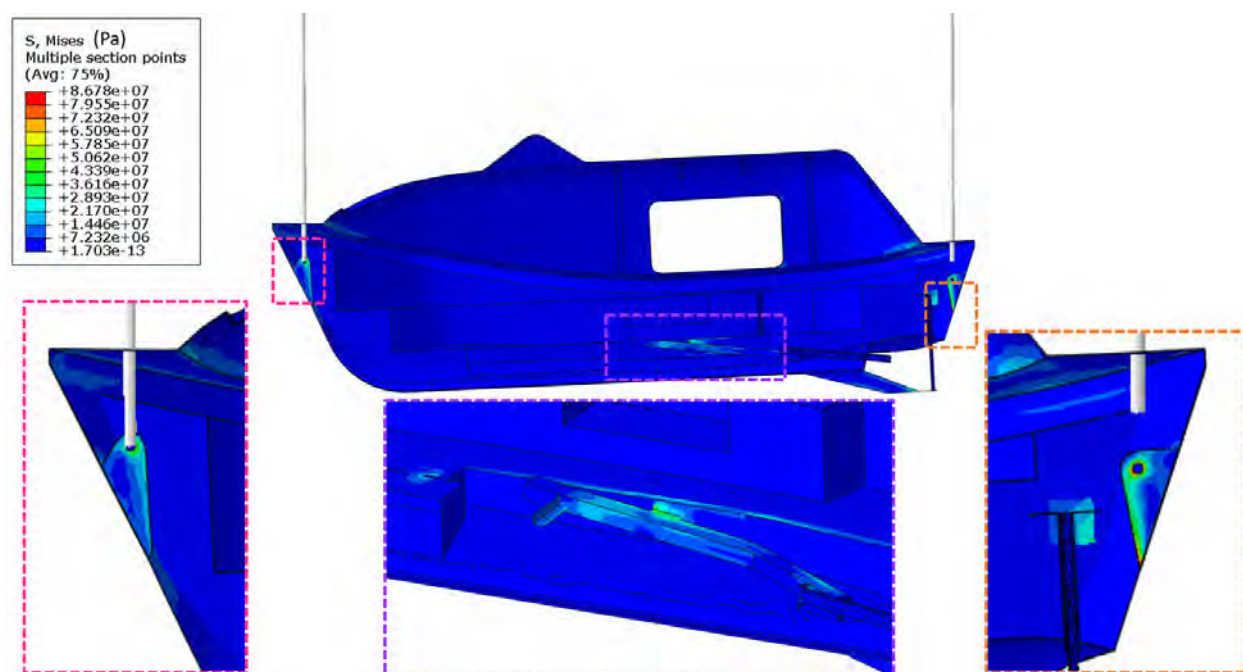


Figure 182. Von Mises Stress Contour of lifeboat in Step 1 with gravity and engine weight only applied to the lifeboat.

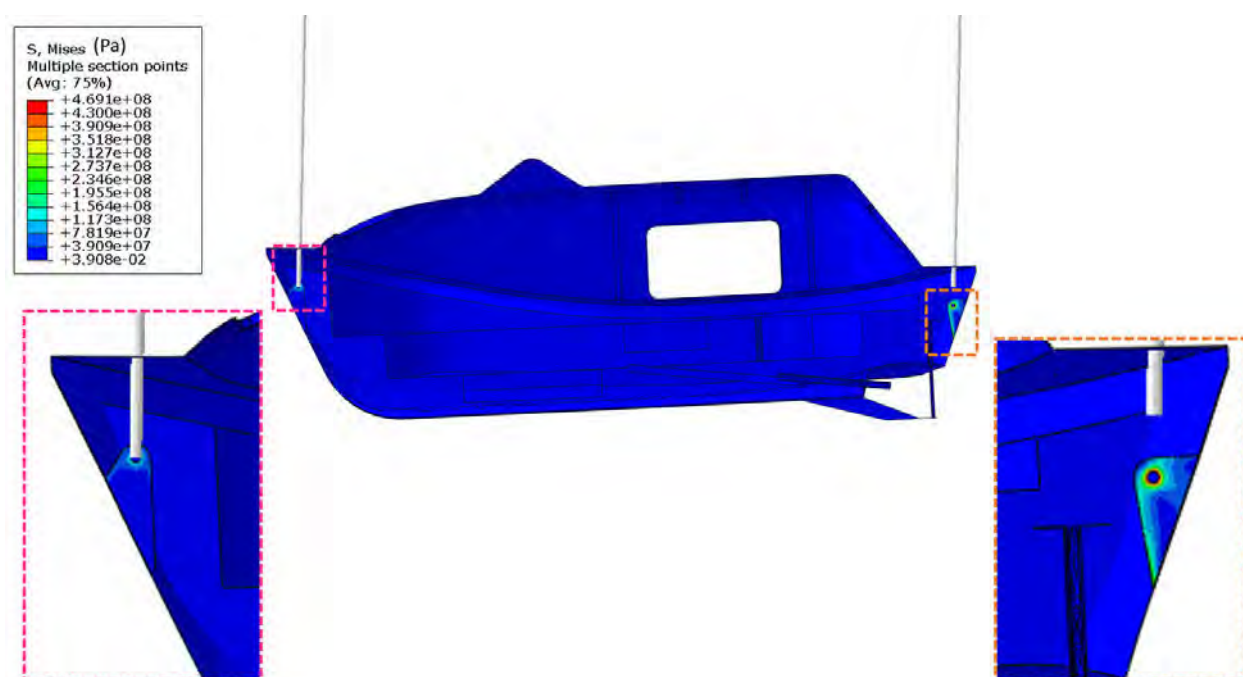


Figure 183. Von Mises Stress Contour of lifeboat in Step 2 with gravity and engine weight and raised ~3.1 inches into the aft davit bumper.

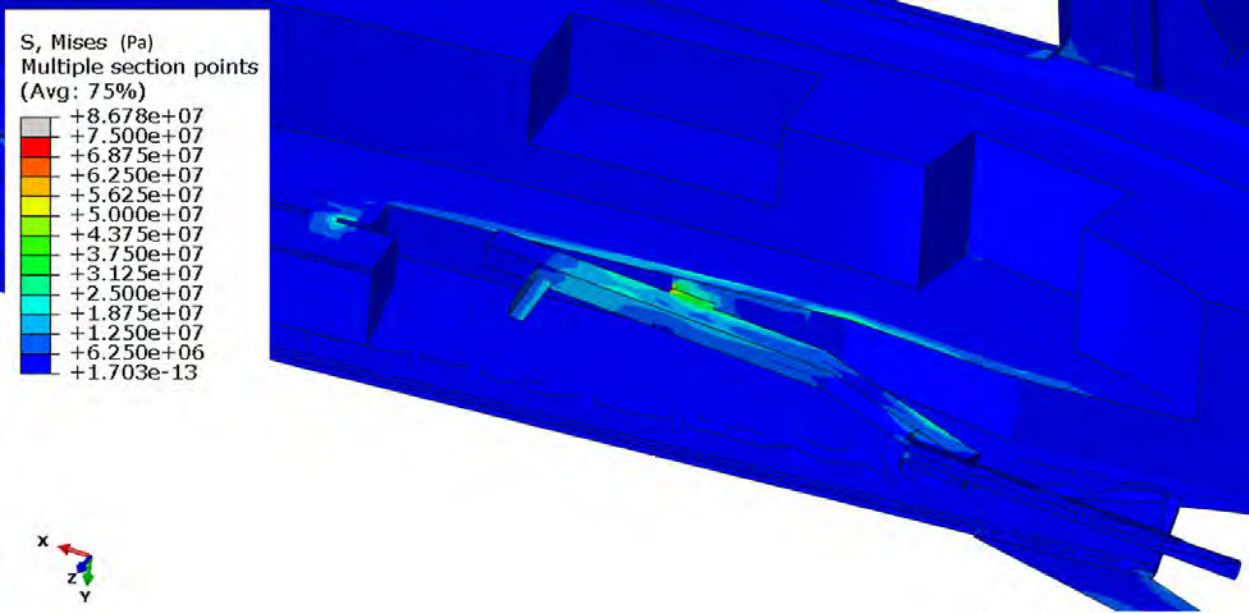


Figure 184. Von Mises Stress Contour of lifeboat in Step 2 with gravity and engine weight and raised ~3.1 inches into the aft davit bumper.

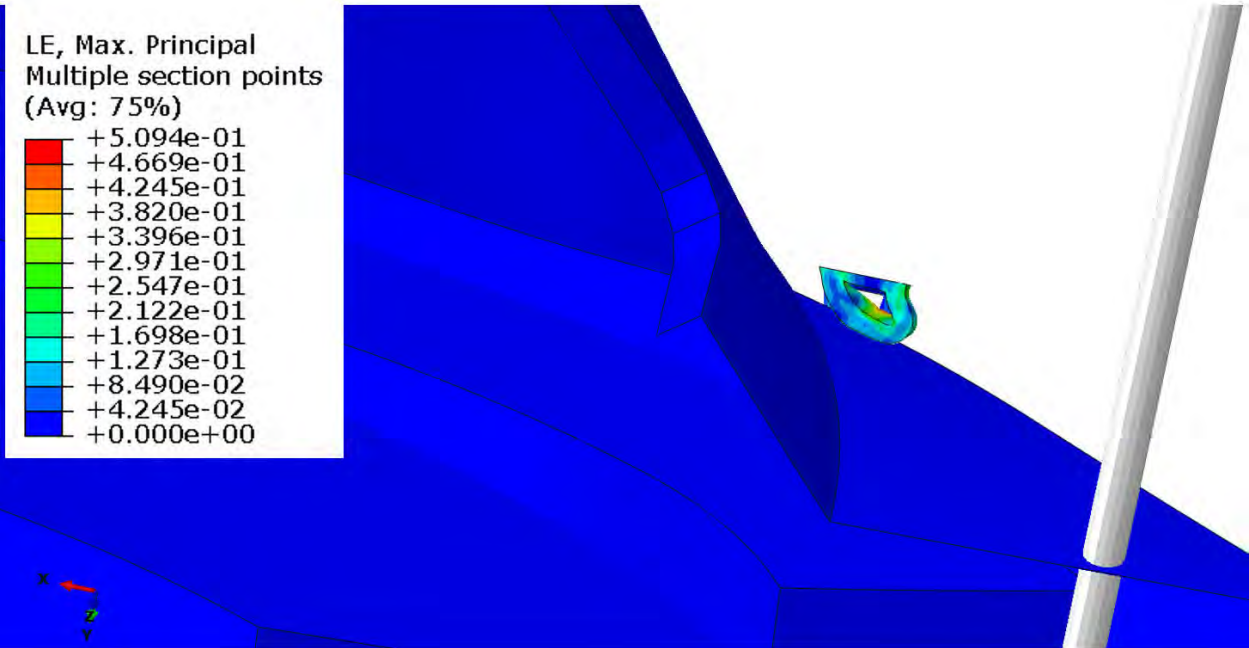


Figure 185. Strain Contours of aft bumper with lifeboat raised ~3.1 inches into the aft davit bumper.

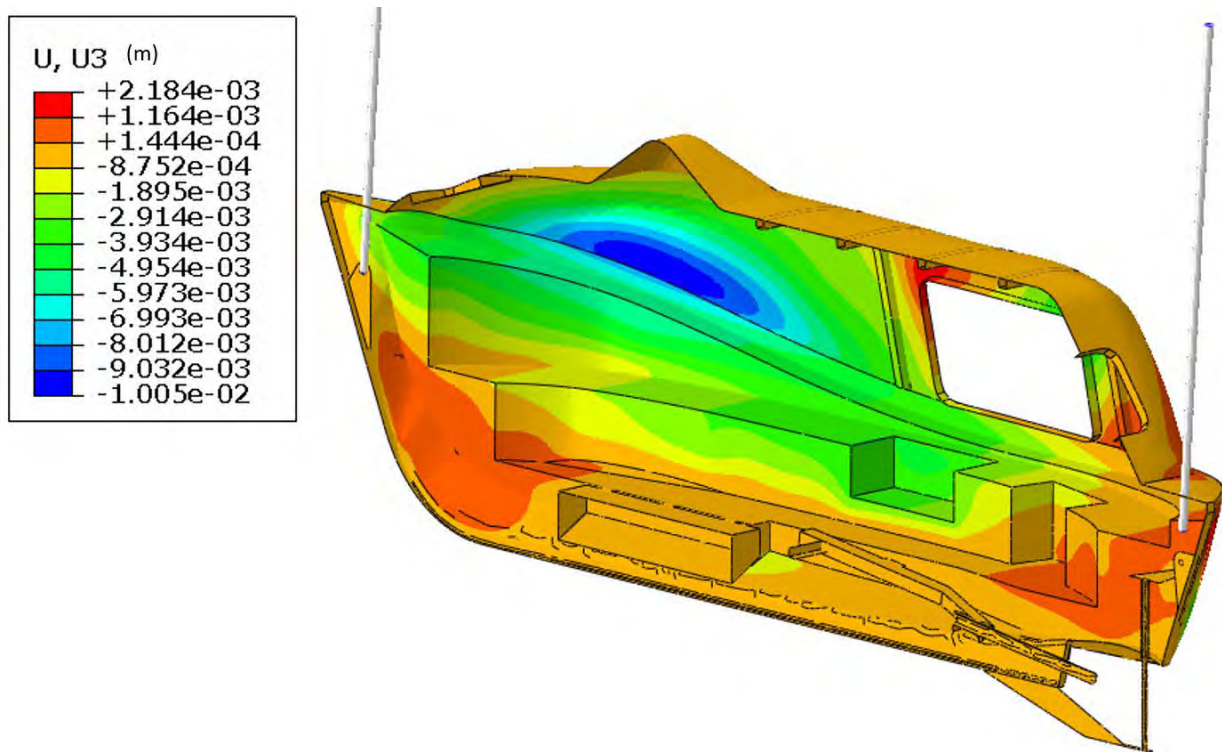


Figure 186. Lateral deflection (port/starboard) of lifeboat raised ~3.1 inches into the aft davit bumper.

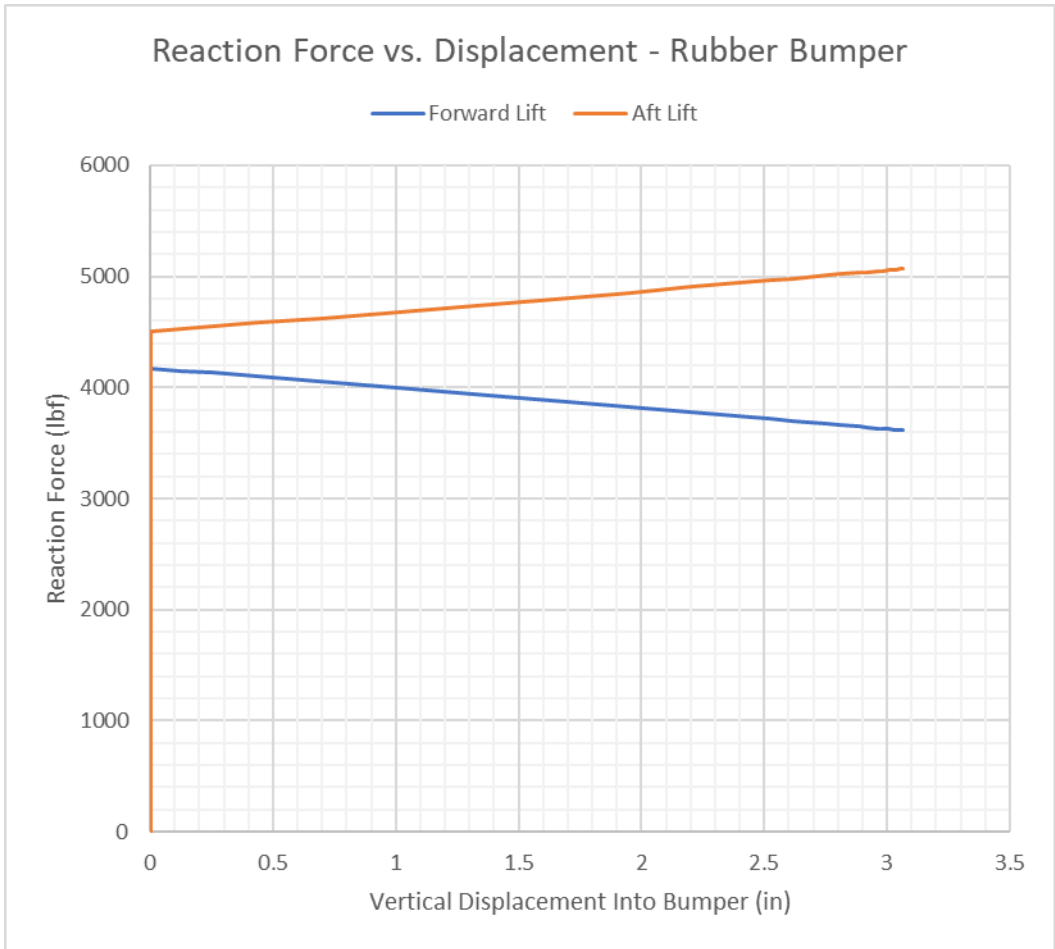


Figure 187. Reaction forces at forward and aft lifting shoes throughout the assessment as a function of vertical displacement considering a bumper.

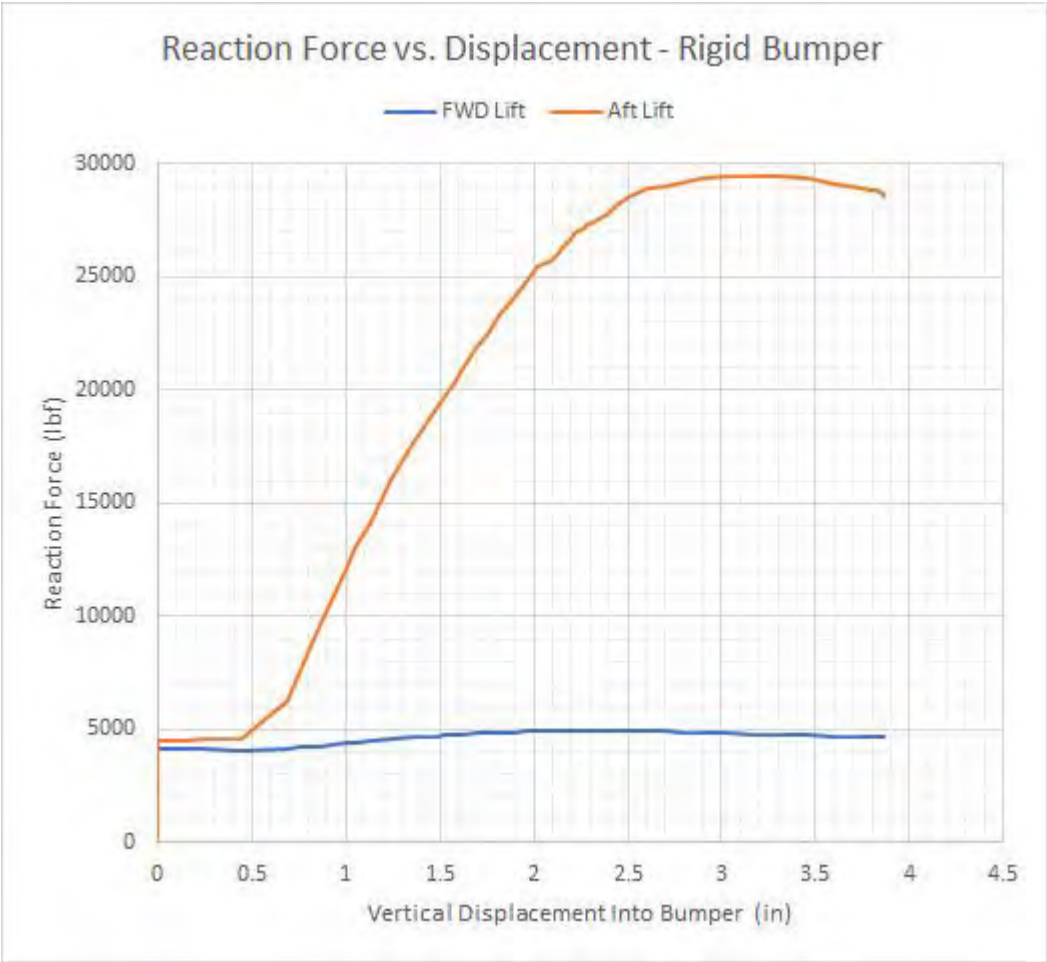


Figure 188. Reaction forces at forward and aft lifting shoes throughout the assessment as a function of vertical displacement considering a rigid bumper.

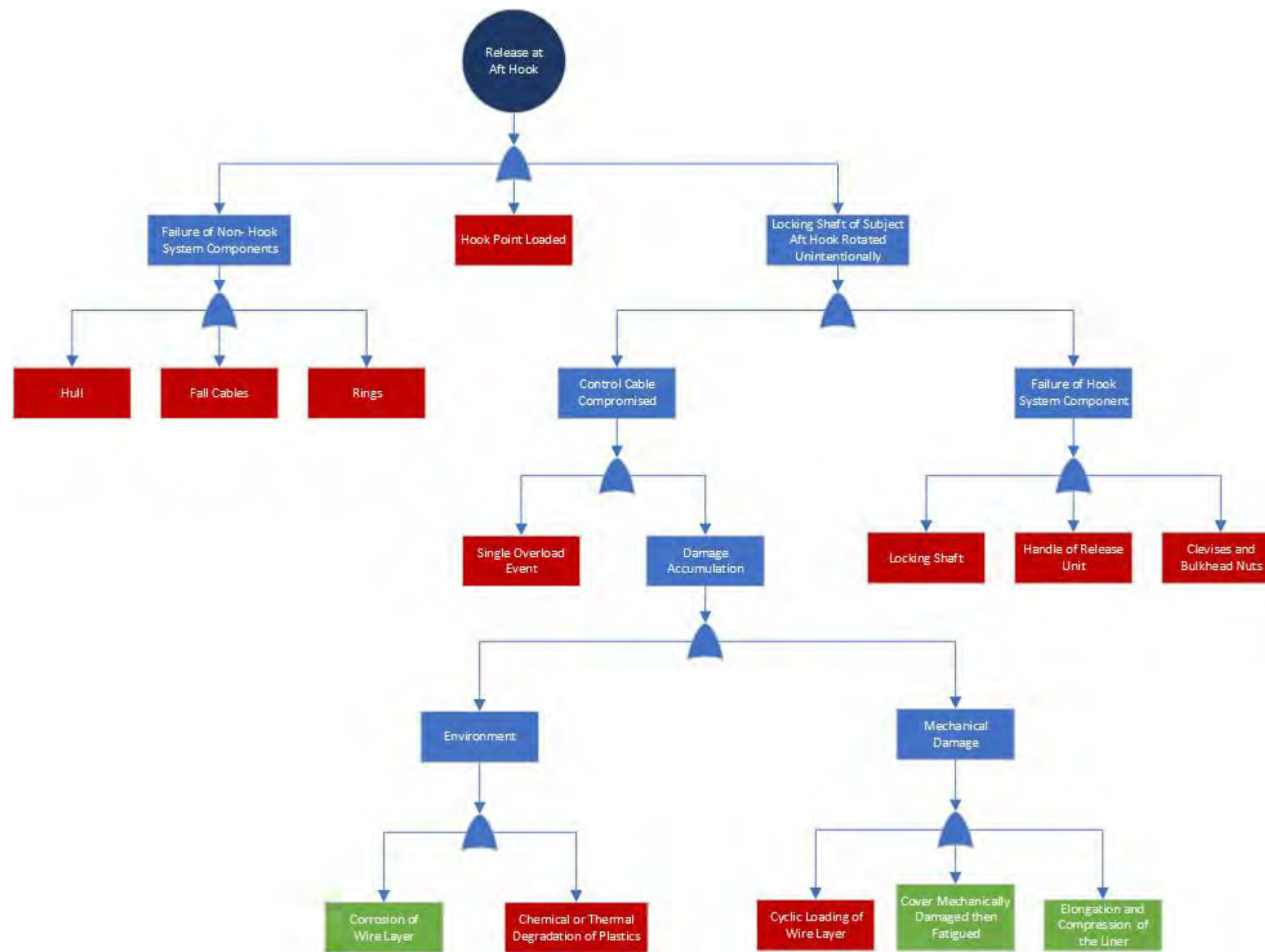


Figure 189. Schematic showing the fault tree used to identify contributing factors to the unintentional release of the Subject Aft Hook. Green: Evidence from site, laboratory testing, and / or document review support that the fault tree event is a contributing factor. Red: Evidence from site, laboratory testing, and / or document review support that the fault tree event is likely not a contributing factor.



ABOUT DNV GL

DNV GL is a global quality assurance and risk management company. Driven by our purpose of safeguarding life, property, and the environment, we enable our customers to advance the safety and sustainability of their business. We provide classification, technical assurance, software, and independent expert advisory services to the maritime, oil and gas, power, and renewables industries. We also provide certification, supply chain, and data management services to customers across a wide range of industries. Operating in more than 100 countries, our experts are dedicated to helping customers make the world safer, smarter, and greener.